

Fall 11-19-2011

Development of Boronic Acid Fluorescent Reporters, Boronic Acid-Modified Thymidine Triphosphates for Sensor Design and Antagonists of Bacterial Quorum Sensing in *Vibrio Harveyi*

Yunfeng Cheng

Follow this and additional works at: https://scholarworks.gsu.edu/chemistry_diss

 Part of the [Chemistry Commons](#)

Recommended Citation

Cheng, Yunfeng, "Development of Boronic Acid Fluorescent Reporters, Boronic Acid-Modified Thymidine Triphosphates for Sensor Design and Antagonists of Bacterial Quorum Sensing in *Vibrio Harveyi*." Dissertation, Georgia State University, 2011.
https://scholarworks.gsu.edu/chemistry_diss/58

This Dissertation is brought to you for free and open access by the Department of Chemistry at ScholarWorks @ Georgia State University. It has been accepted for inclusion in Chemistry Dissertations by an authorized administrator of ScholarWorks @ Georgia State University. For more information, please contact scholarworks@gsu.edu.

DEVELOPMENT OF BORONIC ACID FLUORESCENT REPORTERS, BORONIC ACID-MODIFIED THYMIDINE TRIPHOSPHATES FOR SENSOR DESIGN AND ANTAGONISTS OF BACTERIAL QUORUM SENSING IN VIBRIO HARVEYI

by

YUNFENG CHENG

Under the Direction of Binghe Wang

ABSTRACT

Carbohydrates are known to play important roles in a large number of physiological and pathological processes. Conceivably, “binders” of carbohydrates of biological importance could be used as diagnostic and therapeutic agents. Currently, lectins are the major available tools in research for carbohydrate recognition. However, the available lectins often have cross-reactivity issues, along with the high costs and stability issues. Therefore, there is a critical need to develop alternatives (lectin mimics). In this regard, there have been very active efforts in developing different “binders”, such as small molecule lectinmimics and aptamers. Among all the small molecule lectin mimics developments, boronic acid stands out as the most important building blocks of the sensors design for carbohydrates biomarkers due to its intrinsic binding affinities

with diols. To address a fundamental question that whether boronic acid also binds to six-membered ring sugars, with very limited precedents, we provided a concrete experimental evidence of the binding. Specifically, a series of isoquinolinyboronic acids were found to have remarkably high binding affinities with fluorescence change upon binding to representative sugars. Most importantly, these isoquinolinyboronic acids showed weak but very encouraging bindings with six-membered sugar model. All these promising results paves the way of using boronic acids, especially isoquinolinyboronic acid as building blocks for chemosensors design for biological carbohydrates biomarkers, which universally contain six-membered ring and liner diols.

Aptamer provides another alternative way for sensors development for carbohydrates biomarkers as lectin mimics. Compared to lectins, they are normally cheaper and more stable. However, there is much less options. Another challenging area for aptamer-based lectin mimics development is the difficulty to differentiate changes in glycosylation patterns of a glycoprotein, which affect the function of a glycoprotein and thus recognized as biomarkers. To address this major challenge, our group first demonstrated that the incorporation of a boronic acid into DNA would allow for the aptamer selection process to gravitate towards the glycosylation site. To examine the generality of boronic acid incorporation, increase the structural diversity, and broaden the application of boronic acid-modified DNA, a series of B-TTP analogues with simplified structures were designed, synthesized, and successfully incorporated into DNA. A simple route was also developed using 1,7-octadiyne as a linker for both Sonogashira coupling with thymidine and CuAAC tethering of a boronic acid moiety. This paves the way for the preparation of a large number of B-TTPs with different structural features for aptamer selection

or array analysis.

Finally, bacterial quorum sensing has received much attention in recent years because of its relevance to pathological events such as biofilm formation. As one of the very first groups that developed a series of antagonists for AI-2 mediated quorum sensing, we herein designed and synthesized a series of analogues based on the structures of two lead inhibitors identified through virtual screening. Besides, we also examined their inhibitory activities, twelve of which showed equal or better inhibitory activities compared with the lead inhibitors. The best compound showed an IC_{50} of about 6 μ M in a whole cell assay using *Vibrio harveyi* as the model organism. This encouraging results and SAR discuss also paves the way for the finding of more potent compound through further structure optimization.

INDEX WORDS: Chemosensor, Boronic acid, Fluorescent, Carbohydrate biomarkers, Nucleic acid, Boronolactams, Quorum sensing, AI-2, *Vibrio harveyi*

DEVELOPMENT OF BORONIC ACID FLUORESCENT REPORTERS, BORONIC ACID-
MODIFIED THYMIDINE TRIPHOSPHATES FOR SENSOR DESIGN AND ANTAGONISTS
OF BACTERIAL QUORUM SENSING IN VIBRIO HARVEYI

by

YUNFENG CHENG

A Dissertation Submitted in Partial Fulfillment of the Requirements for the Degree of

Doctor of Philosophy

in the College of Arts and Sciences

Georgia State University

2011

Copyright by
Yunfeng Cheng
2011

DEVELOPMENT OF BORONIC ACID FLUORESCENT REPORTERS, BORONIC ACID-
MODIFIED THYMIDINE TRIPHOSPHATES FOR SENSOR DESIGN AND ANTAGONISTS
OF BACTERIAL QUORUM SENSING IN VIBRIO HARVEYI

by

YUNFENG CHENG

Committee Chair: Dr. Binghe Wang

Committee: Dr. Jenny J. Yang
Dr. Zhen Huang

Electronic Version Approved:

Office of Graduate Studies
College of Arts and Sciences
Georgia State University
Dec 2011

DEDICATION

In endless gratitude to my family, who gave me spiritual as well as material support for my pursuit of knowledge and graduate studies.

ACKNOWLEDGEMENTS

First of all, I would like to express my deep gratitude towards my advisor Prof. Wang, for his advice and encouragement throughout the whole work, and also for his consistent help for my own career goal during the entire process. This dissertation would not have been possible without his help. He is not only a supervisor for my research work, but also a mentor for my personal life, who benefits me a lot through learning from him and thus get a high-level starting point in my career.

Besides, I would also like to sincerely appreciate my committee members, Prof. Yang and Prof. Huang for their time, enthusiasm, and patience in helping me through out my PhD program.

In addition, many other people at the department of chemistry have also offered their support and help during my PhD study. Among them, I would especially thank (1) Dr. Nanting Ni and Dr. Wenqian Yang for their help for the publication of isoquinolinyboronic acids binding study paper, (2) Dr. Chaofeng Dai, Mrs. Hanjing Peng, Dr. Shilong Zheng, Dr. Shan Jin for the help on the project of design, synthesis, and PCR incorporation study of B-TTP analogues, (3) Mrs. Hanjing Peng (co-first author on the quorum sensing paper, the contents of which are included in this dissertation), Dr. Nanting Ni, Dr. Minyong Li, Mr. Gaurav Choudhary, Dr. Hanting Chou, Dr. Chung-Dar Lu, and Dr. Phang C. Tai for their collaborations on the published paper on the development of antagonists of AI-2 mediated bacterial quorum sensing. Besides, I also really appreciate all my other labmates and colleagues, for their great supports and daily discussions during my years of graduate study. Technical support from Dr. Siming Wang, Yanyi (Johnny) Chen, and Dr. Sekar Chandrasekaran in Mass Spectrum and NMR data collection should also be acknowledged.

Finally, financial support from the National Institutes of Health (CA123329, CA1113917, GM086925, and GM084933), University Doctoral Fellowship, Molecular Basis of Disease program at GSU, the Georgia Cancer Coalition, and the Georgia Research Alliance is gratefully acknowledged.

TABLE OF CONTENTS

ACKNOWLEDGEMENTS	v
LIST OF TABLES	viii
LIST OF FIGURES	ix
LIST OF SCHEMES	xiv
CHAPTER	
1. INTRODUCTION	1
Boronic acid-based Chemosensors	1
2. A New Class of Fluorescent Boronic Acids that Have Extraordinarily High Affinities for Diols in Aqueous Solution at Physiological pH	10
Introduction	10
Results and Discussion	12
Conclusions	32
Experimental Section	32
3. Design, Synthesis, and Polymerase-Catalyzed Incorporation of Click-Modified Boronic Acid-TTP Analogues	34
Introduction	34
Results and Discussion	36
Conclusions	43
Experimental Section	43
4. Synthesis and Evaluation of New Antagonists of Bacterial Quorum Sensing in <i>Vibrio harveyi</i>	49
Introduction	49
Results and Discussion	51
Conclusions	69

Experimental Section	70
5. CONCLUSIONS	88
REFERENCES	90
APPENDIX: SUPPORTING INFORMATION	104

LIST OF TABLES

Table 2.1. Apparent association constants (K_a) of isoquinolinyboronic acids with representative sugars	14
Table 2.2. Apparent association constants (K_a) of isoquinolinyboronic acids with representative carbohydrates	19
Table 2.3. Apparent pK_a values of the isoquinolinyboronic acids in the absence and presence of sugars	25
Table 2.4. ^{11}B NMR of isoquinoliny boronic acids alone and in the presence of fructose	26
Table 2.5. Fluorescence quantum yields of the isoquinolinyboronic acids alone and in presence of various sugars	31
Table 4.1. Structures and activities of amides and thioamides	58
Table 4.2. Structures and activities of esters and thioesters	59
Table 4.3. Structures and activities of biaryl compounds	61
Table 4.4. Structures and activities of other compounds	63
Table 4.5. Experimental pIC_{50} , predicted pIC_{50} and residual values of molecules used for CoMFA computation	65

LIST OF FIGURES

Figure 1.1. Structure of BTTP	7
Figure 1.2. Structures of a PBL library	8
Figure 1.3. Structure of <i>p</i> -boronophenylalanine	8
Figure 2.1. Structures of isoquinolinyboronic acids, 8-QBA and 6-MDDCQ	12
Figure 2.2. Fluorescent spectral changes of 8-IQBA upon addition of different diols in phosphate buffer (0.1 M) at pH 7.4: $\lambda_{\text{ex}} = 322 \text{ nm}$, $\lambda_{\text{em}} = 361 \text{ nm}$ (for D-glucose and D-sorbitol); 383 nm (for D-fructose). (A) D-Glucose; (B) D-Sorbitol; (C) D-Fructose; (D) plots of fluorescent intensity changes of 8-IQBA as a function of sugar concentration, $[8\text{-IQBA}] = 1 \times 10^{-5} \text{ M}$.	15
Figure 2.3. Fluorescent spectral changes of 5-IQBA upon addition of different diols in phosphate buffer (0.1 M) at pH 7.4: $\lambda_{\text{ex}} = 272 \text{ nm}$, $\lambda_{\text{em}} = 342 \text{ nm}$ (for D-glucose); 344 nm (for D-sorbitol); 378 nm (for D-fructose). (A) D-Glucose; (B) D-Sorbitol; (C) D-Fructose; (D) plots of fluorescent intensity changes of 5-IQBA as a function of sugar concentration, $[5\text{-IQBA}] = 1 \times 10^{-5} \text{ M}$.	16
Figure 2.4. Fluorescent spectral changes of 4-IQBA upon addition of different diols in phosphate buffer (0.1 M) at pH 7.4: $\lambda_{\text{ex}} = 322 \text{ nm}$, $\lambda_{\text{em}} = 361 \text{ nm}$ (for D-glucose, D-sorbitol,); 370 nm (for D-fructose). (A) D-Glucose; (B) D-Sorbitol; (C) D-Fructose; (D) plots of fluorescent intensity changes of 4-IQBA as a function of sugar concentration, $[4\text{-IQBA}] = 1 \times 10^{-5} \text{ M}$.	17

Figure 2.5. Fluorescent spectral changes of 6-IQBA upon addition of different diols in phosphate buffer (0.1 M) at pH 7.4: $\lambda_{\text{ex}} = 272$ nm, $\lambda_{\text{em}} = 356$ nm (A) D-Glucose; (B) D-Sorbitol; (C) D-Fructose; (D) plots of fluorescent intensity changes of 6-IQBA as a function of sugar concentration, $[6\text{-IQBA}] = 1 \times 10^{-5}$ M. 18

Figure 2.6. Fluorescent spectral changes of isoquinolinyboronic acids upon addition of *cis*-1,2-cyclohexanediol in phosphate buffer (0.1 M) at pH 7.4: (A) 8-IQBA, $\lambda_{\text{ex}} = 332$ nm, $\lambda_{\text{em}} = 442$ nm; (B) 5-IQBA, $\lambda_{\text{ex}} = 272$ nm, $\lambda_{\text{em}} = 341$ nm; (C) 4-IQBA, $\lambda_{\text{ex}} = 322$ nm, $\lambda_{\text{em}} = 440$ nm; (D) 6-IQBA, $\lambda_{\text{ex}} = 272$ nm, $\lambda_{\text{em}} = 355$ nm; Insets: plots of fluorescent intensity changes of IQBAs as a function of sugar concentration $[\text{IQBAs}] = 1 \times 10^{-5}$ M. 20

Figure 2.7. Fluorescent spectral changes of isoquinolinylboronic acids upon addition of methyl- α -D-glucopyranose and cyclohexanol in phosphate buffer (0.1 M) at pH 7.4: (A) 6-IQBA with methyl- α -D-glucopyranose, $\lambda_{\text{ex}} = 272$ nm, $\lambda_{\text{em}} = 356$ nm; (B) 4-IQBA with methyl- α -D-glucopyranose, $\lambda_{\text{ex}} = 322$ nm, $\lambda_{\text{em}} = 361$ nm; (C) plots of fluorescent intensity changes of 4-IQBA and 6-IQBA as a function of methyl- α -D-glucopyranose concentration, (D) 6-IQBA with cyclohexanol, $\lambda_{\text{ex}} = 272$ nm, $\lambda_{\text{em}} = 455$ nm; [IQBAs] = 1×10^{-5} M

Figure 2.8. Fluorescent spectral changes of 8-QBA and 6-MDDCQ upon addition of *cis*-cyclohexanediol in phosphate buffer (0.1 M) at pH 7.4: (A) 8-QBA: $\lambda_{\text{ex}} = 270$ nm, $\lambda_{\text{em}} = 314$ nm, [8-QBA] = 1×10^{-5} M; (B) plot of fluorescent intensity change of 8-QBA as a function of sugar concentration, [8-QBA] = 1×10^{-5} M; (C) 6-MDDCQ: $\lambda_{\text{ex}} = 270$ nm, $\lambda_{\text{em}} = 387$ nm, [6-MDDCQ] = 2×10^{-5} M; (D) plot of fluorescent intensity change of 6-MDDCQ as a function of sugar concentration, [6-MDDCQ] = 2×10^{-5} M.

Figure 2.9. Fluorescent intensity change-6-IQBA concentration relationships in the presence and absence of 0.75 M *cis*-cyclohexanediol in phosphate buffer (0.1 M) at pH 7.4: $\lambda_{\text{ex}} = 272$ nm, $\lambda_{\text{em}} = 354$ nm.

Figure 2.10. pH profiles of the fluorescence intensities of isoquinolinyl boronic acids in the absence and presence of sugars in 0.1 M aqueous phosphate buffer (A) [8-IQBA] 1×10^{-5} M; (B) [5-IQBA] 1×10^{-5} M; (C) [4-IQBA] 1×10^{-5} M; (D) [6-IQBA] 1×10^{-5} M.

Figure 3.1. Chemical structures of B-TTP and NB-TTP

Figure 3.2. Structures of B-TTP analogues 18-21	38
Figure 3.3. Incorporation of B-TTP analogues by Klenow Fragment: 1) Primer only; 2) Primer + dNTPs, no Klenow fragment; 3) Primer + Klenow fragment, no dNTPs; 4) Primer + Klenow fragment + dNTPs; 5) using B-TTP analogue 18 instead of dTTP in 4); 6) using B-TTP analogue 19 instead of dTTP in 4); 7) using B-TTP analogue 20 instead of dTTP in 4); 8) using B-TTP analogue 21 instead of dTTP in 4).	41
Figure 3.4. Group A (analyzed with 15% PAGE) and B (15% denaturing PAGE): PCR incorporation using dTTP (Lane 1), B-TTP analogues 18-21 (Lanes 3-6, respectively), or M-TTP (Lane 7). Lane 2 is negative control with no dTTP. Group C: (analyzed with 15% PAGE): PCR incorporation using B-TTP analogues 18-21 (Lane 1, 3, 5, 7, respectively), DNA being treated with H ₂ O ₂ before analyzing (Lane 2, 4, 6, and 8 for B-TTP analogues 2-5, respectively). All reactions were conducted using <i>Taq</i> polymerase.	42
Figure 4.1. Hit compounds identified from virtual screening	52
Figure 4.2. Optimization of the lead structure	53
Figure 4.3. The molecular alignments of all compounds	65
Figure 4.4. Experimental <i>versus</i> predicted pIC ₅₀ for CoMFA 3D-QSAR model	68

Figure 4.5. 3D contour maps around compound 37a as the result of a CoMFA analysis of the AI-2 inhibitory activities. Regions where substitution enhances (green) or reduces (yellow) the inhibitory affinity (left); the color coding indicates regions where electronegative substituents would enhance (blue) or reduce (red) the inhibitory activities (right).

LIST OF SCHEMES

Scheme 1.1. Overall binding equilibrium of phenylboronic acid with a diol	2
Scheme 2.1. Reagents and condition: i. <i>n</i> -butyllithium, trimethyl borate, THF, -78 °C, 39%.	13
Scheme 2.2. Proposed ionization steps of IQBAs	29
Scheme 2.3. The proposed ionization steps of esters of IQBAs	29
Scheme 3.1. Synthesis of B-TTP analogues 18 to 21	39
Scheme 4.1. Different forms of AI-2	51
Scheme 4.2. Synthesis of Compounds 28-30	53
Scheme 4.3. Synthesis of Compounds 31-35	54
Scheme 4.4. Synthesis of Compounds 36 and 37	55
Scheme 4.5. Synthesis of compounds 39-43	55
Scheme 4.6. Synthesis of Compounds 17-21	56

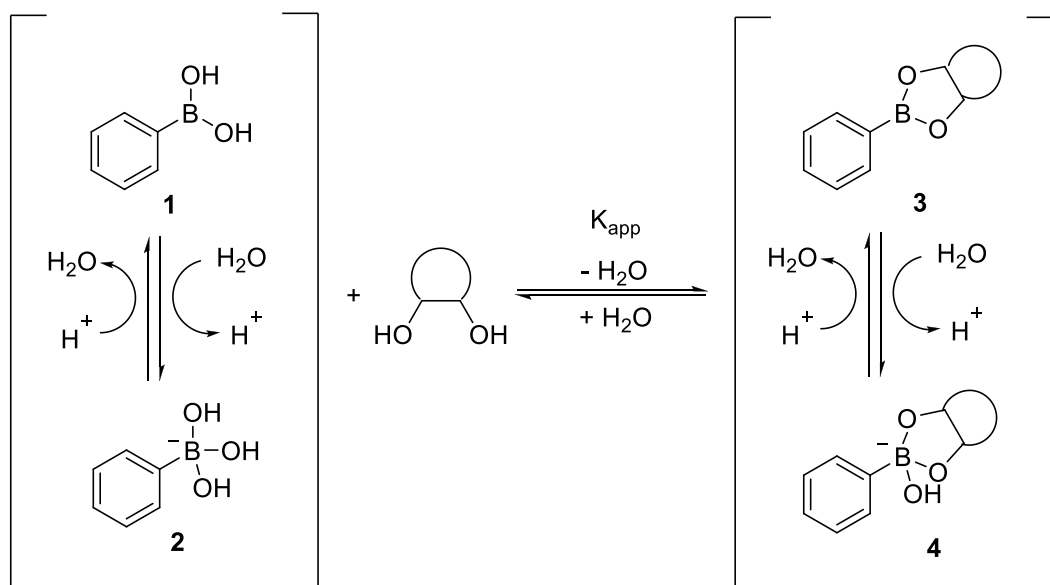
CHAPTER 1.

INTRODUCTION

Boronic acid-based chemosensors

Among all the covalent functional group interactions, boronic acid stands out as the most commonly used in chemosensor construction because of its strong interactions with diols,[1-14] aminoalcohols,[15-17] α -aminoacids,[18] α -hydroxyl acids,[19-22] alcohols[12, 23-38] as well as cyanide[39, 40] and fluoride.[41-45] Among all these interactions, the most commonly used is the complexation between a boronic acid and a diol as described in Scheme 1.1. In early 1990's, Czarnik[6] and Shinkai[46] first recognized the utility of boronic acids in sensor design as described in their seminal papers. This was followed by a decade of very active work in the design and synthesis of sensors for monosaccharides and oligosaccharides. Efforts in recent years have moved to a more biological direction with applications in glycan analysis,[43, 47-49] recognitions of cell-surface carbohydrate biomarkers[5, 50] and glycoproteins[49] as well as array analyses.[51, 52] For biological applications, these boronic acid-based sensors and receptors function in a similar fashion as lectins (carbohydrate-binding proteins). Therefore, the term "boronlectin" was coined to refer to this class of sensors/binders.[12] Along this line, there have been extensive efforts in the design and synthesis of boronic acids that change spectroscopic properties upon binding[12] and the development of combinatorial methods for the rapid search of peptide/protein-based boronlectins (PBL)[43, 47, 53] and nucleic acid-based boronlectins (NBL).[54, 55] Another contribution came from the Schultz lab, who recently reported the successful incorporation of a boronic acid-modified amino acid (phenylalanine) into protein for the selection of lectins with enhanced affinities for carbohydrates.[56, 57] Besides, small molecule boronlectins (SBL) have also shown their tremendous potential in carbohydrate biomarker recognition and targeting.[5, 50]

Several recent reviews and research papers comprehensively summarize the use of boronic acids in sensor designs for carbohydrates,[12, 58] fluoride,[41-45] and cyanides,[39, 40] and have in-depth discussions of factors[12] that should be considered in designing such sensors. In addition, there have also been quite a few reviews[12, 58] and research papers [59-63] on boronic acids that change fluorescent properties upon binding to a nucleophilic analyte or pH changes. Instead of illustrating all the literature details, this section will mainly give a brief description of major factors and issues that need to be considered during boronic-acid based chemosensors design. Along this line, a few selected examples will also be illustrated to highlight the applications.



Scheme 1.1. Overall binding equilibrium of phenylboronic acid with a diol

The unique ability for boronic acids to interact with nucleophiles as described in Scheme 1.1 is due to its special electronic properties. First, the boron atom of a boronic acid has unique electronic properties because of its open shell structure with only 6 valence electrons in its trigonal neutral form, which renders boronic acid a Lewis acid and capable of strong interactions with Lewis bases/nucleophiles such as hydroxyl and amino groups as well as cyanide and fluoride. As a result, the boronic acid (1,

Scheme 1.1) group is able to react with a protic solvent and convert to its anionic tetrahedral form (2) with the concomitant release of a proton, which is the origin of its Brønsted acidity. The boronic acid group is also able to form tight and reversible complexes with 1,2- and 1,3-substituted Lewis base donors such as hydroxyl, amino, and carboxylate groups (Scheme 1.1). Several factors affect the complexation between the boronic acid unit and 1,2- and 1,3-substituted Lewis base donors such as diols, which is the most commonly used form of complexation involving a boronic acid in chemosensor design. It has been widely recognized that a small O-C-C-O dihedral angle, and low pK_a values of the diol and the boronic acid all favor binding at neutral pH.[64, 65] However, the effect of pK_a value is not unidirectional, i.e. this is a bell-shaped relationship with an optimal binding pH somewhere between the pK_a values of the diol and the boronic acid.[12] If the pK_a values of both the diol and boronic acid are low, it is possible that the optimal binding condition is below physiological pH. The combined effect of pK_a and dihedral angle is that boronic acid binding strength normally follows the following order: catechol, *cis*-diols on five-membered ring, linear diols, and then *cis*-diols on six-membered ring. Of course, there are other specific structural features and factors such as buffer, ionic strength, solvent that also affect the complexation.[64]

Because of its strong Lewis acidity, the boronic acid group can also complex with single Lewis bases/nucleophiles. Along this line, boronic acids have been used in the design and synthesis of sensors for fluoride and cyanide. One area that has not been widely recognized is the potential to take advantage of the interactions between a single hydroxyl group and hydroxyl groups on six-membered ring for boronlectin design. This point is especially important because carbohydrates found in glycoproteins, glycolipids, and lipopolysaccharides are almost universally six-membered ring sugars and linear diols. One has to recognize that boronic acids are strong Lewis acids. Depending on their apparent pK_a , their interactions with simple Lewis bases/nucleophiles can be very strong. Furthermore B-O bond is

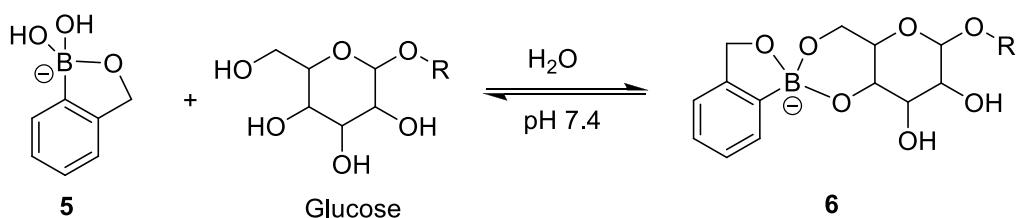
especially strong.[66] There are ample examples of boronic acid interactions with simple hydroxyl groups,[12, 23-38] which can be used for boronlectin design. This property has been extensively used for the design and synthesis of inhibitors of hydrolytic enzymes.[12, 23] There have also been extensive structural studies that clearly indicate covalent interactions between the boronic acid unit and enzyme active site nucleophiles (hydroxyl groups).[28, 31-37, 67-70] For boronic acid-based enzyme inhibitors, once inside the active site, the strong interactions of the boronic acid moiety with a nucleophile are almost always the guiding force in dictating the orientations of other functions groups in an inhibitor.[34-36] The situation of boronic acid-based inhibitor binding to an enzyme in many ways is similar to chemosensor/boronlectin binding to a target where there are many other factors/interactions that help to create synergy with the interactions between a boronic acid and a nucleophile. Therefore, the application of the boronic acid moiety for chemosensor/boronlectin design is not restricted to diols on aryl and five-membered rings and linear structures. As a matter of fact, there are several examples of boronic acid binding to diols/hydroxyl groups on six-membered rings.[5, 50, 71, 72] Furthermore, immobilized boronic acids have been used to isolate glycans and glycoproteins;[73-81] free boronic acids have been used for carbohydrate derivatization for mass spectrometric analysis[73, 82-84] with much success; small molecule boronlectins have been used to recognize cell surface carbohydrate biomarkers which only contains diols on six-membered rings or linear structures;[5] and boronic acid-modified DNA aptamers have been selected to recognize glycoproteins with the ability to differentiate glycosylation variation[56] and carbohydrates with only hydroxyl groups on a six-membered ring. Such reports lend validity to using boronic acids for binding with biologically important carbohydrates that only have hydroxyl groups on six-membered rings. Therefore, literature precedents and a long list of successful studies provide assurance and encouragement to those interested in developing boronlectins for recognition of

carbohydrate-based mammalian biomarkers, which only have hydroxyl groups on linear and six-membered ring structures.

Though the strong interactions between a boronic acid moiety and carbohydrates make it a good candidate for chemosensor design, as in any sensor/binder effort, another key issue is the proper design of the three dimensional scaffold, which allows the desired functional group arrangement and orientation for complementary interactions with the analyte. Generally speaking, there are three ways to achieve this: *de novo* design, template-directed synthesis, and combinatorial library approach. There are successful examples in all three areas in the development of boronolactin/chemosensor by using boronic acid as a key recognition moiety. Briefly, *de novo* design has been used for the successful construction of chemosensors for glucose[85] and dopamine;[86] template-directed synthesis has been used for the construction of sensors for fructose as a model;[87, 88] and combinatorial libraries have been constructed in search of PBLs[43, 47, 53, 56, 57] for carbohydrates and NBLs glycoproteins[54] and carbohydrates. Below are a few specific recent examples of boronic acid-based chemosensors/boronolactins, which demonstrate how such “binders” can be used for biological applications.

In the first example, the Hall lab in 2006 reported an *ortho*-hydroxymethyl phenylboronic acid (5, Scheme 1.2), which was shown to be superior in carbohydrate binding to the well-established diaklyamino (Wulff-type) analogs with better binding affinity and solubility.[89, 90] The most significant finding of compound 5 is the weak but encouraging binding with model glycopyranosides. In neutral aqueous media, 5 could complex hexopyranosides primarily using their 4,6-diol, which is presented on most cell-surface glycoconjugates. The binding constants of 5 with glycopyranosides were obtained by using the alizarin red S-UV assay, developed by the Wang lab, at physiological pH (7.4) in water.[14] The K_a with methyl α -D-glycopyranoside was 22 M^{-1} , which was slightly lower than the binding constant

with glucose ($K_a = 36 \text{ M}^{-1}$). In contrast, the binding constant of phenylboronic acid with glucose is about 5 M^{-1} at physiological pH. Due to the specific property of this unique boronic acid, one can envision a wide variety of applications in the design of oligomeric receptors and sensors toward the selective recognition of glycoconjugates.



Scheme 2. Binding between ortho-hydroxymethyl phenylboronic acid 5 and glycoconjugates

One challenging area of carbohydrate recognition is the differentiation of glycosylation patterns of a glycoprotein. For example, prostate specific antigen (PSA) is a prostate cancer biomarker and a glycoprotein. The glycosylation pattern of PSA from cancer is known to be different from that of normal tissue.[47, 91-101] Tools that allow for detection and differentiation of the various glycoforms of a given glycoprotein will be very useful. The Wang lab is developing an aptamer selection platform for glycoproteins by incorporating boronic acid-modified thymidine into DNA.[54] A boronic acid-labeled thymidine triphosphate (BTTP, Figure 1.1) has been successfully synthesized. It has also been confirmed that DNA polymerase can recognize BTTP as a substrate and the boronic acid-labeled DNA as a template, which are prerequisites for further aptamer selection. Based on the intrinsic affinity of boronic acids for carbohydrates, and well-known aptamer selection method developing about 18 years by the labs of Szostak,[102] Joyce,[103] and Gold,[104] it is very reasonable to believe that incorporation of a

boronic acid into the DNA aptamer would allow the selection process to gravitate toward the “sweet spot” (glycosylation site).

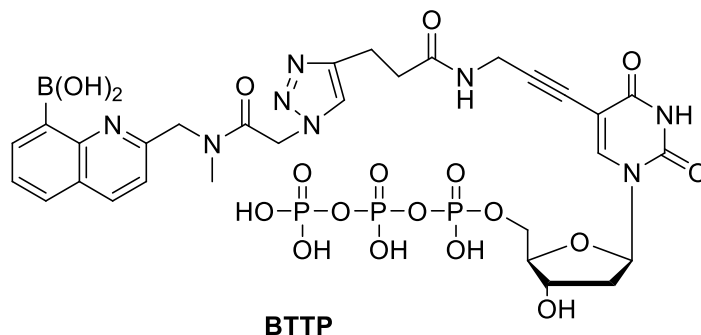


Figure 1.1. Structure of BTTP

In addition to aptamer-based boronic acid libraries, there have been efforts in making peptide-based boronic acid libraries for the same purpose. For examples, the Hall lab developed a general solid-phase approach to the synthesis and isolation of functionalized boronic acids, which should be very useful in combinatorial library synthesis of boronic acid-based carbohydrate sensors.[105] Along a similar line, the Hall lab has established a prototypic bead-supported split-pool library of triamine-derived triboronic acid receptors;[47] the Lavigne lab reported their PBLs for carbohydrate recognition;[43] and Duggan and co-workers prepared solid-supported peptide boronic acids derived from 4-borono-L-phenylalanine and studied their affinity for alizarin.[53] As a specific example, herein we discuss in detail recent work done by the Anslyn lab. A chemosensor array of PBLs (7, Figure 1.2) has been developed for saccharides and saccharide derivatives. This array is fully operational in aqueous media at physiological pH. Binding studies were performed colorimetrically using an indicator (bromopyrogallol red (BPR)) uptake protocol in the taste-chip platform. The binding response signal was recorded and differential indicator uptake rates of these receptors in the presence of saccharides were analyzed to identify patterns within the data set using linear discriminant analysis. This LDA data set could be used for classifying disaccharides and monosaccharides as well as discriminating compounds within each saccharide group. Besides, it can also

identify sucralose in a real world beverage sample as well. This chemosensor assay system has the advantage of good water solubility and high sensitivity. This method was one of the first assays where supramolecular pattern-based sensors were used to identify a specific target in a complex beverage.

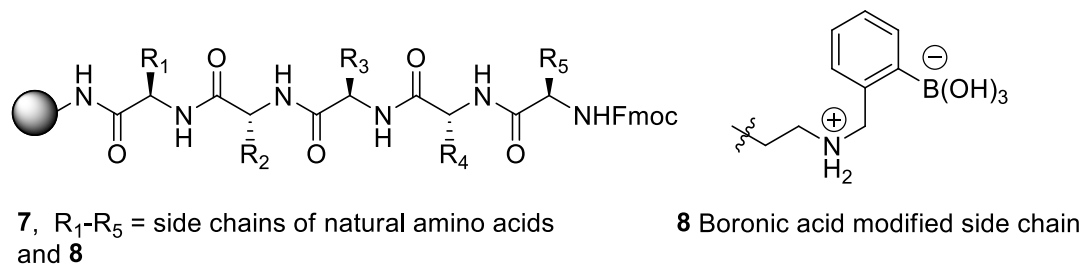


Figure 1.2. Structures of a PBL library

Finally, the Schultz lab recently reported the successful incorporation of the boronate functionality into the genetic code of *E. coli* in high yield and efficiency.[56, 57] Specifically, *p*-boronophenylalanine (9, Figure 1.3) was incorporated into proteins, which can lead to the development of protein-based boronlectins (PBLs) that specifically recognize various glycoproteins or carbohydrates. The ability to incorporate boronophenylalanine into proteins allows for selective chemistry on the boronoprotein based on the intrinsic properties of the boronic acid. Therefore, boronic acid incorporation can be used to purify native protein sequences in a one-step scarless affinity procedure and *in vivo* labeling of boronate containing proteins with polyhydroxylated reporter molecules.

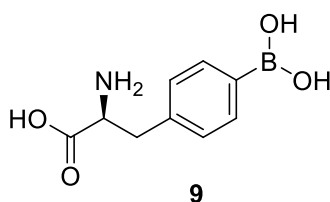


Figure 1.3. Structure of *p*-boronophenylalanine

In summary, among all the covalent interactions, boronic acid stands out as the most powerful building blocks as a key recognition moiety for sensors design, due to its intrinsic binding affinity with diols, aminoalcohols, α -aminoacids, α -hydroxyl acids, alcohols as well as cyanide and fluoride. Among all these interactions, the boronic-acid based chemosensors for carbohydrates are mostly developed. This is due to the reasons that (1) carbohydrates are known to play important roles in a large number of biological and pathological processes, (2) high affinity and specificity boronic-acid based chemosensors for biologically important carbohydrates are potential medicinal and diagnostic agents due to their intrinsic properties. To date, a series of successful boronic acid-based chemosensors have been developed, which could be categorized into *de novo* design, especially for SBLs; template-directed synthesis such as the application in the construction of sensors for fructose as a model; and combinatorial libraries in search of PBLs, and NBLs. Along a similar line, we will report our contributions to this area in following chapters 2 and 3.

CHAPTER 2

A New Class of Fluorescent Boronic Acids that Have Extraordinarily High Affinities for Diols in Aqueous Solution at Physiological pH

Abstract: *This chapter is mainly based on one paper that has been published in Chemistry-A European Journal in 2010 from page 13528 to 13538.* The fluorescent boronic acids that have high affinities for diols at physiological relevant condition play an important role as a key recognition moiety for carbohydrates sensor design. Herein we report a series of isoquinolinyboronic acids that have extraordinarily high affinities for diol-containing compounds at physiological pH. In addition, 5- and 8-isoquinolinyboronic acids also showed fairly high binding affinity with D-glucose ($K_a = 42$ and 46 M^{-1} , respectively). For the very first time, weak but encouraging binding with *cis*-cyclohexanediol was found for these boronic acids. Such binding was coupled with significant fluorescence changes. Furthermore, 4- and 6-isoquinolinyboronic acids also showed ability to complex methyl- α -D-glucopyranose ($K_a = 3$ and 2 M^{-1} , respectively).

Introduction

Boronic acids are commonly used in chemosensor design due to its intrinsic binding affinity with diols (Scheme 1.1), aminoalcohols, α -aminoacids, α -hydroxyl acids, alcohols as well as cyanide and fluoride.[12, 58, 106, 107] The general interaction pathways are shown in Scheme 1.1. Since the rejuvenation of the boronic acid-diol recognition field by Czarnik[6] and Shinkai[106] in the early 1990s', research in this area has undergone some transformations going from binding with simple monosaccharides to recognition of cell-surface carbohydrate biomarkers. Several recent reviews and research papers comprehensively summarized the use of boronic acids in sensor design for

carbohydrates,[12, 58, 108-110] with in-depth discussions of factors[12, 58, 65, 111] that should be considered in designing such sensors.

One critical need in the carbohydrate sensing area is the availability of fluorescent boronic acid reporter compounds that (1) change fluorescent properties upon binding; (2) are water soluble; (3) have high intrinsic affinity for diols, and (4) are chemically and photochemically stable. There have also been quite a few reviews[8, 58] and recent research papers[57, 90, 112-124] on boronic acids that change fluorescent properties upon binding to a nucleophilic/Lewis base analyte.

Despite the impressive progress made in the design and synthesis of fluorescent boronic acid reporter compounds, several key issues remain. First, most fluorescent boronic acid reporter compounds have low to modest intrinsic affinities for diol-containing compounds. Second, boronic acids are known to have high affinity for *cis*-diols on five-membered rings and in linear structures. Binding to six-membered ring diols has commonly believed to be very hard unless the six-membered ring is constrained to give an abnormally small dihedral angle.[58] This point is very important because biologically important cell-surface carbohydrate biomarkers only contain six-membered pyranose, but not five-membered furanose. Boronic acids that can bind diols on pyranose sugars are very important for the design of sensors for carbohydrate biomarkers. It is our working hypothesis that since boronic acids are Lewis acids, under the appropriate conditions they should interact with all nucleophiles/Lewis bases including diols on a six-membered-ring. Indeed, polystyrene-immobilized phenylboronic acid has been used for the separation of *cis*- and *trans*-cyclohexanediol,[125] indicating their interactions. Additional evidence comes from the binding studies with inositols.[71] Recently, the Hall lab reported a compound that can bind to a pyranose model (methyl- α -D-glucopyranose).[89, 90] The boronic acid binds to the 4,6-positions of a pyranose sugar. So far, to our best knowledge there has been no report of monoboronic acid

that can bind methyl- α -D-glucopyranose with fluorescence intensity changes in an aqueous solution. Herein we describe the very unique binding and fluorescent properties of series of isoquinolinyboronic acids (Figure 2.1), which show extraordinarily high binding affinities for carbohydrates. 4- and 6-IQBA also showed detectable binding to methyl- α -D-glucopyranose, with fluorescence changes upon binding. In addition, we also report the unique binding affinity of these boronic acids with *cis*-cyclohexanediol. These boronic acids represent the very first that can bind 1,2-diols on an unconstrained six membered ring in aqueous solution at physiological pH with fluorescence intensity changes.

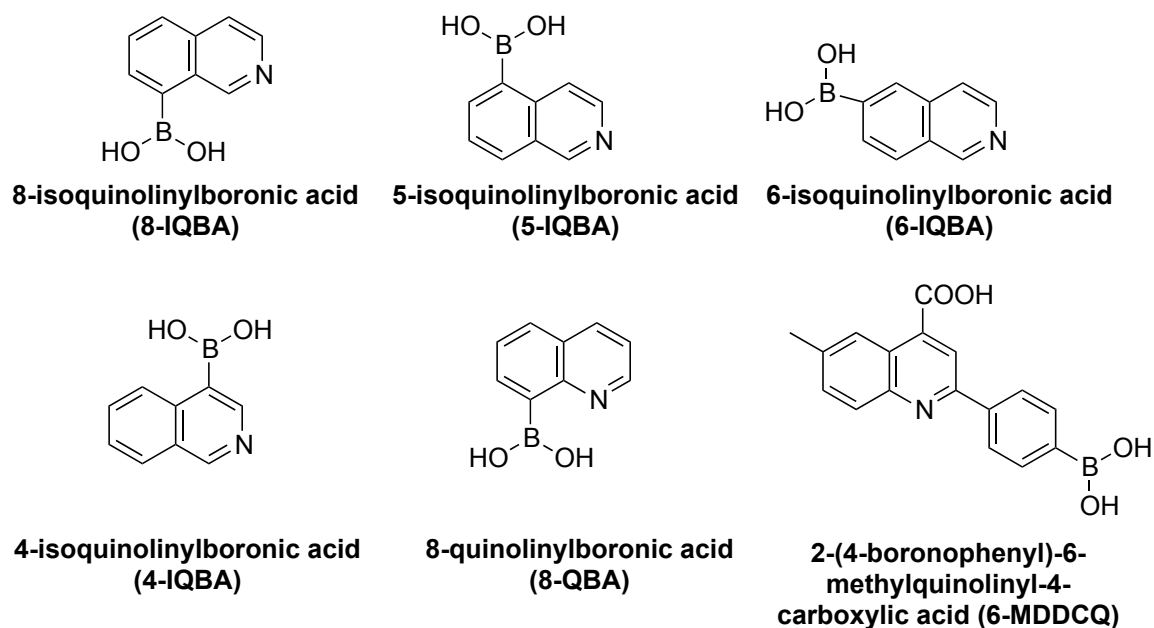
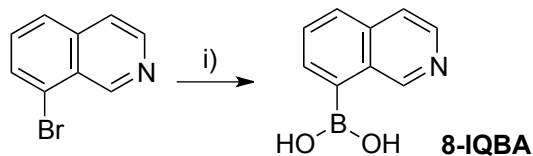


Figure 2.1. Structures of isoquinolinyboronic acids, 8-QBA and 6-MDDCQ

Results and Discussion

8-Isoquinolinyboronic acid (8-IQBA) was synthesized through a one-step borylation reaction (Scheme 2.1) and all other isoquinolinyboronic acids were commercially available.



Scheme 2.1. Reagents and condition: i). *n*-butyllithium, trimethyl borate, THF, -78 °C, 39%.

Since a long-standing goal in our lab is the search for boronic acids that change fluorescent properties upon binding, we examined whether these isoquinolinyboronic acids (IQBAs) would have such properties. Three representative sugars were used for this study: D-fructose, D-glucose, and D-sorbitol. It was found that all IQBAs changed fluorescent properties upon sugar addition, though the direction and magnitude of the changes were different for the various boronic acids. For example, 8-IQBA showed a maximum of 35-fold increase in fluorescent intensity upon fructose addition at physiological pH in phosphate buffer (Figure 2.2 and Table 2.1). On the other hand, addition of sorbitol only induced a 1-fold fluorescent intensity increase and glucose addition induced a 60% decrease in fluorescent intensity. The opposite directions of fluorescent intensity changes when fructose and glucose were added were something that had not been observed before, indicating the idiosyncratic nature 8-IQBA in its fluorescent response to binding. Interestingly, 5-IQBA showed similar properties in fluorescent responses upon sugar binding (Figure 2.3): fluorescent intensity increased with fructose or sorbitol addition and decreased with glucose addition. On the other hand, 4-IQBA only showed fluorescent intensity increases upon sugar additions (Figure 2.4); while 6-IQBA only showed fluorescent intensity decreases (Figure 2.5). The observed fluorescent changes upon sugar binding also allowed for the easy determination of the apparent binding constants of these boronic acids. Table 2.1 summarizes the results. The apparent association constants (K_a) with D-fructose, D-glucose, and D-sorbitol were 1493, 46, and 1588 M^{-1} for 8-IQBA; 1432, 42, and 2934 M^{-1} for 5-IQBA; 2170, 25, and 1001 M^{-1} for 4-IQBA; and

1353, 28, and 1620 M^{-1} for 6-IQBA; respectively. It needs to be note the K_a was determined due to the central hypothesis that the stoichiometry of the bindings of IQBAs with sugars are due to 1:1 binding, which is a well developed method in our previous binding studies.[12] In this case, the linear correlation of $I_0/\Delta I$ with the reciprocal of concentration confirmed the stoichiometry 1:1 binding in the tested conditions (see appendix for a specific example of the binding equation development). Several things are worth mentioning regarding these binding results. The first thing that stands out among all these binding constants is the extraordinarily high affinity of these isoquinolinylboronic acids for the monosaccharides studied. For example, the binding constants with fructose for all isoquinolinylboronic acids studied were in the range of 1353-2170 M^{-1} . In contrast, the binding constant between 8-quinolinylboronic acid and fructose was 108 M^{-1} . [126] The difference is over 13-fold. Second, it is also interesting to note that these isoquinolinylboronic acids showed much higher affinity for glucose than phenylboronic acid. For example, the apparent binding constants of 8-IQBA and 5-IQBA with glucose were 46 and 42 M^{-1} , respectively. In contrast, the binding constant between phenylboronic acid and glucose was about 5 M^{-1} . Third, the apparent association constants trend with 4-IQBA followed the order of D-fructose > D-sorbitol > D-glucose. This is different from that for other arylboronic acids,[65, 127, 128] which has the order of D-sorbitol > D-fructose > D-glucose. Even in the case of 8-IQBA, its binding constants with sorbitol and fructose were essentially the same, which was unexpected. Fourth, the binding constants are not directly correlated with the intensity of fluorescent changes. This is also different from most of the fluorescent boronic acids that we have reported, which show higher magnitude changes for tight binders.

Table 2.1. Apparent association constants (K_a) of isoquinolinylboronic acids with representative sugars^a

Isoquinolinyl	D-Fructose	D-Glucose	D-Sorbitol

boronic acids ^[a]	K_a (M^{-1})	$\Delta I_{\max}/I_0$	K_a (M^{-1})	$\Delta I_{\max}/I_0$	K_a (M^{-1})	$\Delta I_{\max}/I_0$
8-IQBA	1493 ± 25	35	46 ± 12	-60%	1588 ± 266	1
5-IQBA	1432 ± 242	9	42 ± 6	-60%	2934 ± 61	1
4-IQBA	2170 ± 184	16	25 ± 7	2	1001 ± 10	2
6-IQBA	1353 ± 274	-60%	28 ± 4	-82%	1620 ± 247	-80%
8-QBA	$108^{[b]}$	$47^{[b]}$	3 ± 2	11	616 ± 150	13

[a] Binding studies were conducted in phosphate buffer (0.1 M) at pH 7.4 (All the experiments were duplicated). [b] reference number[126]

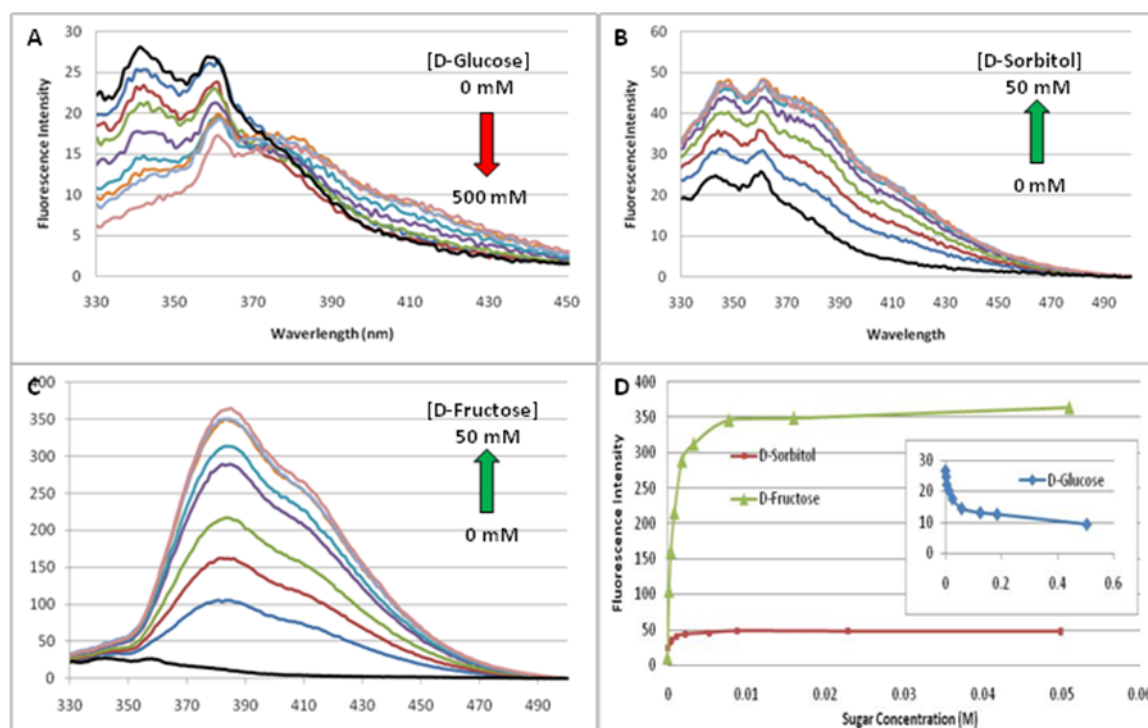


Figure 2.2. Fluorescent spectral changes of 8-IQBA upon addition of different diols in phosphate buffer (0.1 M) at pH 7.4: $\lambda_{\text{ex}} = 322$ nm, $\lambda_{\text{em}} = 361$ nm (for D-glucose and D-sorbitol); 383 nm (for D-fructose).

(A) D-Glucose; (B) D-Sorbitol; (C) D-Fructose; (D) plots of fluorescent intensity changes of 8-IQBA as a function of sugar concentration, $[8\text{-IQBA}] = 1 \times 10^{-5} \text{ M}$.

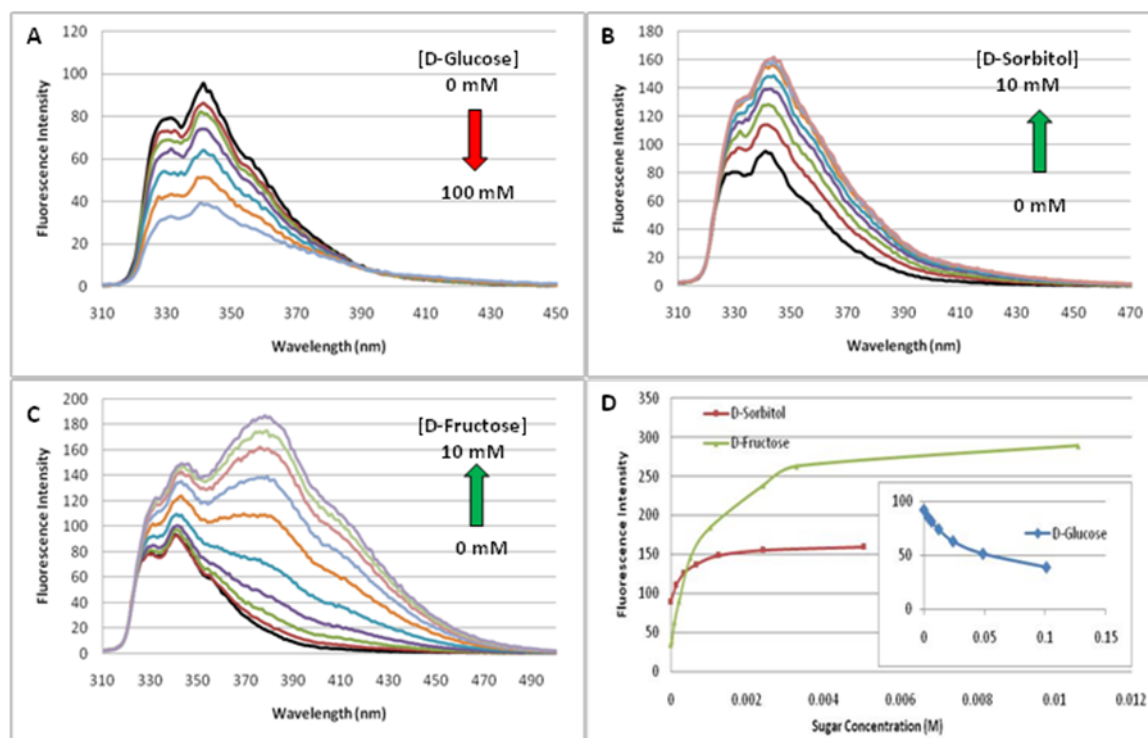


Figure 2.3. Fluorescent spectral changes of 5-IQBA upon addition of different diols in phosphate buffer (0.1 M) at pH 7.4: $\lambda_{\text{ex}} = 272 \text{ nm}$, $\lambda_{\text{em}} = 342 \text{ nm}$ (for D-glucose); 344 nm (for D-sorbitol); 378 nm (for D-fructose). (A) D-Glucose; (B) D-Sorbitol; (C) D-Fructose; (D) plots of fluorescent intensity changes of 5-IQBA as a function of sugar concentration, $[5\text{-IQBA}] = 1 \times 10^{-5} \text{ M}$.

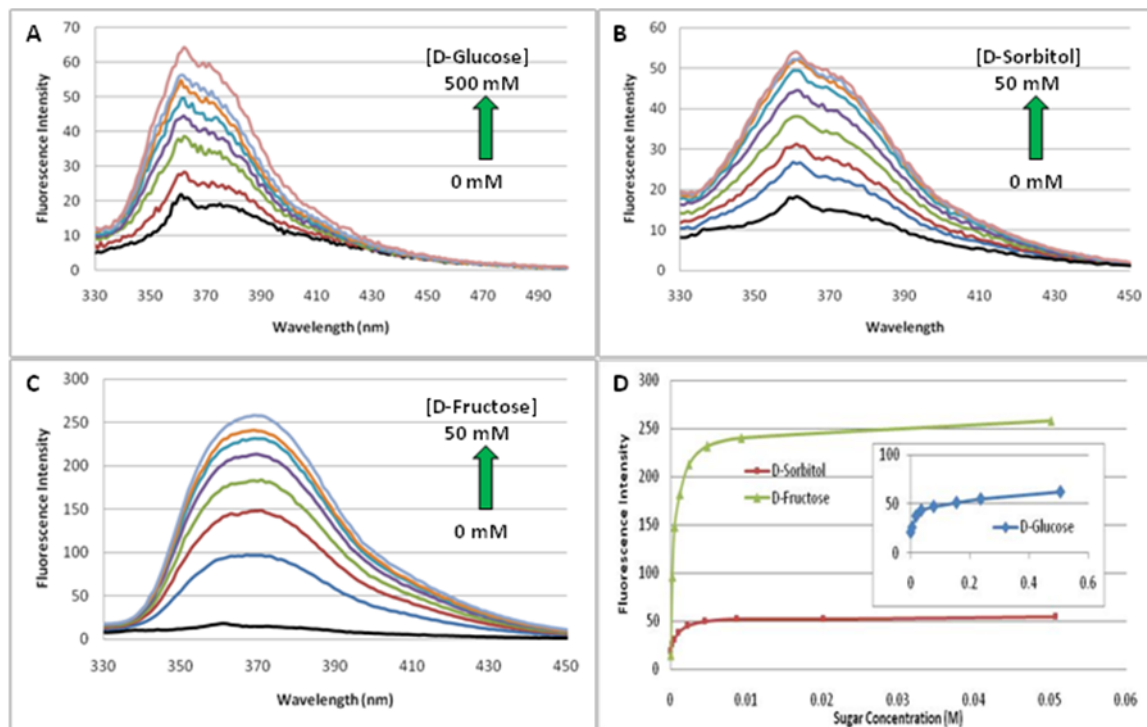


Figure 2.4. Fluorescent spectral changes of 4-IQBA upon addition of different diols in phosphate buffer (0.1 M) at pH 7.4: $\lambda_{ex} = 322$ nm, $\lambda_{em} = 361$ nm (for D-glucose, D-sorbitol,); 370 nm (for D-fructose). (A) D-Glucose; (B) D-Sorbitol; (C) D-Fructose; (D) plots of fluorescent intensity changes of 4-IQBA as a function of sugar concentration, $[4\text{-IQBA}] = 1 \times 10^{-5}$ M.

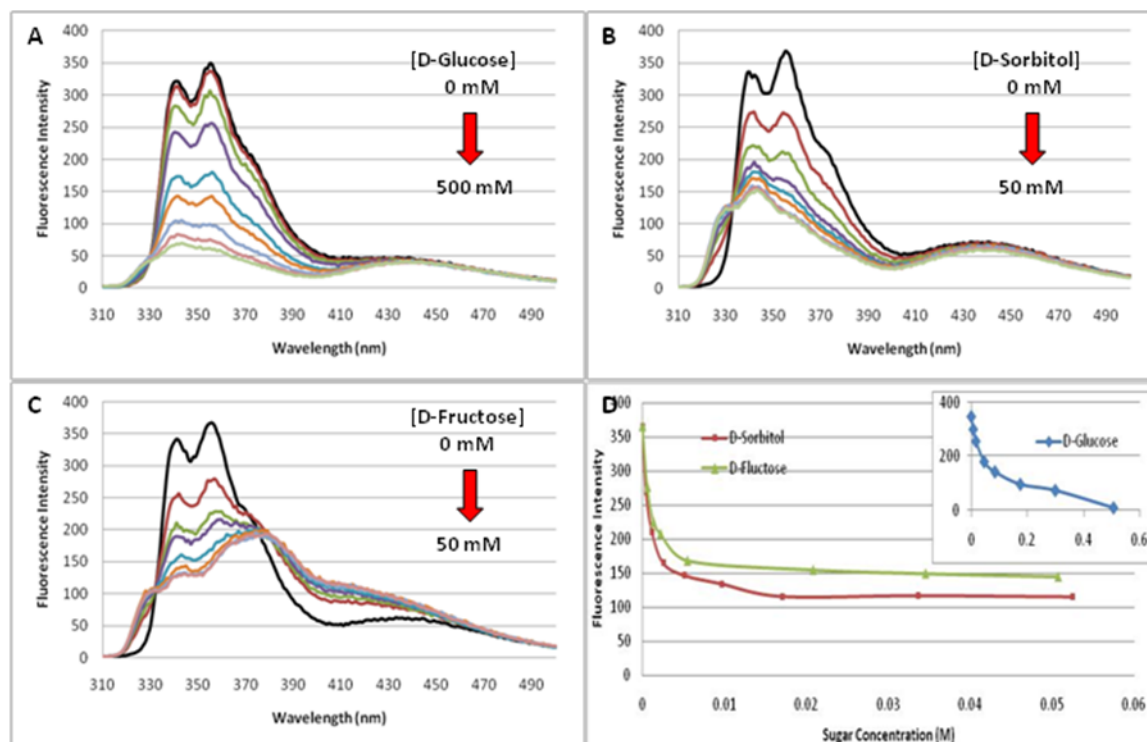


Figure 2.5. Fluorescent spectral changes of 6-IQBA upon addition of different diols in phosphate buffer (0.1 M) at pH 7.4: $\lambda_{\text{ex}} = 272$ nm, $\lambda_{\text{em}} = 356$ nm (A) D-Glucose; (B) D-Sorbitol; (C) D-Fructose; (D) plots of fluorescent intensity changes of 6-IQBA as a function of sugar concentration, $[6\text{-IQBA}] = 1 \times 10^{-5}$ M.

Encouraged by the high affinity of these IQBAs, especially with glucose, we were interested in probing the ability for them to bind with the pyranose form of a sugar. This interest stems from the fact that cell surface carbohydrates only contain sugars in the pyranose form and one of the important goals in our carbohydrate sensor effort is the design and synthesis of probes for cell surface carbohydrate biomarkers. However, the “general consensus” seems to be that arylboronic acids do not bind to vicinal diols on six-membered ring, and thus application of boronic acids in recognizing glycans in mammalian systems would be difficult. To address this fundamental question, we also tested the binding affinities of isoquinolinyboronic acids with methyl- α -D-glucopyranose and *cis*-cyclohexanediol. The selection of methyl- α -D-glucopyranose is to ensure that the sugar is in its cyclic form. However, the disadvantage is

that the 1-position hydroxyl group is no longer available for binding. *cis*-Cyclohexanediol was selected as a representative of *cis*-diols on a six-membered ring. The summary binding results are shown in Table 2.2, and Figures 2.6 and 2.7. Several special binding properties were observed. First, weak but encouraging binding with *cis*-cyclohexanediol was observed for 8-IQBA, 5-IQBA and 4-IQBA, with the apparent association constants (K_a) being 0.1 (6-fold fluorescence intensity change), 2.4 (7-fold fluorescence intensity change), and 1.5 M^{-1} (2-fold fluorescence intensity change), respectively. In control experiments, cyclohexanol did not show appreciable binding or fluorescent changes when added to the same boronic acid solutions. Second, these isoquinolinylboronic acids showed binding with a model glycoside, methyl- α -D-glucopyranose, under physiologically relevant conditions. The apparent binding constants (K_a) for 4-IQBA and 6-IQBA were 3 and 2 M^{-1} , respectively. It should be noted that the Hall lab has reported *ortho*-hydroxymethyl phenylboronic acid as binders for methyl- α -D-glucopyranose.[89, 90] However, they do not change fluorescence upon binding. To our best knowledge, these are the very first examples of boronic acid derivatives that can bind to methyl- α -D-glucopyranose with fluorescence changes.

Table 2.2. Apparent association constants (K_a) of isoquinolinylboronic acids with representative carbohydrates^[a]

Isoquinolinyl boronic acids ^[a]	Methyl- α -D-glucopyranose		Cis-cyclohexanediol		cyclohexanol	
	$K_a (\text{M}^{-1})$	$\Delta I_{\text{max}}/I_0$	$K_a (\text{M}^{-1})$	$\Delta I_{\text{max}}/I_0$	$K_a (\text{M}^{-1})$	$\Delta I_{\text{max}}/I_0$
8-IQBA	Not observed	×	0.4 ± 0.0	15	Not observed	×
5-IQBA	Not observed	×	1.1 ± 0.8	-66%	Not observed	×

4-IQBA	3.3 ± 0.9	1	0.8 ± 0.2	6	Not observed	×
6-IQBA	2.1 ± 1.4	-30%	1.0 ± 0.2	-71%	4 ± 1	3
8-QBA	Not observed	×	1.2 ± 0.7	23	Not observed	×
6-MDDCQ	Not observed	×	2.0 ± 0.2	-75%	Not observed	×

[a] Binding studies were conducted in phosphate buffer (0.1 M) at pH 7.4 (All the experiments were duplicated)

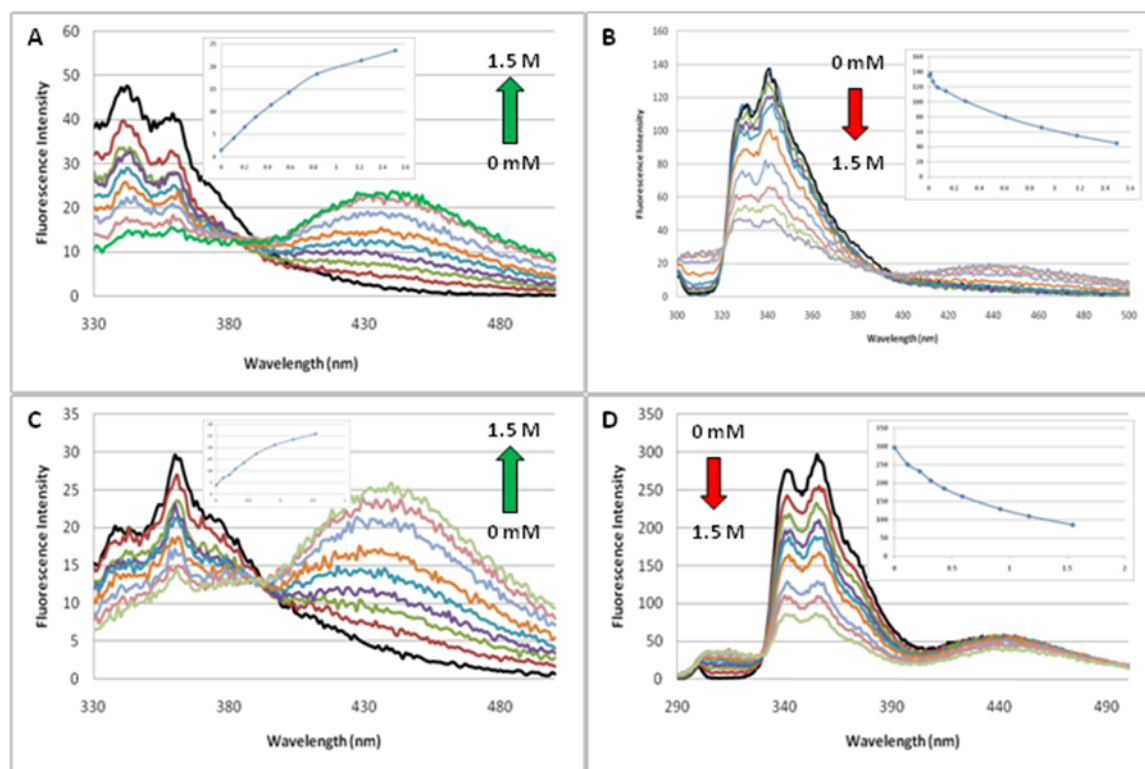


Figure 2.6. Fluorescent spectral changes of isoquinolinyboronic acids upon addition of *cis*-1,2-cyclohexanediol in phosphate buffer (0.1 M) at pH 7.4: (A) 8-IQBA, $\lambda_{\text{ex}} = 332 \text{ nm}$, $\lambda_{\text{em}} = 442 \text{ nm}$; (B) 5-IQBA, $\lambda_{\text{ex}} = 272 \text{ nm}$, $\lambda_{\text{em}} = 341 \text{ nm}$; (C) 4-IQBA, $\lambda_{\text{ex}} = 322 \text{ nm}$, $\lambda_{\text{em}} = 440 \text{ nm}$; (D) 6-IQBA, $\lambda_{\text{ex}} = 272 \text{ nm}$, $\lambda_{\text{em}} = 355 \text{ nm}$; Insets: plots of fluorescent intensity changes of IQBAs as a function of sugar concentration $[\text{IQBAs}] = 1 \times 10^{-5} \text{ M}$.

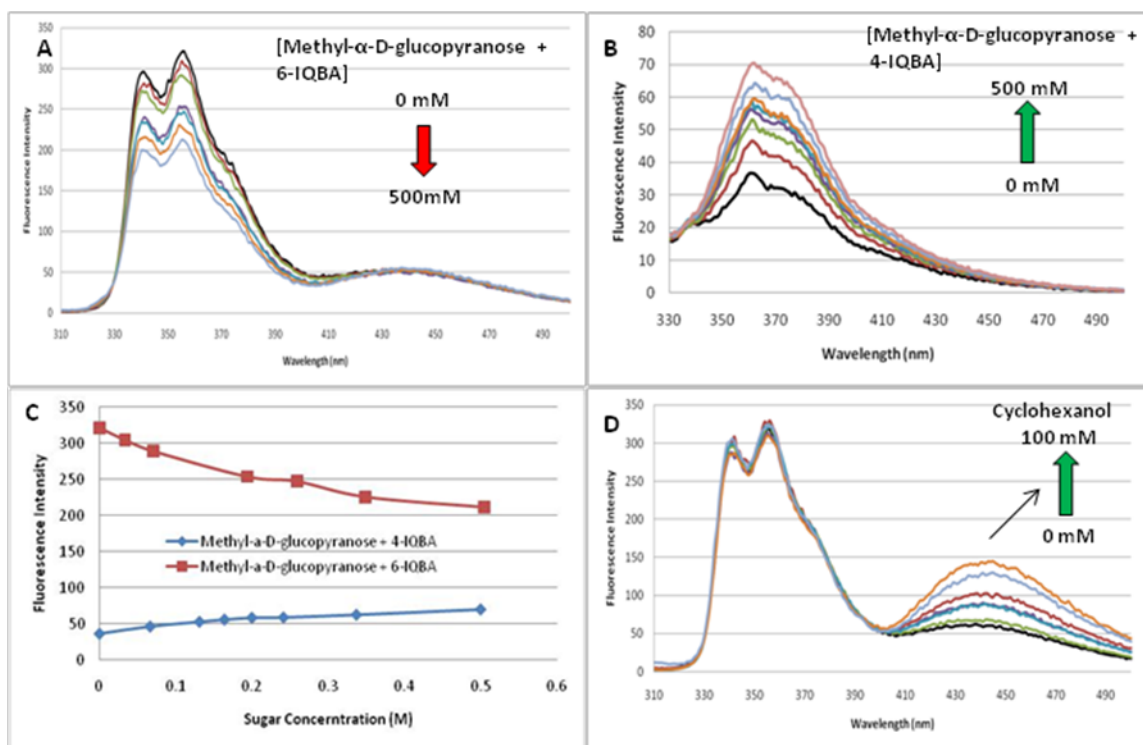


Figure 2.7. Fluorescent spectral changes of isoquinolinyboronic acids upon addition of methyl- α -D-glucopyranose and cyclohexanol in phosphate buffer (0.1 M) at pH 7.4: (A) 6-IQBA with methyl- α -D-glucopyranose, $\lambda_{\text{ex}} = 272$ nm, $\lambda_{\text{em}} = 356$ nm; (B) 4-IQBA with methyl- α -D-glucopyranose, $\lambda_{\text{ex}} = 322$ nm, $\lambda_{\text{em}} = 361$ nm; (C) plots of fluorescent intensity changes of 4-IQBA and 6-IQBA as a function of methyl- α -D-glucopyranose concentration, (D) 6-IQBA with cyclohexanol, $\lambda_{\text{ex}} = 272$ nm, $\lambda_{\text{em}} = 455$ nm; [IQBAs] = 1×10^{-5} M.

As a control, we also studied the binding of these isoquinolinyboronic acids with cyclohexanol in order to see whether their apparent binding was due to interactions with a single hydroxyl group (boronic acid interactions with single hydroxyl groups do have precedents).[58] As can be seen from Table 2.2, 6-IQBA was found to bind both *cis*-cyclohexanediol ($K_a = 1 \text{ M}^{-1}$) and cyclohexanol ($K_a = 4 \text{ M}^{-1}$) and the others did not show any binding with cyclohexanol. Such results indicate that single hydroxyl group binding might play an important role in the binding of 6-IQBA with methyl- α -D-glucopyranose and

cyclohexanediol. At this time, it is not clear as to exactly which way 6-IQBA binds to these six-membered ring diols.

With the weak but encouraging binding with *cis*-cyclohexanediol for all the isoquinolinyboronic acids discussed above, it becomes important to address the questions of whether the ability to bind *cis*-diols on a six-membered ring is unique to isoquinolinyboronic acids. As a control, phenylboronic acid should be considered first. Binding between phenylboronic acid with cyclohexanediol had been studied before and no binding was observed.[127] Such results indicate that the ability to bind to *cis*-diols on a six-membered ring is not universal to all boronic acids. Next we studied the binding of 8-QBA and 6-MDDCQ (Figure 2.1) with *cis*-cyclohexanediol. 8-QBA was selected since it is a quinolinyboronic acid. 6-MDDCQ was selected because the boronic acid was attached to phenyl ring but the compound also contains a quinoline moiety. Both boronic acids also showed binding with *cis*-cyclohexanediol (Figure 2.8). For 8-QBA, a 23-fold fluorescence change was found upon the addition of 1.5 M *cis*-cyclohexanediol at physiological pH in phosphate buffer. These results indicated that binding with *cis*-cyclohexanediol is not a unique binding affinity of isoquinolinyboronic acids.

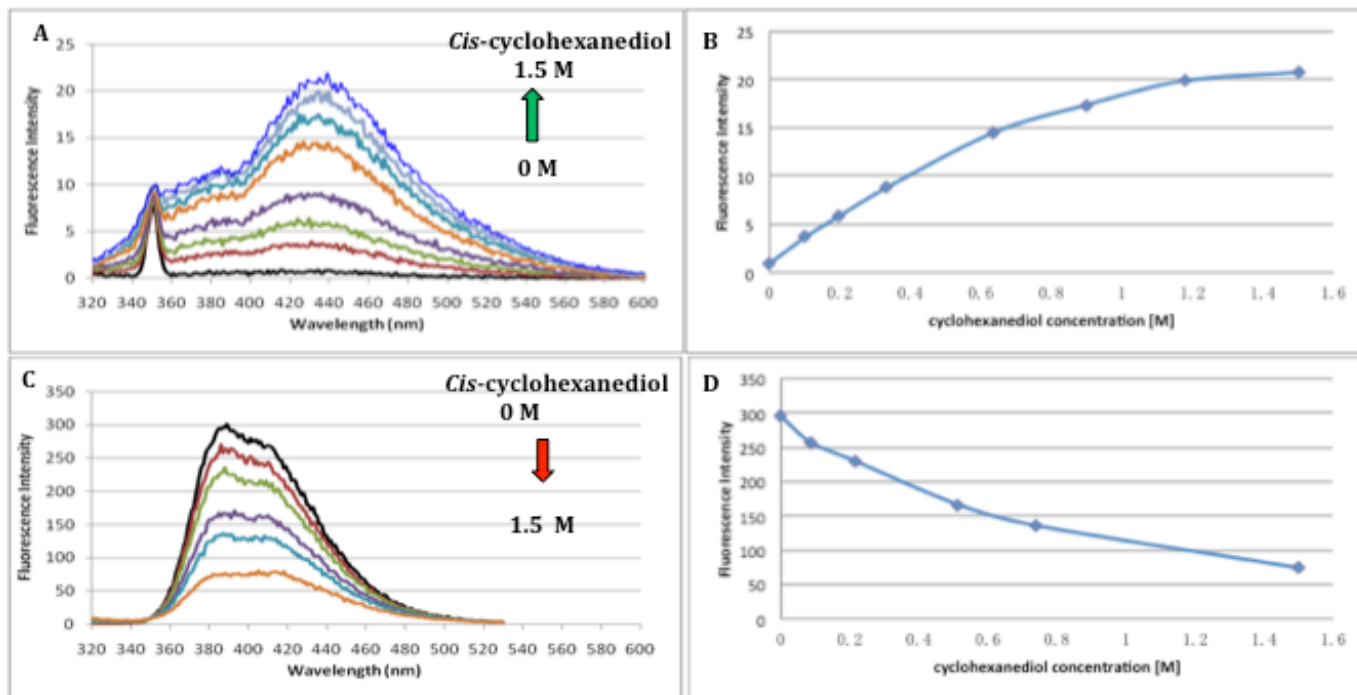


Figure 2.8. Fluorescent spectral changes of 8-QBA and 6-MDDCQ upon addition of *cis*-cyclohexanediol in phosphate buffer (0.1 M) at pH 7.4: (A) 8-QBA: $\lambda_{\text{ex}} = 270$ nm, $\lambda_{\text{em}} = 314$ nm, $[8\text{-QBA}] = 1 \times 10^{-5}$ M; (B) plot of fluorescent intensity change of 8-QBA as a function of sugar concentration, $[8\text{-QBA}] = 1 \times 10^{-5}$ M; (C) 6-MDDCQ: $\lambda_{\text{ex}} = 270$ nm, $\lambda_{\text{em}} = 387$ nm, $[6\text{-MDDCQ}] = 2 \times 10^{-5}$ M; (D) plot of fluorescent intensity change of 6-MDDCQ as a function of sugar concentration, $[6\text{-MDDCQ}] = 2 \times 10^{-5}$ M.

One cautionary note related to all the binding constants with six-membered diols is their small magnitude, which could severely affect the accuracy of determination. The other issue to consider is the change of solvent bulk properties due to diol addition at high concentrations, which could affect fluorescence. This aspect is especially important for 6-IQBA because it showed tighter “binding” with cyclohexanol than with *cis*-cyclohexanediol. To specifically differentiate the effect of bulk properties and binding on fluorescence and to probe whether the observed fluorescent changes were due to specific binding, we conducted additional experiments to study boronic acid-concentration (6-IQBA, 10-30 μM) dependent fluorescent changes in the presence and absence of 0.75 M *cis*-cyclohexanediol. From Figure

2.9, it can be seen clearly that the fluorescence intensity increases have a linear relationship with 6-IQBA concentrations in the absence of added *cis*-cyclohexanediol. On the other hand, significant curvature was observed in the presence of 0.75 M *cis*-cyclohexanediol. Such results cannot be explained by the bulk effect of the added sugar and are consistent with specific binding interactions, which are concentration dependent. Bulk effect of the added sugar on fluorescent properties should only result in two parallel lines with different intercepts.

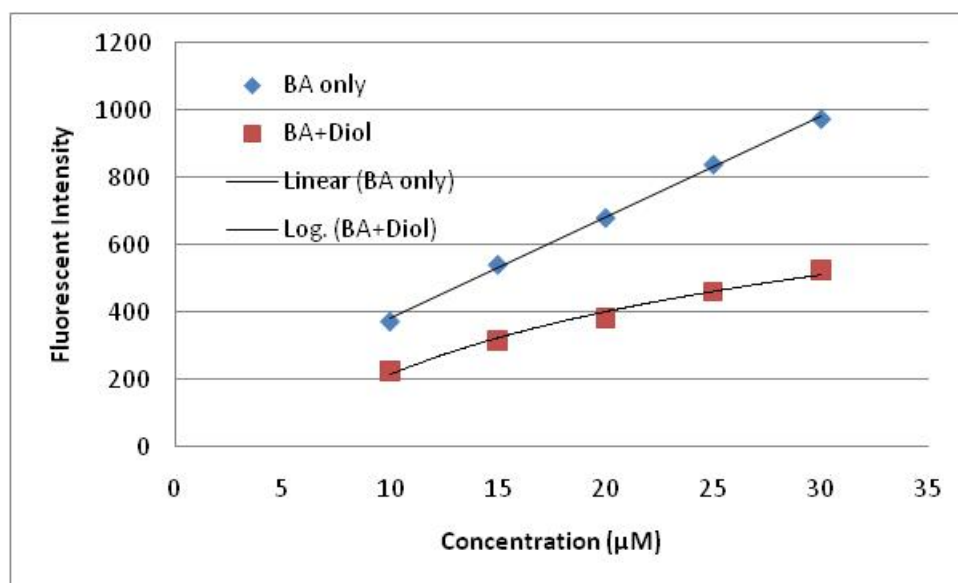


Figure 2.9. Fluorescent intensity change-6-IQBA concentration relationships in the presence and absence of 0.75 M *cis*-cyclohexanediol in phosphate buffer (0.1 M) at pH 7.4: $\lambda_{\text{ex}} = 272$ nm, $\lambda_{\text{em}} = 354$ nm. ■: 6-IQBA only; ◆ : 6-IQBA with 0.75 M *cis*-cyclohexanediol.

p*K*_a and quantum yields

Aimed at understanding the basic mechanism through which fluorescent intensity changes occur, we also studied the pH profiles of the fluorescence intensity in the absence and presence of sugars. Figure 2.10 and Table 2.3 summarized the results of apparent p*K*_a values of the isoquinolinyboronic acids in the

absence and presence of sugars. As can be seen in Figure 2.10, fluorescent intensities change with pH for both the boronic acids and their presumed esters with various sugars. Numerous previous reports have demonstrated that such fluorescent changes are associated with the pK_a of individual species. Since each boronic acid has two ionizable functional groups, the boronic acid group and the isoquinolinyl nitrogen, there is the question of which pK_a each fluorescent change corresponds to.

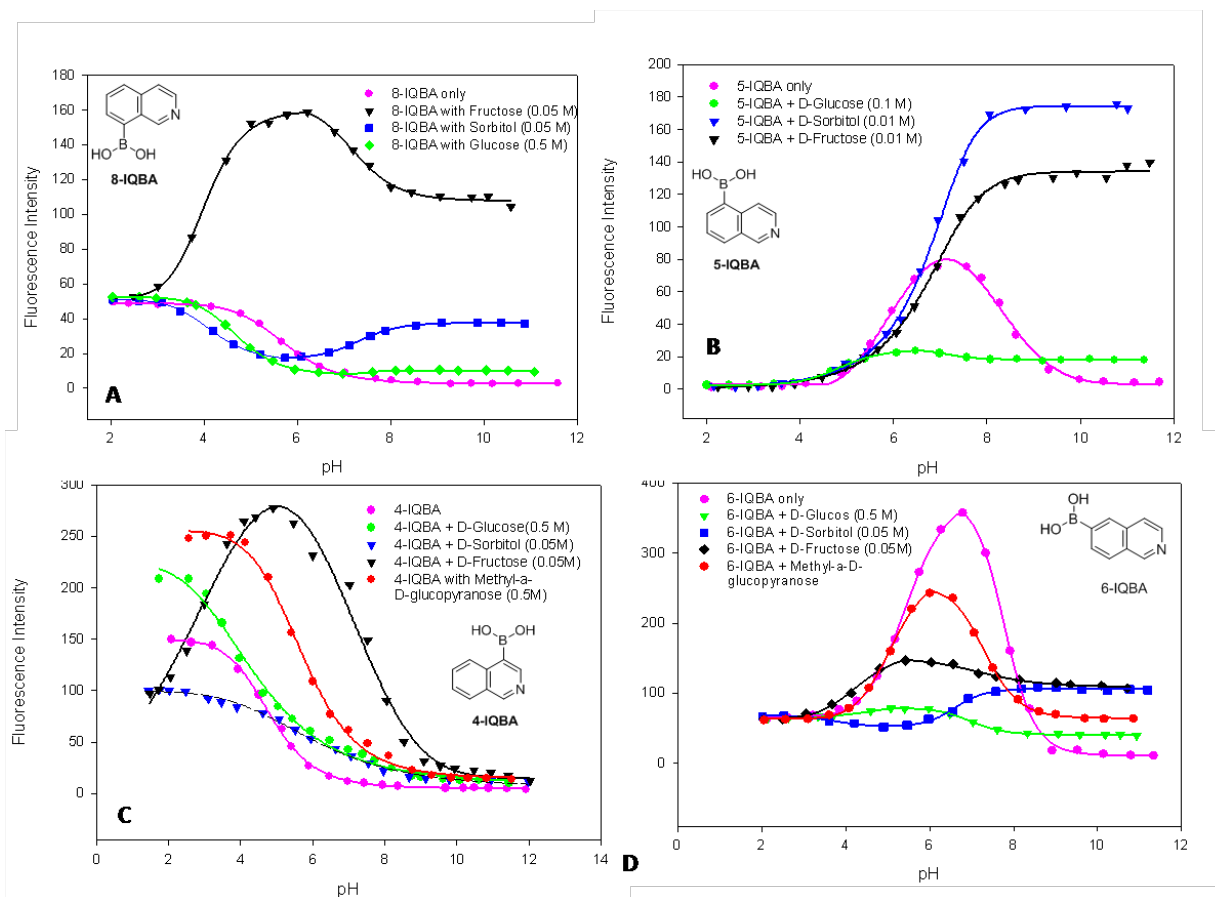


Figure 2.10. pH profiles of the fluorescence intensities of isoquinolinyl boronic acids in the absence and presence of sugars in 0.1 M aqueous phosphate buffer (A) [8-IQBA] 1×10^{-5} M; (B) [5-IQBA] 1×10^{-5} M; (C) [4-IQBA] 1×10^{-5} M; (D) [6-IQBA] 1×10^{-5} M.

Table 2.3. Apparent pK_a values of the isoquinolinylboronic acids in the absence and presence of sugars^[a]

pK_a	In the absence of a diol	In the presence of D-fructose	In the presence of D-glucose	In the presence of D-sorbitol	In the presence of methyl- α -D-glucopyranose
8-IQBA	5.7;	4.1; 7.2	4.8; 7.5	4.1; 7.3	×
5-IQBA	5.9; 8.5	6.9	4.9; 6.8	6.8	×
4-IQBA	5.0	3.4; 7.6	4.4	6.0	5.7
6-IQBA	5.4; 7.7	4.2; 6.8	4.8; 7.0	3.8; 6.6	5.1; 7.4
8-QBA	4 ^[b] ; 10 ^[b]	2.5 ^[b] ; 9 ^[b]	ND	ND	ND

[a] All the results were duplicated. [b][126]

As shown in Schemes 2.2 and 2.3, there are two possible routes for the ionization steps of IQBAs and their esters. For example, in route A, pK_{a1} was assigned to the deprotonation of isoquinolinium nitrogen and pK_{a2} was assigned to the hybridization state change of the boronic acid group. While in route B, pK_{a3} was assigned to the hybridization state change of the boronic acid group and pK_{a4} was assigned to the deprotonation of isoquinolinium nitrogen. In order to assign each pK_a , we recorded the ^{11}B NMR spectra of IQBAs and their esters in a mixed deuterated methanol-water (1:1) solvent at different pH. Since it has been reported that 50% methanol of water solution resulted in minimal changes of the solution pH, methanol was used to increase the boronic acid solubility. The results are shown in Table 2.4.

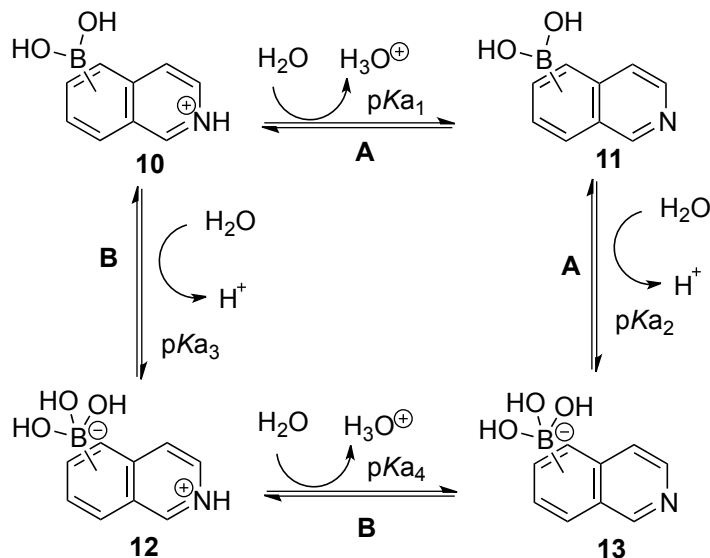
Table 2.4. ^{11}B NMR of isoquinolinyl boronic acids alone and in the presence of fructose

Entry	δ ppm/pH-1	δ ppm/pH-2	δ ppm/pH-2
8-IQBA ^[a]	28.9/1.3	29.5/7.3	3.2/11.9
8-IQBA and Fructose ^[b]	29.3/1.3	8.2/7.2	7.6/11.1
5-IQBA ^[a]	30.1&20.3/1.6	29.3&19.3/7.3	4.6/12.8
5-IQBA and Fructose ^[b]	29.7/2.1	7.3/7.6	10.2/11.7
4-IQBA ^[a]	28.1&19.1/1.5	24.6&19.2/5.7	3.5&2.3/12.2
4-IQBA and Fructose ^[b]	20.4/2.0	7.6&11.1/6.6	7.6/12.0
6-IQBA ^[a]	27.8&18.9/1.6	28.3&18.9/7.6	2.6/12.6
6-IQBA and Fructose ^[b]	28.8&18.8/1.5	20.7&9.0/5.7	8.0/12.1

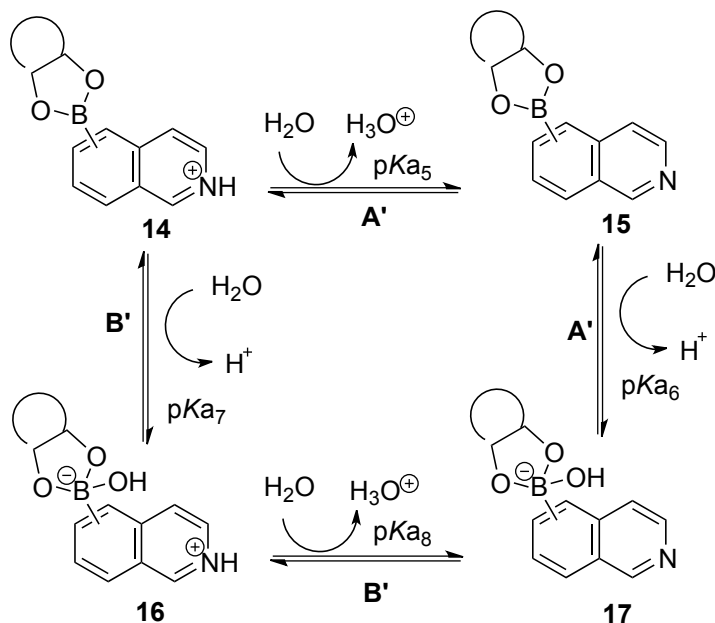
[a] [IQBAs] = 30 mM; [b] [fructose] = 50 mM

In the case of 8-IQBA, the boron signal of 8-IQBA appeared at 28.5 ppm at pH 1.3 and 29.5 at pH 7.3 respectively, consistent with the neutral trigonal boron (10 or 11). At pH 11.9, the boron signal of 3.2 ppm was observed indicating the presence of the anionic tetrahedral state (13). These results indicated that the boron atom of the free acid changed hybridization from sp^2 to sp^3 between pH 7.3 and 11.9. So 5.7 was assigned to pK_{a1} and pK_{a2} was assigned to be >7 , which was consistent with route A (Scheme 2.2). The esters of 8-IQBA all have two pK_a values based on the fluorescent data. The only difference is that the fluorescence of the fructose ester increases first, followed by a decrease. On the other hand the fluorescence of glucose ester and sorbitol ester only decreases slightly, followed by an increase. So it is

reasonable to assign the pK_a values for all the esters of 8-IQBA in the same way. ^{11}B NMR spectra of the fructose ester of 8-IQBA were studied as a model case. Single peaks of 29.3 ppm at pH 1.3 and 8.2 ppm at pH 7.2 were observed respectively. These chemical shifts clearly indicated that the boron atom in the ester form changes hybridization state between pH 1.3 and 7.2. Based on this, 4.1 was assigned to pK_{a7} and 7.2 was assigned to pK_{a8} , consistent with route B' (Scheme 2.3). Such results indicate that the pK_a of the boronic acid group is higher in the absence of a sugar, but lower in the presence of a sugar than that of the protonated quinolinium group. Such a pK_a -switch seems to correspond to the highest fluorescence intensity change at pH 6 (Figure 2.9A), and suggests that the zwitterionic specie 16 (Scheme 2.3) is the more fluorescent one. At pH 7.4, the 8-IQBA fructose ester exists predominantly in the boronate form 17 and 8-IQBA itself exists as a mixture of the neutral trigonal boron form 11 and the boronate form 13. Both 11 and 13 are almost non-fluorescent, and yet the boronate ester form 17 is fluorescent. It seems that the fluorescence increase is due to diol binding as that of 8-QBA.[126] All the pK_a values of other IQBAs in the absence and presence of a sugar were assigned by the same method. The results showed that they have similar pK_a assignments as those of 8-IQBA, going through route A with IQBA only and route B' in the presence of a sugar. It should be noted that these pK_a assignments are opposite to that of 8-QBA[126] and consistent with that of 5-QBA[129] described previous reports.



Scheme 2.2. Proposed ionization steps of IQBAs.



Scheme 2.3. The proposed ionization steps of esters of IQBAs.

In the case of 5-IQBA, at pH 7.4, 5-IQBA fructose ester exists predominantly in a mixture of zwitterionic quinolinium boronate form 16 and boronate form 17. 5-IQBA itself also exists in a mixture of neutral trigonal boron form 11 and boronate form 13. It should be pointed out that the boronate form

13 of 5-IQBA itself is non-fluorescent, while the boronate form 17 of 5-IQBA fructose ester is the most fluorescent species. In the case of 4-IQBA at pH 7.4, its fructose ester exists predominantly in the zwitterionic quinolinium boronate form 16 and 4-IQBA itself exists in a mixture of neutral trigonal boron form 11 and boronate form 13. Both 11 and 13 are non-fluorescent, and yet the zwitterionic quinolinium boronate form 16 is fluorescent. So it also seems that the fluorescence increase is due to diol binding as that of 8-QBA. Finally, at pH 7.4, 6-IQBA fructose ester exists predominantly in the boronate form 17, while 6-IQBA itself exists in the neutral trigonal boron form 11. Although both 11 and 17 are fluorescent, the neutral trigonal boron form 11 seems to have higher fluorescence intensity than 13. This might explain the fluorescence intensity decrease after binding with fructose. One thing needs to be mentioned here is that in some cases two peaks were found for IQBA or its ester. For example, the ^{11}B NMR spectra of 4-IQBA showed two peaks at 28 and 19 ppm. It is possible that the second peak might be the methyl ester of boronic acid. This is reasonable since a mixed deuterated methanol-water (1:1) solvent was used to increase the boronic acid solubility. Another possibility is the formation of a cyclic dimeric boronic anhydride -O-B-O-B-O- via a 2:1 boronic acid:diol binding mode. However, the likelihood of this cyclic structure is probably high only in organic solvent, but not in aqueous solution.

The fluorescent quantum yields for these boronic acids and their sugar esters were determined with 4-indolylboronic acid as the reference compound and [130] using Eq. 1, [131] where Q represents quantum yield, I is the integrated intensity, OD is the optical density, and subscript R denotes reference compound. The results are shown in Table 2.5.

$$Q = Q_R (I/I_R) (OD_R/OD) \quad (1)$$

The quantum yields trend of 8-IQBA and its esters followed the order of D-fructose ester > D-sorbitol ester > 8-IQBA alone > D-glucose ester. For example, the quantum yield of the D-fructose ester of 8-IQBA is 24%, while that of 8-IQBA alone and its D-glucose ester is only about 2%, giving about a 12-fold difference. In the case of other isoquinolinylboronic acids, the following orders were observed for the respective apparent quantum yield: D-fructose ester > D-sorbitol ester > D-glucose ester > 5-IQBA alone; D-fructose ester > methyl- α -D-glucopyranose ester > D-sorbitol ester > D-glucose ester > 4-IQBA alone, and 6-IQBA alone > D-fructose ester > D-sorbitol ester > D-glucose ester > methyl- α -D-glucopyranose. All the isoquinolinylboronic acids have different trends and are not directly correlated with the apparent pK_a of each compound. This is understandable since many other factors such as flexibility, solvation, and excited state electron density distribution are expected to affect the quantum yields of these compounds as well.

Table 2.5. Fluorescence quantum yields of the isoquinolinylboronic acids alone and in the presence of various sugars^[a]

FQY (%)	Isoquinolinyl boronic acids	D-Fructose (M)	D-Glucose (M)	D-Sorbitol (M)	Methyl- α -D-glucopyranose
8-IQBA	2.2 \pm 0.02	24 \pm 0.8	2.1 \pm 0.2	6.9 \pm 0.6	×
5-IQBA	2.5 \pm 0.02	19 \pm 0.01	3.7 \pm 0.4	7.7 \pm 2.0	×
4-IQBA	1.0 \pm 0.08	17 \pm 0.01	1.7 \pm 0.2	2.5 \pm 0.7	3.4 \pm 0.02
6-IQBA	13.2 \pm 3.2	12 \pm 0.3	4.8 \pm 0.9	10.1 \pm 0.7	1.9 \pm 0.2

8-QBA	ND	28 ^[b]	ND	ND	ND
-------	----	-------------------	----	----	----

[a] All the results were duplicated. [b][126]

Conclusions

In conclusion, we have described a series of water-soluble isoquinolinyboronic acids that change fluorescent properties significantly upon binding. These isoquinoliny boronic acids bind to three representative sugars, D-fructose, D-glucose, and D-sorbitol, much more tightly than 8-QBA and most other simple arylboronic acids. Besides, all the isoquinolinyboronic acids, especially 5-IQBA and 8-IQBA, showed modest binding affinity with D-glucose ($K_a = 42$ and 46 M^{-1} , respectively). These numbers are much higher than that observed with phenylboronic acid. All isoquinolinyboronic acids also showed weak but encourage binding affinity with *cis*-cyclohexanediol with significant fluorescence changes. These are the very first examples of the binding of boronic acids with a six-membered vicinal diol with fluorescence intensity change. Also very significant are the findings that 4-IQBA and 6-IQBA can complex methyl- α -D-glucopyranose ($K_a = 3$ and 2 M^{-1} , respectively) under physiologically relevant conditions. The above findings are especially important because carbohydrates found in glycoproteins, glycolipids, and lipopolysaccharides are almost universally six-membered ring sugars and linear diols, and one area that has not been widely recognized is the potential to take advantage of the interactions between hydroxyl groups on six-membered ring with a boronic acid for boronlectin design.

Synthesis of 8-isoquinolinyboronic acid (8-IQBA). To a flask charged with 8-bromoisoquinoline (20 mg, 0.096 mmol, 1 equiv) in a nitrogen atmosphere was added anhydrous THF (0.5 mL). The mixture was stirred at -78 °C. n-Butyl-lithium (2.0 M solution in pentane, 0.2 mL, 0.4 mmole, 4 equiv) was added, then the solution was stirred at -78 °C for 45 min. After adding trimethyl borate (0.05 mL, 0.45 mmol, 4.7 equiv), the reaction mixture was stirred at -78 °C for another 5 min. Then the reaction was allowed to room temperature and left to react for an additional hour. H₂O (0.5 mL) and saturated NaHCO₃ (1.0 mL) was added to quench the reaction. The mixture was extracted with ethyl acetate (2 × 30 mL), washed with H₂O (2 × 5 mL), brine (2 × 5 mL), and dried over anhydrous Na₂SO₄. The residue was purified by chromatography (MeOH/CH₂Cl₂ = 5/1) to yield a brown solid (6.5 mg, 39%). ¹H NMR (400 MHz, DMSO-d₆) δ9.7 (1H, s), 8.6 (2H, s), 8.5 (1H, d, *J* = 5.6 Hz), 8.0 (1H, d, *J* = 8.0 Hz), 7.9 (1H, d, *J* = 6.4 Hz), 7.8 (1H, d, *J* = 5.6 Hz), 7.7 (1H, dd, *J* = 6.4, 8.0 Hz); ¹³C NMR (100 Hz, DMSO-d₆) δ153.0, 142.2, 135.1, 133.7, 130.8, 129.6, 127.8, 120.8; ESI-MS, *m/z* 174, *M*+1; HRMS, 174.0735.

CHAPTER 3.

Design, Synthesis, and Polymerase-Catalyzed Incorporation of Click-Modified Boronic Acid-TTP

Analogues

Abstract: *This chapter is mainly based on one paper that has been published in Chemistry – An Asian Journal in 2011 from page 2747 to 2752. As discussed in the previous chapters, though the very active work in the design and synthesis of sensors for monosaccharides and oligosaccharides, efforts in recent years have moved to a more biological direction with applications in glycan analysis, recognition of cell-surface carbohydrates biomarkers and glycoproteins as well as array analysis. DNA molecules are known to be important materials in sensing, aptamer selection, nanocomputing, and construction of unique architects. The incorporation of modified nucleobases affords DNA unique properties for applications in areas that are otherwise difficult or not possible. Earlier, we have demonstrated that the boronic acid moiety can be introduced into DNA through polymerase-catalyzed reactions. In order to study whether such incorporation by polymerase is a general phenomenon, we designed and synthesized four boronic acid-modified TTP analogues. The synthesis of analogues 20 and 21 was through the use of a single dialkyne tether for both the Sonogashira coupling with thymidine and later Cu-mediated [3+2] cycloaddition for linking the boronic acid moiety. This approach is much more efficient than the previously described method, and paves the way for the preparation of a large number of boronic acid-modified TTPs with a diverse set of structural features. All analogues showed very good stability under PCR conditions and were recognized as a substrate by DNA polymerase, and thus incorporated into DNA.*

Introduction

The same properties that afford DNA the kind of unique features suitable as genomic materials also allow it to be used in a wide variety of applications such as nanosensing,[132] aptamer selection,[133-135] nanocomputing,[136] and reaction encoding.[137, 138] Along these lines, modifications of nucleobases often endow DNA with additional properties for enhanced applications. For example, 5-position modified thymidine analogues have been widely used in aptamer selections.[139, 140] On the other hand, it is also well-known that boronic acid is one of the most commonly used building blocks for the design of chemosensors for carbohydrates, due to its intrinsic affinity with diols, single hydroxy groups, as well as other nucleophiles/Lewis bases.[6, 12, 46, 58, 141, 142] One of our long-standing interests is developing an aptamer selection platform specifically for biological important carbohydrates and glycoproteins through the incorporation of a boronic acid group into DNA.[58, 143, 144]

This is based on the central hypothesis that the incorporation of a boronic acid-modified nucleotide into DNA would allow for enhanced recognition of carbohydrate moieties, which contain many hydroxyl groups.[49] Along this line, we have previously reported the design and synthesis of a thymidine analogue (B-TTP, Figure 3.1) modified with 8-quinolinyboronic acid at the 5-position, which can be introduced into DNA through polymerase-catalyzed reactions, as well as the feasibility of boronic acid-modified DNA aptamer selection for biological important glycoproteins.[49, 143] In addition, there are boronic acids that change fluorescent properties upon binding.[58] Incorporation of such boronic acids allows DNA to be used in sensing applications without the need for an additional reporting unit. As a specific example, we have also demonstrated the synthesis and incorporation of a long wavelength boronic acid-modified TTP (NB-TTP, Figure 3.1), which shows fluorescence intensity change upon carbohydrate addition.[144] In order to examine the generality of boronic acid incorporation and to

broaden the application of boronic acid-modified DNA, we are interested in studying the incorporation of additional boronic acids with different structural features. At the same time, we are also interested in developing a synthetic approach, which is more efficient than the previous described method and would allow for easy analogue synthesis. The resulting increase in structural diversity of boronic acid-modified thymidine analogues will be very important in future applications such as aptamer selection for biologically important carbohydrate biomarkers as well as glycoproteins.

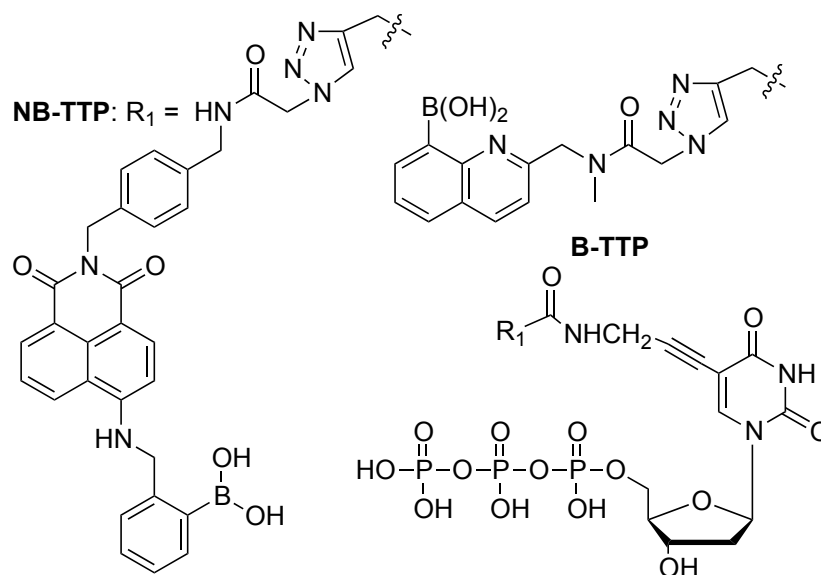


Figure 3.1. Chemical structures of B-TTP and NB-TTP.

Results and Discussion

In our initial design, we were interested in the introduction of *ortho*- and *meta*-substituted phenylboronic acid, which are much easier to synthesize than the previously used boronic acids (B-TTP and NB-TTP, Figure 3.1). In applications, where the fluorescent properties are not important, these phenylboronic acid-modified thymidine would be very useful and easy to prepare. Figure 3.2 shows the new analogues design. In the preparation of these new analogues, we initially followed the general

procedures developed for the synthesis of B-TTP (Figure 3.1). Thus M-TTP (Scheme 3.1) was synthesized following a four-step procedure starting from 5-iodo-2'-deoxyuridine (22, Scheme 3.1) as published previously.[143] Substituted azidomethylphenylboronic acid (23 or 24, Scheme 3.1) were easily obtained from their bromomethylphenylboronic acid precursors (25 or 26, Scheme 3.1), respectively. Then coupling of the appropriately substituted azidomethylphenylboronic acid (23 or 24) via a copper (I)-catalyzed azide-alkyne cycloaddition (CuAAC)[145-147] 18 and 19 in 31% yield after HPLC purification.

The key design in linking the boronic acid moiety to the 5-position of thymidine is the availability of a terminal alkyne group after the initial coupling. In order to shorten the synthesis, we designed an approach by using a single dialkyne tether for both the Sonogashira coupling with thymidine and later CuAAC for linking the boronic acid moiety. Such a design shortens the synthesis by two steps and simplifies the structural features of the side chain. Specifically, M(C)-TTP (Scheme 3.1) was prepared through Sonogashira coupling of 5-iodo-2'-deoxyuridine (22, Scheme 3.1) with 1,7-octadiyne, and the subsequent triphosphorylation using a modified procedure.[148, 149] Then CuAAC led to the final products, 20 and 21, in 29% and 14% yield, respectively after HPLC purification.

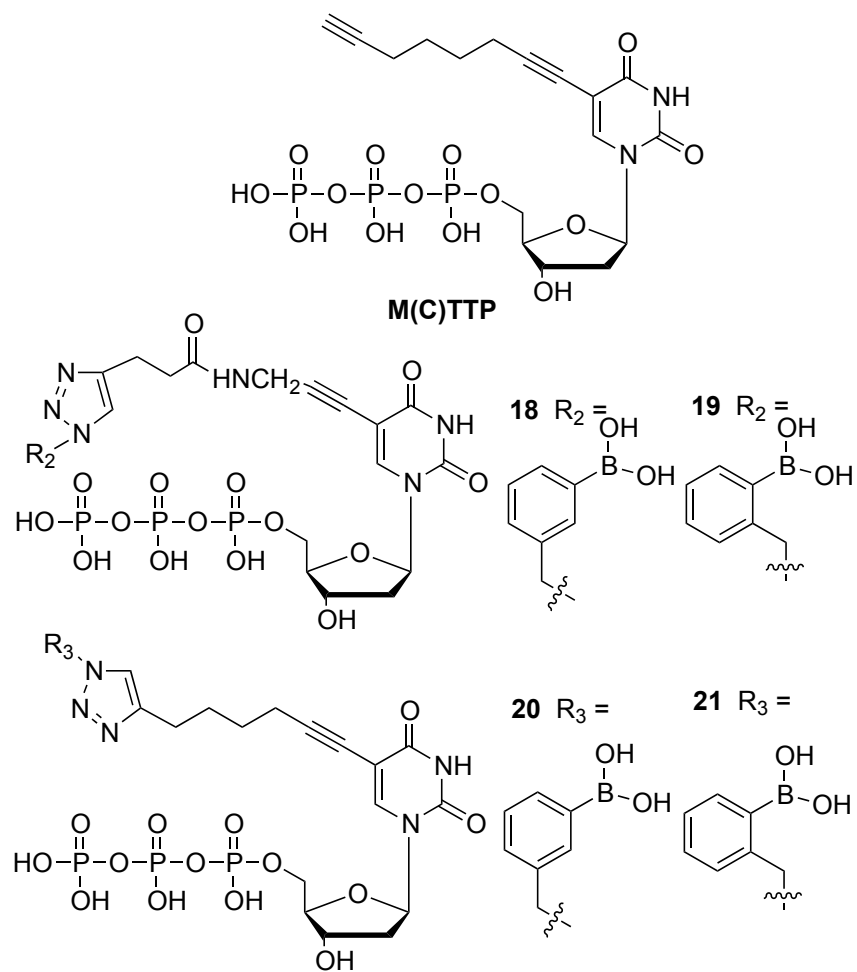
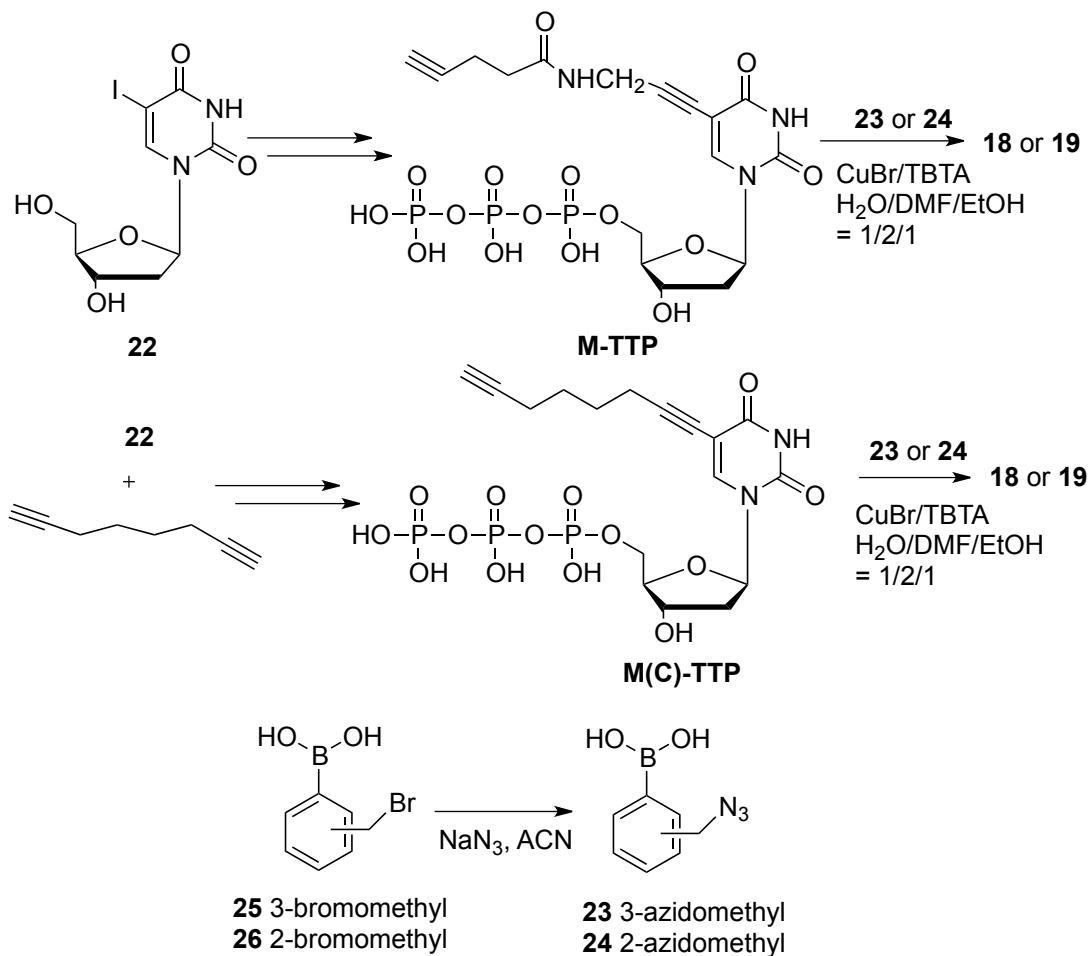


Figure 3.2. Structures of B-TTP analogues 18-21.



Scheme 3.1. Synthesis of B-TTP analogues 18 to 21.

Stability test of B-TTP analogues under PCR conditions

After obtaining the B-TTP analogues, we first studied whether these analogues were stable under PCR conditions needed for polymerase-mediated incorporation. HPLC was used to monitor the stability of these synthesized B-TTP analogues 18-21 (Figure 3.2). The results showed that all B-TTP analogues are very stable under PCR conditions including three rounds of thermal cycling at 94 °C for 2 min, then 94 °C for 1 min, 46 °C for 1 min, and 72 °C for 1 min and denaturing treatment (95 °C for 7 min). The HPLC chromatograms of B-TTP analogues 18-21 are shown in Figure S3.1-S3.4 (supporting information). No noticeable degradation was observed.

Incorporation of B-TTP analogues by Klenow fragment-catalyzed primer extension

Next, we studied whether these B-TTP analogues 18-21 could be incorporated into DNA in an enzyme-catalyzed reaction as we have done previously with B-TTP (Figure 3.1). Specifically, primer extension using 18-21 and the Klenow fragment was conducted using a short sequence of 21-nt oligonucleotide (5' -GGTTCCACCAGCAACCCGCTA-3') as the template and a 14-nt primer (5'-TAGCGGGTTGCTGG-3') as shown in Figure 3.3. The primer and template were designed in such a way that the first incorporated base would be a T, so there are two possible scenarios in the extension, either fully extended product or no extension at all. The latter case could be due to either no incorporation of the modified nucleotide or the inability to extend of the sequence with the incorporation of this modified nucleotide. The obtained DNA products were studied using PAGE. The primer was radio-labeled with ^{32}P at the 5'-end using $\gamma\text{-}^{32}\text{P}\text{-ATP}$ and T4 kinase (lane 1, Figure 3.3). Negative control without the Klenow fragment (lane 2, Figure 3.3) and without dNTPs (lane 3, Figure 3.3) showed no full length DNA sequence. The shorter DNA in Lane 3 without dNTPs could have resulted from the 3'-5' exonuclease activity of Klenow fragment.[144] The positive control with Klenow fragment and natural dNTPs showed full length DNA sequence (lane 4, Figure 3.3). Primer extension using B-TTP analogues 18-21 (lane 5-8, Figure 3.3) also gave a full length DNA sequence, which clearly indicated that these synthesized B-TTP analogues 18-21 were recognized as a substrate by the polymerase, and incorporated into DNA.

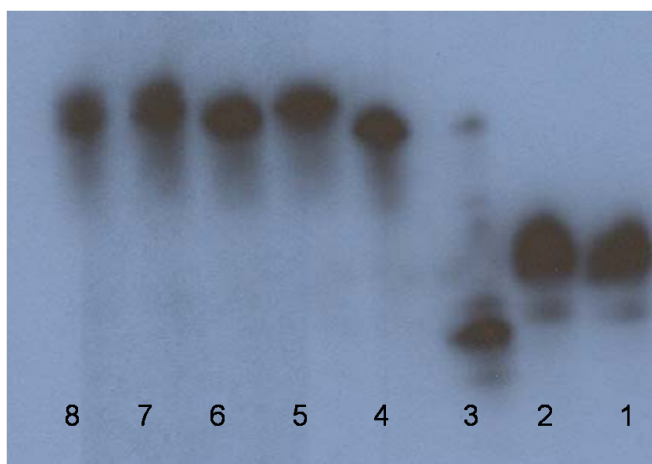


Figure 3.3. Incorporation of B-TTP analogues by Klenow Fragment: 1) Primer only; 2) Primer + dNTPs, no Klenow fragment; 3) Primer + Klenow fragment, no dNTPs; 4) Primer + Klenow fragment + dNTPs; 5) using B-TTP analogue 18 instead of dTTP in 4); 6) using B-TTP analogue 19 instead of dTTP in 4); 7) using B-TTP analogue 20 instead of dTTP in 4); 8) using B-TTP analogue 21 instead of dTTP in 4).

To further confirm the results, besides PAGE analysis, we also conducted MALDI analyses of the primer extension product. B-TTP analogue 18 was chosen as an example. From the MALDI spectra (Figure S3.5-S3.6, supporting information), the following results were obtained. In the control reaction, full extension of the primer using natural dNTPs yielded a DNA with m/z of 6519 (calculated $[M + H]^+$: 6519) as the extended strand peak in MALDI. On the other hand, when B-TTP analogue 18 was used instead of TTP, primer extension yielded a DNA with m/z of 6772 and m/z of 6787 as new peaks for the corresponding extended strand. Each was assigned as the deborylated (calc. $[M + H - HBO_2]^+$: 6771) and oxidative deborylated sequence (calc. $[M + H - HBO]^+$: 6787). Such behavior in MALDI is common in our past experience with boronic acid compounds.[143, 144] Results obtained further confirmed the full incorporation of the boronic acid-modified TTP analogues.

PCR Investigation

Encouraged by the successful incorporation of B-TTP analogues 18-21 into a short sequence by Klenow fragment-mediated primer extension, we further investigated the PCR amplification of a longer DNA with 90 bases template that we used previously.[143] As can be seen from Figure 3.4, all four analogues were successfully incorporated. Specifically, very similar bands were found with the PCR products of B-TTP analogues 18-21 (Lanes 3-6, respectively, group A) compared to those products using dTTP (Lane 1, group A) and M-TTP (Lane 7, group A). The slightly reduced mobility of DNA with boronic acid incorporation can be explained by the interaction of the boronic acid functional group (a

Lewis acid) with PAGE gel. This can be further confirmed by the results of Group C, which represents the gel results of the PCR products after treating with H_2O_2 (final concentration of 10 mM, 2 h). All PCR products of B-TTP analogues 18-21 after treating with H_2O_2 (Lane 2, 4, 6, and 8, respectively, group C) showed almost the same mobility. However, before treatment, different mobility was observed for PCR products of B-TTP analogues 18-21 (Lane 1, 3, 5, 7, respectively, Group C). As an example, PCR products obtained through incorporation of B-TTP analogue 20 shows the biggest difference in mobility (Lane 5: before H_2O_2 treatment, and Lane 6: after H_2O_2 treatment, Group C). The most significant evidence of the full incorporation of all the B-TTP analogues came from the denaturing PAGE gel results (15% denaturing PAGE containing 8M urea). A very clear single band was observed for all the PCR products of B-TTP analogues 18-21 (Lanes 3-6, Group B), compared to that of dTTP (Lane 1, group B). Besides, as shown in the image quant for the bands in Group B (see appendix for details), BTTP analogues showed the relative band intensity of 73%, 82%, 84%, 76%, and 79% for B-TTP analogues 2-5, and MTTP, respectively. This also clearly indicated the high incorporation efficiency.

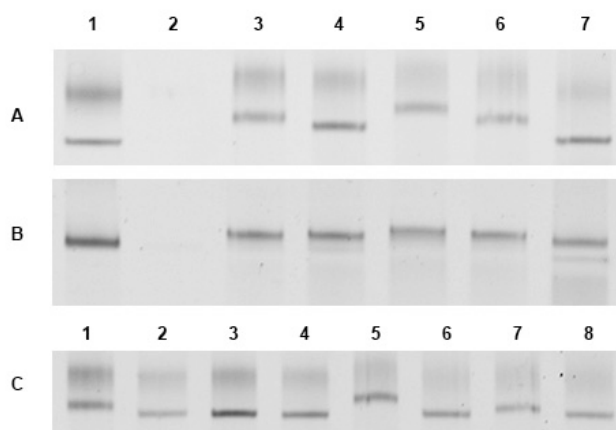


Figure 3.4. Left: Group A (analyzed with 15% PAGE) and B (15% denaturing PAGE): PCR incorporation using dTTP (Lane 1), B-TTP analogues 18-21 (Lanes 3-6, respectively), or M-TTP (Lane 7). Lane 2 is negative control with no dTTP. Group C: (analyzed with 15% PAGE): PCR incorporation

using B-TTP analogues 18-21 (Lane 1, 3, 5, 7, respectively), DNA being treated with H₂O₂ before analyzing (Lane 2, 4, 6, and 8 for B-TTP analogues 18-21, respectively). All reactions were conducted using *Taq* polymerase (See Supporting information for full gel pictures).

Conclusions

Four boronic acid-modified TTP analogues have been successfully synthesized. Two of them were synthesized using an improved procedure, which uses 1,7-octadiyne as a linker for both the Sonogashira coupling with thymidine and CuAAC tethering of the boronic acid moiety. All four boronic acid-modified TTP analogues were characterized thorough ¹H NMR, ³¹P NMR, and MS. The purities were confirmed by HPLC. Moreover, these analogues were successfully incorporated into DNA, suggesting that linker differences and the structural features of the boronic acid part do not have much bearing on polymerase-mediated incorporation. The newly developed synthetic method also paves the way for the preparation of a large number of boronic acid-modified TTP with a diverse set of structural features for future applications such as aptamer selection.

Experimental Section

General. Chemicals were obtained from Aldrich and Acros, unless indicated otherwise. For all reactions, analytical grade solvents were used. Anhydrous solvents were used for all moisture-sensitive reactions. NMR data were collected on a Bruker 400 MHz spectrophotometer. The chemical shifts are relative to TMS as an internal standard for ¹H NMR, and 85% H₃PO₄ as an external reference for ³¹P NMR. Mass spectra were recorded on a Waters Micromass LC-Q-TOF micro spectrometer or an ABI4800 MALDI-TOF-TOF mass spectrometer at Georgia State University Mass Spectrometry Facilities. HPLC condition for the purification of B-TTP analogues 2-5 were as follows: column: Agilent,

semi-preparation column; flow rate: 2.0 mL/min; solvents: A: 0.1 M NH_4HCO_3 , B: MeOH; program: 0.02-15 min 25% (B%), 35-45 min, 100%, 55-65 min 25%, stop; temperature: 20 °C, detection wavelength: 280 nm.

Synthesis of M (C)-TTP. The synthesis of M(C)-TTP was following Carell's procedure with revision:[148, 149] M(C)-T[148, 149] (300 mg, 0.9 mmol, 1 eq) and proton sponge (232 mg, 1.08 mmole, 1.2 eq) were dried in vacuo over P_2O_5 overnight and then dissolved in anhydrous trimethylphosphate (2.5 mL) under nitrogen in an ice-bath. Then fresh distilled POCl_3 (0.10 mL, 1.2 eq) dissolved in anhydrous trimethylphosphate (0.5 mL) was added drop wise via a syringe with stirring. The reaction mixture was further stirred in an ice-bath for 2 h and then a solution of bis-tri-*n*-butylammonium pyrophosphate (2.5 g, 5.27 mmole, 3.5 eq) and tri-*n*-butylamine (2.14 mL) in 3.0 mL of anhydrous DMF was added in one portion. The mixture was stirred at room temperature for 10 min and then triethylammonium bicarbonate solution (0.1 M, pH 8, 70 mL) was added. The reaction mixture was stirred at room temperature for an additional hour and concentrated, then purified with a DEAE-Sephadex A-25 column using a linear gradient of ammonium bicarbonate (0-0.6 M) collected portions eluted out by 0.12M-0.15M according the UV absorbance at 290 nM followed by freeze drying to give the final product as a white powder (93 mg, 18 %). ^1H NMR (D_2O): δ = 8.00 (s, 1H), 6.27 (t, J = 6.8 Hz, 1H), 4.60 (s, 1H), 4.22 (d, J = 4.8 Hz, 3H), 2.46 (t, J = 6.8 Hz, 2 H), 2.41 (m, 2H), 2.36 (t, J = 2.8 Hz, 1H), 2.27 (m, 2H), 1.68 ppm (m, 2H); ^{31}P NMR (161 MHz, D_2O): δ = -6.1, -11.1, -21.7 ppm; MS (-ESI) m/z : 571 ($[\text{M} - \text{H}]^-$).

Synthesis of B-TTP analogue 18. To a solution of M-TTP (5.0 mg, 0.0083 mmol, 1.0 eq) and 3-(azidomethyl)-phenyl-boronic acid (8.0 mg, 0.045 mmol, 5.4 eq) in 120 μL of a mixed solvent ($\text{H}_2\text{O}/\text{DMF}/\text{EtOH}$ = 1/2/1) was added 50 μL of a solution of TBTA (2.8 mg, 0.0052 mmole, 0.60 eq) and

CuBr (0.2 mg, 0.0026 mmole, 0.30 eq) in 100 μ L DMF. Then the mixture was stirred vigorously at room temperature for 3 h and centrifuged. Supernatant was removed, and the remaining was washed twice with 100 mM NH_4HCO_3 buffer (0.7 mL). The combined washings and supernatant was purified by HPLC to give a white powder after lyophilization (1.9 mg, 31%). ^1H NMR (D_2O): δ = 7.68 (s, 1H), 7.66 (s, 1H), 7.00 (t, J = 8.4 Hz, 1H), 6.53 (d, J = 8.4 Hz, 1H), 6.34 (s, 1H), 6.05 (t, J = 6.8 Hz, 1H), 5.33 (s, 2H), 4.34 (m, 1H), 4.00 (m, 3H), 3.92 (s, 2H), 2.91 (t, J = 6.4 Hz, 2H), 2.45 (t, J = 6.4 Hz, 2H), 2.12 ppm (m, 2H); ^{31}P NMR (161 MHz, D_2O): δ = -5.9, -10.8, -19.2 ppm; MS (-ESI) m/z : 733 ($[\text{M} - \text{BOH} - \text{H}_2\text{O} - \text{H}]^-$).

Synthesis of B-TTP analogue 19. To a solution of M-TTP (5.0 mg, 0.0083 mmol, 1.0 equivalent) and 2-(azidomethyl)-phenyl-boronic acid (5.1 mg, 0.029 mmol, 3.4 eq) in 120 μ L of a mixed solvent ($\text{H}_2\text{O}/\text{DMF}/\text{EtOH} = 1/2/1$) was added 45 μ L of a solution of TBTA (2.8 mg, 0.0052 mmole, 0.62 eq) and CuBr (0.4 mg, 0.0028 mmole, 0.34 eq) in 90 μ L DMF. Then the mixture was stirred vigorously at room temperature for 3 h and centrifuged. Supernatant was removed, and the remaining was washed twice with 100 mM NH_4HCO_3 buffer (0.7 mL). The combined washings and supernatant was purified by HPLC to give a white powder after lyophilization (2.0 mg, 31%). ^1H NMR (D_2O): δ = 7.69 (s, 1H), 7.65 (s, 1H), 7.01 (m, 1H), 6.57 (m, 1H), 6.37 (m, 2H), 6.04 (t, J = 6.8 Hz, 1H), 5.61 (s, 2H), 4.35 (m, 1H), 4.04 (m, 3H), 3.92 (s, 2H), 2.92 (t, J = 6.4 Hz, 2H), 2.46 (t, J = 6.4 Hz, 2H), 2.11 ppm (m, 2H); ^{31}P NMR (161 MHz, D_2O): δ = -5.1, -10.0, -18.5 ppm; MS (-ESI) m/z : 669 ($[\text{M} - \text{BOH} - \text{PO}_3\text{H} - \text{H}]^-$).

Synthesis of B-TTP analogue 20. To a solution of M(C)-TTP (5.0 mg, 0.0087 mmol, 1.0 eq) and 3-(azidomethyl)-phenyl-boronic acid (8.0 mg, 0.045 mmol, 5.2 eq) in 120 μ L of a mixed solvent ($\text{H}_2\text{O}/\text{DMF}/\text{EtOH} = 1/2/1$) was added 50 μ L of a solution of TBTA (2.8 mg, 0.0052 mmol, 0.60 eq) and CuBr (0.4 mg, 0.0026 mmol, 0.30 eq) in 100 μ L DMF. The mixture was stirred vigorously at room temperature for 3 h and centrifuged. Supernatant was removed, and the remaining was washed twice with

100 mM NH_4HCO_3 buffer (0.7 mL). The combined washings and supernatant was purified by HPLC to give a white powder after lyophilization (1.9 mg, 29%) was obtained. ^1H NMR (D_2O): $\delta = 7.86$ (s, 2H), 7.63 (d, $J = 7.2$ Hz, 1H), 7.55 (s, 1H), 7.36 (t, $J = 7.2$ Hz, 1H), 7.24 (d, $J = 7.6$ Hz, 1H), 6.25 (t, 1H), 5.59 (s, 1H), 4.58 (m, 2H), 4.22 (m, 3H), 2.76 (t, $J = 6.8$ Hz, 2H), 2.41 (m, 4H), 1.79 (t, $J = 6.4$ Hz, 2H), 1.57 ppm (t, $J = 6.4$ Hz, 2H); ^{31}P NMR (161 MHz, D_2O): $\delta = -5.4, -10.3, -18.7$ ppm; MS (-ESI) m/z : 355.6 ($[\text{M} - 2\text{H}_2\text{O} - 2\text{H}]^{2-}$).

Synthesis of B-TTP analogue 21. To a solution of M(C)-TTP (5.0 mg, 0.0087 mmole, 1.0 eq) and 2-(azidomethyl)-phenyl-boronic acid (8.0 mg, 0.045 mmol, 5.2 eq) in 120 μL of a mixed solvent ($\text{H}_2\text{O}/\text{DMF}/\text{EtOH} = 1/2/1$) was added 50 μL of a solution of TBTA (2.8 mg, 0.0052 mmole, 0.60 eq) and CuBr (0.4 mg, 0.0026 mmole, 0.30 eq) in 100 μL DMF. The mixture was stirred vigorously at room temperature for 3 h and centrifuged. Supernatant was removed, and then the remaining was washed twice with 100 mM NH_4HCO_3 buffer (0.7 mL). The combined washings and supernatant was purified by HPLC to give a white powder after lyophilization (0.9 mg, 14%). ^1H NMR (D_2O): $\delta = 7.70$ (s, 1H), 7.60 (s, 1H), 7.41 (d, $J = 6.4$ Hz, 1H), 7.24 (m, 1H), 7.09 (d, $J = 6.4$ Hz, 1H), 6.74 (m, 1H), 6.07 (t, $J = 6.4$ Hz, 1H), 5.53 (s, 2H), 4.41 (m, 1H), 4.04 (m, 3H), 2.56 (t, $J = 6.8$ Hz, 2H), 2.20 (m, 4H), 1.59 (t, $J = 7.6$ Hz, 2H), 1.37 ppm (t, $J = 7.6$ Hz, 2H); ^{31}P NMR (161 MHz, D_2O): $\delta = -5.1, -10.0, -18.5$ ppm; MS (-ESI) m/z : 355.6 ($[\text{M} - 2\text{H}_2\text{O} - 2\text{H}]^{2-}$).

PAGE analysis of Klenow fragment-catalyzed primer extension: The mixture of 14-nt primer DNA (50 μM), T4 polynucleotide kinase (0.5 units/ μL , Biolabs, Inc.) and γ - ^{32}P -ATP (0.6 μL , from Perkin-Elmer Corp.) in 12 μL T4 kinase buffer solution was incubated at 37 $^\circ\text{C}$ for 1 h. The harvested ^{32}P -labeled DNA was then purified using Microcon YM-3 centrifugal filter (Millipore Corp.) to remove low molecular weight molecules. Using a similar primer extension protocol as previously described, the

³²P-labeled primer alone, reaction mixture without enzyme, reaction mixture without dNTPs, reaction mixture with both enzyme and natural dNTPs, and reaction mixture with B-TTP analogues 18-21 together with the other 3 dNTPs as well as enzyme were incubated at 37 °C for 1 h. After reaction, the mixtures were quenched with 2× DNA loading dye. 3µL of samples from each reaction was taken and run on 15% PAGE at 300V for 3 h. After being isolated, fixed and dried, the gel was developed using autoradiography (overnight) to obtain the film.

Primer extension using the Klenow fragment for MALDI-TOF-MS studies: 10 µL of 21-nt template (100 µM), 15 µL of 14-nt primer (100 µM), 1 µL of Klenow (5 units/µL), 4µL of dNTPs (0.2 mM each), 5 µL of 10 × NEB buffer 2, 15 µL of deionized water in total volume of 50 µL of solution was prepared for the control experiment; 10 µL of 21-nt template (100 µM), 15 µL of 14-nt primer (100 µM), 1 µL of Klenow (5 units/µL), 4 µL of B-TTP analogue 18 (2.5 mM), 4 µL of three other dNTPs (0.2 mM each), 5 µL of 10 × NEB buffer 2, and 11 µL of de-ionized water in total volume of 50 µL of solution was prepared for the reaction by using B-TTP analogue 18. The prepared solutions were then incubated at 37 °C for 1 h. After further purification using Microcon YM-3 centrifugal filter (Millipore Corp.) to remove dNTPs and other low molecular weight molecules, the harvested DNA was directly sent for MALDI analysis.

PCR incorporation using B-TTP analogues: PCR was performed on an Eppendorf Mastercycler thermal cycler with ethidium bromide fluorescent imaging. *Taq*. DNA polymerase was purchased from New England Biolabs. Reaction buffer was used as provided by the vendor. 50 µL reaction mixture contains template (90-mer single-strand DNA pool 5'-CCTTCGTTGTCTGCCTTCGT-50N-ACCCTTCAGAATTCGCACCA-3', with a final concentration 10 nM, where 50N stands for 50 randomized positions), primer 1 (100 µM, 5'-TGGTGCGAATTCTGAAGGGT-3'), primer 2 (1 µM, 5'-

CCTTCGTTGTCTGCCTTCGT-3'), dATP, dCTP, dGTP, dTTP or one of the B-TTP analogues or M-TTP (each with a final concentration of 200 mM), 1 × reaction buffer, and *Taq.* polymerase (0.5 U). Reaction thermocycling is composed of initial denaturation (95 °C 2 min), 30 cycles of 95 °C 20 s, 48 °C 20 s and 72 °C 30 s, and final extension (72 °C 10 min) then hold at 4 °C. Reaction product was purified by washing with H₂O in a Millipore Amicon Ultra 10 kDa spin column. The product was then analyzed with 15% PAGE by loading with 1 × gel-loading dye (2.5% Ficoll 400, 11 mM EDTA, 3.3 mM Tris-HCl, 0.017% SDS, 0.015% bromophenol blue at pH 8.0). Denaturing gel analysis was performed by denaturing the purified PCR product at 95 °C for 2 min, followed by addition of 1 × loading dye with 8 M urea at 70 °C and kept for 2 min. The sample was then loaded onto 15% denaturing PAGE containing 8 M urea. One portion of purified PCR product was treated with H₂O₂ (final concentration 10 mM) at rt. for 2 h before loading onto 15% PAGE.

CHAPTER 4.

Synthesis and Evaluation of New Antagonists of Bacterial Quorum Sensing in *Vibrio harveyi*

Abstract: This chapter is mainly based on one paper that has been published in *ChemMedChem* in 2009 from page 1457 to 1468 with Mrs. Hangjing Peng from the same group as a co-first author. Specifically, I initiated this project through design and synthesis of 12 analogues. Dr. Nanting Ni from the same group performed the biological assays of these 12 compounds. Ms. Peng and I contributed to further analogues design based on the preliminary results. Ms. Peng completed the synthesis of further designed analogues, and the biological assays with the help from Dr. Ni. Dr. Mingyong Li from the same group conducted the computational study. Bacterial quorum sensing has received much attention in recent years because of its relevance to pathological events such as biofilm formation. Based on the structures of two lead inhibitors (IC_{50} : 35-55 mM) against AI-2 mediated quorum sensing identified through virtual screening, we have synthesized 39 analogs and examined their inhibitory activities. Twelve of the new analogs showed equal or better inhibitory activities compared with the lead inhibitors. The best compound showed an IC_{50} of about 6 mM in a whole cell assay using *Vibrio harveyi* as the model organism. The structure-activity relationship is also discussed in this chapter.

Introduction

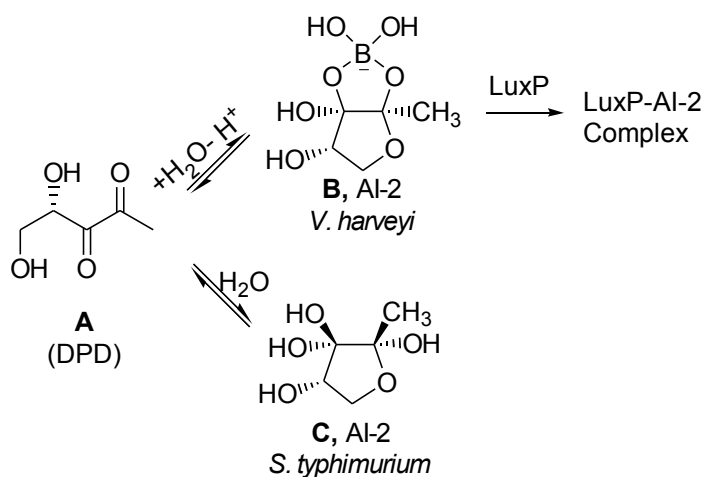
It is known that bacteria can coordinate community wide activities upon environmental stimulation, behave like multi-cellular organisms in some sense, and thus adapt themselves to the changing environmental conditions by taking advantage of an intercellular communication process known as quorum sensing. Quorum sensing can modulate gene expression and consequently control the behavior of bacterial processes such as bioluminescence, biofilm formation, virulence factor

expression,[150] conjugation, sporulation, and swarming mobility.[151] Quorum sensing is regulated by the production and detection of small signaling molecules called autoinducers (AIs).[86, 152] Several major types of small molecules are used as autoinducers in bacteria quorum sensing. For instance, acyl homoserine lactones (AHLs) are mostly used by Gram-negative bacteria[153] and autoinducing peptides (AIPs) are used in Gram-positive bacteria.[154] Autoinducer-2 (AI-2) seems to mediate quorum sensing in a remarkably wide range of bacteria including Gram-negative and Gram-positive bacteria.[155] As a result, it was proposed that AI-2 could serve as an “universal signal”, which affects interspecies communications among bacteria.[155] The causative agent of the disease cholera, human pathogen *Vibrio cholerae*, also possesses the AI-2 mediated quorum sensing pathway.[156, 157] Related research has indicated that quorum sensing can control virulence factor expression and biofilm formation in *V. cholerae*. [156, 158]

Because quorum sensing is involved in the regulation of pathologically relevant events, it is conceivable that inhibitors of quorum sensing could have therapeutic applications. Furthermore, quorum sensing inhibitors are important research tools in mechanistic studies. Recent years have seen an increasing interest in quorum sensing inhibitor/antagonist and agonist development.[152, 159-178] Our lab has also discovered several classes of inhibitors against AI-2 mediated quorum sensing.[151, 179, 180] In this chapter, we describe our effort in developing and optimizing quorum sensing inhibitors against the AI-2 pathway using *Vibrio harveyi* as a model organism.

AI-2 constitutes a group of compounds that can be inter-converted to each other upon hydration and binding with boric acid. Scheme 4.1 shows three examples of the AI-2 family of compounds. The key precursor, DPD (A), is synthesized by LuxS from *S*-ribosylhomocysteine.[181] Among the different forms of AI-2, compound B is the active species in regulating quorum sensing in *V. harveyi* through

binding to its receptor, LuxP.[181, 182] The crystal structure of the AI-2-receptor (LuxP) complex in *V. harveyi* has been solved.[181] Using this crystal structure and through virtual screening, we identified two hit inhibitors of AI-2 quorum sensing with IC₅₀ values in the range of 35-55 mM (Figure 1).[86] In order to further improve potency and achieve an initial understanding of the structure-activity relationship, we have designed and synthesized 39 analogs of these two hit compounds. Several potent quorum sensing inhibitors with IC₅₀ values in the single digit micromolar range have been found.



Scheme 4.1. Different forms of AI-2

Results and Discussion

Again, the optimization work is based on two inhibitors (KM-03009 and SPB-02229, Figure 4.1) identified previously through virtual screening.[86] Though these were not especially potent inhibitors, they represented the first AI-2 inhibitors at that time and the structural scaffold was novel and small, which allows for easy modification. In the crystal structure of *V. harveyi* LuxP-AI-2 complex, the positively charged side chains of Arg 215 and Arg 310 were known to interact with three of the four

borate oxygen atoms and thus stabilize the anionic tetrahedral boron. The two hydroxyl groups and the furanoyl oxygen are also involved in hydrogen bonding with Trp 82, Gln 77 and Asn 159.[183]

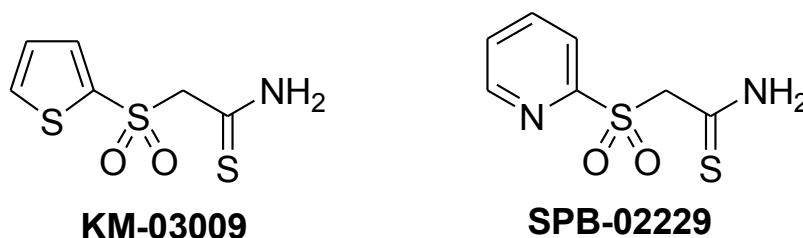


Figure 4.1. Hit compounds identified from virtual screening

Compounds KM-03009 and SPB-02229 seem to interact with LuxP by using the sulfone group at the position of the borate portion of the natural ligand.[183] Specifically, the two oxygen atoms of the sulfone group can interact with Arg 215 and Arg 310, mimicking the borate oxygen atoms.[86] The aryl ring is involved in some hydrophobic interactions. Based on these findings and comparison of these two lead compounds with the other inactive hit compounds, it seems that the sulfone group should be directly attached to an aryl group and the thioamide group should be separated from the sulfone group by one atom.[86] With the above information in hand, we were interested in modifying the structure of the two lead compounds by changing both ends (R^1 and R^2 , Figure 4.2), while retaining the middle skeleton of the structure. In addition, analogs were also prepared to examine the importance of the sulfone moiety (part B) and the thioamide/thioester structure (part C).

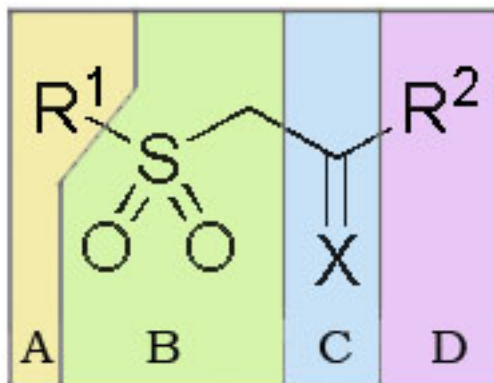
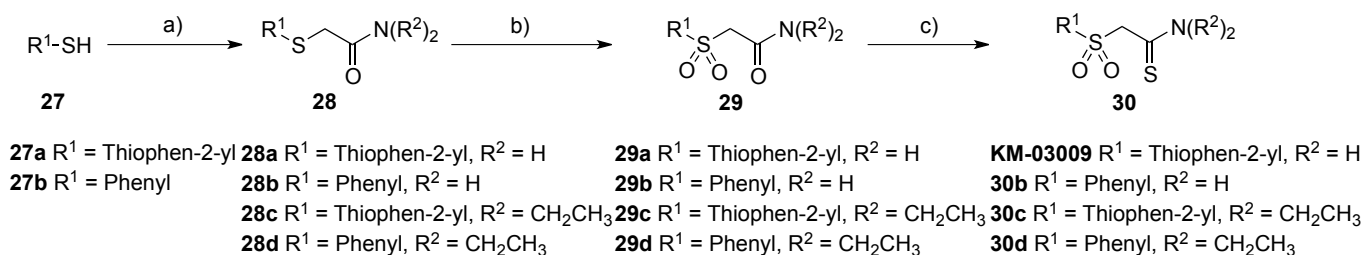


Figure 4.2. Optimization of the lead structure

For part A of the structure (Figure 4.2), the following aryl groups were used: thiophenyl, pyridinyl, phenyl, or substituted phenyl groups including phenyl groups bearing a simple substituent or extended by connecting to an additional aryl group. The impact of the polarity and the size of the substitution on the phenyl group were studied. The effects of substituents at different positions (*para*- or *meta*-) of the phenyl ring were also explored. For Part B of the structure, the effect of changing the sulfone to a sulfoxide group was examined. For part C, the influence of replacing the thiocarbonyl by a carbonyl group was explored. In optimizing part D, the terminal functional group of the structure, different classes of compounds were synthesized and compared, including amides, alkylamides, esters, acids, isoxazole and hydroxylamine (Schemes 4.2-4.6).

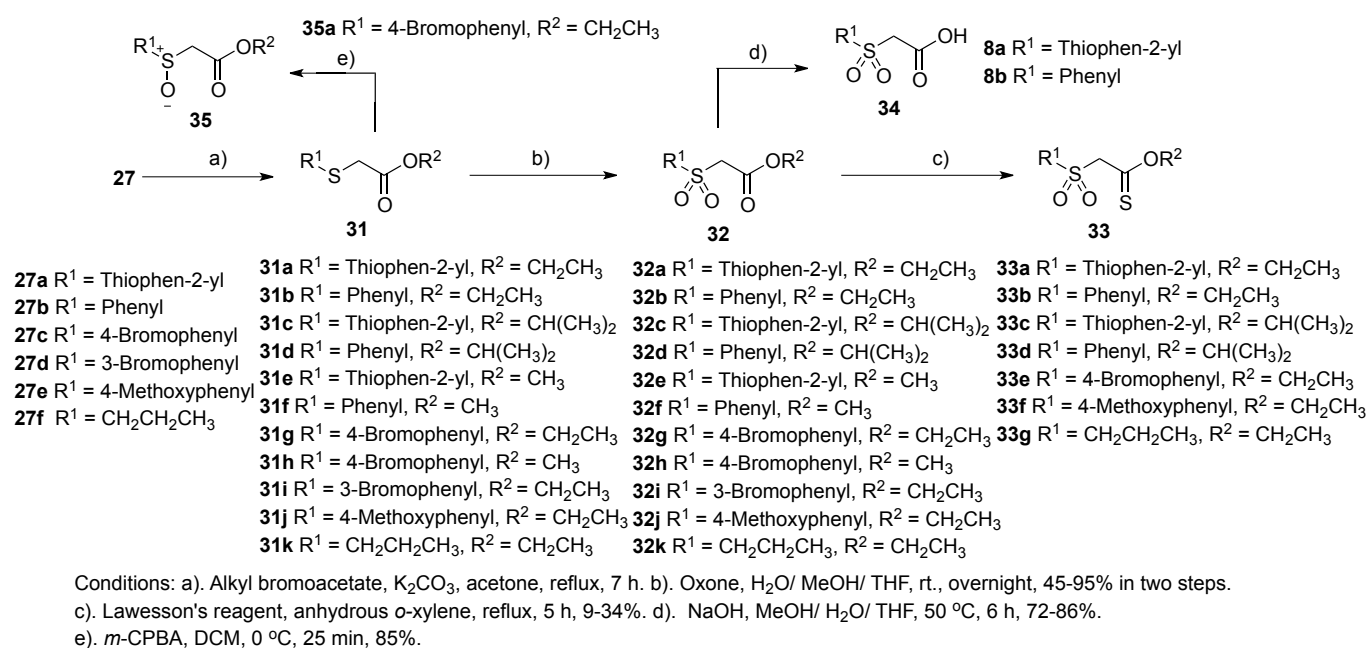


Conditions: a). Bromoacetamide or *N,N*-diethylbromoacetamide, K₂CO₃, acetone, reflux, 7 h.

b). Oxone, H₂O/ MeOH/ THF, rt., overnight, 44-78% in two steps. c). Lawesson's reagent, anhydrous THF, reflux, 2 h, 25-61%.

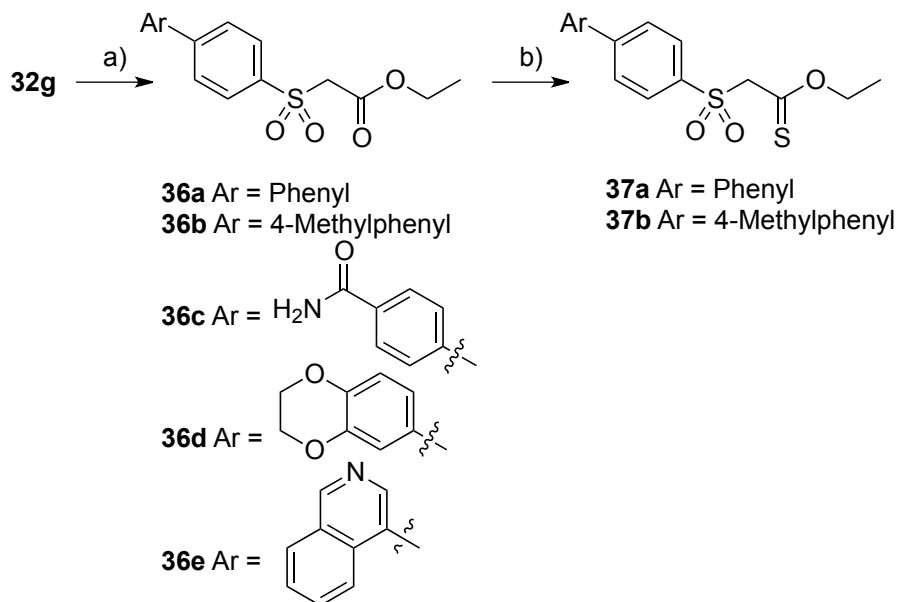
Scheme 4.2. Synthesis of compounds 28-30

Scheme 2 describes the synthesis of amide and thioamide compounds 28-30. Specifically, arylsulfonyl amides (29) were synthesized in two steps from aryl thiols (27) and the corresponding α -haloacetamides through substitution in the presence of potassium carbonate under reflux, followed by oxidation with oxone at room temperature.[184] Thiation of arylsulfonyl amides (29) was accomplished by using Lawesson's reagent in THF [185] with yields in the range of 25-60%.



Scheme 4.3. Synthesis of compounds 31-35

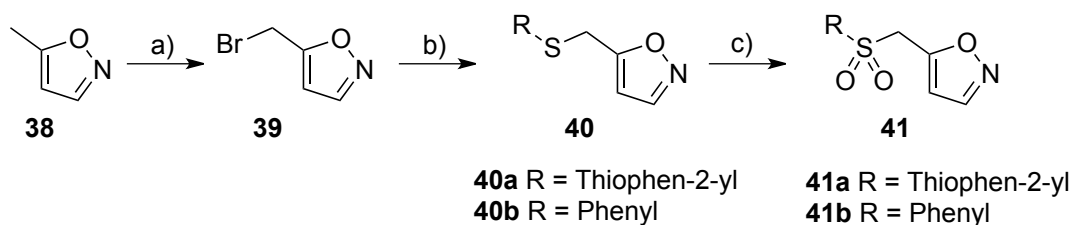
The ester, thioester and acid analogs were synthesized as described in Scheme 4.3. Specifically, the synthesis of arylsulfonyl esters (32) was very similar to that of arylsulfonyl amides (29) except for that *o*-xylene was used in the thiation reaction as the solvent instead of THF because esters are less reactive toward the Lawesson's reagent and requires higher temperature.[185, 186] The sulfonyl acetic acids (34) were synthesized through hydrolysis of the corresponding methyl esters (32) at 50 °C under basic conditions. Arylsulfonyl acetate (35) was synthesized in high yield through the oxidation of arylthioacetate (31) using *m*-CPBA in DCM at 0 °C.[187]



Conditions: a). 4-Carbamoylphenylboronic acid or 2,3-dihydrobenzo[*b*][1,4]dioxin-6-yl-6-boronic acid or isoquinolin-4-yl-4-boronic acid, Pd(OAc)₂, PPh₃, K₂CO₃, MF, 90 °C, 8 h, 30-88%. b). Lawesson's reagent, anhydrous *o*-xylene, reflux, 6 h, 17-21%.

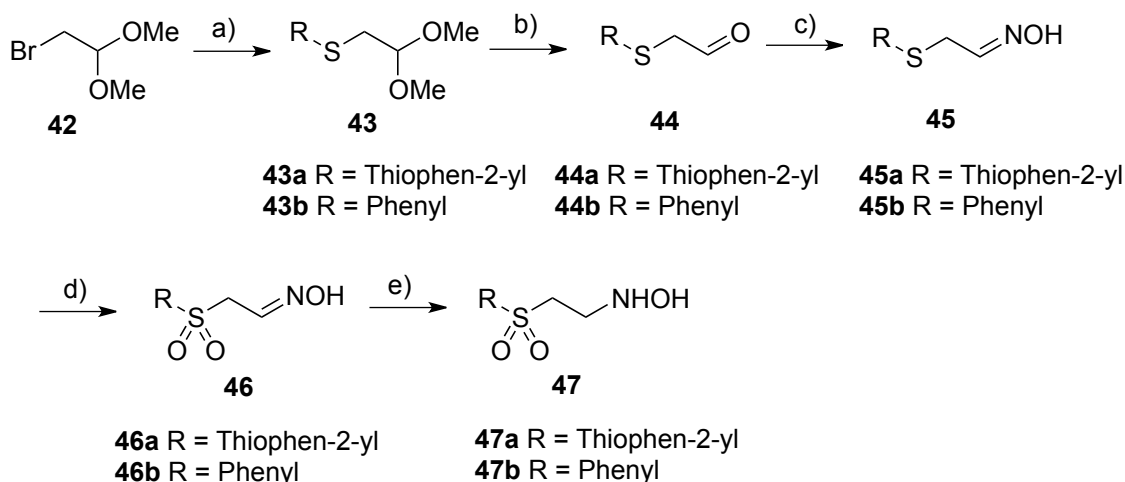
Scheme 4.4. Synthesis of compounds 36 and 37

Compounds with extended phenyl rings were synthesized using the procedure shown in Scheme 4.4. Specifically, Suzuki coupling reaction was used for the addition of an extra aryl ring to give 36.[188] Conversion of the ester group to a thioester (37) was accomplished using Lawesson's reagent as described above.



a). AIBN, NBS, CCl₄, reflux/ *hν* 4.5 h, 40%; b). Thiophene-2-thiol (**27a**) or thiophenol (**27b**), K₂CO₃, acetone, reflux, 6 h; c). MeOH/ THF, oxone/ H₂O, rt, overnight, 54-69% in two steps.

Scheme 4.5. Synthesis of compounds 39-41



a). Thiophene-2-thiol (**27a**) or thiophenol (**27b**), EtONa, reflux, 2 h, 48-59%; b). 1% HCl, acetone, 1.5 h, 51-94%; c). NH₂OH HCl, KHCO₃, MeOH, rt, 1.5 h, 67-91%; d). MeOH/ THF, oxone/ H₂O, rt, overnight, 84%; e). NaCNBH₃, 4.0 M HCl in dioxane, MeOH, rt, 2.5 h, 30-38%.

Scheme 4.6. Synthesis of compounds 43-47

Compounds 39-41 and 43-47 were synthesized using the procedures described in Schemes 4.5 and 4.6. The sulfonylmethyl isoxazoles (41) were synthesized in two steps from the reaction between aryl thiols (27) and bromomethyl isoxazole (49) followed by oxidation using oxone. The synthesis of sulfonyl *N*-hydroxyethylamines (47) were completed in five steps. The substitution reaction between an aryl thiol (27) and bromoacetaldehyde acetal (42) was accomplished in the presence of sodium ethoxide (1 equivalent). Acidic hydrolysis of the dimethyl acetal (43) yielded the aldehyde (44),[189] which was then converted to oxime (45). Sulfone (46) was prepared through oxidation using oxone and then the oxime moiety was reduced to *N*-hydroxyethylamine (47) using NaCNBH₃ at room temperature.[190]

All compounds synthesized were evaluated for their ability to inhibit AI-2-mediated quorum sensing following literature procedures.[151, 183, 191-193] In doing so, the MM32 strain of *V. harveyi* was used. As discussed above, *V. harveyi* produces bioluminescence upon quorum sensing and the intensity of bioluminescence is controlled by the level of AI-2 stimulation.[152] The MM32 strain lacks the LuxN receptor, which is required to respond to AI-1[183], and LuxS, which catalyzes the biosynthesis of DPD.

Therefore, the bioluminescence can only be produced if a proper amount of DPD is added to the culture because there is no endogenous AI-2, and the level of AI-1 does not interfere with the AI-2 inhibition assay.

Inhibition of luminescence production by the synthesized compounds was studied in the presence 5 mM of DPD, which was chosen to ensure that luminescence production stays in a sensitive region as described previously.[151] DMSO, which is used to dissolve the compounds for making the stock solutions, was found to have significant influence on the bioluminescence.[151] Therefore, a constant concentration of DMSO (0.4% in volume) was maintained in the final test solutions so as to exclude its possible side effect on the results. A 96-well plate reader was used for the luminescence determination in an inhibitor concentration range from 400 to 0 mM. The IC_{50} values were then calculated according to the inhibition curves.

Since the MM32 strain does not respond to AI-1, we also utilized the BB886 strain of *V. harveyi*, which lacks the AI-2 receptor, to test the AI-1 inhibition activities of the synthesized compounds and to check their selectivity toward AI-2-mediated quorum sensing. Before the inhibition test, the two strains were checked for their specificity for AI-2 and AI-1 by incubation in the presence of boric acid/DPD and cell-free medium from MM32 (Lacks luxS enzyme which produces AI-2), respectively. The results confirmed that the MM32 strain did not respond to AI-1 and the BB886 strain did not respond to AI-2. Among all the compounds tested, 12 compounds (Compounds 33a-f, 6g, 36a-c, and 37a-b) were observed to have significant inhibition activities against AI-2 mediated quorum sensing with IC_{50} at or below 40 mM and 4 compounds (36a-b, 37a-b) have IC_{50} in the single digit micromolar range. Among the 12 active compounds, five compounds (33c-d, 36a, 36c, and 37b) showed good selectivity towards AI-2 with the IC_{50} values for AI-1 inhibition above 200 mM.

In analyzing the AI-2 inhibition results, we were interested in achieving some basic understanding of the structural features, which are essential and/or beneficial for AI-2 inhibition. The first thing that we examined was whether the thioamide structure (part C, Figure 4.2) was important. From the compounds listed in Table 4.1, one can see that the “thio” structure feature was important for activity, but not essential. For example, the only difference between KM-03009 and 29a was that one was the thioamide (KM-03009) and the other one was a simple amide. However, their activities differ by over ten-fold with the thioamide compound being more active. The situations are similar when comparing 29b vs. 30b, 29c vs. 30c, and 29d vs. 30d.

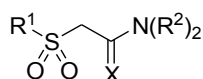


Table 4.1. Structures and activities of amides and thioamides					
Compound	R ¹ =	R ² =	X =	IC ₅₀ for AI-2 (mM)	IC ₅₀ for AI-1 (mM)
KM-03009	Thiophen-2-yl	H	S	35±3	71±5
29a	Thiophen-2-yl	H	O	>400	--
29b	Phenyl	H	O	>400	>400
30b	Phenyl	H	S	89±10	158±22
29c	Thiophen-2-yl	Ethyl	O	>400	>400
30c	Thiophen-2-yl	Ethyl	S	138±25	143±18
29d	Phenyl	Ethyl	O	>400	>400
30d	Phenyl	Ethyl	S	91±14	>400

Next we examined the comparison between thioesters and esters (Table 4.2). The same conclusions can be drawn, i.e., “thiation” is very important for AI-2 activities in this series with the thioesters having higher or equal activities compared with regular esters. For example, the only difference between 32a and 33a is that 32a is an ester and 33a is a thioester and yet their IC₅₀ values differ by about 6-fold. The situations are similar when comparing between 32b and 33b, and 32c and 33c. However, there are also other cases, such as 32d vs. 33d and 32g vs. 33e, where the thioesters and the esters have similar activities.

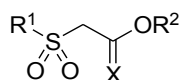


Table 4.2. Structures and activities of esters and thioesters

Compound	R ¹ =	R ² =	X =	IC ₅₀ for AI-2 (mM)	IC ₅₀ for AI-1 (mM)
32a	Thiophen-2-yl	Ethyl	O	124±16	>400
33a	Thiophen-2-yl	Ethyl	S	22±2	54±6
32b	Phenyl	Ethyl	O	170±30	>400
33b	Phenyl	Ethyl	S	33±4	96±20
32c	Thiophen-2-yl	Isopropyl	O	127±21	>400
33c	Thiophen-2-yl	Isopropyl	S	34±2	>400
32d	Phenyl	Isopropyl	O	38±15	217±101
33d	Phenyl	Isopropyl	S	33±4	>400
32e	Thiophen-2-yl	Methyl	O	>400	>400
32f	Phenyl	Methyl	O	>400	>400
32g	4-Bromophenyl	Ethyl	O	17±3	11±1
33e	4-Bromophenyl	Ethyl	S	14±2	35±10

32h	4-Bromophenyl	Methyl	O	81±3	115±35
32i	3-Bromophenyl	Ethyl	O	163±22	319±23
32j	4-Methoxyphenyl	Ethyl	O	87±6	79±15
33f	4-Methoxyphenyl	Ethyl	S	26±4	33±4
32k	Propyl	Ethyl	O	>400	>400
33g	Propyl	Ethyl	S	122±36	51±6

In comparing between esters and amides (Part D), higher inhibition activities of the ethyl and isopropyl esters were observed compared to their corresponding amides. For example, thioesters 33a-d (Table 4.2, between 22 and 34 mM) have lower IC₅₀ values compared to their corresponding thioamides such as KM-03009 (35 mM) and 30b-d (around 100 mM), though it is hard to say whether some of these small differences are meaningful given the intrinsic fluctuation of whole cell assay results. For the substituents of part D of the ester series, there is essentially no difference between ethyl esters and isopropyl esters, but methyl esters are obviously weaker inhibitors. For example, compounds 32e and 32f are inactive toward AI-2. However, the same trend was not observed with the amide compounds. One thing worth mentioning is that the isopropyl ester compounds (32c, d and 33c, d) seem to show the highest selectivity between AI-1 and AI-2 inhibition.

As for Part A, the aryl ring of the structure seems to be an important component for activities because the replacement of the aryl ring by an alkyl group led to a significant decrease in the activity. This becomes very clear when the IC₅₀ values of compounds with an alkyl chain at the Part A position such as 32k (Table 4.2, ester, >400 mM) and 33g (Table 4.2, thioester, 122 mM) are compared with most of the other ethyl esters (around 150 mM for esters and 30 mM for thioesters). A heterocycle, such as the thiophenyl group, is slightly better than a phenyl group. For example the IC₅₀ values of

compounds 32a/33a (thiophenyl) are slightly lower than that of compounds 32b/33b (phenyl). Additional substituents on the aryl ring seem to favor inhibition activities. For example, adding a bromo or a methoxyl group at the *para*- position of the phenyl ring resulted in significantly improved activities from an IC_{50} of 170 mM (6b) to 17 mM (6g) and 87 mM (6j). However, if the substituent is on the *meta*-position, no improvement was observed. A case in point is compound 6i, which has an IC_{50} of 163 mM.

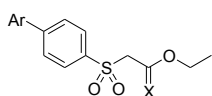
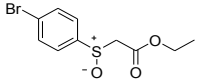
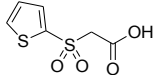
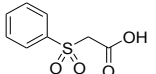
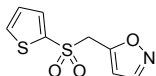
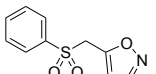
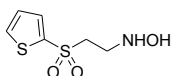
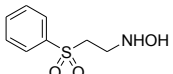


Table 4.3. Structures and activities of biaryl compounds				
Compound	Ar =	X =	IC_{50} for AI-2 (mM)	IC_{50} for AI-1 (mM)
36a	Phenyl	O	8.7±2.9	293±108
37a	Phenyl	S	5.7±0.8	32±2
36b	4-Methylphenyl	O	8.2±2.3	66±32
37b	4-Methylphenyl	S	5.6±1.3	>400
36c		O	31±2	>200
36d		O	158±43	>400
36e		O	>400	>400

Because of the promising results with *para*-substituted phenyl group in part A, we synthesized additional compounds with a bulky substituent at the *para*-position (Table 4.3). Several points are readily noticeable in this series of compounds. First, the “biaryl” compounds tend to be more active than

the single aryl compounds unless the second aryl group has ring heteroatom and/or a substitution. For example, biaryl compounds 36a, b (8.2-8.7 mM) and 37a, b (5.6-5.7 mM) all have IC_{50} values in the single digit micromolar range, while their corresponding “single aryl ring” analogs compounds 32b (170 mM) and 33b (33 mM) have much lower activities. However, with an isoquinolinyl (36c) or dihydrobenzodioxinyl (36d) group as the second ring, the IC_{50} values are over 150 mM. Second, a methyl group on the additional phenyl ring does not seem to make much difference. However, when a bulky group is attached, the molecule starts to lose its activity. This point is demonstrated by the activity change from 36a to 36e, which has a quinoline as the second ring. Third, as for the selectivity in inhibition against AI-2 and AI-1, a phenyl group extended by a second phenyl ring seems to improve the selectivity in biaryl compound 36a (about 34 fold), whereas a polar substituent on the phenyl ring seems to decrease the selectivity for AI-2 (e.g., 32g-j and 33e-f). Fourth, the effect of “thiation” of the carbonyl group in the biaryl series seems to be less significant compared to those with only one aryl group. For example, the IC_{50} of biaryl compounds 36a-b (esters, 8.2-8.7 mM) are close to those of compounds 37a-b (thioesters, about 5.6-5.7 mM). Overall, the introduction of a second aryl ring is advantageous for improved activity and selectivity.

The results of inhibition evaluation also revealed that reducing the sulfone group to a sulfoxide seems to result in diminished activities. For example, compound 32g (sulfone) has an IC_{50} of 17 mM, while the corresponding sulfoxide (35a, Table 4.4) has an IC_{50} of 48 mM. The possible reason for the activity difference may be due to the better structure mimicry of the borate group in AI-2 by a sulfone group than a sulfoxide. Additionally, a charged or polar terminal group (part D) also results in significantly reduced activities (34a, b, 41a, b, 47a, b)

Table 4.4. Structures and activities of other compounds			
Compound	Structure	IC ₅₀ for AI-2 (mM)	IC ₅₀ for AI-1 (mM)
35a		48±14	303±10
34a		>400	>400
34b		>400	>400
41a		>400	>400
41b		150±30	>400
47a		>400	Agonist
47b		267±49	--

In order to exclude potentially misleading results caused by possible cytotoxicity, the effect of selected synthesized active inhibitors with IC₅₀ values below 150 mM (30c, 30d, 32a, 33a, 33b, 32c, 33c, 32d, 33d, 32g, 33e, 32h, 32j, 33f, 36a, 37a, 36b, 37b, 36c, and 35a,) on bacterial growth was tested on the MM32 strain of *V. harveyi* by following procedures published earlier.[86] The results showed that none of these compounds has cytotoxicity at concentrations, which are twice the IC₅₀ value. That means the decrease of bioluminescence production observed was solely due to the inhibition of quorum sensing. To further explore the influence of the compounds on the growth of bacteria and to normalize the bioluminescence to cell density, especially during the same time point in which we assayed for the inhibition of fluorescence, a plate counting test was performed for the following compounds: KM-03009,

36a, 36b, 36c, 37a and 37b, using the MM32 strain of *V. harveyi*. The bacteria culture incubated for 5 hours in the presence of a compound at a concentration, which was close to its IC_{50} was diluted to 1:100 and 1:1000, and plated onto fresh LM plates and incubated at 30 °C for 24-48 hr. The colonies appeared were counted and compared to the blank (bacteria incubated without any inhibitor). The number of CFU (colony forming unit) of the bacteria incubated in the presence of an inhibitor at about the IC_{50} concentration was about the same as that of the blank. For example, the number of colonies appeared in the presence of the inhibitors ranged from 80-170% of that of the controls (without any inhibitors), while the bioluminescence intensity of these experiments with inhibitors at IC_{50} concentrations was only 30-60% of the controls. Such results further suggested that the compounds indeed inhibited the luminescence production (quorum sensing), not bacteria growth.

Aimed at achieving further understanding of the structure-activity relationship, we also conducted a Comparative Molecular Field Analysis (CoMFA). The CoMFA methodology is a 3D Quantitative Structure-Activity Relationship (3D-QSAR) technique by analyzing the steric and electrostatic fields.[194] In this case all compounds were optimized by the semi-empirical MOPAC/AM1 method[195] and then assigned with AM1BCC charges.[196-198] These conformations were then aligned with compound 37a (the most potent compound) for CoMFA computation as depicted in Figure 4.3.

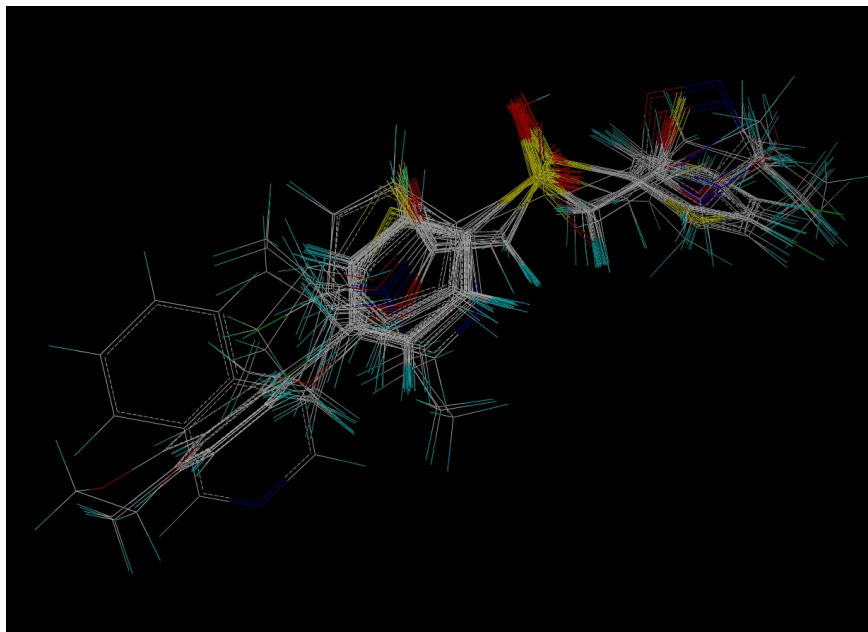


Figure 4.3. Molecular alignments of all compounds

CoMFA results suggest that the steric and electrostatic fields contribute 56% and 44% to AI-2 inhibitory activities, respectively. Statistically, the resulting standard error (SE) of 0.207, noncross-validated correlation coefficient (r^2) of 0.931, cross-validated coefficient (q^2) of 0.922 and F value of 76.72 confirm the reliability of our CoMFA model. Table 4.5 shows that comparison of the calculated pIC_{50} and experimentally determined pIC_{50} values using the CoMSIA model developed and Figure 4 shows the schematic correlation of such data.

Table 4.5. Experimental pIC_{50} , predicted pIC_{50} and residual values of molecules used for CoMFA computation			
Compound	Experimental pIC_{50}	Predicted pIC_{50}	Residual
KM-03009	4.46	3.87	0.59
SPB-02229	4.26	4.44	-0.18
29a	3.00	3.22	-0.22

29b	3.00	3.25	-0.25
30b	4.05	3.87	0.18
29c	3.00	3.13	-0.13
30c	3.86	3.91	-0.05
29d	3.00	3.30	-0.30
30d	4.04	3.71	0.33
32a	3.91	3.91	0.00
33a	4.66	4.32	0.33
32b	3.77	3.62	0.15
33b	4.48	4.55	-0.07
32c	3.90	4.11	-0.21
33c	4.47	4.38	0.09
32d	4.42	4.32	0.10
33d	4.48	4.56	-0.08
32e	3.00	3.01	-0.01
32f	3.00	3.12	-0.12
32g	4.77	4.51	0.26
33e	4.85	4.94	-0.08
32h	4.09	3.76	0.34
32i	3.79	3.83	-0.04
32j	4.06	4.13	-0.07
33f	4.59	4.73	-0.14
32k	3.00	3.04	-0.04
33g	3.91	4.00	-0.09
36a	5.05	4.89	0.15

37a	5.22	5.51	-0.28
36b	5.10	4.95	0.15
37b	5.22	5.48	-0.26
36c	4.51	4.40	0.11
36d	3.80	3.67	0.14
36e	3.00	2.97	0.03
35a	4.32	4.40	-0.08
34a	3.00	3.10	-0.10
34b	3.00	2.95	0.05
41a	3.00	3.08	-0.08
41b	3.82	3.85	-0.03
47a	3.00	3.01	-0.01
47b	3.57	3.69	-0.11

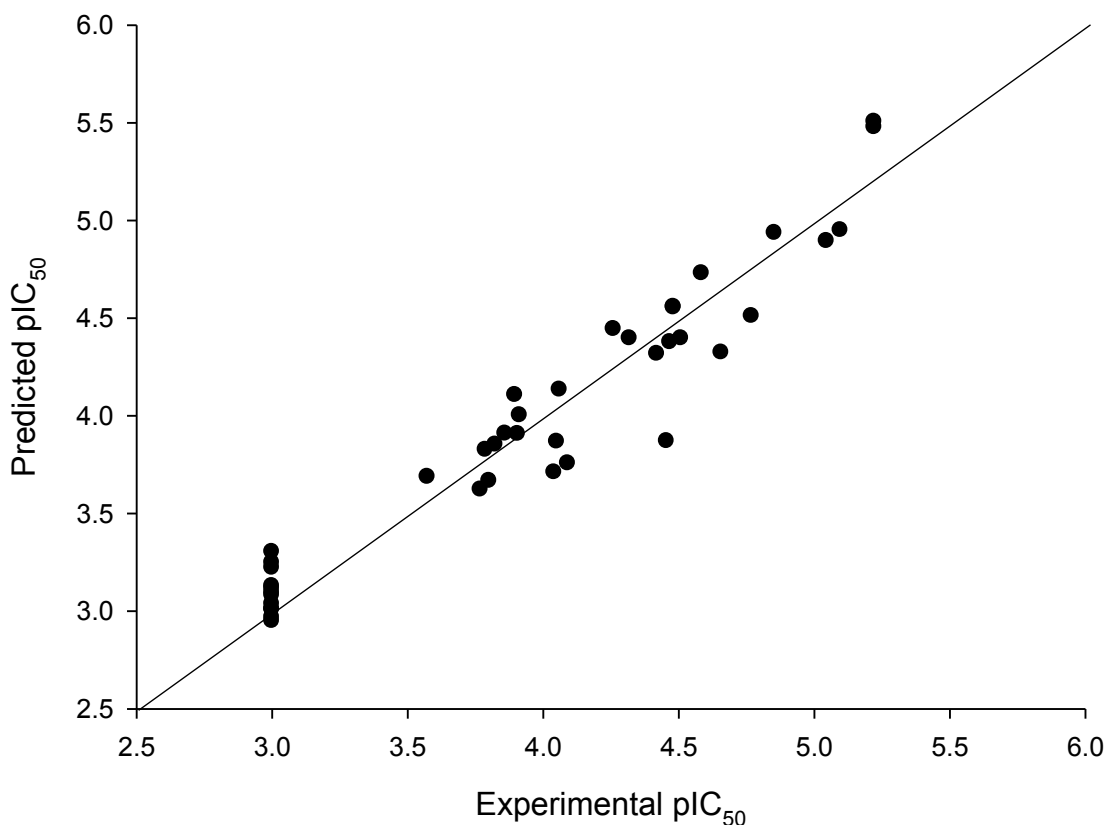


Figure 4.4. Experimental *versus* predicted pIC₅₀ for CoMFA 3D-QSAR model

For clarity in presentation, two 3D contour maps are shown in Figure 4.5. In the steric contour map, a high density of green and yellow colors around the R₁ substituent (Figure 4.2) suggests that a moderate bulky aromatic ring, such as diphenyl ring, is favorable; in the meanwhile the yellow color around the R₂ substituent also indicates a less bulky group here is desired. In the electrostatic contour map, a red color around the sulfonyl moiety and the R₂ substituent suggests that the less electronegative substituents in these positions could enhance the biological activity. The CoMFA model may provide useful insight into the future design of novel AI-2 inhibitors.

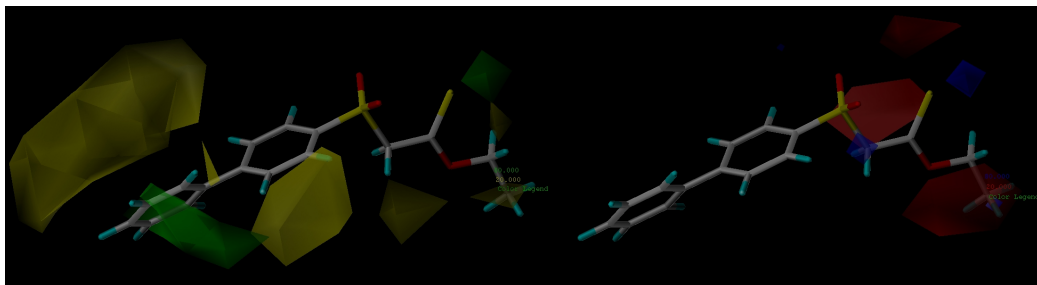


Figure 4.5. 3D contour maps around compound 37a as the result of a CoMFA analysis of the AI-2 inhibitory activities. Regions where substitution enhances (green) or reduces (yellow) the inhibitory affinity (left); the color coding indicates regions where electronegative substituents would enhance (blue) or reduce (red) the inhibitory activities (right).

Though the studies presented give an initial understanding of the structure-activity relationship, it should be noted that whole cell bacterial assays have certain intrinsic experimental variations that may not allow us to draw firm conclusions related to structural variations that only resulted in small changes in activities. When the same compound was tested using an entirely new batch of bacteria from the same source, IC_{50} variations of up to 1-3 fold were observed in some extreme cases. Though such variations are common in whole cell bacterial assay, one does need to be careful in drawing quantitative conclusions. The results presented can be viewed as a qualitative trend.

Conclusions

In this study, structure optimization was performed with two hit compounds obtained from virtual screening. Thirty nine new analogs were successfully synthesized and tested. Among all the synthesized analogs, 12 were found to show good inhibition activity with IC_{50} values below 40 μ M, 4 of which showed single digit micromolar IC_{50} values, while 6 out of the 12 possess good selectivity toward AI-2 mediated quorum sensing. Overall, the following structural features are beneficial to AI-2 inhibition activities: a sulfone group (part B), “thiation” of the carbonyl group of part C, a hydrophobic group of modest size in part D, and a biphenyl system in part A.

Experimental Section

General Chemistry

All reagents were purchased from Acros and Aldrich. Boronic acids were provided by Frontier Scientific, Inc. DPD was synthesized following literature procedures.[169, 177] 1H -NMR and ^{13}C -NMR spectra were recorded at 400 and 100 MHz, respectively, on a Bruker 400 NMR spectrometer. Mass spectral analyses were performed by the mass spectrometry facilities at Georgia State University.

Synthesis

General Experimental Procedure for Substitution Reaction of Thiol and Haloacetamides, Haloacetates or 5-(Bromomethyl)isoxazole. Representative Procedure for Substitution of Thiophene-2-thiol (27a) and 2-Iodoacetamide (Schemes 4.2 and 4.3, reaction a; Scheme 4.5, reaction b): A mixture of thiophene-2-thiol (27a, 690 mg, 5.94 mmol, 2.2 equiv.), 2-iodoacetamide (499 mg, 2.7 mmol, 1.0 equiv.) and potassium carbonate (560 mg, 4.05 mmol, 1.5 equiv.) in acetone (20 mL) was heated under reflux for 6 h (TLC). The solution was filtered and

solvent was evaporated. Dichloromethane (50 mL) was added to dissolve the residue. The solution was washed with saturated NaHCO₃ (8 mL × 2), H₂O (5 mL × 2) and brine (10 mL), and dried over Na₂SO₄. Evaporation of solvent afforded the crude product which was purified by column chromatography (Hex/EtOAc, 2:1) to give 2-(thiophen-2-ylthio)acetamide (28a, 229 mg, 49%) as light yellow oil. The crude product can also be used in the next step without purification.

Ethyl 2-(phenylthio)acetate (31b). Yellow oil; yield 64%; ¹H NMR (CD₃OD) δ 7.39-7.40 (d, *J* = 7.2 Hz, 2H), 7.28-7.31 (t, *J* = 7.2 Hz, 7.68 Hz, 2H), 7.20-7.24 (t, *J* = 6.8 Hz, 7.6 Hz, 1H), 4.08-4.13 (t, *J* = 7.2 Hz, 2H), 3.68 (s, 2H), 1.16-1.19 (t, *J* = 7.2 Hz, 3H); GC-MS, *m/z* 196 (M⁺).

Ethyl 2-(4-bromophenylthio)acetate (31g). Colorless oil; yield 87%; ¹H NMR (CDCl₃) δ 7.41-7.43 (d, *J* = 8.4, 2H), 7.26-7.30 (d, *J* = 8.4 Hz, 2H), 4.14-4.19 (q, *J* = 7.2 Hz, 2H), 3.61 (s, 2H), 1.21-1.25 (t, *J* = 7.2 Hz, 3H); ¹³C NMR (CDCl₃) δ 169.4, 134.2, 132.1, 131.5, 121.0, 61.7, 36.6, 14.1; MS (ES⁺), *m/z* 275.0 (M+1)⁺.

Methyl 2-(4-bromophenylthio)acetate (31h). Colorless oil; yield 56%; ¹H NMR (CDCl₃) δ 7.42-7.44 (d, *J* = 8.4 Hz, 1H), 7.26-7.29 (d, *J* = 8.8 Hz, 1H), 3.72 (s, 3H), 3.63 (s, 2H), ¹³C NMR (CDCl₃) δ 169.9, 134.1, 132.1, 131.5, 121.1, 52.6, 36.4; MS (ES⁺), *m/z* 282.9 (M+23)⁺.

Ethyl 2-(4-methoxyphenylthio)acetate (31j). Colorless oil; yield 99%; ¹H NMR (CDCl₃) δ 7.41-7.43 (d, *J* = 8.8 Hz, 2H), 6.83-6.86 (d, *J* = 8.8 Hz, 2H), 4.11-4.17 (q, *J* = 7.2 Hz, 2H), 3.79 (s, 3H), 3.51 (s, 2H), 1.20-1.23 (t, *J* = 7.2 Hz, 3H); ¹³C NMR (CDCl₃) δ 169.9, 159.6, 134.2, 124.9, 114.6, 61.3, 55.3, 38.6, 14.1; MS (ES⁺), *m/z* 227.1 (M+1)⁺.

Ethyl 2-(propylthio)acetate (31k). Colorless oil; yield 77%; ¹H NMR (CDCl₃) δ 4.17-4.22 (q, *J* = 7.2 Hz, 2H), 3.21 (s, 2H), 2.60-2.64 (t, *J* = 14.8 Hz, 2H), 1.59-1.68 (m, *J* = 7.2 Hz, 2H), 1.27-1.31 (t, *J* = 7.2 Hz, 3H), 0.98-1.01 (t, *J* = 7.2 Hz, 3H); ¹³C NMR (CDCl₃) δ 170.6, 61.2, 34.6, 33.6, 22.3, 14.1, 13.3; MS (ES⁺), *m/z* 163.1 (M+1)⁺.

5-(Phenylthiomethyl)isoxazole (40b). Yellow oil; yield 87%; ^1H NMR (CDCl_3) δ 8.15 (s, 1H), 7.25-7.38 (m, 5H), 6.07 (s, 1H), 4.19 (s, 2H); GC-MS, m/z , 191 (M^+).

General Experimental Procedure for Oxone Oxidation Reaction. Representative Procedure for Oxidation of 2-(Thiophen-2-ylthio)acetamide (28a) (Schemes 4.2 and 4.3, reaction b; Scheme 4.5, reaction c, Scheme 4.6, reaction d): To a stirred solution of 2-(thiophen-2-ylthio)acetamide (28a, 229 mg, 1.32 mmol, 1.0 equiv.) in MeOH (5.4 mL) and THF (5.4 mL) was added the solution of oxone (1.12 g, 1.82 mmol, 1.38 equiv.) in H_2O (7.2 mL) dropwise. The mixture was stirred at room temperature overnight. The solution was filtered and solvent was removed. Then dichloromethane (50 mL) was added and the solution was washed with H_2O (8 mL), brine (8 mL \times 2), and dried over Na_2SO_4 . Evaporation of solvent afforded the crude product which was purified by column chromatography (Hex/EtOAc 2:1 – 1:1) to give 2-(thiophen-2-ylsulfonyl)acetamide (29a, 241 mg, 89%) as white solid.

2-(Thiophen-2-ylsulfonyl)acetamide (29a). White solid; yield 44% for two steps; ^1H NMR (CD_3OD): δ 7.97 (s, 1H), 7.78 (s, 1H), 7.23-7.24 (d, 1H), 4.23 (s, 2H); ^{13}C NMR (CD_3OD): δ 164.4, 139.5, 135.0, 127.7, 62.4; MS (ES^+), m/z 206 ($\text{M}+1$) $^+$, 228 ($\text{M}+\text{Na}$) $^+$.

2-(Phenylsulfonyl)acetamide (29b). White solid; yield 89% in two steps. ^1H NMR ($(\text{CD}_3)_2\text{CO}$) δ 7.95-7.97 (m, 2H), 7.73-7.77 (m, 1H), 7.63-7.67 (m, 2H), 6.71-7.18 (br, 2H), 4.17 (s, 2H); ^{13}C NMR ($(\text{CD}_3)_2\text{CO}$) δ 162.4, 139.9, 133.8, 129.1, 128.3, 61.4; MS (ES^+), m/z 200 ($\text{M}+1$) $^+$, 222 ($\text{M}+\text{Na}$) $^+$.

N,N-Diethyl-2-(thiophen-2-ylsulfonyl)acetamide (29c). Light yellow crystals; yield 78% in 2 steps; ^1H NMR (CDCl_3) δ 7.74-7.76 (m, $J = 4.8$ Hz, 2H), 7.15-7.18 (t, $J = 4.8$ Hz, 1H), 4.29 (s, 2H), 3.45-3.50 (q, $J = 7.2$ Hz, 2H), 3.34-3.40 (q, $J = 7.2$ Hz, 2H), 1.20-1.24 (t, $J = 7.2$ Hz, 3H),

1.11-1.14 (t, $J = 7.2$ Hz, 3H), ^{13}C NMR (CDCl_3) δ 160.6, 139.6, 135.6, 135.0, 128.0, 61.0, 43.3, 41.1, 14.4, 13.0; MS (ES^-), m/z 260.0 ($\text{M}-1$) $^-$, m.p. = 89-90 °C.

N,N-Diethyl-2-(phenylsulfonyl)acetamide (29d). White crystals 72% for 2 steps; ^1H NMR (CDCl_3) δ 7.92-7.94 (d, $J = 7.2$ Hz, 2H), 7.65-7.69 (t, $J = 7.2$ Hz, 1H), 7.55-7.59 (t, $J = 7.6$ Hz, 2H), 4.21 (s, 2H), 3.45-3.51 (q, $J = 7.2$ Hz, 2H), 3.32-3.37 (q, $J = 7.2$ Hz, 2H), 1.20-1.24 (t, $J = 7.2$ Hz, 3H), 1.08-1.11 (t, $J = 7.2$ Hz, 3H), ^{13}C NMR (CDCl_3) δ 160.6, 139.0, 134.3, 129.2, 128.8, 60.0, 43.3, 41.0, 14.4, 12.9; MS (ES^-), m/z 255.0 ($\text{M}-1$) $^-$; m.p. = 84-85 °C.

Ethyl 2-(thiophen-2-ylsulfonyl)acetate (32a). colorless oil; yield 71% in two steps; ^1H NMR (CDCl_3) δ 7.80-7.81 (dd, $J = 1.2$ Hz, 3.6 Hz, 4.8 Hz, 1H), 7.76-7.78 (dd, $J = 1.2$ Hz, 4.0 Hz, 4.8 Hz, 1H), 7.18-7.20 (q, $J = 1.2$ Hz, 3.6 Hz, 4.0 Hz, 1H), 4.22 (s, 1H), 4.16-4.21 (q, $J = 7.2$ Hz, 2 H), 1.21-1.25 (t, $J = 7.2$ Hz, 3 H); ^{13}C NMR (CDCl_3) δ 162.3, 139.3, 135.4, 135.1, 128.0, 62.5, 62.0, 13.9; MS (ES^+), m/z , 235 (M^+), 257 ($\text{M}+\text{Na}$) $^+$.

Ethyl 2-(phenylsulfonyl)acetate (32b). White solid; yield 71%; ^1H NMR (CDCl_3) δ 7.95-7.97 (d, $J = 7.6$ Hz, 2H), 7.68 – 7.72 (t, $J = 7.2$ Hz, 1H), 7.57-7.61 (t, $J = 7.2$ Hz, 7.6 Hz, 2H), 4.17 (s, 1H), 4.12-4.15 (q, $J = 7.2$ Hz, 2H), 1.17–1.26 (t, $J = 7.2$ Hz, 3H); ^{13}C NMR (CDCl_3) δ 162.3, 138.7, 134.3, 129.2, 128.6, 62.4, 61.0, 13.9; MS (ES^+), m/z , 229 ($\text{M}+1$) $^+$, 251 ($\text{M}+\text{Na}$) $^+$; m.p. = 43-44 °C.

Isopropyl 2-(thiophen-2-ylsulfonyl)acetate (32c). Colorless oil, yield 95% in two steps; ^1H NMR (CDCl_3) δ 7.69-7.71 (m, 2H), 7.10 – 7.12 (t, $J = 4.0$ Hz, 1H), 4.94- 4.97 (m, $J = 6.0$ Hz, 1H) 4.11 (s, 2H), 4.15 – 4.20 (d, $J = 6.0$ Hz, 6H). ^{13}C NMR (CDCl_3) δ 161.7, 139.4, 135.3, 134.8, 127.8, 70.6, 62.3, 21.5; MS (ES^-), m/z , 247 ($\text{M}-1$) $^-$

Isopropyl 2-(phenylsulfonyl)acetate (32d). Colorless oil; yield 92% in two steps; ^1H NMR (CDCl_3) δ 7.92-7.94 (d, $J = 8.0$ Hz, 2H), 7.64 – 7.68 (m, 1H), 7.54-7.58 (m, 2H), 4.91-

4.97 (m, $J = 6.0$ Hz, 1H) 4.07 (s, 2H), 4.13, 4.14 (d, $J = 6.0$ Hz, 6H). ^{13}C NMR (CDCl_3) δ 161.8, 138.8, 134.2, 129.1, 128.5, 70.4, 61.2, 21.4; MS (ES^-), m/z 241 ($\text{M}-1$) $^-$.

Methyl 2-(thiophen-2-ylsulfonyl)acetate (32e). Colorless oil; yield 73% in two steps; ^1H NMR (CDCl_3) δ 7.76-7.68 (m, 2H), 7.17-7.19 (t, $J = 4.4$ Hz, 1H), 4.21 (s, 1H), 3.75 (s, 3H); MS (ES^+), m/z 221 ($\text{M}+1$) $^+$, 243 ($\text{M}+\text{Na}$) $^+$.

Methyl 2-(phenylsulfonyl)acetate (32f). Colorless oil; yield 80% in two steps; ^1H NMR (CDCl_3) δ 7.88-7.90 (d, $J = 8.0$ Hz, 2H), 7.62 – 7.66 (t, $J = 7.2$ Hz, 1H), 7.51-7.55 (m, $J = 7.2$ Hz, 8.0 Hz, 2H), 4.07 (s, 1H), 3.64 (s, 3H); MS (ES^-), m/z 213 ($\text{M}-1$) $^-$.

Ethyl 2-(4-bromophenylsulfonyl)acetate (32g). Colorless crystal, yield 90%; ^1H NMR (CDCl_3) δ 7.81-7.83 (d, $J = 8.8$ Hz, 2H), 7.72-7.74 (d, $J = 8.4$ Hz, 2H), 4.14-4.19 (q, $J = 7.2$ Hz, 2H), 4.11 (s, 2H), 1.21-1.24 (t, $J = 7.2$ Hz, 3H); ^{13}C NMR (CDCl_3) δ 162.2, 137.6, 132.5, 130.2, 129.8, 62.5, 60.9, 13.9; MS (ES^+), m/z 328.9 ($\text{M}+23$) $^+$; m.p. = 49-50 $^\circ\text{C}$.

Methyl 2-(4-bromophenylsulfonyl)acetate (32h). White crystals; yield 88%; ^1H NMR (CDCl_3) δ 7.81-7.83 (d, $J = 8.8$ Hz, 2H), 7.72-7.75 (d, $J = 8.8$ Hz, 2H), 4.13 (s, 2H), 3.73 (s, 3H); ^{13}C NMR (CDCl_3) δ 162.7, 137.6, 132.6, 130.1, 129.9, 60.6, 53.2; MS (ES^+), m/z 314.9 ($\text{M}+23$) $^+$; m.p. = 78-79 $^\circ\text{C}$.

Ethyl 2-(3-bromophenylsulfonyl)acetate (32i). Colorless crystals; yield 75% in two steps; ^1H NMR (CDCl_3) δ 8.11 (s, 1H), 7.90-7.92 (d, $J = 7.9$ Hz, 1H), 7.82-7.84 (d, $J = 7.9$ Hz, 1H), 7.47-7.51 (t, $J = 7.9$ Hz, 1H), 4.15-4.21 (q, $J = 7.1$ Hz, 2H), 4.15 (s, 2H); ^{13}C NMR (CDCl_3) δ 162.0, 140.4, 137.3, 131.5, 130.7, 127.2, 123.1, 62.5, 60.9, 13.8; MS (ES^+), m/z 329.1 ($\text{M}+23$) $^+$; m.p. = 36-37 $^\circ\text{C}$.

Ethyl 2-(4-methoxyphenylsulfonyl)acetate (32j). Colorless oil; yield 71%; ^1H NMR (CDCl_3) δ 7.86-7.88 (d, $J = 8.8$ Hz, 2H), 7.02-7.04 (d, $J = 9.2$ Hz, 2H), 4.13-4.18 (q, $J = 6.8$ Hz,

2H), 4.09 (s, 2H), 3.89 (s, 3H), 1.20-1.24 (t, $J = 6.8$ Hz, 3H); ^{13}C NMR (CDCl_3) δ 164.2, 162.6, 130.8, 130.2, 114.3, 62.3, 61.2, 55.7, 13.9; MS (ES^+), m/z 281.0 ($\text{M}+23$) $^+$.

Ethyl 2-(propylsulfonyl)acetate (32k). Colorless oil; yield 84%; ^1H NMR (CDCl_3) δ 4.25-4.31 (q, $J = 7.2$, 2H), 3.95 (s, 2H), 3.22-3.26 (m, $J = 8.0$ Hz, $J = 2.4$, 2H), 1.90-1.95 (m, $J = 7.6$ Hz, $J = 2.4$ Hz, 2H), 1.31-1.35 (t, $J = 7.2$ Hz, 3H), 1.10-1.13 (t, $J = 7.2$ Hz, 3H); ^{13}C NMR (CDCl_3) δ 163.1, 62.6, 57.4, 55.2, 15.7, 13.9, 13.0; MS (ES^+), m/z 317.0 ($\text{M}+23$) $^+$.

5-((Thiophen-2-ylsulfonyl)methyl)isoxazole (41a). Yellow solid, yield 69% in two steps; ^1H NMR (CDCl_3) δ 8.25-8.26 (d, 1H), 7.53-7.77 (dd, $J = 1.2$ Hz, 1.6 Hz, 5.2 Hz, 1H), 7.57-7.58 (dd, $J = 1.6$ Hz, 4.0 Hz), 7.13-7.16 (q, $J = 4.0$ Hz, 5.2 Hz, 1H), 7.45-7.46 (d, 1H), 4.69 (s, 2H); ^{13}C NMR (CDCl_3) δ 159.7, 150.7, 137.9, 135.6, 135.4, 128.2, 105.6, 55.0; MS (ES^+), m/z 230 ($\text{M}+1$) $^+$.

5-(Phenylsulfonylmethyl)isoxazole (41b). Yellow solid, yield 62%; ^1H NMR (CDCl_3) δ 8.22 (s, 1H), 7.77-7.79 (d, $J = 8.0$ Hz, 2H), 7.66-7.70 (t, $J = 7.2$ Hz, 2H), 7.26-7.56 (t, $J = 7.6$ Hz, 2H), 6.38 (s, 1H), 4.60 (s, 2H); ^{13}C NMR (CDCl_3) δ 159.7, 150.6, 137.6, 134.6, 129.4, 128.4, 105.4, 53.8; MS (ES^+), m/z 224 ($\text{M}+1$) $^+$, 246($\text{M}+\text{Na}$) $^+$, m.p. = 87-88 °C.

2-(Phenylsulfonyl)acetaldehyde oxime (46b). White solid; yield 84%; ^1H NMR ($(\text{CD}_3)_2\text{CO}$, mixture of isomers, ratio 1/1) δ 10.69 (s, 0.5H), 10.49 (s, 0.5 H), 7.66-7.98 (m, 5H), 7.33 (t, 0.5H), 6.82 (t, 0.5H), 4.37 (d, 1H), 4.11(d, 1H); MS (ES^+), m/z 200 ($\text{M}+1$) $^+$, 222($\text{M}+\text{Na}$) $^+$; m.p. = 91-94 °C.

General Experimental Procedure for Thiation Reaction of Amides. Representative Procedure for Thiation of 2-(Phenylsulfonyl)acetamide (29a) (Scheme 2, reaction c): To a solution of 2-(thiophen-2-ylsulfonyl)acetamide (29a, 33 mg, 0.17 mmol, 1.0 equiv.) in anhydrous THF (5 mL) was added Lawesson's reagent (67 mg, 0.17 mmol, 1.0 equiv.) at room temperature

under N₂; then the reaction was heated at reflux for 2 h. After solvent was evaporated, the residue was dissolved in dichloromethane (50 mL). The solution was washed with H₂O (5 mL), brine (5 mL), and dried over Na₂SO₄. Evaporation of solvent afforded the crude product which was purified by column chromatography (Hex/EtOAc/Acetone 1:1:0.01) to give 2-(Phenylsulfonyl)ethanethioamide (KM-03009, 22 mg, 61%) as white solid.

2-(Thiophen-2-ylsulfonyl)ethanethioamide (KM-03009). White solid, yield 38%; ¹H NMR ((CD₃)₂CO) δ 9.13 (br, 1H), 8.70 (br, 1H), 8.05-8.06 (dd, *J* = 1.2 Hz, 4.8 Hz, 1H), 7.77-7.79 (dd, *J* = 1.2 Hz, 4.0 Hz), 7.26-7.28 (dd, *J* = 4.0 Hz, 4.8 Hz, 1H), 4.66 (s, 2H); ¹³C NMR ((CD₃)₂CO) δ 192.7, 139.0, 135.5, 135.2, 127.9, 70.5; MS (ES⁺), *m/z* 222 (M+1)⁺, 244 (M+Na)⁺; m.p. = 154-155 °C.

2-(Phenylsulfonyl)ethanethioamide (30b). White solid; yield 61%; ¹H NMR ((CD₃)₂CO) δ 8.61-9.12 (br, 2H), 7.94-7.96 (m, 2H), 7.74-7.78 (m, 1H), 7.63-7.67 (m, 2H), 4.60 (s, 2H); ¹³C NMR ((CD₃)₂CO) δ 192.9, 138.6, 134.1, 129.0, 128.7, 69.1; MS (ES⁺), *m/z* 216 (M+1)⁺, 238 (M+Na)⁺, m.p. = 165-166 °C.

N,N-Diethyl-2-(thiophen-2-ylsulfonyl)ethanethioamide (30c). Light yellow solid; yield 25%; ¹H NMR (CDCl₃) δ 7.76-7.77 (d, *J* = 5.0 Hz, 1H), 7.69-7.71 (d, *J* = 3.8 Hz, 1H), 7.16-7.18 (m, *J* = 3.8 Hz, *J* = 5.0 Hz, 1H), 4.80 (s, 2H), 3.92-3.97 (q, *J* = 7.2 Hz, 2H), 3.84-3.89 (q, *J* = 7.2 Hz, 2H), 1.29-1.32 (t, *J* = 7.2 Hz, 3H), 1.25-1.29 (t, *J* = 7.2 Hz, 3H), ¹³C NMR (CDCl₃) δ 185.0, 138.2, 136.1, 134.9, 127.7, 69.3, 48.2, 47.6, 13.3, 10.8; MS (ES⁺), *m/z* 278.2 (M+1)⁺, m.p. = 98-99 °C.

N,N-Diethyl-2-(phenylsulfonyl)ethanethioamide (30d). White solid, yield 30%,; ¹H NMR (CDCl₃) δ 7.88-7.90 (d, *J* = 7.2 Hz, 2H), 7.66-7.70 (t, *J* = 7.4 Hz, 1H), 7.54-7.58 (t, *J* = 8.0 Hz, 2H), 4.73 (s, 2H), 3.91-3.96 (q, *J* = 7.2 Hz, 2H), 3.86-3.90 (q, *J* = 7.2 Hz, 2H), 1.31-1.33 (t, *J* =

7.2 Hz, 3H), 1.25-1.28 (t, $J = 7.2$ Hz, 3H), ^{13}C NMR (CDCl_3) δ 185.2, 137.8, 134.2, 129.2, 128.8, 68.4, 48.1, 47.6, 13.3, 10.8; MS (ES^+), m/z 272.2 ($\text{M}+1$) $^+$, m.p. = 103-105 °C.

General Experimental Procedure for Thiation Reaction of Esters. Representative Procedure for Thiation of Ethyl 2-(Thiophen-2-ylsulfonyl)acetate (32a) (Scheme 4.3, reaction c; Scheme 4.4, reaction b): To a solution of ethyl 2-(thiophen-2-ylsulfonyl)acetate (32a, 50 mg, 0.22 mmol, 1.0 equiv.) in anhydrous *o*-xylene (2 mL) was added Lawesson's reagent (174 mg, 0.43 mmol, 2.0 equiv.) under N_2 . The reaction was heated under reflux for 6 h. After solvent was evaporated, the residue was dissolved in dichloromethane (50 mL) and the solution was washed with H_2O (5 mL), brine (5 mL \times 2), and dried over Na_2SO_4 . Evaporation of solvent afforded the crude product, which was purified by column chromatography (Hex/EtOAc, 6:1) to give *O*-ethyl 2-(thiophen-2-ylsulfonyl)ethanethioate (33a, 18 mg, 34%) as light yellow solid.

O-Ethyl 2-(thiophen-2-ylsulfonyl)ethanethioate (33a). Light yellow solid; yield 34%; ^1H NMR ($(\text{CD}_3)_2\text{CO}$) δ 8.10 (s, 1H), 7.78 (s, 1H), 7.31 (d, 1H), 4.79 (s, 2H), 4.43-4.45 (d, $J = 6.8$ Hz, 2H), 1.27-1.30 (t, $J = 6.8$ Hz, 3H); ^{13}C NMR ($(\text{CD}_3)_2\text{CO}$) δ 206.1, 139.4, 135.5, 135.4, 128.1, 72.3, 69.6, 12.7; MS (ES^+), m/z 251 ($\text{M}+1$) $^+$, 268 ($\text{M}+\text{H}_2\text{O}$) $^+$, 273 ($\text{M}+\text{Na}$) $^+$; m.p. = 50-51 °C.

O-Ethyl 2-(phenylsulfonyl)ethanethioate (33b). White solid; yield 31%; ^1H NMR ($(\text{CD}_3)_2\text{CO}$) δ 7.92-7.94 (m, 2H), 7.77-7.91 (m, 1H), 7.66-7.70 (m, 2H), 4.72 (s, 2H), 4.35-3.38 (q, $J = 7.2$ Hz, 2H), 1.18-1.22 (t, $J = 7.2$ Hz, 3H); ^{13}C NMR ($(\text{CD}_3)_2\text{CO}$) δ 206.4, 139.0, 134.1, 129.1, 128.6, 71.1, 69.4, 12.5; MS (ES^+), m/z , 245 ($\text{M}+1$) $^+$, 267 ($\text{M}+\text{Na}$) $^+$; m.p. = 33-34 °C.

O-Isopropyl 2-(thiophen-2-ylsulfonyl)ethanethioate (33c). Yellow solid; yield 24%; ^1H NMR ($(\text{CD}_3)_2\text{CO}$) δ 8.07 – 8.09 (m, 1H), 7.77-7.78 (m, 1H), 7.31 – 7.29 (m, 1H), 5.47- 5.50 (m, $J = 6.0$ Hz, 1H) 4.75 (s, 2H), 1.27,1.29 (d, $J = 6.0$ Hz, 6H); ^{13}C NMR ($(\text{CD}_3)_2\text{CO}$) δ 206.7, 141.0, 136.9, 136.7, 129.5, 78.5, 74.1, 21.4; MS (ES^+), m/z 287 ($\text{M}+\text{Na}$) $^+$; m.p. = 53-55 °C.

O-Isopropyl 2-(phenylsulfonyl)ethanethioate (33d). Yellow solid; yield 27%; ^1H NMR ($(\text{CD}_3)_2\text{CO}$) δ 7.93, 7.95 (d, $J = 7.6$ Hz, 2H), 7.77-7.79 (d, $J = 7.2$ Hz, 1H), 7.66-7.70 (t, $J = 7.6$ Hz, 8.0 Hz, 2H), 5.41- 5.43 (m, $J = 6.4$ Hz, 1H) 4.70 (s, 2H), 1.19-1.21 (d, $J = 6.4$ Hz, 6H); ^{13}C NMR ($(\text{CD}_3)_2\text{CO}$) δ 206.9, 140.5, 135.4, 130.6, 130.0, 78.3, 72.8, 21.3; MS (ES $^-$), m/z 257 (M-1) $^-$; m.p. = 36-37 $^\circ\text{C}$.

O-Ethyl 2-(4-bromophenylsulfonyl)ethanethioate (33e). Light yellow solid; yield 20%; ^1H NMR (CDCl_3) δ 7.74-7.76 (d, $J = 8.8$ Hz, 2H), 7.70-7.72 (d, $J = 8.8$ Hz, 2H) , 4.52 (s, 2H), 4.40-4.45 (q, $J = 7.2$ Hz, 2H), 1.29-1.33 (t, $J = 7.2$ Hz, 3H); ^{13}C NMR (CDCl_3) δ 204.3, 137.0, 132.4, 130.3, 129.6, 71.4, 69.7, 13.3; MS (ES $^+$), m/z 344.9 (M+23) $^+$; m.p. = 84-85 $^\circ\text{C}$.

O-Ethyl 2-(4-methoxyphenylsulfonyl)ethanethioate (33f). Light yellow solid; yield 18%; ^1H NMR (CDCl_3) δ 7.80-7.82 (d, $J = 9.2$ Hz, 2H), 7.00-7.02 (d, $J = 9.2$ Hz, 2H) , 4.51 (s, 2H), 4.40-4.45 (q, $J = 7.2$ Hz, 2H), 3.90 (s, 3H), 1.29-1.33 (t, $J = 7.2$ Hz, 3H); ^{13}C NMR (CDCl_3) δ 205.1, 164.1, 131.0, 129.7, 114.2, 71.8, 69.5, 55.7, 13.3; MS (ES $^+$), m/z 297.0 (M+23) $^+$; m.p. = 58-59 $^\circ\text{C}$.

O-Ethyl 2-(propylsulfonyl)ethanethioate (33g). Light yellow oil; yield 9.4%; ^1H NMR (CDCl_3) δ 4.56-4.62 (q, $J = 7.2$, 2H), 4.37 (s, 2H), 3.21-3.25 (m, $J = 7.9$ Hz, $J = 2.4$ Hz, 2H) , 1.91-1.97 (m, $J = 7.6$ Hz, $J = 2.0$ Hz, 2H), 1.44-1.48 (t, $J = 7.2$ Hz, 3H), 1.09-1.12 (t, $J = 7.2$ Hz, 3H); ^{13}C NMR (CDCl_3) δ 205.7, 69.9, 68.1, 54.4, 29.7, 16.0, 13.4, 13.0; MS (ES $^+$), m/z 233.0 (M+23) $^+$.

Compound 37a. Light yellow solid; yield 17%; ^1H NMR (CDCl_3) δ 7.93-7.95 (d, $J = 8.6$ Hz, 2H), 7.73-7.76 (d, $J = 8.6$ Hz, 2H), 7.59-7.61 (d, $J = 6.9$ Hz, 2H), 7.46-7.50 (t, $J = 7.0$ Hz, 2H), 7.42-7.44 (t, $J = 7.1$ Hz, 1H), 4.55 (s, 2H), 4.41-4.47 (q, $J = 7.1$ Hz, 2H), 1.27-1.31 (t, $J =$

7.1 Hz, 3H); ^{13}C NMR (CDCl_3) δ 204.7, 147.1, 139.0, 136.6, 129.3, 129.1, 128.8, 127.6, 127.4, 71.6, 69.6, 13.3; MS (ES^-), m/z 319.0 ($\text{M}-1$) $^-$; m.p. = 70-72 °C.

Compound 37b. White solid; yield 21%; ^1H NMR (CDCl_3) δ 7.92-7.94 (d, J = 8.8 Hz, 2H), 7.74-7.76 (d, J = 8.4 Hz, 2H), 7.52-7.54 (d, J = 8.0 Hz, 2H), 7.29-7.31 (d, J = 7.6 Hz, 2H), 4.56 (s, 2H), 4.41-4.44 (q, J = 7.2 Hz, 2H), 2.42 (s, 1H), 1.26-1.29 (t, J = 7.2 Hz, 3H); ^{13}C NMR (CDCl_3) δ 162.4, 147.2, 138.9, 136.8, 136.0, 129.8, 129.1, 127.5, 127.2, 62.4, 61.1, 21.1, 13.9; MS (ES^+), m/z 357.1 ($\text{M}+23$) $^+$; m.p. = 98-100 °C.

General Experimental Procedure for Cross Coupling Reaction. Representative Procedure for Cross Coupling of Ethyl 2-(4-Bromophenylsulfonyl)acetate (32g) and Phenylboronic Acid (Scheme 4.4, reaction a): A mixture of ethyl 2-(4-bromophenylsulfonyl)acetate (32g, 188.7 mg, 0.61 mmol, 1 equiv.), phenylboronic acid (180 mg, 1.47 mmol, 2.4 equiv.), $\text{Pd}(\text{OAc})_2$ (11 mg, 0.049 mmol, 0.08 equiv.), PPh_3 (39 mg, 0.147 mmol, 0.24 equiv.) and K_2CO_3 (255 mg, 1.84 mmol, 3.0 equiv.) in DMF (3.3 mL) was degassed using vacuum pump and backfilled with N_2 . Then the reaction mixture was heated and stirred at 90 °C overnight. After cooling to room temperature, the resulting mixture was poured into 5.0 mL 1N HCl (in ice bath). Then the mixture was extracted with EtOAc (40 mL). The organic extract was washed with brine (8 mL) and dried over Na_2SO_4 . Evaporation of solvents and purification of the residue by column chromatography (Hexanes:EtOAc 8:1 – 5:1) gave the pure compound (36) as white solid (79 mg, 42%).

Compound 36a. White solid; 42%; ^1H NMR (CDCl_3) δ 8.00-8.02 (d, J = 8.8 Hz, 2H), 7.76-7.79 (d, J = 8.4 Hz, 2H), 7.61-7.63 (d, J = 6.8 Hz, 2H), 7.47-7.51 (t, J = 6.8 Hz, 2H), 7.44-7.46 (t, J = 7.2 Hz, 1H), 4.15-4.20 (q, J = 7.2 Hz, 2H), 4.15 (s, 2H), 1.20-1.23 (t, J = 7.2 Hz, 3H);

^{13}C NMR (CDCl_3) δ 162.4, 147.2, 139.0, 137.2, 129.1, 128.8, 127.8, 127.4, 62.4, 61.1, 13.7; MS (ES^+), m/z 327.2 ($\text{M}+23$) $^+$, m.p. = 108-110 $^\circ\text{C}$.

Compound 36b. White solid; yield 49%; ^1H NMR (CDCl_3) δ 7.98-7.80 (d, J = 8.8 Hz, 2H), 7.74-7.77 (d, J = 8.4 Hz, 2H), 7.50-7.53 (d, J = 8.0 Hz, 2H), 7.29-7.31 (d, J = 8.0 Hz, 2H), 4.15-4.19 (q, J = 7.2 Hz, 2H), 4.15 (s, 2H), 2.42 (s, 1H), 1.19-1.23 (t, J = 7.2 Hz, 3H); ^{13}C NMR (CDCl_3) δ 162.4, 147.2, 138.9, 136.8, 136.0, 129.8, 129.1, 127.5, 127.2, 62.4, 61.1, 21.1, 13.9; MS (ES^+), m/z 341.3 ($\text{M}+23$) $^+$; m.p. = 83-85 $^\circ\text{C}$.

Compound 36c. White solid; yield 37%; ^1H NMR ($(\text{CD}_3)_2\text{CO}$) δ 8.06-8.11 (m, J = 8.4 Hz, J = 8.8 Hz, 4H), 8.01-8.03 (d, J = 8.8 Hz, 2H), 7.86-7.89 (d, J = 8.8 Hz, 2H), 4.42 (s, 2H), 4.10-4.12 (q, J = 7.2 Hz, 2H), 1.12-1.16 (t, J = 7.2 Hz, 3H); ^{13}C NMR (Acetone- d_6) δ 168.4, 163.5, 146.5, 142.6, 139.8, 135.5, 130.2, 129.3, 128.7, 128.3, 62.6, 61.5, 14.2; MS (ES^+), m/z 370.2 ($\text{M}+23$) $^+$; m.p. = 181-183 $^\circ\text{C}$.

Ethyl 2-(4-(2,3-dihydrobenzo[*b*][1,4]dioxin-6-yl)phenylsulfonyl)acetate (36d). White solid; yield 88%; ^1H NMR (CDCl_3) δ 7.95-7.97 (d, J = 8.8 Hz, 2H), 7.70-7.72 (d, J = 8.4 Hz, 2H), 7.14-7.15 (t, J = 2.4 Hz, 1H), 7.11-7.13 (m, J = 8.4 Hz, J = 2.4 Hz, 1H), 6.96-6.98 (d, J = 8.4 Hz, 1H), 4.31 (s, 4H), 4.14 (s, 2H), 4.14-4.17 (q, J = 7.2 Hz, 2H), 1.19-1.23 (t, J = 7.2 Hz, 3H); ^{13}C NMR (CDCl_3) δ 162.4, 146.6, 144.4, 143.9, 136.6, 132.3, 129.1, 127.2, 120.5, 117.9, 116.2, 64.5, 64.4, 62.4, 61.1, 13.9; MS (ES^+), m/z 385.3 ($\text{M}+23$) $^+$; m.p. = 116-118 $^\circ\text{C}$.

Ethyl 2-(4-(isoquinolin-4-yl)phenylsulfonyl)acetate (36e). Light yellow solid; yield 30%; ^1H NMR (CDCl_3) δ 9.33 (s, 1H), 8.50 (s, 1H), 8.11-8.14 (d, J = 8.4 Hz, 2H), 8.08-8.11 (d, J = 7.6 Hz, 1H), 7.80-7.82 (d, J = 8.4 Hz, 1H), 7.73-7.77 (m, J = 8.4 Hz, 2H), 7.67-7.72 (t, J = 8.4 Hz, 2H), 4.20-4.25 (q, J = 7.2 Hz, 2H), 4.23 (s, 2H), 1.24-1.28 (t, J = 7.2 Hz, 3H); ^{13}C NMR

(CDCl₃) δ 162.4, 153.1, 143.5, 142.8, 138.3, 133.6, 131.2, 130.8, 128.9, 128.1, 127.7, 124.0, 62.5, 61.0, 13.9; MS (ES⁺), m/z 356.0 (M+1)⁺; m.p. = 123-125 °C.

Experimental Procedure for *m*-CPBA Oxidation of Ethyl 2-(4-Bromophenylthio)acetate (32g). (Scheme 4.3, reaction v): A solution of *m*-CPBA (110 mg, 75% pure, 0.48 mmol, 1 equiv.) in DCM (3.5 mL) was added dropwise to a stirred solution of ethyl 2-(4-bromophenylthio)acetate (132 mg, 0.48 mmol, 1 equiv.) at 0 °C. Then the reaction mixture was stirred at 0 °C for 25 min. The reaction solution was filtered and diluted with DCM (10 mL) and was washed with saturated NaHCO₃ (8 mL \times 2), H₂O (8 mL) and brine (10 mL). The organic layer was dried over Na₂SO₄. Then the solvent was removed under vacuum to give the crude product, which was purified by column chromatography (Hex/EtOAc 3:1) to give pure ethyl 2-(4-bromophenylsulfinyl)acetate (35a, 119 mg, 85%) as colorless crystals.

Ethyl 2-(4-bromophenylsulfinyl)acetate (35a). Colorless crystals, yield 85%; ¹H NMR (CDCl₃) δ 7.68-7.70 (d, J = 8.4 Hz, 2H), 7.56-7.59 (d, J = 8.8 Hz, 2H), 4.14-4.20 (q, J = 7.2 Hz, 2H), 3.83-3.86 (d, J = 13.6 Hz, 1H), 3.65-3.69 (d, J = 13.6 Hz, 1H), 1.22-1.25 (t, J = 7.2 Hz, 3H); ¹³C NMR (CDCl₃) δ 164.4, 142.2, 132.6, 126.3, 125.8, 62.1, 61.5, 14.0; MS (ES⁺), m/z 290.9 (M+1)⁺; m.p. = 62-63 °C.

General Experimental Procedure for Hydrolysis of Esters. Representative Procedure for Hydrolysis of Methyl 2-(Thiophen-2-ylsulfonyl)acetate (31e) (Scheme 3, reaction d): To a stirred solution of methyl 2-(thiophen-2-ylsulfonyl)acetate (31e, 115 mg, 0.52 mmol, 1 equiv.) in MeOH (5 mL) and THF (1 mL) was added a solution of NaOH (209 mg, 5.22 mmol, 10 equiv.) in H₂O (1 mL) dropwise. The reaction mixture was heated and stirred at 50 °C for 5 h. Then the organic solvents were evaporated and the mixture was diluted with 10 mL H₂O. The solution was adjusted to pH 10 with NaOH (5 M aqueous solution) and extracted with DCM (10 mL \times 3). The

aqueous phase was acidified to pH 2, and further extracted with DCM (30 mL \times 3). The organic phase was dried over Na₂SO₄, and the solvent was removed to get 2-(thiophen-2-ylsulfonyl)acetic acid (34a) as white solid (78 mg, 72%).

2-(Thiophen-2-ylsulfonyl)acetic acid (34a). White solid; yield 72%; ¹H NMR (CD₃OD) δ 7.97 – 7.98 (d, J = 4.8 Hz, 1H), 7.79-7.81 (d, J = 4.0 Hz, 1H), 7.22-7.24 (m, J = 4.0 Hz, J = 4.8 Hz, 1H), 4.36 (s, 2H); ¹³C NMR (CD₃OD) δ 165.7, 141.2, 136.6, 136.5, 129.2, 62.9; MS (ES⁻), m/z 205 (M-1)⁻; m.p. = 124-126 °C.

2-(Phenylsulfonyl)acetic acid (34b). White solid; yield 86%; ¹H NMR (CD₃OD) δ 7.96-7.98 (d, J = 7.6 Hz, 2H), 7.71-7.75 (t, J = 7.6 Hz, 1H), 7.61-7.65 (t, J = 8.0 Hz, 2H), 4.29 (s, 2H); ¹³C NMR (CD₃OD) δ 165.7, 140.7, 135.4, 130.4, 129.7, 61.6; MS (ES⁻), m/z 200 (M-1)⁻; m.p. = 105-107 °C.

Experimental Procedure for the Synthesis of 5-(Bromomethyl)isoxazole (39) (Scheme 4.5, reaction a): A mixture of 5-methylisoxazole (38, 622 mg, 0.6 mL, 7.48 mmol, 1.0 equiv.), NBS (1.33 g, 7.48 mmol, 1.0 equiv.) and 2,2'-azobis(2-methyl-propionitrile) (AIBN, 25 mg, 0.15 mmol, 2% equiv.) in carbon tetrachloride (40 mL) was heated at reflux under irradiation with a tungsten light for 4.5 h. After the solvent was evaporated, ethyl acetate was added (40 mL) and the solution was washed with H₂O (5 mL \times 2), brine (10 mL), and dried over Na₂SO₄. Evaporation of solvent afforded the crude product, which was purified by column chromatography (Hex/EtOAc, 5:1) to give 5-(bromomethyl)-isoxazole (39, 480 mg, 40%) as colorless oil.

5-(Bromomethyl)isoxazole (39). Colorless oil; yield 40%; ¹H NMR (CDCl₃) δ 8.22 (s, 1H), 6.33 (s, 1H), 4.50 (s, 2H).

General Experimental Procedure for Substitution Reaction Between Thiols and 2-Bromo-1,1-dimethoxyethane (42). Representative Procedure for Substitution Between Thiophene-2-thiol (27a) and 2-Bromo-1,1-dimethoxyethane (42) (Scheme 4.6, reaction a): A mixture of absolute ethanol (3 mL) and sodium (152 mg, 6.6 mmol, 1.2 equiv.) in a dry flask was heated to reflux until the solution was clear and cooled in an ice bath (under nitrogen). Thiophene-2-thiol (27a, 767 mg, 0.6 mL, 6.6 mmol, 1.2 equiv.) was added at 0 °C under N₂ and the reaction was stirred for another 15 min at 0 °C. Then 2-bromo-1,1-dimethoxyethane (42, 97%, 930 mg, 0.67 mL, 5.5 mmol, 1.0 equiv.) was added and the reaction was heated at reflux for 2 h. The solution was filtered and solvent was evaporated. Ethyl acetate (50 mL) was added and the solution was washed with H₂O (8 mL × 2), saturated NaCl (8 mL), and dried over Na₂SO₄. Evaporation of solvent gave the crude product which was purified by chromatography (Hex/EtOAc, 20:1) to give 2-(2,2-dimethoxyethylthio)-thiophene (43a, 538 mg, 48%) as colorless oil.

2-(2,2-Dimethoxyethylthio)thiophene (43a). Colorless oil; yield 48%; ¹H NMR (CDCl₃) δ 7.35-7.37 (dd, *J* = 1.2 Hz, *J* = 5.2 Hz), 7.17-7.19 (dd, *J* = 1.2 Hz, *J* = 3.6 Hz, 1H), 6.97-6.99 (t, *J* = 3.6 Hz, *J* = 5.2 Hz, 1H), 3.52-3.54 (t, *J* = 5.6 Hz, 1H), 3.37 (s, 6H), 2.99-3.00 (d, *J* = 5.6 Hz, 2H); ¹³C NMR (CDCl₃) δ 134.0, 134.0, 129.6, 127.5, 103.3, 53.5, 40.9.

(2,2-Dimethoxyethyl)(phenyl)sulfane (43b). Colorless oil; yield 59%; ¹H NMR (CDCl₃) δ 7.40-7.42 (m, 2H), 7.28-7.33 (m, 2H), 7.21-7.23 (t, 1H), 4.54-4.57 (t, *J* = 5.6 Hz, 1H), 3.39 (s, 1H), 3.14-3.15 (d, 5.6 Hz); ¹³C NMR (CDCl₃) δ 136.1, 129.5, 129.1, 129.0, 126.3, 103.2, 53.6, 36.5.

General Experimental Procedure for Hydrolysis of Aldehyde Dimethyl Acetals (43). Representative Procedure for Hydrolysis of 2-(2,2-dimethoxyethylthio)-thiophene (43a) (Scheme 4.6, reaction b): To a solution of 43a (113 mg, 0.55 mmol) in acetone (0.6 mL) was added 1%

HCl (0.6 mL); then the reaction was heated under reflux for 1.5 h. Solvent was evaporated and ethyl acetate (50 mL) was added. The organic layer was washed with saturated NaHCO₃ (8 mL), H₂O (8 mL × 3), brine (8 mL), and dried over Na₂SO₄. The evaporation of solvent afforded the crude product, which was purified by column chromatography (Hex/EtOAc 6:1) to give 2-(thiophen-2-ylthio)acet-aldehyde (44a, 44 mg, 51%) as light yellow oil.

2-(Thiophen-2-ylthio)acetaldehyde (44a). Light yellow oil; yield 51%; ¹H NMR (CDCl₃) δ 9.63-9.65 (t, *J* = 3.2 Hz, 1H), 7.40-7.43 (m, 1H), 7.19-7.20 (m, 1H), 7.99-7.04 (m, 1H), 3.46-3.49 (m, *J* = 3.2 Hz, 2H); MS (ES⁺), *m/z* 159 (M+1)⁺.

2-(Phenylthio)acetaldehyde (44b). Colorless oil, yield 94%; ¹H NMR (CDCl₃) δ 9.54-9.55 (t, *J* = 3.2 Hz, 1H), 7.25-7.38 (m, 5H), 3.60-3.61 (d, *J* = 3.2 Hz, 2H); MS (ES⁺), *m/z* 153 (M+1)⁺.

General Experimental Procedure for Synthesis of Aldoximes from Aldehydes (45). Representative Procedure for Synthesis of 2-(thiophen-2-ylthio)acetaldehyde oxime (45a) (Scheme 4.6, reaction c): A mixture of 2-(thiophen-2-ylthio)acetaldehyde (44a, 144 mg, 0.91 mmol, 1.0 equiv.), hydroxylamine hydrochloride (95 mg, 1.37 mmol, 1.5 equiv.) and potassium bicarbonate (137 mg, 1.37, 1.5 equiv.) in MeOH (14 mL) was stirred at room temperature overnight. The solution was filtered and solvent was evaporated. Then ethyl acetate (50 mL) was added and the solution was washed with H₂O (10 mL × 2), saturated NaCl (8 mL), and dried over anhydrous Na₂SO₄. Evaporation of solvent afforded crude product which was purified by chromatography (Hex/EtOAc, 6:1) to give 2-(thiophen-2-ylthio)acetaldehyde oxime (45a, 106 mg, 67%) as light yellow oil.

2-(Thiophen-2-ylthio)acetaldehyde oxime (45a). Light yellow oil; yield 67%; ^1H NMR ($(\text{CD}_3)_2\text{CO}$, mixture of isomers, ratio 1/1.5) δ 9.94, 10.31(s, 1H), 6.81-7.59 (m, 4H), 3.53-3.55, 3.72-3.74 (d, 2H); MS (ES^+), m/z 174 ($\text{M}+1$) $^+$.

2-(Phenylthio)acetaldehyde oxime (45b). Colorless oil; yield 91%; ^1H NMR ($(\text{CD}_3)_2\text{CO}$, mixture of isomers, ratio 1/1) δ 10.49 (s, 0.5 H), 10.50 (s, 0.5H), 7.66-7.98 (m, 5H), 7.33 (t, 0.5 H), 6.82 (t, 0.5 H), 4.36-4.37 (d, 1H), 4.12-4.13 (d, 1H); MS (ES^+), m/z 168 ($\text{M}+1$) $^+$.

General Experimental Procedure for the Reduction Reaction. Representative Procedure for Reduction of *N*-(2-(thiophen-2-ylsulfonyl)ethyl)-hydroxylamine (47a) (Scheme 6, reaction e): To a solution of 2-(thiophen-2-ylsulfonyl)acetaldehyde oxime (46a, 46 mg, 0.22 mmol, 1.0 equiv.) in MeOH (2 mL) was added sodium cyanoborohydride (37 mg, 0.59 mmol, 2.68 equiv.); then the solution of 4.0 M HCl in 1,4-dioxane (0.2 mL) was added in three portions to maintain PH = 3.0 during the reaction time (3.5 h). Then the solution of 5 N NaOH was added to adjust the pH to 11.0 and then solvent was evaporated. Dichloromethane (50 mL) was added and the solution was washed with saturated NaCl (8 mL \times 2), and dried over anhydrous Na_2SO_4 . Evaporation of solvent afforded the crude product, which was purified by column chromatography (Hex/EtOAc, 2:3) to give *N*-(2-(thiophen-2-ylsulfonyl)ethyl)-hydroxylamine (47a, 14 mg, 30%) as white solid.

N-(2-(Thiophen-2-ylsulfonyl)ethyl)hydroxylamine (47a). White solid, 30% in two steps; ^1H NMR (CDCl_3) δ 7.73-7.77 (m, 2H), 7.17-7.19 (m, 1H), 7.53-7.56 (t, $J = 6.4$ Hz, 2H), 3.37-3.40 (t, $J = 6.4$ Hz, 2H); ^{13}C NMR (CDCl_3) δ 140.2, 134.3, 128.1, 54.7, 47.6; MS (ES^+), m/z 208 ($\text{M}+1$) $^+$.

N-(2-(phenylsulfonyl)ethyl)hydroxylamine (47b). White solid; yield 38%; ^1H NMR (CDCl_3) δ 7.93-7.95 (m, 2H), 7.67-7.71 (m, 1H), 7.57-7.61 (m, 2H), 5.50 (br, 1H), 3.42-3.45 (t, J

= 6.0 Hz, 2H), 3.33-3.36 (t, J = 6.0 Hz, 2H); ^{13}C NMR (CDCl_3) δ 139.3, 133.9, 129.4, 128.0, 53.1, 47.3; 135.8, 129.1, 128.5, 126.0, 57.0, 30.0; MS (ES^+), m/z 202 ($\text{M}+1$) $^+$; m.p. = 67-68 °C.

Bacterial assay

All compounds tested were of high purity (about 98% with impurities being mostly solvents) as judged by ^1H -NMR. The NMR spectra of all final compounds are provided in the Supplemental Section. MM32 and BB886 strains of *V. harveyi* were purchased from ATCC (MM32 #BAA-1121, BB886 #BAA-1118). The quorum sensing assays were performed by following literature.[86, 151, 191] In the AI-1 bioassays, cell-free culture (5% of the test medium volume) from BB886 with OD_{600} of 0.8 -1.2 was added as the source of AI-1. Kanamycin (50 mg/mL) was used as antibiotics in incubation and inoculation.

Cell growth test (MM32)

Cell growth test was performed according to literature protocol.[86] MM32 strain of *V. harveyi* (ATCC #BAA-1121) was grown for 16 h with aeration (175 rpm) at 30 °C in 2 mL of AB medium with antibiotics (kanamycin 50 mg/mL and chloramphenicol 10 mg/mL). Then this bacterial culture was diluted 100-fold with 20 mL AB medium in a 250 mL flask, tested compounds were added and incubated at 30 °C (175 rpm). The OD_{600} values were determined every 20 min. The doubling time was calculated based on the OD_{600} values.

Plate counting test (MM32)

Plate counting test was performed on the basis of the MM32 test.[191] MM32 bacteria were streak-seeded on fresh LM plates and then cultured in the presence of kanamycin 50 mg/mL and chloramphenicol 10 mg/mL. Colonies appeared after overnight incubation at 30 °C. Single colonies were picked from the LM plates and were grown for 16 h with aeration (175 r.p.m.) at 30 °C in 2 mL of Autoinducer Bioassay (AB) medium[192] with antibiotics

(kanamycin 50 mg/mL and chloramphenicol 10 mg/mL). Then the solution was diluted to OD_{600} 0.7 and the bacteria preinoculum was grown in AB-Fe medium with 1.2 mM of iron to a OD_{600} of 1.0-1.1 with shaking at 30 °C (175 r.p.m.) for 1-1.5 h.[101] The resulting inoculum culture was then diluted 5000-fold in fresh AB medium. Solutions of the test compounds in AB medium at concentrations ranging from 0 to 400 mM were prepared in 96-well plates. To these solutions, freshly synthesized DPD solution (pH 7) was added for a final concentration of 5 mM. Boric acid was added to give a final concentration of 1 mM. After addition of bacteria in AB medium, the micro plates were covered with a non-toxic plate sealer and incubated at 30 °C with aeration for 3-5 h. Light production was measured every hour using a Perkin-Elmer luminescence microplate reader. The bacteria solution incubated for 5 h in the presence of a compound at a concentration, which was close to its IC_{50} was diluted to 1:100 and 1:1000, and plated onto fresh LM plates and incubated at 30 °C for 24-48 h. The colonies appeared were counted. The concentration of bacteria, which yielded 30-300 colonies was considered valid and CFU was recorded. The CFU (colony forming unit) ratio ($CFU_{1/2}/CFU_{blank}$) and the luminescence ratio ($Luminescence_{1/2}/Luminescence_{blank}$) were compared.

CHAPTER 5.

CONCLUSIONS

In summary, carbohydrates are known to play important roles in a large number of biological and pathological processes, including cancer metastasis, cell signaling, cell adhesion, embryo development, protein function regulation, cellular communication, and so on. Conceivably, “binders” of carbohydrates of biological importance could be used as diagnostic and therapeutic agents. Currently, lectins are the major available tools in research for carbohydrate recognition. However, the available lectins often have cross-reactivity issues, along with the high costs and stability issues. Therefore, there is a critical need to develop alternatives (lectin mimics). In this regard, there have been very active efforts in developing different “binders”, such as small molecule lectin mimics and aptamers (short DNA or RNA sequence that can bind to the target specifically with high binding affinity). Among all the small molecule lectin mimics developments, boronic acid stands out as the most important building blocks of the sensors design for carbohydrates biomarkers due to its intrinsic binding affinities with diols. The boronic acid-based sensors for carbohydrates are termed “boronlectins”. However, there is always a paradox in boronic acid based sensors design area, that is on one hand, the carbohydrates are universally six-membered ring diols or linear diols. On the other hand, the general consensus always thinks that boronic acids do not bind to six-membered ring sugars. This hinders a lot in the field of boronic acid-based sensors design for biological carbohydrate biomarkers. However, it is always our working hypothesis, that since boronic acid is a lewis acid, under appropriate condition, it could bind to any lewis base/nucleophile, which also includes six-membered ring diols. To address this fundamental question, along with very limited precedents, we provided a concrete experimental evidence of our long-term working hypothesis. Specifically,

a new class of boronic acid, isoquinolinyboronic acid, was found to have remarkably high binding affinities with fluorescence change upon binding to representative sugars. Most importantly, these isoquinolinyboronic acids showed weak but very encouraging bindings with six-membered ring diols. All the tested isoquinolinyboronic acid showed bindings with *cis*-1,2-cyclohexanediol. 4-IQBA and 6-IQBA also showed bindings with methyl- α -D-glucopyranose. All these promising results paves the way of using boronic acids, especially isoquinolinyboronic acid as building blocks for chemosensors design for biological carbohydrates biomarkers, which universally contain six-membered ring and linear diols. Aptamer provides another alternative way for sensors development for carbohydrates biomarkers as lectin mimics. Compared to lectins, they are normally cheaper and more stable. However, there is much less options. Another challenging area for aptamer-based lectin mimics development is the difficulty to differentiate changes in glycosylation patterns of a glycoprotein, which affect the function of a glycoprotein and thus recognized as biomarkers. To address this major challenge, our group first demonstrated that the incorporation of a boronic acid into DNA would allow for the aptamer selection process to gravitate towards the “sweet spot” (glycosylation site). To examine the generality of boronic acid incorporation, increase the structural diversity, and broaden the application of boronic acid-modified DNA, a series of B-TTP analogues with simplified structures were designed, synthesized, and successfully incorporated into DNA. A simple route was also developed using 1,7-octadiyne as a linker for both Sonogashira coupling with thymidine and CuAAC tethering of the boronic acid moiety. This paves the way for the preparation of a large number of B-TTPs with different structural features for aptamer selection or array analysis. Finally, bacterial quorum sensing has received much attention in recent years because of its relevance to pathological events such as biofilm formation. As one of the very first groups that developed a

series of antagonists for AI-2 mediated quorum sensing, we herein designed and synthesized a series of analogues based on the structures of two lead inhibitors identified through virtual screening. Besides, we also examined their inhibitory activities, twelve of which showed equal or better inhibitory activities compared with the lead inhibitors. The best compound showed an IC_{50} of about 6 mM in a whole cell assay using *Vibrio harveyi* as the model organism. This encouraging results and SAR discuss also paves the way for the finding of more potent compound through further structure optimization.

REFERENCES

1. Asher, S.A., Alexeev, V.L., Goponenko, A.V., Sharma, A.C., Lednev, I.K., Wilcox, C.S., and Finegold, D.N., *Photonic Crystal Carbohydrate Sensors: Low Ionic Strength Sugar Sensing*. J. Am. Chem. Soc., 2003. **125**: p. 3322 -3329.
2. Bielecki, M., Eggert, H., and Norrild, J.C., *A Fluorescent Glucose Sensor Binding Covalently to All Five Hydroxy Groups of α -D-Glucose. A Reinvestigation*. J. Chem. Soc., Perkin Trans. 2, 1999: p. 449-455.
3. Eggert, H., Frederiksen, J., Morin, C., and Norrild, J.C., *A New Glucose-selective Fluorescent Bisboronic Acid. First Report of Strong α -Furanose Complexation in Aqueous Solution at Physiological pH*. J. Org. Chem., 1999. **64**: p. 3846-3852.
4. James, T.D., Sandanayake, K.R.A.S., Iguchi, R., and Shinkai, S., *Novel Saccharide-Photoinduced Electron Transfer Sensors Based on the Interaction of Boronic Acid and Amine*. J. Am. Chem. Soc., 1995. **117**: p. 8982-8987.
5. Yang, W., Fan, H., Gao, S., Gao, X., Ni, W., Karnati, V., Hooks, W.B., Carson, J., Weston, B., and Wang, B., *The First Fluorescent Diboronic Acid Sensor Specific for Hepatocellular Carcinoma Cells Expressing Sialyl Lewis X*. Chem. Biol., 2004. **11**: p. 439-448.
6. Yoon, J. and Czarnik, A.W., *Fluorescent Chemosensors of Carbohydrates. A Means of Chemically Communicating the Binding of Polyols in Water Based on Chelation-Enhanced Quenching*. J. Am. Chem. Soc., 1992. **114**: p. 5874-5875.
7. Badugu, R., Lakowicz, J.R., and Geddes, C.D., *Anion Sensing Using Quinolinium Based Boronic Acid Probes*. Curr. Anal. Chem., 2005. **1**(2): p. 157-170.
8. Cao, H.S. and Heagy, M.D., *Fluorescent Chemosensors for Carbohydrates: A Decade's worth of Bright Spies for Saccharides in Review*. J. Fluor., 2004. **14**: p. 569-584.
9. Kim, S.K., Kim, H.N., Xiaoru, Z., Lee, H.N., Lee, H.N., Soh, J.H., Swamyand, K.M.K., and Yoon, J., *Recent Development of Anion Selective Fluorescent Chemosensors*. Supramol. Chem., 2007. **19**(4-5): p. 221-227.

10. Mader, H.S. and Wolfbeis, O.S., *Boronic Acid Based Probes for Microdetermination of Saccharides and Glycosylated Biomolecules*. *Microchimica Acta*, 2008. **162**(1-2): p. 1-34.
11. Pickup, J.C., Hussain, F., Evans, N.D., Rolinski, O.J., and Birch, D.J.S., *Fluorescence-Based Glucose Sensors*. *Biosens. & Bioelectr.*, 2005. **20**(12): p. 2555-2565.
12. Yan, J., Fang, H., and Wang, B., *Boronolectins and Fluorescent Boronolectins-An Examination of the Detailed Chemistry Issues Important for their Design*. *Med. Res. Rev.*, 2005. **25**: p. 490-520.
13. Norrild, J.C. and Eggert, H., *Evidence for Mono- and Bidentate Boronate Complexes of Glucose in the Furanose Form. Application of $^1J_{C-C}$ Coupling Constants as a Structural Probe*. *J. Am. Chem. Soc.*, 1995. **117**: p. 1479-1484.
14. Springsteen, G. and Wang, B., *Alizarin Red as a General Fluorescent Reporter for Studying the Binding of Boronic Acids and Carbohydrates*. *Chem. Commun.*, 2001: p. 1608-1609.
15. Aharoni, R., Bronstheyn, M., Jabbour, A., Zaks, B., Srebnik, M., and Steinberg, D., *Oxazaborolidine Derivatives Inducing Autoinducer-2 signal Transduction in *Vibrio harveyi**. *Bioorg. Med. Chem.*, 2008. **16**(4): p. 1596-1604.
16. Cho, B.T., *Oxazaborolidines as Asymmetric Inducers for the Reduction of Ketones and Ketimines*. *Boronic Acids*, 2005: p. 411-439.
17. Jabbour, A., Steinberg, D., Dembitsky, V.M., Moussaieff, A., Zaks, B., and Srebnik, M., *Synthesis and Evaluation of Oxazaborolidines for Antibacterial Activity against *Streptococcus Mutans**. *J. Med. Chem.*, 2004. **47**: p. 2409-2410.
18. Mohler, L.K. and Czarnik, A.W., *α -Amino Acid Chelative Complexation by an Arylboronic Acid*. *J. Am. Chem. Soc.*, 1994. **116**: p. 2233.
19. Gamsey, S., Miller, A., Olmstead, M.M., Beavers, C.M., Hirayama, L.C., Pradhan, S., Wessling, R.A., and Singaram, B., *Boronic Acid-Based Bipyridinium Salts as Tunable Receptors for Monosaccharides and α -Hydroxycarboxylates*. *J. Am. Chem. Soc.*, 2007. **129**(5): p. 1278-1286.
20. Gray Jr., C.W. and Houston, T.A., *Boronic Acid Receptors for α -Hydroxycarboxylates: High Affinity of Shinkai's Glucose Receptor for Tartrate*. *J. Org. Chem.*, 2002. **67**: p. 5426-5428.
21. Wang, Z., Zhang, D.Q., and Zhu, D.B., *A New Saccharide Sensor Based on a Tetrathiafulvalene-Anthracene Dyad with a Boronic Acid Group*. *J. Org. Chem.*, 2005. **70**: p. 5729-5732.
22. Wiskur, S.L., Lavigne, J.L., Ait-Haddou, H., Lynch, V., Chiu, Y.H., Canary, J.W., and Anslyn, E.V., *pKa Values and Geometries of Secondary and Tertiary Amines Complexed to Boronic Acids-Implications for Sensor Design*. *Org. Lett.*, 2001. **3**: p. 1311-1314.
23. Yang, W., Gao, S., and Wang, B., *Biologically Active Boronic Acid Compounds*, in *Organoboronic Acids*, D. Hall, Editor 2005, John Wiley and Sons: New York. p. 481-512.
24. Hiratake, J. and Oda, J., *Aminophosphonic and Aminoboronic Acids as Key Elements of a Transition State Analogue Inhibitor of Enzymes*. *Biosci. Biotech. Biochem.*, 1997. **61**: p. 211-218.

25. Gallardo-Williams, M.T., Maronpot, R.R., Wine, R.N., Brunssen, S.H., and Chapin, R.E., *Inhibition of the Enzymatic Activity of Prostate-specific Antigen by Boric Acid and 3-Nitrophenyl Boronic Acid*. *Prostate*, 2003. **54**: p. 44-49.
26. Adams, J. and Kauffman, M., *Development of the Proteasome Inhibitor Velcade((TM)) (Bortezomib)*. *Can. Invest.*, 2004. **22**: p. 304-311.
27. Bacha, U., Barrila, J., Velazquez-Campoy, A., Leavitt, S.A., and Freire, E., *Identification of Novel Inhibitors of the SARS Coronavirus Main Protease 3CLpro*. *Biochemistry*, 2004. **43**: p. 4906-4912.
28. Holyoak, T., Wilson, M.A., Fenn, T.D., Kettner, C.A., Petsko, G.A., Fuller, R.S., and Ringe, D., *2.4 Angstrom Resolution Crystal Structure of the Prototypical Hormone-processing Protease Kex2 in Complex with an Ala-Lys-Arg Boronic Acid Inhibitor*. *Biochemistry*, 2003. **42**: p. 6709-6718.
29. Snow, R.J., Bachovchin, W.W., Barton, R.W., Campbell, S.J., Coutts, S.J., Freeman, D.M., Gutheil, W.G., Kelly, T.A., Kennedy, C.A., Krolikowski, D.A., Leonard, S.F., Pargellis, C.A., Tong, I., and Adams, J., *Studies on Proline Boronic Acid Dipeptide Inhibitors of Dipeptidyl Peptidase-iv - Identification of a Cyclic Species Containing a B-N Bond*. *J. Am. Chem. Soc.*, 1994. **116** p. 10860-10869.
30. Geele, G., Garrett, E., and Hageman, H.J., *Effect of Benzene Boronic Acids on Sporulation and on Production of Enzymes in Bacillus subtilis Cells. Spores VI*. *Am. Soc. Micro.*, 1975: p. 391-396.
31. Farr-Jones, S., Smith, S.O., Kettner, C.A., Griffin, R.G., and Bachovchin, W.W., *Crystal Versus Solution Structure of Enzymes: NMR Spectroscopy of a Peptide Boronic Acid-serine Protease Complex in the Crystalline State*. *Proc. Natl. Acad. Sci. U S A*, 1989. **86**(18): p. 6922-6924.
32. Groll, M., Berkers, C.R., Ploegh, H.L., and Ovaa, H., *Crystal Structure of the Boronic Acid-based Proteasome Inhibitor Bortezomib in Complex with the Yeast 20S Proteasome*. *Structure*, 2006. **14**(3): p. 451-456.
33. Matthews, D.A., Alden, R.A., Birktoft, J.J., Freer, S.T., and Kraut, J., *X-ray Crystallographic Study of Boronic Acid Adducts with Subtilisin BPN' (Novo). A Model for the Catalytic Transition State*. *J. Biol. Chem.*, 1975. **250**(18): p. 7120-7126.
34. Powers, R.A., Blazquez, J., Weston, G.S., Morosini, M.I., Baquero, F., and Shoichet, B.K., *The Complexed Structure and Antimicrobial Activity of a Non-beta-lactam Inhibitor of AmpC Beta-lactamase*. *Protein Sci.*, 1999. **8**(11): p. 2330-2337.
35. Powers, R.A. and Shoichet, B.K., *Structure-based Approach for Binding Site Identification on AmpC Beta-lactamase*. *J. Med. Chem.*, 2002. **45**(15): p. 3222-3234.
36. Stoll, V.S., Eger, B.T., Hynes, R.C., Martichonok, V., Jones, J.B., and Pai, E.F., *Differences in Binding Modes of Enantiomers of 1-acetamido Boronic Acid Based Protease Inhibitors: Crystal Structures of Gamma-chymotrypsin and Subtilisin Carlsberg Complexes*. *Biochemistry*, 1998. **37**(2): p. 451-462.
37. Zhong, S., Jordan, F., Kettner, C.A., and Polgar, L., *Observation of Tightly Bound Boron-11 Nuclear Magnetic Resonance Signals on Serine Proteases. Direct Solution Evidence for Tetrahedral Geometry around the Boron in the Putative Transition-state Analogs*. *J. Am. Chem. Soc.*, 1991. **113**: p. 9429-9435.
38. Bone, R., Frank, D., Kettner, C.A., and Agard, D.A., *Structural Analysis of Specificity: a-Lytic Protease Complexes with Analogues of Reaction Intermediates*. *Biochemistry*, 1989. **28**: p. 7600-7609.

39. Badugu, R., Lakowicz, J.R., and Geddes, C.D., *Excitation and Emission Wavelength Ratiometric Cyanide-Sensitive Probes for Physiological Sensing*. *Anal. Chem.*, 2004. **327**: p. 82-90.
40. Badugu, R., Lakowicz, J.R., and Geddes, C.D., *Cyanide-Sensitive Fluorescent Probes*. *Dyes Pigm.*, 2005. **64**: p. 49-55.
41. Badugu, R., Lakowicz, J.R., and Geddes, C.D., *A Wavelength-Ratiometric Fluoride-Sensitive Probe based on the Quinolinium Nucleus and Boronic Acid Moiety*. *Sensors Actuators B-Chem.*, 2005. **104**: p. 103-110.
42. DiCesare, N. and Lakowicz, J.R., *New Sensitive and Selective Fluorescent Probes for Fluoride Using Boronic Acids*. *Anal. Biochem.*, 2002. **301**: p. 111-116.
43. Oehlke, A., Auer, A.A., Jahre, I., Walfort, B., Ruffer, T., Zoufala, P., Lang, H., and Spange, S., *Nitro-substituted Stilbeneboronate Pinacol Esters and their Fluoro-adducts. Fluoride Ion Induced Polarity Enhancement of Arylboronate Esters*. *J. Org. Chem.*, 2007. **72**(12): p. 4328-4339.
44. Swamy, K.M.K., Lee, Y.J., Lee, H.N., Chun, J., Kim, Y., Kim, S.J., and Yoon, J., *A New Fluorescein Derivative Bearing a Boronic Acid Group as a Fluorescent Chemosensor for Fluoride Ion*. *J. Org. Chem.*, 2006. **71**: p. 8626-8628.
45. Cooper, C.R., Spencer, N., and James, T.D., *Selective Fluorescence Detection of Fluoride Using Boronic Acids*. *Chem. Commun.*, 1998: p. 1365-1366.
46. Kondo, K., Shiomi, Y., Saisho, M., Harada, T., and Shinkai, S., *Specific Complexation of Disaccharides with Diphenyl-3,3'-diboronic Acid that Can Be Detected by Circular Dichroism*. *Tetrahedron*, 1992. **48**: p. 8239-8252.
47. Manku, S. and Hall, D.G., *Synthesis, Decoding, and Preliminary Screening of a Bead-supported Split-pool Library of Triboronic Acid Receptors for Complex Oligosaccharides*. *Aust. J. Chem.*, 2007. **60**(11): p. 824-828.
48. Sorensen, M.D., Martins, R., and Hindsgaul, O., *Assessing the Terminal Glycosylation of a Glycoprotein by the Naked Eye*. *Angew. Chem. Int. Ed. Engl.*, 2007. **46**(14): p. 2403-2407.
49. Li, M., Lin, N., Huang, Z., Du, L., Fang, H., Altier, C., and Wang, B., *Selecting Aptamers for a Glycoprotein through the Incorporation of the Boronic Acid Moiety*. *J. Am. Chem. Soc.*, 2008. **130**: p. 12636-12638.
50. Yang, W., Gao, S., Gao, X., Karnati, V.R., Ni, W., Wang, B., Hooks, W.B., Carson, J., and Weston, B., *Diboronic Acids as Fluorescent Probes for Cells Expressing Sialyl Lewis X*. *Bioorg. Med. Chem. Lett*, 2002. **12**: p. 2175-2177.
51. Zhong, Z. and Anslyn, E.V., *A Colorimetric Sensing Ensemble for Heparin*. *J. Am. Chem. Soc.*, 2002. **124**: p. 9014 -9015.
52. Zhu, L., Zhong, Z., and Anslyn, E.V., *Guidelines in Implementing Enantioselective Indicator-Displacement Assays for α -Hydroxycarboxylates and Diols*. *J. Am. Chem. Soc.*, 2005. **127**: p. 4260 -4269.
53. Duggan, P.J. and Offermann, D.A., *The Preparation of Solid-supported Peptide Boronic Acids Derived from 4-Borono-L-phenylalanine and their Affinity for Alizarin*. *Aust. J. Chem.*, 2007. **60**(11): p. 829-834.
54. Lin, N., Yan, J., Huang, Z., Altier, C., Li, M.Y., Carrasco, N., Suyemoto, M., Johnston, L., Wang, S.M., Wang, Q., Fang, H., Caton-Williams, J., and Wang, B.H., *Design and Synthesis of Boronic-acid-labeled Thymidine Triphosphate for Incorporation into DNA*. *Nucleic Acids Res.*, 2007. **35**(4): p. 1222-1229.

55. Manimala, J.C., Wiskur, S.L., Ellington, A.D., and Anslyn, E.V., *Tuning the Specificity of a Synthetic Receptor Using a Selected Nucleic Acid Receptor*. *J. Am. Chem. Soc.*, 2004. **126**: p. 16515-16519.
56. Liu, C.C., Mack, A.V., Tsao, M.L., Mills, J.H., Lee, H.S., Choe, H., Farzan, M., Schultz, P.G., and Smider, V.V., *Protein Evolution with an Expanded Genetic Code*. *Proc. Nat. Acad. Sci. U.S.A.*, 2008. **105**(46): p. 17688-17693.
57. Brustad, E., Bushey, M.L., Lee, J.W., Groff, D., Liu, W., and Schultz, P.G., *A Genetically Encoded Boronate-Containing Amino Acid*. *Angew. Chem. Int. Ed. Engl.*, 2008. **47**(43): p. 8220-8223.
58. Jin, S., Cheng, Y.F., Reid, S., Li, M., and Wang, B., *Carbohydrate Recognition by Boronolactams, Small Molecules, and Lectins*. *Med. Res. Rev.*, 2010. **30**: p. 171-257.
59. Gao, X., Zhang, Y., and Wang, B., *A Highly Fluorescent Water-soluble Naphthalene-based Boronic Acid Reporter for Saccharide Sensing that also Shows Ratiometric UV Changes*. *Tetrahedron*, 2005. **61**: p. 9111-9117.
60. Gao, X., Zhang, Y., and Wang, B., *Naphthalene-Based Water-Soluble Fluorescent Boronic Acid Isomers Suitable for Ratiometric and Off-On Sensing of Saccharides at Physiological pH*. *New J. Chem.*, 2005. **29**: p. 579-586.
61. Zhang, Y., Ballard, C.E., Zheng, S., Gao, X., Ko, K.C., Yang, H., Brandt, G., Lou, X., Tai, P.C., Lu, C.-D., and Wang, B., *Design, Synthesis and Evaluation of Efflux Substrate-metal Chelator Conjugates as Potential Anti-microbial Agents*. *Bioorg. Med. Chem. Lett.*, 2007. **17**: p. 707-711.
62. Zhang, Y., Li, M., Chandrasekaran, S., Gao, X., Fang, X., Lee, H.-W., Hardcastle, K., Yang, J., and Wang, B., *A Unique Quinolineboronic Acid-based Supramolecular Structure that Relies on Double Intermolecular B-N Bonds for Self-assembly in Solid State and in Solution*. *Tetrahedron*, 2007. **63**: p. 3287-3292.
63. Liu, S.J., Zhao, Q., Xu, W.J., and Huang, W., *Fluoride Probe Based on Organoboron Compounds*. *Progress in Chemistry*, 2008. **20**(11): p. 1708-1715.
64. Springsteen, G. and Wang, B., *A Detailed Examination of Boronic Acid-Diol Complexation*. *Tetrahedron*, 2002. **58**: p. 5291-5300.
65. Yan, J., Springsteen, G., Deeter, S., and Wang, B., *The Relationship among pKa, pH, and Binding Constants in the Interactions between Boronic Acids and Diols-It is not as Simple as It Appears*. *Tetrahedron*, 2004. **60**: p. 11205-11209.
66. Hall, D.G., *Structure, Properties and Preparation of Boronic Acid Derivatives. Overview of their Reactions and Applications*, in *Boronic Acids*, D.G. Hall, Editor 2005, Wiley-VCH: Weinheim. p. 1-99.
67. Bachovchin, W.W., Wong, W.Y., Farr-Jones, S., Shenvi, A.B., and Kettner, C.A., *Nitrogen-15 NMR Spectroscopy of the Catalytic-triad Histidine of a Serine Protease in Peptide Boronic Acid Inhibitor Complexes*. *Biochemistry*, 1988. **27**(20): p. 7689-7697.
68. Ivanov, D., Bachovchin, W.W., and Redfield, A.G., *Boron-11 Pure Quadrupole Resonance Investigation of Peptide Boronic Acid Inhibitors Bound to Alpha-lytic Protease*. *Biochemistry*, 2002. **41**(5): p. 1587-1590.
69. Tsilikounas, E., Kettner, C.A., and Bachovchin, W.W., *11B NMR Spectroscopy of Peptide Boronic Acid Inhibitor Complexes of Alpha-lytic Protease. Direct Evidence for Tetrahedral Boron in both Boron-Histidine and Boron-serine Adduct Complexes*. *Biochemistry*, 1993. **32**(47): p. 12651-12655.

70. Weston, G.S., Blazquez, J., Baquero, F., and Shoichet, B.K., *Structure-based Enhancement of Boronic Acid-based Inhibitors of AmpC Beta-lactamase*. J. Med. Chem., 1998. **41**(23): p. 4577-4586.
71. Gray, C.W., Johnson, L.L., Walker, B.T., Sleevi, M.C., Campbell, A.S., Plourde, R., and Houston, T.A., *Specific Sensing Between Inositol Epimers by a bis(Boronate)*. Bioorg. Med. Chem. Lett., 2005. **15**: p. 5416-5418.
72. Karnati, V., Gao, X., Gao, S., Yang, W., Sabapathy, S., Ni, W., and Wang, B., *A Selective Fluorescent Sensor for Glucose*. Bioorg. Med. Chem. Lett., 2002. **12**: p. 3373-3377.
73. Hageman, J.H. and Kuehn, G.D., *Boronic Acid Matrices for the Affinity Chromatography of Glycoproteins and Enzymes*. Met. Mol. Biol., 1992. **11**: p. 45-71.
74. Kajjout, M., Rolando, M., and Cren-Olivé, C. *A New Reagent for the Selective Characterization of Glycoproteins, on 2D Gel*. in *Second International Symposium on Separation and Characterization of Natural and Synthetic Macromolecules (SCM-2)*, Amsterdam. 2005.
75. Lee, J.H., Kim, Y., Ha, M.Y., Lee, E.K., and Choo, J., *Immobilization of Aminophenylboronic Acid on Magnetic Beads for the Direct Determination of Glycoproteins by Matrix Assisted Laser Desorption Ionization Mass Spectrometry*. J. Am. Soc. Mass Spectrom., 2005. **16**(9): p. 1456-1460.
76. Bouriotis, V., Galpin, I.J., and Dean, P.D.G., *Applications of Immobilized Phenylboronic Acids as Supports for Group-Specific Ligands in the Affinity-Chromatography of Enzymes*. J. Chromatogr., 1981. **210**: p. 267-278.
77. Psotova, J. and Janiczek, O., *Boronate Affinity-Chromatography and the Applications*. Chem. Listy, 1995. **89**: p. 641-648.
78. Seliger, H. and Genrich, V., *Synthesis of M-Aminophenylboronic Acid, Effector in Affinity Chromatography of Nucleic-Acids*. Experientia, 1974. **30**(12): p. 1480-1481.
79. Singhal, R.P., Ramamurthy, B., Govindraj, N., and Sarwar, Y., *New Ligands for Boronate Affinity-Chromatography - Synthesis and Properties*. J. Chromatogr., 1991. **543**(1): p. 17-38.
80. Breitenbach, J.M. and Hausinger, R.P., *Proteus mirabilis Urease. Partial Purification and Inhibition by Boric Acid and Boronic Acids*. Biochem. J., 1988. **250**(3): p. 917-920.
81. Soundaramani, S., Badawi, M., Montañó-Kohlrust, C., and Hageman, J.H., *Boronic Acids for Affinity Chromatography: Spectral Methods for Determination of Ionization and Diol-binding Constants*. Anal. Biochem., 1989. **178**: p. 125-134.
82. Gao, X.B., Yang, J.H., Huang, F., Wu, X., Li, L., and Sun, C.X., *Progresses of Derivatization Techniques for Analyses of Carbohydrates*. Analy. Lett., 2003. **36**: p. 1281-1310.
83. Williams, D., Lee, T.D., Dinh, N., and Young, M.K., *Oligosaccharide Profiling: the Facile Detection of Mono-, Di- and Oligosaccharides by Electrospray Orthogonal Time-Of-Flight Mass Spectrometry using 3-Aminophenylboronic Acid Derivatization*. Rapid Commun. Mass Spectrom., 2000. **14**: p. 1530-1537.
84. Zaikin, V.G. and Halket, J.M., *Derivatization in Mass Spectrometry - 4. Formation of Cyclic Derivatives*. Eur. J. Mass Spectrom., 2004. **10**: p. 555-568.
85. Yang, W., He, H., and Drucekhammer, D.G., *Computer-Guided Design in Molecular Recognition: Design and Synthesis of a Glucopyranose Receptor*. Angew. Chem. Int. Ed., 2001. **40**: p. 1714-1718.

86. Jin, S., Li, M., Zhu, C., Tran, V., and Wang, B., *Computer-based De Novo Design, Synthesis, and Evaluation of Boronic Acid-based Artificial Receptors for Selective Recognition of Dopamine*. *ChemBioChem*, 2008. **9**(9): p. 1431-1438.
87. Wang, W., Gao, S., and Wang, B., *Building Fluorescent Sensors by Template Polymerization: The Preparation of a Fluorescent Sensor for D-Fructose*. *Org. Lett.*, 1999. **1**: p. 1209-1212.
88. Gao, S., Wang, W., and Wang, B., *Building Fluorescent Sensors for Carbohydrates Using Template-directed Polymerizations*. *Bioorg. Chem.*, 2001. **29**: p. 308-320.
89. Dowlut, M. and Hall, D.G., *An Improved Class of Sugar-Binding Boronic Acids, Soluble and Capable of Complexing Glycosides in Neutral Water*. *J. Am. Chem. Soc.*, 2006. **128**: p. 4226 -4227.
90. Berube, M., Dowlut, M., and Hall, D.G., *Benzoboroxoles as Efficient Glycopyranoside-binding Agents in Physiological Conditions: Structure and Selectivity of Complex Formation*. *J. Org. Chem.*, 2008. **73**(17): p. 6471-6479.
91. Basu, P.S., Majhi, R., and Batabyal, S.K., *Lectin and Serum-PSA Interaction as a Screening Test for Prostate Cancer*. *Clin. Biochem.*, 2003. **36**(5): p. 373-376.
92. Belanger, A., van Halbeek, H., Graves, H.C., Grandbois, K., Stamey, T.A., Huang, L., Poppe, I., and Labrie, F., *Molecular Mass and Carbohydrate Structure of Prostate Specific Antigen: Studies for Establishment of an International PSA Standard*. *Prostate*, 1995. **27**(4): p. 187-197.
93. Dudkin, V.Y., Miller, J.S., and Danishefsky, S.J., *Chemical Synthesis of Normal and Transformed PSA Glycopeptides*. *J. Am. Chem. Soc.*, 2004. **126**: p. 736 -738.
94. Huber, P.R., Schmid, H.P., Mattarelli, G., Strittmatter, B., van Steenbrugge, G.J., and Maurer, A., *Serum Free Prostate Specific Antigen: Isoenzymes in Benign Hyperplasia and Cancer of the Prostate*. *Prostate*, 1995. **27**(4): p. 212-219.
95. Huizen, I.V., Wu, G., Moussa, M., Chin, J.L., Fenster, A., Lacefield, J.C., Sakai, H., Greenberg, N.M., and Xuan, J.W., *Establishment of a Serum Tumor Marker for Preclinical Trials of Mouse Prostate Cancer Models*. *Clin. Cancer Res.*, 2005. **11**(21): p. 7911-7919.
96. Jankovic, M.M. and Kosanovic, M.M., *Glycosylation of Urinary Prostate-specific Antigen in Benign Hyperplasia and Cancer: Assessment by Lectin-binding Patterns*. *Clin. Biochem.*, 2005. **38**(1): p. 58-65.
97. Kano, Y., Mashiko, T., Danbara, M., Takayama, Y., Ohtani, S., Egawa, S., Baba, S., and Akahoshi, T., *Changes in Serum IgG Oligosaccharide Chains with Prostate Cancer Progression*. *Anticancer Res.*, 2004. **24**(5B): p. 3135-3139.
98. Ohyama, C., Hosono, M., Nitta, K., Oh-eda, M., Yoshikawa, K., Habuchi, T., Arai, Y., and Fukuda, M., *Carbohydrate Structure and Differential Binding of Prostate Specific Antigen to Maackia Amurensis Lectin between Prostate Cancer and Benign Prostate Hypertrophy*. *Glycobiology*, 2004. **14**(8): p. 671-679.
99. Tabares, G., Jung, K., Reiche, J., Stephan, C., Lein, M., Peracaula, R., de Llorens, R., and Hoesel, W., *Free PSA forms in Prostatic Tissue and Sera of Prostate Cancer Patients: Analysis by 2-DE and Western Blotting of Immunopurified Samples*. *Clin. Biochem.*, 2007. **40**(5-6): p. 343-350.
100. Tabares, G., Radcliffe, C.M., Barrabes, S., Ramirez, M., Aleixandre, R.N., Hoesel, W., Dwek, R.A., Rudd, P.M., Peracaula, R., and de Llorens, R., *Different Glycan Structures*

- in Prostate-specific Antigen from Prostate Cancer Sera in Relation to Seminal Plasma PSA*. *Glycobiology*, 2006. **16**(2): p. 132-145.
101. Villoutreix, B.O., Getzoff, E.D., and Griffin, J.H., *A Structural Model for the Prostate Disease Marker, Human Prostate-specific Antigen*. *Protein Sci.*, 1994. **3**(11): p. 2033-2044.
 102. Ellington, A.D. and Szostak, J.W., *In Vitro Selection of RNA Molecules that Bind Specific Ligands*. *Nature*, 1990. **346** p. 818 - 822
 103. Robertson, D.L. and Joyce, G.F., *Selection in vitro of an RNA Enzyme that Specifically Cleaves Single-stranded DNA*. *Nature*, 1990. **344**: p. 467-468.
 104. Gold, L. and Tuerk, C., *Systematic Evolution of Ligands by Exponential Enrichment: RNA Ligands to Bacteriophage T4 DNA Polymerase*. *Science*, 1990. **249**(4968): p. 505-10.
 105. Gravel, M., Thompson, K.A., Zak, M., Berube, C., and Hall, D.G., *Universal Solid-phase Approach for the Immobilization, Derivatization, and Resin-to-resin Transfer Reactions of Boronic Acids*. *J. Org. Chem.*, 2002. **67**(1): p. 3-15.
 106. James, T.D. and Shinkai, S., *Artificial Receptors as Chemosensors for Carbohydrates*. *Top. Curr. Chem.*, 2002. **218**: p. 159-200.
 107. Striegler, S., *Selective Carbohydrate Recognition by Synthetic Receptors in Aqueous Solution*. *Curr. Org. Chem.*, 2003. **7**(1): p. 81-102.
 108. Norrild, J.C. and Sotofte, I., *Design, Synthesis and Structure of New Potential Electrochemically Active Boronic Acid-Based Glucose Sensors*. *J. Chem. Soc., Perkin Trans. 2*, 2002(2): p. 303-311.
 109. Zou, Y., Broughton, D.L., Bicker, K.L., Thompson, P.R., and Lavigne, J.J., *Peptide Boronic Lectins (PBLs): A New Tool for Glycomics and Cancer Diagnostics*. *ChemBioChem.*, 2007. **8**(17): p. 2048-2051.
 110. Duggan, P.J. and Offermann, D.A., *Remarkably Selective Saccharide Recognition by Solid-supported Peptide Boronic Acids*. *Tetrahedron*, 2009. **65**(1): p. 109-114.
 111. Jiang, S., Escobedo, J.O., Kim, K.K., Alpturk, O., Samoei, G.K., Fakayode, S.O., Warner, I.M., Rusin, O., and Strongin, R.M., *Stereochemical and Regiochemical Trends in the Selective Detection of Saccharides*. *J. Am. Chem. Soc.*, 2006. **128**(37): p. 12221-12228.
 112. Zheng, S.L., Lin, N., Reid, S., and Wang, B.H., *Effect of Extended Conjugation with a Phenylethynyl Group on the Fluorescence Properties of Water-soluble Arylboronic Acids*. *Tetrahedron*, 2007. **63**(25): p. 5427-5436.
 113. Jin, S., Wang, J.F., Li, M.Y., and Wang, B.H., *Synthesis, Evaluation, and Computational Studies of Naphthalimide-based Long-wavelength Fluorescent Boronic Acid Reporters*. *Chem. Eur. J.*, 2008. **14**(9): p. 2795-2804.
 114. Akay, S., Yang, W.Q., Wang, J.F., Lin, L., and Wang, B.H., *Synthesis and Evaluation of Dual Wavelength fluorescent benzo[b]thiophene Boronic Acid Derivatives for Sugar Sensing*. *Chem. Biol. Drug Des.*, 2007. **70**(4): p. 279-289.
 115. Edwards, N.Y., Sager, T.W., McDevitt, J.T., and Anslyn, E.V., *Boronic Acid Based Peptidic Receptors for Pattern-based Saccharide Sensing in Neutral Aqueous Media, an Application in Real-life Samples*. *J. Am. Chem. Soc.*, 2007. **129**(44): p. 13575-13583.
 116. Schiller, A., Wessling, R.A., and Singaram, B., *A Fluorescent Sensor Array for Saccharides based on Boronic Acid Appended Bipyridinium Salts*. *Angew. Chem. Int. Ed. Engl.*, 2007. **46**(34): p. 6457-6459.

117. Chi, L., Zhao, J.Z., and James, T.D., *Chiral Mono Boronic Acid as Fluorescent Enantioselective Sensor for Mono α -Hydroxyl Carboxylic Acids*. *J. Org. Chem.*, 2008. **73**(12): p. 4684-4687.
118. Liang, X.F., James, T.D., and Zhao, J.Z., *6,6'-Bis-substituted BINOL Boronic Acids as Enantio Selective and Chemoselective Fluorescent Chemosensors for D-sorbitol*. *Tetrahedron*, 2008. **64**(7): p. 1309-1315.
119. Luvino, D., Gasparutto, D., Reynaud, S., Smietana, M., and Vasseur, J.J., *Boronic acid-based Fluorescent Receptors for Selective Recognition of Thymine Glycol*. *Tetrahedron Lett.*, 2008. **49**(42): p. 6075-6078.
120. Swamy, K.M.K., Ko, S.K., Kwon, S.K., Lee, H.N., Mao, C., Kim, J.M., Lee, K.H., Kim, J., Shin, I., and Yoon, J., *Boronic acid-linked Fluorescent and Colorimetric Probes for Copper Ions*. *Chem. Commun.*, 2008(45): p. 5915-5917.
121. Xu, W.Z., Huang, Z.T., and Zheng, Q.Y., *Highly Efficient Fluorescent Sensing for α -Hydroxy acids with C-3-symmetric Boronic Acid-based Receptors*. *Tetrahedron Lett.*, 2008. **49**(33): p. 4918-4921.
122. Cao, Z., Nandhikonda, P., and Heagy, M.D., *Highly Water-Soluble Monoboronic Acid Probes That Show Optical Sensitivity to Glucose Based on 4-Sulfo-1,8-naphthalic Anhydride*. *J. Org. Chem.*, 2009. **74**(9): p. 3544-3546.
123. Han, F., Chi, L.N., Liang, X.F., Ji, S.M., Liu, S.S., Zhou, F.K., Wu, Y.B., Han, K.L., Zhao, J.Z., and James, T.D., *3,6-Disubstituted Carbazole-Based Bisboronic Acids with Unusual Fluorescence Transduction as Enantioselective Fluorescent Chemosensors for Tartaric Acid*. *J. Org. Chem.*, 2009. **74**(3): p. 1333-1336.
124. Jin, S., Zhu, C.Y., Li, M.Y., and Wang, B.H., *Identification of the First Fluorescent α -Amidoboronic Acids that Change Fluorescent Properties upon Sugar Binding*. *Bioorg. Med. Chem. Lett.*, 2009. **19**(6): p. 1596-1599.
125. Seymour, E. and Frechet, J.M.J., *Separation of Cis Diols from Isomeric Cis-trans Mixtures by Selective Coupling to a Regenerable Solid Support*. *Tetrahedron Lett.*, 1976. **41**: p. 3669-3672.
126. Yang, W.Q., Yan, J., Springsteen, G., Deeter, S., and Wang, B.H., *A Novel Type of Fluorescent Boronic Acid that Shows Large Fluorescence Intensity Changes Upon Binding With a Carbohydrate in Aqueous Solution at Physiological pH*. *Bioorg. Med. Chem. Lett.*, 2003. **13**(6): p. 1019-1022.
127. Springsteen, G., *A Detailed Examination of Boronic Acid-Carbohydrate Complexation Using Alizarin Red S. as a General Optical Reporter*, in *Department of Chemistry 2002*, North Carolina State University: Raleigh. p. 183.
128. Wang, J.F., Jin, S., Akay, S., and Wang, B.H., *Design and Synthesis of Long-wavelength Fluorescent Boronic Acid Reporter Compounds*. *Eur. J. Org. Chem.*, 2007(13): p. 2091-2099.
129. Yang, W., Lin, L., and Wang, B., *A Novel Type of Fluorescent Boronic Acid for Carbohydrate Recognition*. *Tetrahedron Lett.*, 2005. **46**: p. 7981-7984.
130. Wang, J.F., Jin, S., Lin, N., and Wang, B.H., *Fluorescent Indolylboronic Acids That Are Useful Reporters for The Synthesis of Boronolactams*. *Chem. Biol. Drug Des.*, 2006. **67**(2): p. 137-144.
131. Lakowicz, J.R., *Principles of Fluorescence Spectroscopy*. 2nd Edition ed2004, New York: Springer Science+Business Media, Inc.

132. Metzler, R., Ambjornsson, T., Hanke, A., Zhang, Y.L., and Levene, S., *Single DNA Conformations and Biological Function*. Journal of Computational and Theoretical Nanoscience, 2007. **4**(1): p. 1-49.
133. Bock, L.C., Griffin, L.C., Latham, J.A., Vermaas, E.H., and Toole, J.J., *Selection of Single-Stranded-DNA Molecules that Bind and Inhibit Human Thrombin*. Nature, 1992. **355**(6360): p. 564-566.
134. Proske, D., Blank, M., Buhmann, R., and Resch, A., *Aptamers - Basic Research, Drug Development, and Clinical Applications*. Appl. Microbiol. Biotechnol., 2005. **69**(4): p. 367-374.
135. Syed, M.A. and Pervaiz, S., *Advances in Aptamers*. Oligonucleotides, 2010. **20**(5): p. 215-224.
136. Maojo, V., Martin-Sanchez, F., Kulikowski, C., Rodriguez-Paton, A., and Fritts, M., *Nanoinformatics and DNA-Based Computing: Catalyzing Nanomedicine*. Pediatr Res., 2010. **67**(5): p. 481-489.
137. Pregibon, D.C., Toner, M., and Doyle, P.S., *Multifunctional Encoded Particles for High-throughput Biomolecule Analysis*. Science, 2007. **315**(5817): p. 1393-1396.
138. Scheuermann, J. and Neri, D., *DNA-Encoded Chemical Libraries: A Tool for Drug Discovery and for Chemical Biology*. ChemBioChem, 2010. **11**(7): p. 931-937.
139. Sakthivel, K. and Barbas, C.F., *Expanding the Potential of DNA for Binding and Catalysis: Highly Functionalized dUTP Derivatives that are Substrates for Thermostable DNA Polymerases*. Angew. Chem. Int. Edit., 1998. **37**(20): p. 2872-2875.
140. Vaught, J.D., Bock, C., Carter, J., Fitzwater, T., Otis, M., Schneider, D., Rolando, J., Waugh, S., Wilcox, S.K., and Eaton, B.E., *Expanding the Chemistry of DNA for in Vitro Selection*. J. Am. Chem. Soc., 2010. **132**(12): p. 4141-4151.
141. Wang, W., Gao, X., and Wang, B., *Boronic Acid-based Sensors for Carbohydrates*. Curr. Org. Chem., 2002. **6**: p. 1285-1317.
142. Yang, W., Gao, X., and Wang, B., *Boronic Acid Compounds as Potential Pharmaceutical Agents*. Med. Res. Rev., 2003. **23**: p. 346-368.
143. Lin, N., Yan, J., Huang, Z., Altier, C., Li, M., Carrasco, N., Suyemoto, M., Johnston, L., Wang, S., Wang, Q., Fang, H., Caton-Williams, J., and Wang, B., *Design and Synthesis of Boronic-acid-labeled Thymidine Triphosphate for Incorporation into DNA*. Nucleic Acids Res., 2007. **35**(4): p. 1222-1229.
144. Yang, X.C., Dai, C.F., Dayan, A., Molina, C., and Wang, B.H., *Boronic acid-modified DNA that Changes Fluorescent Properties upon Carbohydrate Binding*. Chem. Comm., 2010. **46**(7): p. 1073-1075.
145. Huisgen, R., in *1,3-Dipolar Cycloaddition Chemistry*, A. Padwa, Editor 1984, John Wiley: New York. p. 1-176.
146. Rostovtsev, V.V., Green, L.G., Fokin, V.V., and Sharpless, K.B., *A Stepwise Huisgen Cycloaddition Process: Copper(I)-catalyzed Regioselective "ligation" of Azides and Terminal Alkynes*. Angew. Chem. Int. Ed. Engl., 2002. **41**(14): p. 2596-2599.
147. Tornøe, C.W., Christensen, C., and Meldal, M., *Peptidotriazoles on Solid Phase: [1,2,3]-Triazoles by Regiospecific Copper(I)-Catalyzed 1,3-dipolar Cycloadditions of Terminal Alkynes to Azides*. J. Org. Chem., 2002. **67**(9): p. 3057-3064.

148. Gierlich, J., Burley, G.A., Gramlich, P.M.E., and Carell, T., *Click Chemistry as a Reliable Method for the High-Density Postsynthetic Functionalization of Alkyne-Modified DNA*. *Org. Lett.*, 2006. **8**(17): p. 3639-3642.
149. Gierlich, J., Gutsmedl, K., Gramlich, P.M.E., Schmidt, A., Burley, G.A., and Carell, T., *Synthesis of Highly Modified DNA by A Combination of PCR with Alkyne-bearing Triphosphates and Click Chemistry*. *Chem. Eur. J.*, 2007. **13**(34): p. 9486-9494.
150. Camilli, A. and Bassler, B.L., *Bacterial Small-molecule Signaling Pathways*. *Science*, 2006. **311**(5764): p. 1113-6.
151. Ni, N., Chou, H.-T., Wang, J., Li, M., Lu, C.-D., Tai, P.C., and Wang, B., *Identification of Boronic Acids as Antagonists of Bacterial Quorum Sensing in *Vibrio harveyi**. *Biochem. Biophys. Res. Commun.*, 2008. **369**(2): p. 590-594.
152. Waters, C.M. and Bassler, B.L., *Quorum Sensing: Cell-to-cell Communication in Bacteria*. *Annu. Rev. Cell. Dev. Biol.*, 2005. **21**: p. 319-346.
153. Fuqua, C., Parsek, M.R., and Greenberg, E.P., *Regulation of Gene Expression by Cell-to-cell Communication: Acyl-homoserine Lactone Quorum Sensing*. *Annu. Rev. Genet.*, 2001. **35**: p. 439-68.
154. Kleerebezem, M., Quadri, L.E., Kuipers, O.P., and de Vos, W.M., *Quorum Sensing by Peptide Pheromones and Two-component Signal-transduction Systems in Gram-positive Bacteria*. *Mol. Microbiol.*, 1997. **24**(5): p. 895-904.
155. Xavier, K.B. and Bassler, B.L., *LuxS Quorum Sensing: More than Just a Numbers Game*. *Curr. Opin. Microbiol.*, 2003. **6**(2): p. 191-7.
156. Zhu, J., Miller, M.B., Vance, R.E., Dziejman, M., Bassler, B.L., and Mekalanos, J.J., *Quorum-sensing Regulators Control Virulence Gene Expression in *Vibrio cholerae**. *Proc. Natl. Acad. Sci. U S A*, 2002. **99**(5): p. 3129-3134.
157. Miller, M.B., Skorupski, K., Lenz, D.H., Taylor, R.K., and Bassler, B.L., *Parallel Quorum Sensing Systems Converge to Regulate Virulence in *Vibrio cholerae**. *Cell*, 2002. **110**(3): p. 303-14.
158. Hammer, B.K. and Bassler, B.L., *Quorum Sensing Controls Biofilm Formation in *Vibrio cholerae**. *Mol. Microbiol.*, 2003. **50**(1): p. 101-4.
159. Ni, N., Li, M., Wang, J., and Wang, B., *Inhibitors and Antagonists of Bacterial Quorum Sensing*. *Med. Res. Rev.*, 2009. **29**(1): p. 65-124.
160. Whitehead, N.A., Barnard, A.M., Slater, H., Simpson, N.J., and Salmond, G.P., *Quorum-sensing in Gram-negative Bacteria*. *FEMS. Microbiol. Rev.*, 2001. **25**(4): p. 365-404.
161. Meijler, M.M., Hom, L.G., Kaufmann, G.F., McKenzie, K.M., Sun, C., Moss, J.A., Matsushita, M., and Janda, K.D., *Synthesis and Biological Validation of a Ubiquitous Quorum-sensing Molecule*. *Angew. Chem. Int. Ed. Engl.*, 2004. **43**(16): p. 2106-8.
162. Niu, C., Afre, S., and Gilbert, E.S., *Subinhibitory Concentrations of Cinnamaldehyde Interfere with Quorum Sensing*. *Lett. Appl. Microbiol.*, 2006. **43**(5): p. 489-94.
163. Singh, V., Shi, W., Almo, S.C., Evans, G.B., Furneaux, R.H., Tyler, P.C., Painter, G.F., Lenz, D.H., Mee, S., Zheng, R., and Schramm, V.L., *Structure and Inhibition of a Quorum Sensing Target from *Streptococcus pneumoniae**. *Biochemistry*, 2006. **45**(43): p. 12929 -12941.
164. Muh, U., Schuster, M., Heim, R., Singh, A., Olson, E.R., and Greenberg, E.P., *Novel *Pseudomonas aeruginosa* Quorum-sensing Inhibitors Identified in an Ultra-high-throughput Screen*. *Antimicrob. Agents. Chemother.*, 2006. **50**(11): p. 3674-9.

165. Shen, G., Rajan, R., Zhu, J., Bell, C.E., and Pei, D., *Design and Synthesis of Substrate and Intermediate Analogue Inhibitors of S-ribosylhomocysteinase*. J. Med. Chem., 2006. **49**(10): p. 3003-11.
166. Zhu, J., Hu, X., Dizin, E., and Pei, D., *Catalytic Mechanism of S-ribosylhomocysteinase (LuxS): Direct Observation of Ketone Intermediates by ¹³C NMR Spectroscopy*. J. Am. Chem. Soc., 2003. **125**(44): p. 13379-81.
167. Zhu, J., Patel, R., and Pei, D., *Catalytic Mechanism of S-ribosylhomocysteinase (LuxS): Stereochemical Course and Kinetic Isotope Effect of Proton Transfer Reactions*. Biochemistry, 2004. **43**(31): p. 10166-10172.
168. De Keersmaecker, S.C., Varszegi, C., van Boxel, N., Habel, L.W., Metzger, K., Daniels, R., Marchal, K., De Vos, D., and Vanderleyden, J., *Chemical Synthesis of (S)-4,5-dihydroxy-2,3-pentanedione, a Bacterial Signal Molecule Precursor, and Validation of its Activity in Salmonella typhimurium*. J. Biol. Chem., 2005. **280**(20): p. 19563-8.
169. Semmelhack, M.F., Campagna, S.R., Federle, M.J., and Bassler, B.L., *An Expeditious Synthesis of DPD and Boron Binding Studies*. Org. Lett., 2005. **7**(4): p. 569-72.
170. Semmelhack, M.F., Campagna, S.R., Hwa, C., Federle, M.J., and Bassler, B.L., *Boron Binding with the Quorum Sensing Signal AI-2 and Analogues*. Org. Lett., 2004. **6**(15): p. 2635-7.
171. Lowery, C.A., McKenzie, K.M., Meijler, M.M., and Janda, K.D., *Quorum Sensing in Vibrio harveyi: Probing the Specificity of the LuxP Binding Site*. Bioorg. Med. Chem. Lett., 2005. **15**: p. 2395-2398.
172. Frezza, M., Castang, S., Estephane, J., Soulere, L., Deshayes, C., Chantegrel, B., Nasser, W., Queneau, Y., Reverchon, S., and Doutheau, A., *Synthesis and Biological Evaluation of Homoserine Lactone Derived Ureas as Antagonists of Bacterial Quorum Sensing*. Bioorg. Med. Chem., 2006. **14**(14): p. 4781-4791.
173. Ren, D., Zuo, R., Gonzalez Barrios, A.F., Bedzyk, L.A., Eldridge, G.R., Pasmore, M.E., and Wood, T.K., *Differential Gene Expression for Investigation of Escherichia coli Biofilm Inhibition by Plant Extract Ursolic Acid*. Appl. Environ. Microbiol., 2005. **71**(7): p. 4022-34.
174. Lee, J., Bansal, T., Jayaraman, A., Bentley, W.E., and Wood, T.K., *Enterohemorrhagic Escherichia coli biofilms are inhibited by 7-hydroxyindole and stimulated by isatin*. Appl. Environ. Microbiol., 2007. **73**(13): p. 4100-9.
175. Ren, D., Sims, J.J., and Wood, T.K., *Inhibition of Biofilm Formation and Swarming of Escherichia coli by (5Z)-4-bromo-5-(bromomethylene)-3-butyl-2(5H)-furanone*. Environ. Microbiol., 2001. **3**(11): p. 731-6.
176. Widmer, K.W., Soni, K.A., Hume, M.E., Beier, R.C., Jesudhasan, P., and Pillai, S.D., *Identification of Poultry meat-derived Fatty Acids Functioning as Quorum Sensing Signal Inhibitors to Autoinducer-2 (AI-2)*. J. Food. Sci., 2007. **72**(9): p. M363-8.
177. Miller, M.B. and Bassler, B.L., *Quorum Sensing in Bacteria*. Annu. Rev. Microbiol., 2001. **55**: p. 165-99.
178. Higgins, D.A., Pomianek, M.E., Kraml, C.M., Taylor, R.K., Semmelhack, M.F., and Bassler, B.L., *The Major Vibrio cholerae Autoinducer and its Role in Virulence Factor Production*. Nature, 2007. **450**(7171): p. 883-6.
179. Pultar, J., Sauer, U., Domnanich, P., and Preininger, C., *Aptamer-antibody On-chip Sandwich Immunoassay for Detection of CRP in Spiked Serum*. Biosens Bioelectron., 2009. **24**(5): p. 1456-1461.

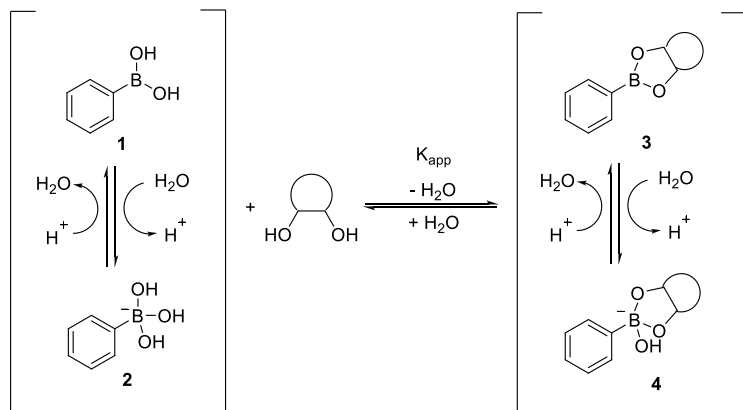
180. Defoirdt, T., Verstraete, W., and Bossier, P., *Luminescence, Virulence and Quorum Sensing Signal Production by Pathogenic Vibrio campbellii and Vibrio harveyi isolates*. J. Appl. Microbiol., 2008. **104**(5): p. 1480-1487.
181. Chen, X., Schauder, S., Potier, N., Van Dorselaer, A., Pelczar, I., Bassler, B.L., and Hughson, F.M., *Structural Identification of a Bacterial Quorum-sensing Signal Containing Boron*. Nature, 2002. **415**(6871): p. 545-549.
182. Winzer, K., Hardie, K.R., and Williams, P., *LuxS and Autoinducer-2: Their Contribution to Quorum Sensing and Metabolism in Bacteria*. Adv. Appl. Microbiol., 2003. **53**: p. 291-396.
183. Bassler, B.L., Wright, M., Showalter, R.E., and Silverman, M.R., *Intercellular Signaling in Vibrio harveyi: Sequence and Function of Genes Regulating Expression of Luminescence*. Mol. Microbiol., 1993. **9**(4): p. 773-786.
184. Aranapakam, V., Grosu, G.T., Davis, J.M., Hu, B.H., Ellingboe, J., Baker, J.L., Skotnicki, J.S., Zask, A., DiJoseph, J.F., Sung, A., Sharr, M.A., Killar, L.M., Walter, T., Jin, G.X., and Cowling, R., *Synthesis and Structure-activity Relationship of Alpha-sulfonylhydroxamic Acids as Novel, Orally Active Matrix Metalloproteinase Inhibitors for the Treatment of Osteoarthritis*. J. Med. Chem., 2003. **46**(12): p. 2361-2375.
185. Yokoyama, M., Menjo, Y., Ubukata, M., Irie, M., Watanabe, M., and Togo, H., *Transformation of Alkyl N-(vinyloxy)benzimidates to Alkyloxazoles. Mechanism and Extension*. Bull. Chem. Soc. Jpn., 1994. **67**(8): p. 2219- 2226.
186. Ozturk, T., Ertas, E., and Mert, O., *Use of Lawesson's Reagent in Organic Syntheses*. Chemical Reviews, 2007. **107**(11): p. 5210-5278.
187. O'Sullivan, O.C.M., Collins, S.G., Maguire, A.R., Böhm, M., and Sander, W., *Photochemistry of cis-3-Diazo-5,6-dimethyl-1,4-oxathian-2-one S-Oxide in Argon Matrices*. Eur. J. Org. Chem., 2006. **2006**(13): p. 2918- 2924.
188. Ooi, T., Uematsu, Y., Kameda, M., and Maruoka, K., *Asymmetric Phase-transfer Catalysis of Homo- and Heterochiral Quaternary Ammonium Salts: Development and Application of Conformationally Flexible Chiral Phase-transfer Catalysts*. Tetrahedron, 2006. **62**(49): p. 11425- 11436.
189. Ishibashi, H., Kameoka, C., Iriyama, H., Kodama, K., Sato, T., and Ikeda, M., *Sulfur-directed Regioselective Radical Cyclization Leading to Beta-lactams - Formal Synthesis of (+/-)-PS-5 and (+)-thienamycin*. J. Org. Chem., 1995. **60**(5): p. 1276-1284.
190. Artman III, G.D., Waldman, J.H., and Weinreb, S.M., *β -Tosylethylhydroxylamine: Preparation and Use as a Hydroxylamine Equivalent in Amidyl Radical-olefin Cyclizations*. Synthesis, 2002. **14**: p. 2057-2063
191. Miller, S.T., Xavier, K.B., Campagna, S.R., Taga, M.E., Semmelhack, M.F., Bassler, B.L., and Hughson, F.M., *Salmonella typhimurium Recognizes a Chemically Distinct Form of the Bacterial Quorum-Sensing Signal AI-2*. Mol. Cell., 2004. **15**(5): p. 677-87.
192. Taga, M.E., *Methods for Analysis of Bacterial Autoinducer-2 Production*. Curr. Proto. Microbiol., John Wiley & Sons Inc., 2006: p. 1C.1.1-1C.1.8.
193. Vilchez, R., Lemme, A., Thiel, V., Schulz, S., Sztajer, H., and Wagner-Do"bler, I., *Analysing Traces of Autoinducer-2 Requires Standardization of the Vibrio harveyi Bioassay*. Anal. Bioanal. Chem., 2007 **387** p. 489-496.
194. Cramer, R.D., Patterson, D.E., and Bunce, J.D., *Comparative Molecular Field Analysis (CoMFA). 1. Effect of Shape on Binding of Steroids to Carrier Proteins*. J. Am. Chem. Soc., 1988. **110**(18): p. 5959-5967.

195. Stewart, J.J., *MOPAC: A Semiempirical Molecular Orbital Program*. J. Comput. Aided. Mol. Des., 1990. **4**(1): p. 1-105.
196. Jakalian, A., Bush, B.L., Jack, D.B., and Bayly, C.I., *Fast, Efficient Generation of High-Quality Atomic Charges. AM1-BCC Model: I. Method*. J. Comput. Chem., 2000. **21**(2): p. 132-146.
197. Jakalian, A., Jack, D.B., and Bayly, C.I., *Fast, Efficient Generation of High-Quality Atomic Charges. AM1-BCC Model: II. Parameterization and Validation*. J. Comput. Chem., 2002. **23**(16): p. 1623-41.
198. Tsai, K.-C., Wang, S.-H., Hsiao, N.-W., Li, M., and Wang, B., *The Effect of Different Electrostatic Potentials on Docking Accuracy: A Case Study Using DOCK5.4*. Bioorg. Med. Chem. Lett., 2008. **18**(12): p. 3509-3512.

APPENDIX: SUPPORTING INFORMATION

General Method for the K_a determination

K_a equation development in spectroscopic methods



This scheme can be simplified as $B + S \rightleftharpoons BS$, based on 1:1 stoichiometry binding.

Assumption: $[B] = mI_0$ $[BS] = n\Delta I$

$$K_a = [BS]/([B]-[BS])([S]-[BS])$$

Since $[S] \gg [B]$, so $[S] \gg [BS]$

$$K_a = [BS]/([B]-[BS])[S]$$

$$= n\Delta I/(mI_0 - n\Delta I)[S]$$

$$K_a[S] (mI_0 - n\Delta I) = n\Delta I$$

$$K_a[S]mI_0 - K_a[S]n\Delta I = n\Delta I$$

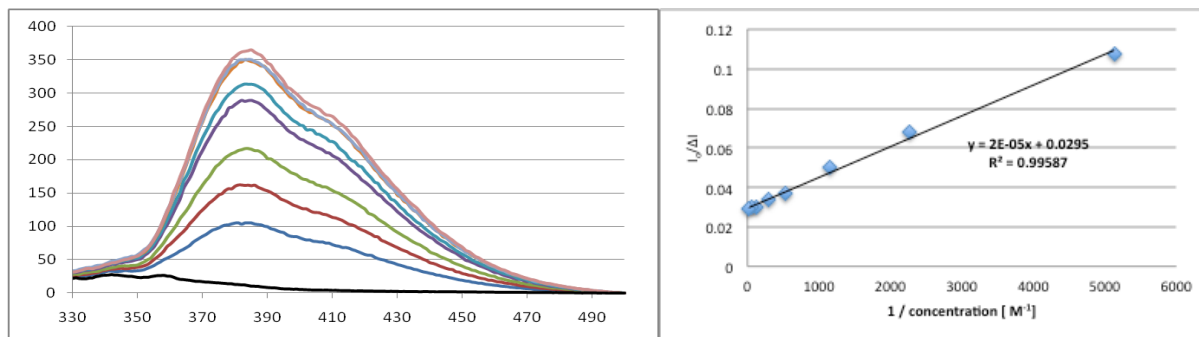
$$K_a[S]mI_0 = n\Delta I + K_a[S]n\Delta I$$

$$I_0/\Delta I = (1+K_a[S])n/mK_a[S]$$

$$= n/mK_a \times 1/[S] + n/m$$

So in a chart of fluorescence intensity change of IQBA as a function of the reciprocal of concentration, we can easily determine the K_a by following equation: $K_a = \text{intercept/slope} = (n/m)/(n/mK_a) = K_a$, and the linearity further confirm the hypothesis of 1:1 binding.

By using the binding of 8-IQBA with fructose as an example:



1/conc.	$\Delta I/I_0$	$I_0/\Delta I$	$K_a =$ Intercept/slope	$= 1475 \text{ M}^{-1}$
5129.976233	9.280140804	0.107756986		
2273.212226	14.73041948	0.067886729		
1142.156863	20.07949545	0.049802048		
539.3657463	27.2851276	0.036650003		
299.5936293	29.59714481	0.033787043		
128.0209758	32.92412242	0.030372867		
62.36232626	33.18822724	0.030131166		
19.60784314	34.64280825	0.02886602		

General Calculation of the quantum yields:

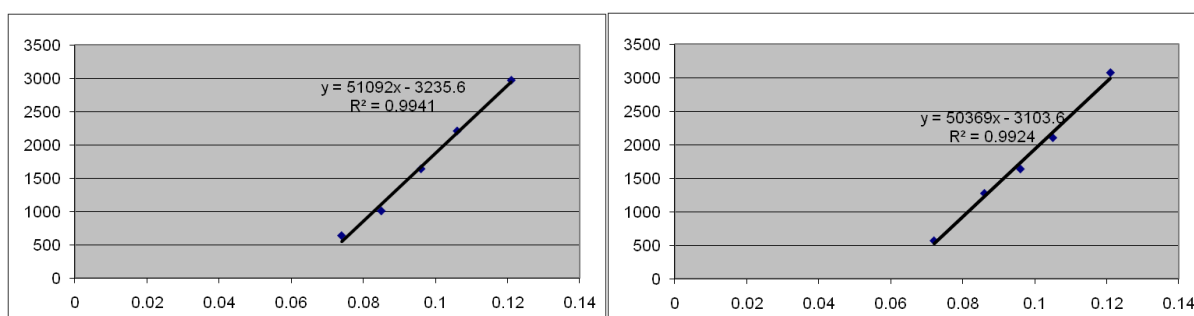
$$Q = Q_R (I/I_R) (OD_R/OD)$$

Use 8-IQBA in the absence of analytes as a specific example.

UV (272 nm) absorbance (1)	Fluorescence intensity are (310-500 nm) (1)	UV (272 nm) absorbance (2)	Fluorescence intensity are (310-500 nm) (2)
0.121	2968.285	0.121	3078.287
0.106	2206.451	0.105	2105.18
0.096	1636.396	0.096	1637.44
0.085	1004.19	0.086	1273.51

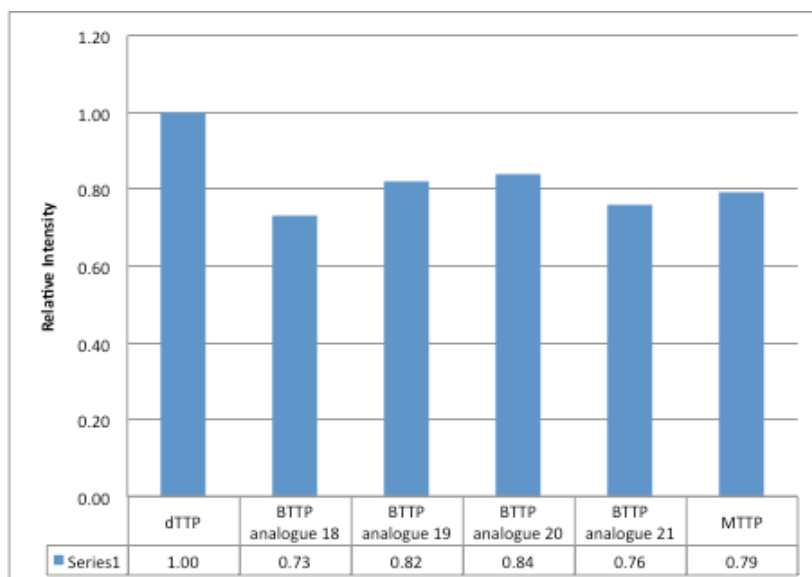
0.074**633.361****0.072****564.929**

A plot of fluorescence intensity against UV absorbance was drawn to obtain I/OD, 51092 and 50369 in this specific case. IR/ODR was also obtained by the same method to be 1000000. Then $Q = QR (I/IR) (ODR/OD) = QR (I/OD)/(IR/ODR) = 0.44 * 51092$ (or $50369)/1000000 = 2.2 \pm 0.02$

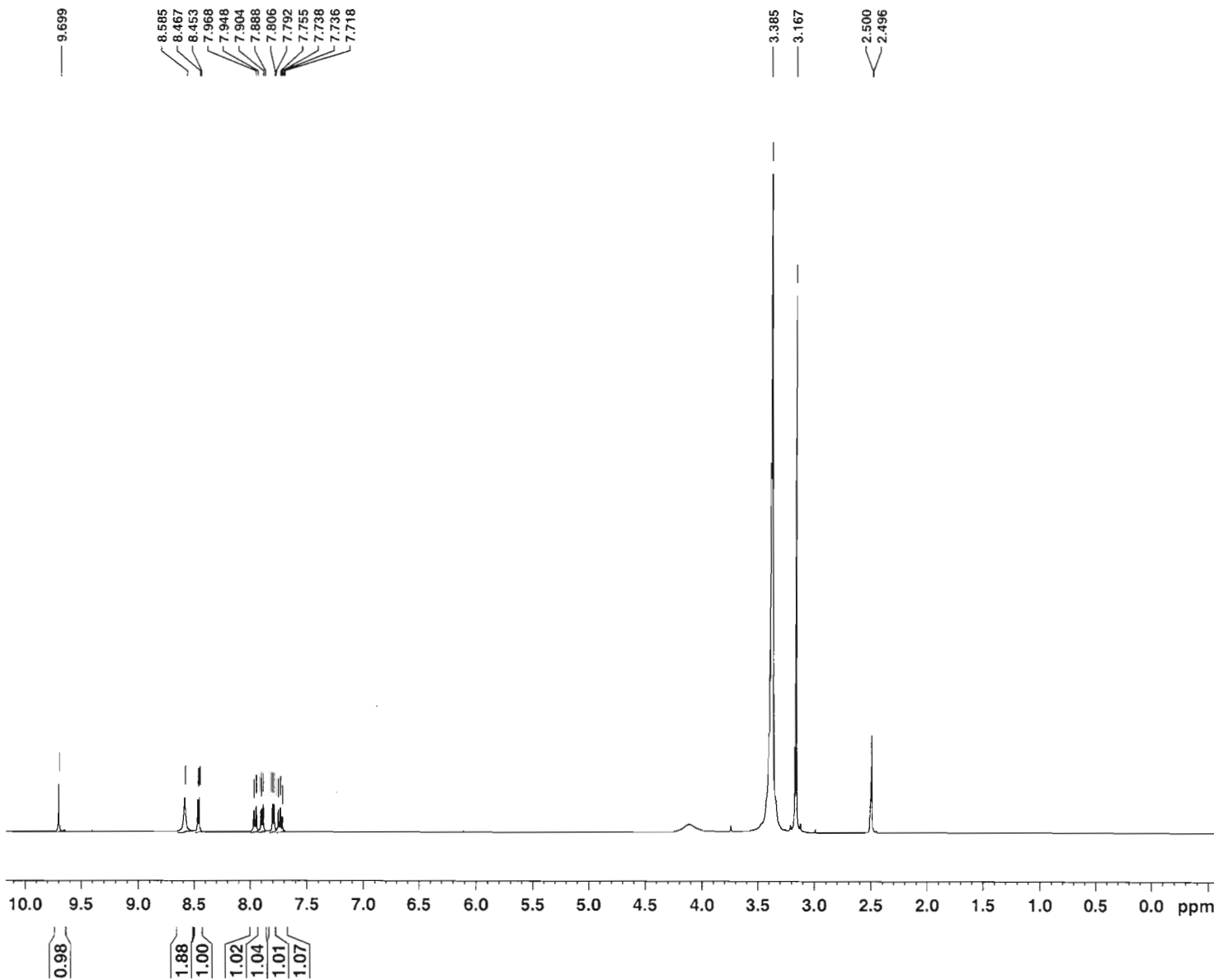


Relative band intensity of B-TTP analogues 2-5, and M-TTP compared to dNTTP in Figure 3.4

(Group B)



¹H NMR of 8-IQBA



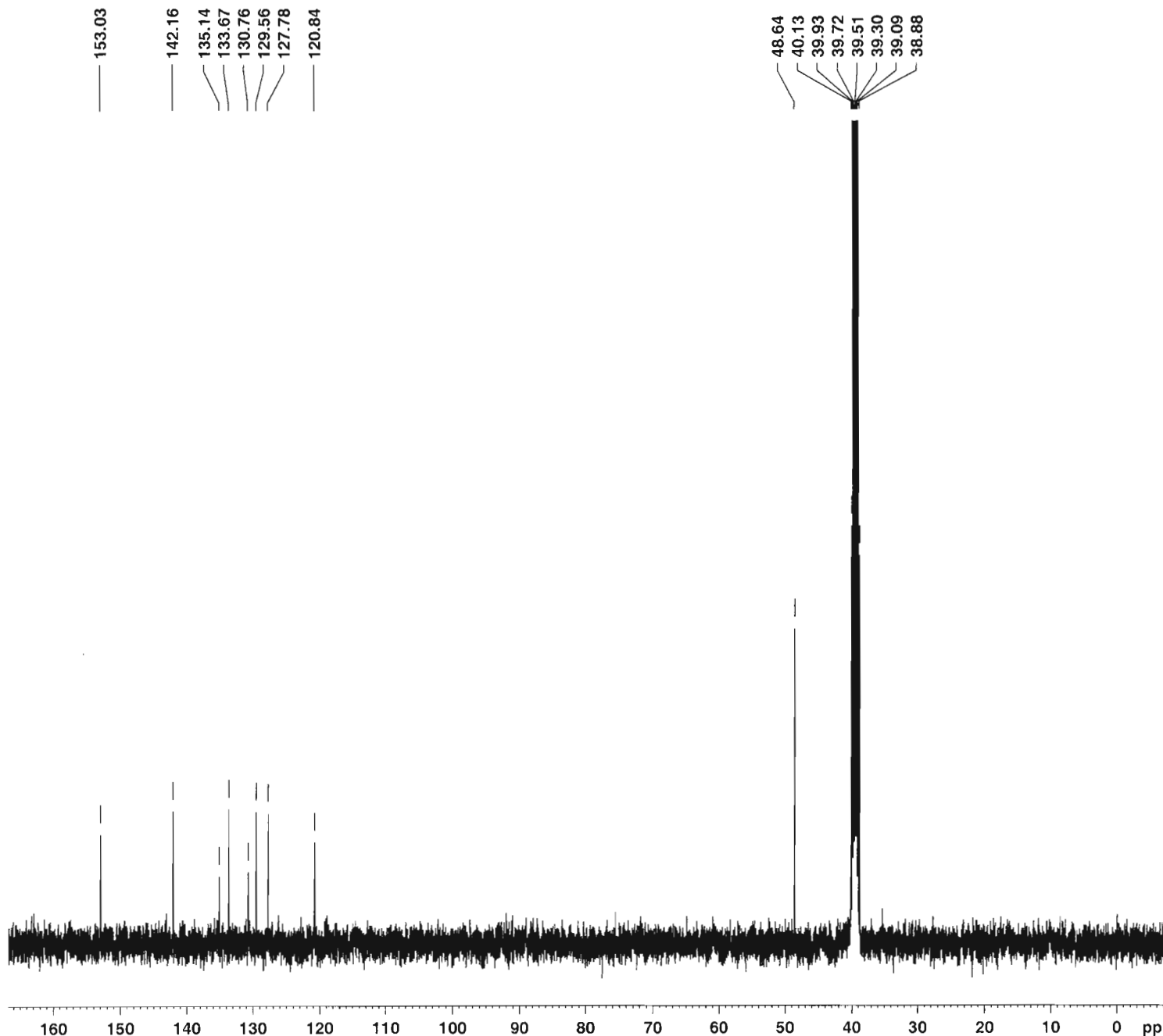
Current Data Parameters
 NAME JC-8IQBA-1H
 EXPNO 1
 PROCNO 1

F2 - Acquisition Parameters
 Date_ 20090923
 Time 19.28
 INSTRUM spect
 PROBHD 5 mm PABBO BB-
 PULPROG zg30
 TD 65536
 SOLVENT DMSO
 NS 16
 DS 2
 SWH 8278.146 Hz
 FIDRES 0.126314 Hz
 AQ 3.9584243 sec
 RG 161.3
 DW 60.400 usec
 DE 7.00 usec
 TE 298.2 K
 D1 1.0000000 sec
 MCREST 0.0000000 sec
 MCWRK 0.0150000 sec

==== CHANNEL f1 =====
 NUC1 1H
 P1 12.80 usec
 PL1 0.00 dB
 SFO1 400.1324710 MHz

F2 - Processing parameters
 SI 32768
 SF 400.1300041 MHz
 WDW EM
 SSB 0
 LB 0.30 Hz
 GB 0
 PC 1.00

¹³C NMR of 8-IQBA



Current Data Parameters
 NAME JC-8IQBA-13C
 EXPNO 1
 PROCNO 1

F2 - Acquisition Parameters
 Date_ 20090923
 Time 19.32
 INSTRUM spect
 PROBHD 5 mm PABBO BB-
 PULPROG zgpg30
 TD 65536
 SOLVENT D2O
 NS 173
 DS 4
 SWH 23980.814 Hz
 FIDRES 0.365918 Hz
 AQ 1.3664756 sec
 RG 14596.5
 DW 20.850 usec
 DE 7.00 usec
 TE 298.2 K
 D1 2.00000000 sec
 d11 0.03000000 sec
 DELTA 1.89999998 sec
 MCREST 0.00000000 sec
 MCWRK 0.01500000 sec

==== CHANNEL f1 =====
 NUC1 13C
 P1 8.00 usec
 PL1 -3.00 dB
 SFO1 100.6228298 MHz

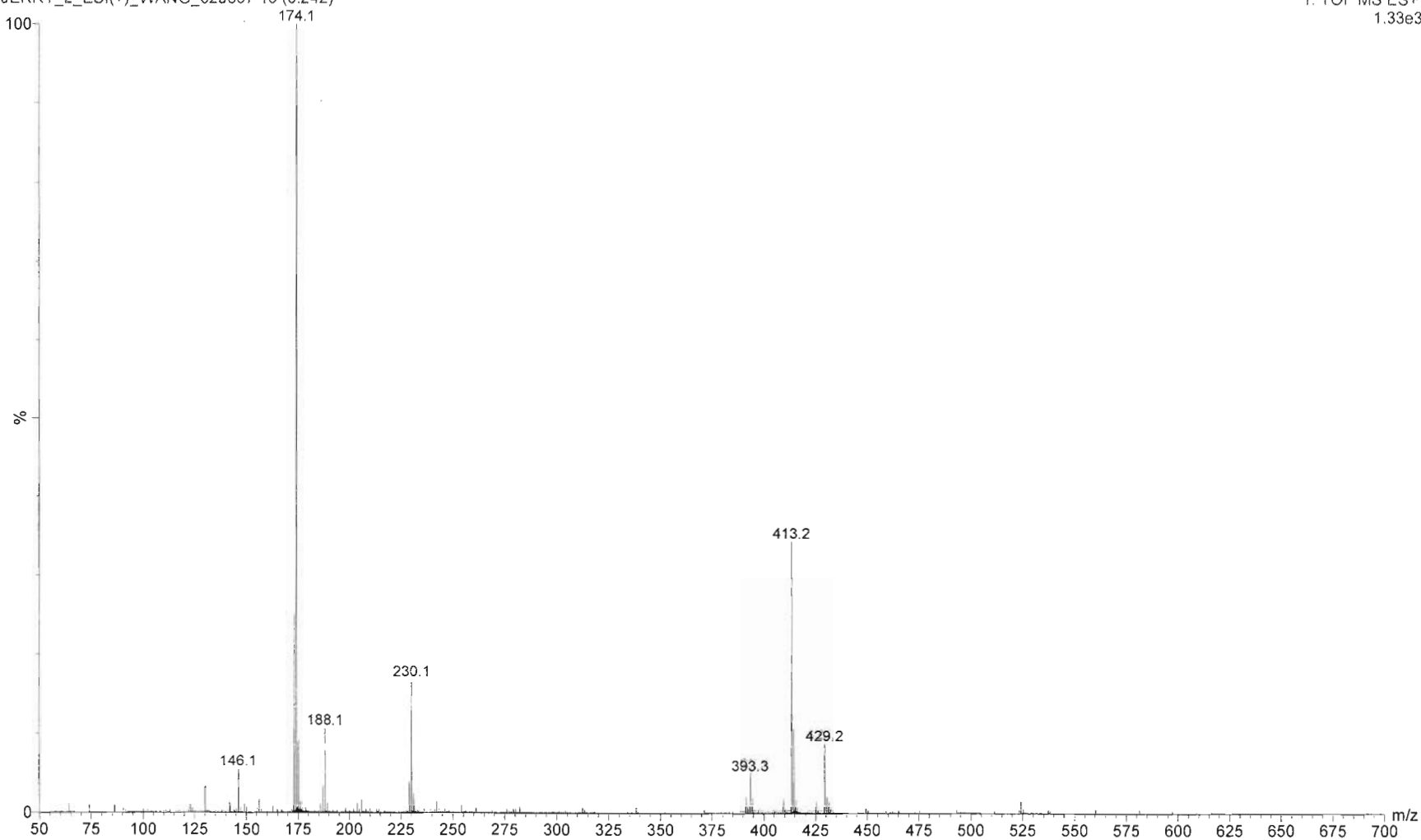
==== CHANNEL f2 =====
 CPDPRG2 waltz16
 NUC2 1H
 PCPD2 70.00 usec
 PL2 -1.00 dB
 PL12 14.00 dB
 PL13 14.00 dB
 SFO2 400.1316005 MHz

F2 - Processing parameters
 SI 32768
 SF 100.6128118 MHz
 WDW EM
 SSB 0
 LB 1.00 Hz
 GB 0
 PC 1.40

ESI-MS of 8-IQBA

in 50% ACN+0.1%HCOOH
JERRY_2_ESI(+)_WANG_020607 13 (0.242)

1: TOF MS ES+
1.33e3



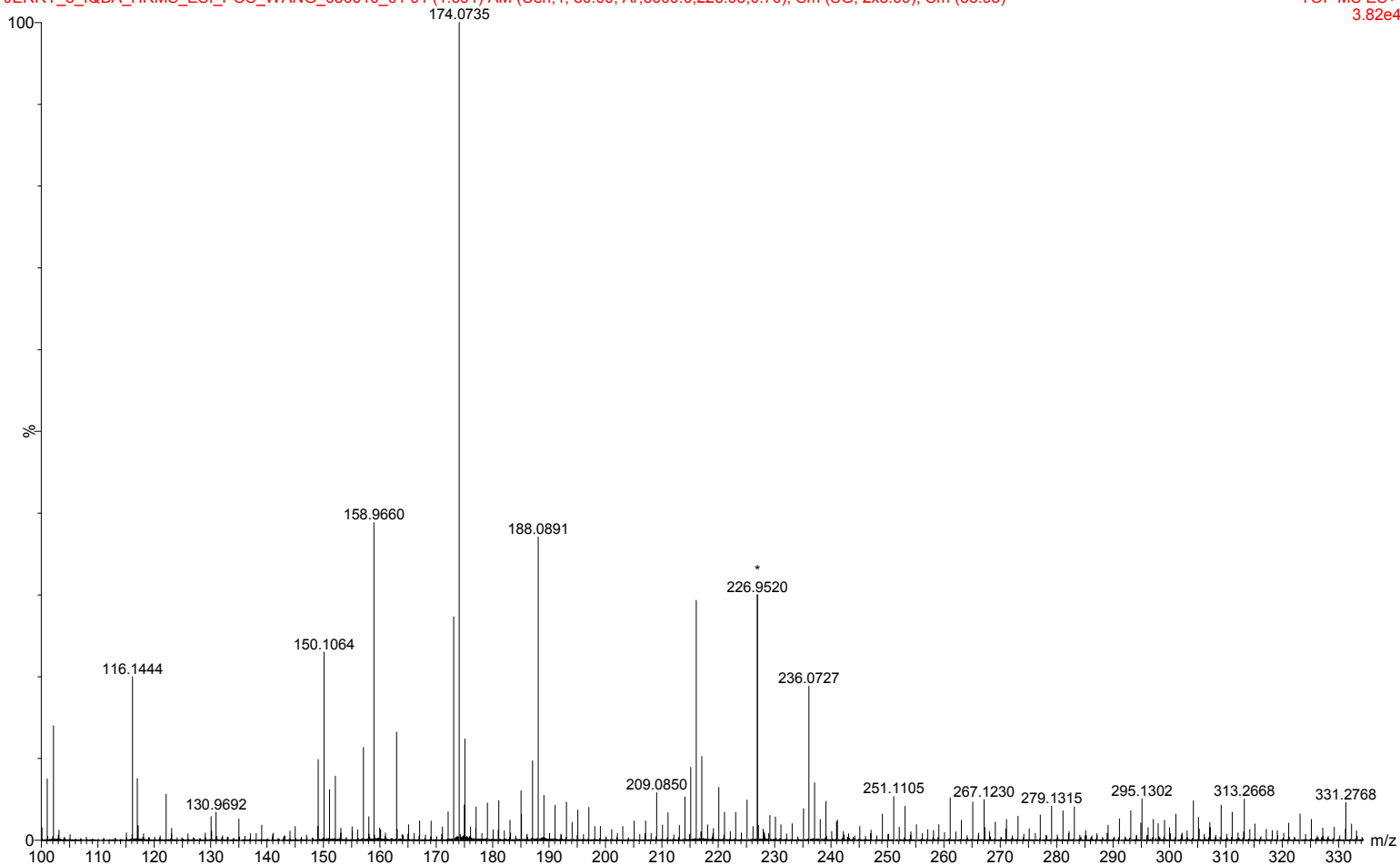
HRMS of 8-IQBA

50%MEOH+0.1%HCOOH, NaFormate as ITSD 226.9520Da

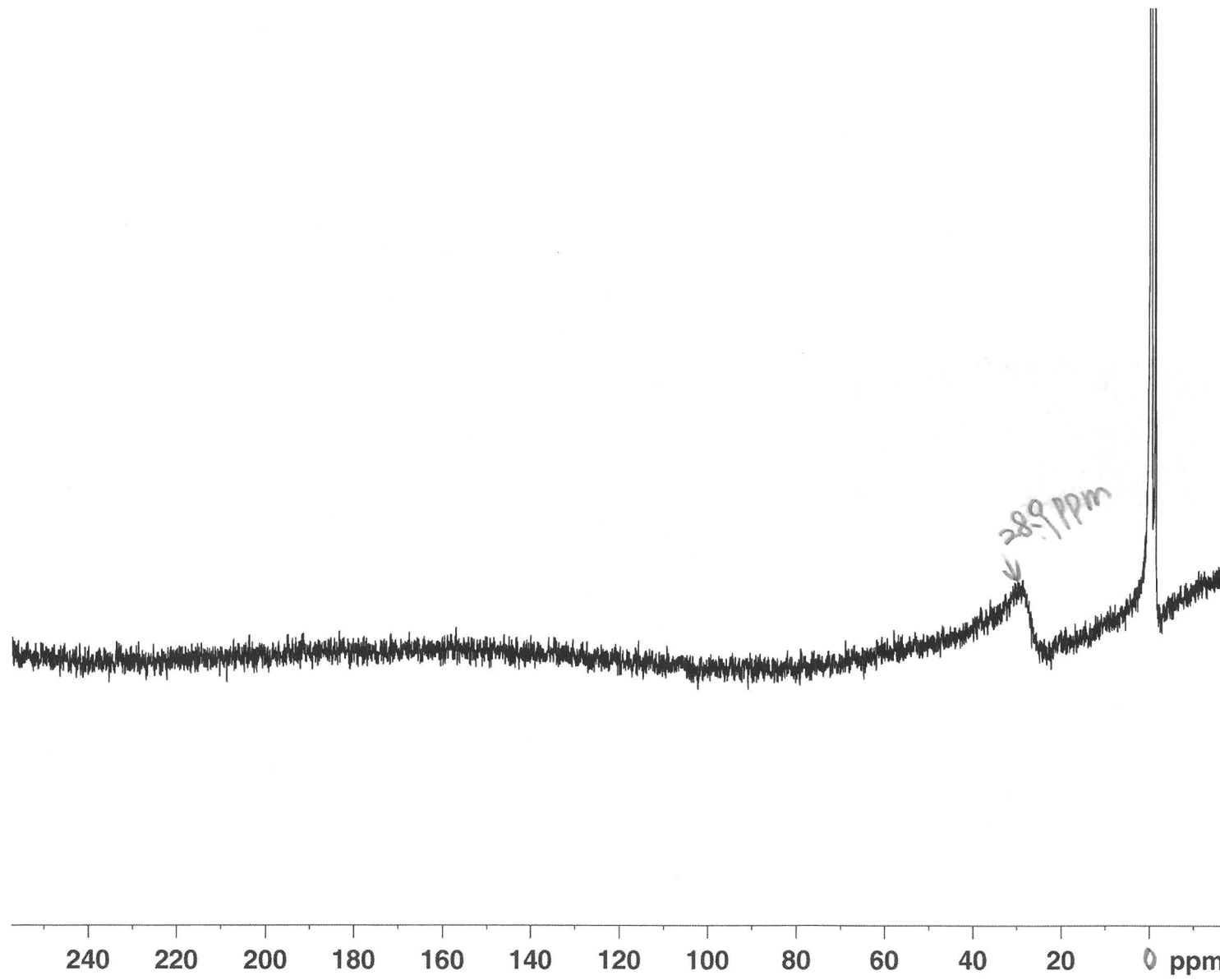
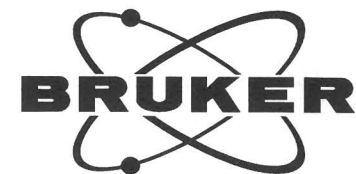
14:51:25 14:51:25

JERRY_8_IQBA_HRMS_ESI_POS_WANG_050610_01 91 (1.691) AM (Cen,4, 80.00, Ar,5000.0,226.95,0.70); Sm (SG, 2x3.00); Cm (35:93)

TOF MS ES+
3.82e4



^{11}B NMR of 8-IQBA (pH = 1.3)



Current Data Parameters
NAME JC-III-8IQBA-1.34-11B
EXPNO 1
PROCNO 1

F2 - Acquisition Parameters
Date_ 20091021
Time 17.50
INSTRUM spect
PROBHD 5 mm PABBO BB-
PULPROG zg30
TD 16384
SOLVENT CDC13
NS 189
DS 0
SWH 50125.312 Hz
FIDRES 3.059406 Hz
AQ 0.1634804 sec
RG 2896.3
DW 9.975 usec
DE 25.00 usec
TE 295.8 K
D1 2.00000000 sec
MCREST 0.00000000 sec
MCWRK 0.01500000 sec

==== CHANNEL f1 =====
NUC1 11B
P1 5.00 usec
PL1 0.00 dB
SFO1 128.3876799 MHz

F2 - Processing parameters
SI 32768
SF 128.3775012 MHz
WDW EM
SSB 0
LB 4.00 Hz
GB 0
PC 1.40

^{11}B NMR of 8-IQBA (pH = 7.3)

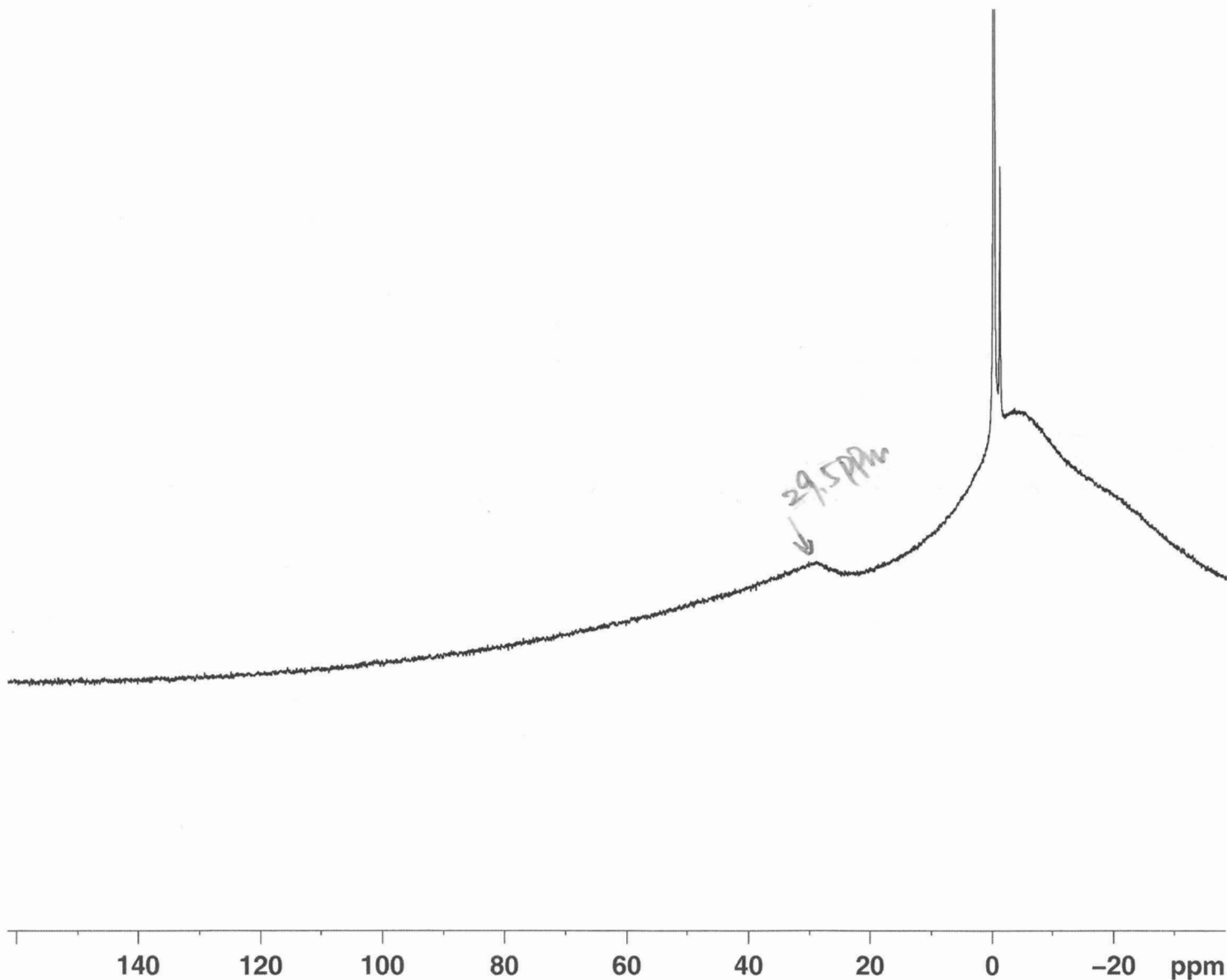


Current Data Parameters
NAME JC-III-8IQBA-7.34-11B
EXPNO 1
PROCNO 1

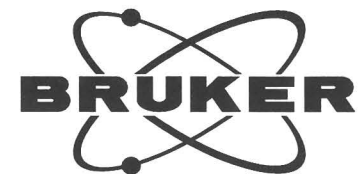
F2 - Acquisition Parameters
Date_ 20091021
Time 18.07
INSTRUM spect
PROBHD 5 mm PABBO BB-
PULPROG zg30
TD 16384
SOLVENT CDC13
NS 239
DS 0
SWH 50125.312 Hz
FIDRES 3.059406 Hz
AQ 0.1634804 sec
RG 1024
DW 9.975 usec
DE 25.00 usec
TE 295.8 K
D1 2.00000000 sec
MCREST 0.00000000 sec
MCWRK 0.01500000 sec

==== CHANNEL f1 =====
NUC1 11B
P1 5.00 usec
PL1 0.00 dB
SFO1 128.3876799 MHz

F2 - Processing parameters
SI 32768
SF 128.3774691 MHz
WDW EM
SSB 0
LB 4.00 Hz
GB 0
PC 1.40



^{11}B NMR of 8-IQBA (pH = 11.9)



Current Data Parameters

NAME JC-III-8IQBA-11.9-11B
EXPNO 1
PROCNO 1

F2 - Acquisition Parameters

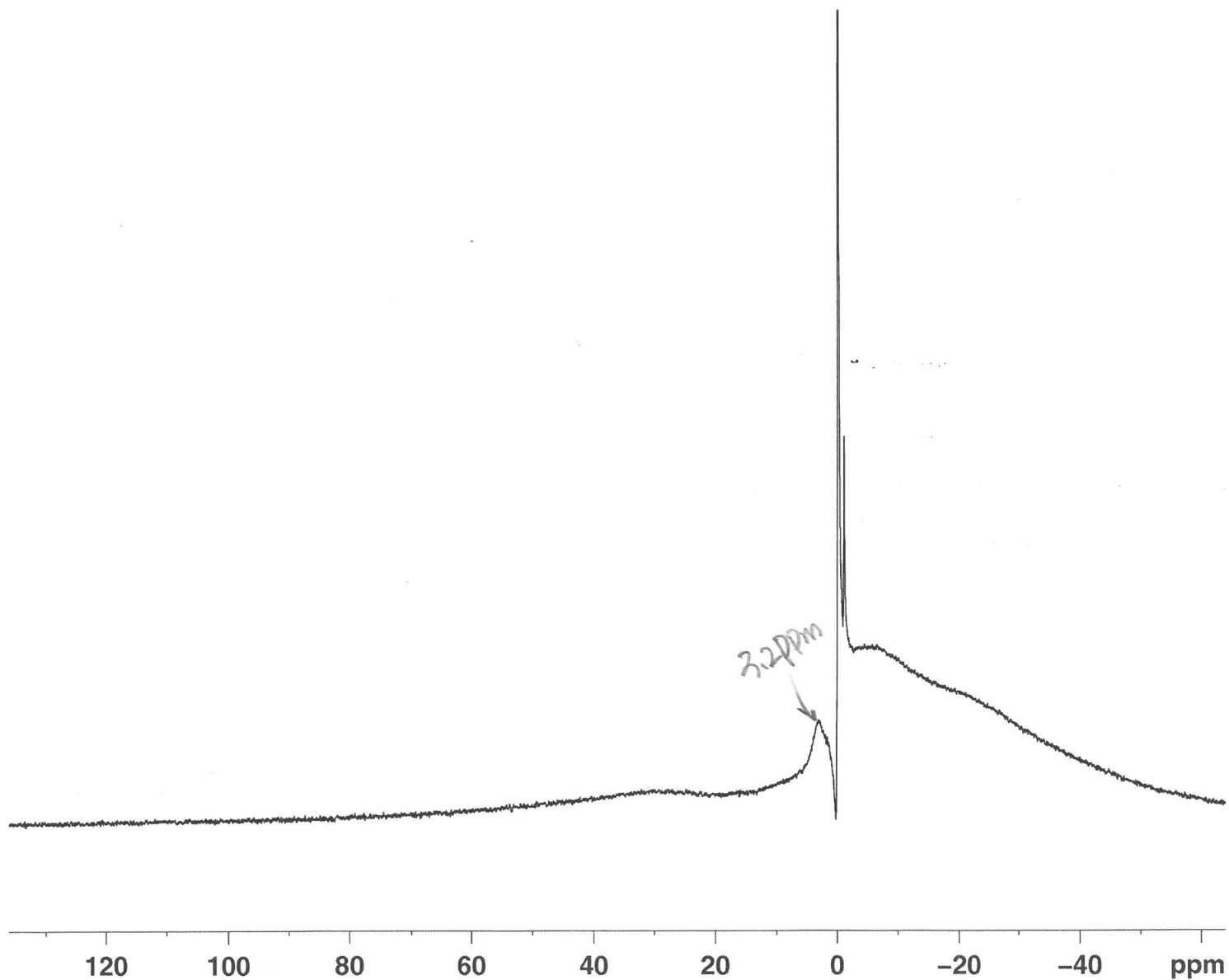
Date_ 20091021
Time 19.01
INSTRUM spect
PROBHD 5 mm PABBO BB-
PULPROG zg30
TD 16384
SOLVENT MeOD
NS 246
DS 0
SWH 50125.312 Hz
FIDRES 3.059406 Hz
AQ 0.1634804 sec
RG 1024
DW 9.975 usec
DE 25.00 usec
TE 295.8 K
D1 2.00000000 sec
MCREST 0.00000000 sec
MCWRK 0.01500000 sec

==== CHANNEL f1 =====

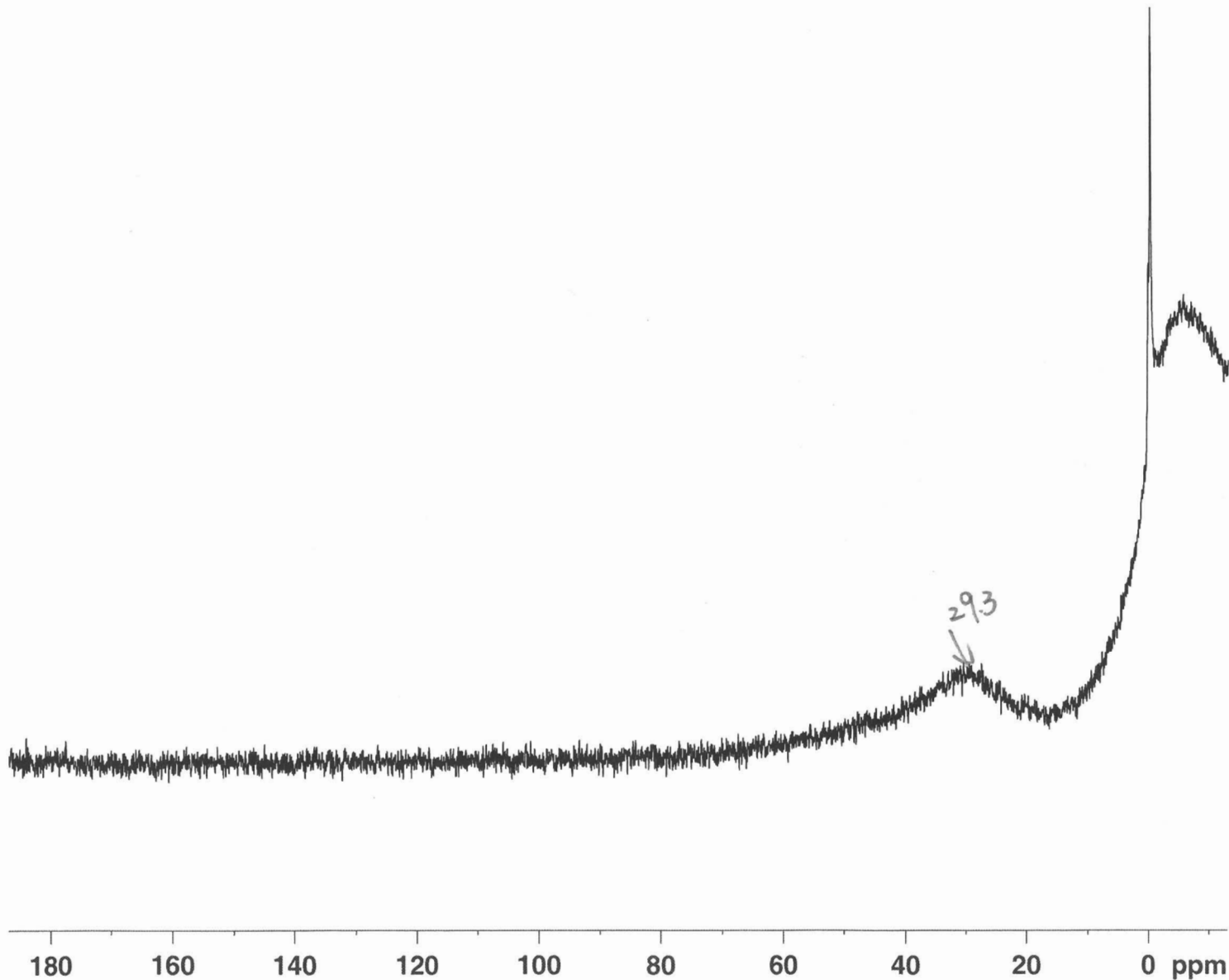
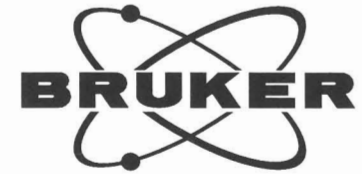
NUC1 11B
P1 5.00 usec
PL1 0.00 dB
SFO1 128.3876799 MHz

F2 - Processing parameters

SI 32768
SF 128.3776802 MHz
WDW EM
SSB 0
LB 4.00 Hz
GB 0
PC 1.40



^{11}B NMR of fructose ester of 8-IQBA (pH = 1.3)



Current Data Parameters
NAME JC-III-8IQBA+Fru-1.3-11B
EXPNO 1
PROCNO 1

F2 - Acquisition Parameters
Date_ 20091022
Time 17.14
INSTRUM spect
PROBHD 5 mm PABBO BB-
PULPROG zg30
TD 16384
SOLVENT MeOD
NS 79
DS 0
SWH 50125.312 Hz
FIDRES 3.059406 Hz
AQ 0.1634804 sec
RG 1024
DW 9.975 usec
DE 25.00 usec
TE 296.1 K
D1 2.00000000 sec
MCREST 0.00000000 sec
MCWRK 0.01500000 sec

==== CHANNEL f1 =====
NUC1 11B
P1 5.00 usec
PL1 0.00 dB
SFO1 128.3876799 MHz

F2 - Processing parameters
SI 32768
SF 128.3775639 MHz
WDW EM
SSB 0
LB 4.00 Hz
GB 0
PC 1.40

^{11}B NMR of fructose ester of 8-IQBA (pH = 7.2)

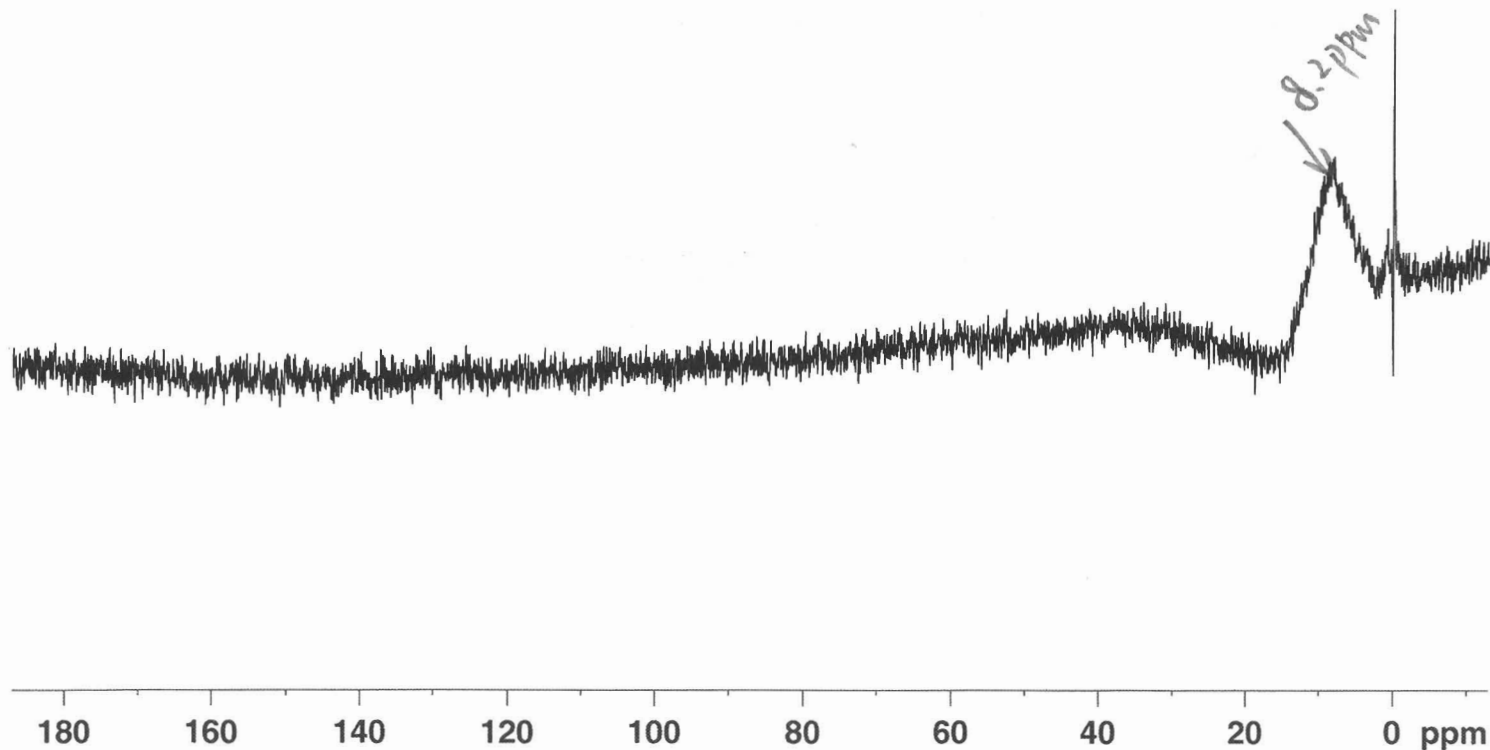


Current Data Parameters
NAME JC-III-8IQBA+Fru-7.2-11B
EXPNO 1
PROCNO 1

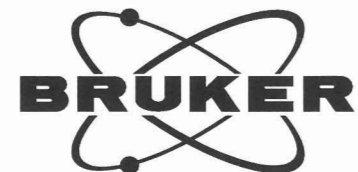
F2 - Acquisition Parameters
Date_ 20091022
Time 17.24
INSTRUM spect
PROBHD 5 mm PABBO BB-
PULPROG zg30
TD 16384
SOLVENT CDC13
NS 155
DS 0
SWH 50125.312 Hz
FIDRES 3.059406 Hz
AQ 0.1634804 sec
RG 2896.3
DW 9.975 usec
DE 25.00 usec
TE 296.1 K
D1 2.0000000 sec
MCREST 0.0000000 sec
MCWRK 0.0150000 sec

==== CHANNEL f1 =====
NUC1 11B
P1 5.00 usec
PL1 0.00 dB
SFO1 128.3876799 MHz

F2 - Processing parameters
SI 32768
SF 128.3774324 MHz
WDW EM
SSB 0
LB 4.00 Hz
GB 0
PC 1.40



^{11}B NMR of fructose ester of 8-IQBA (pH = 11.1)

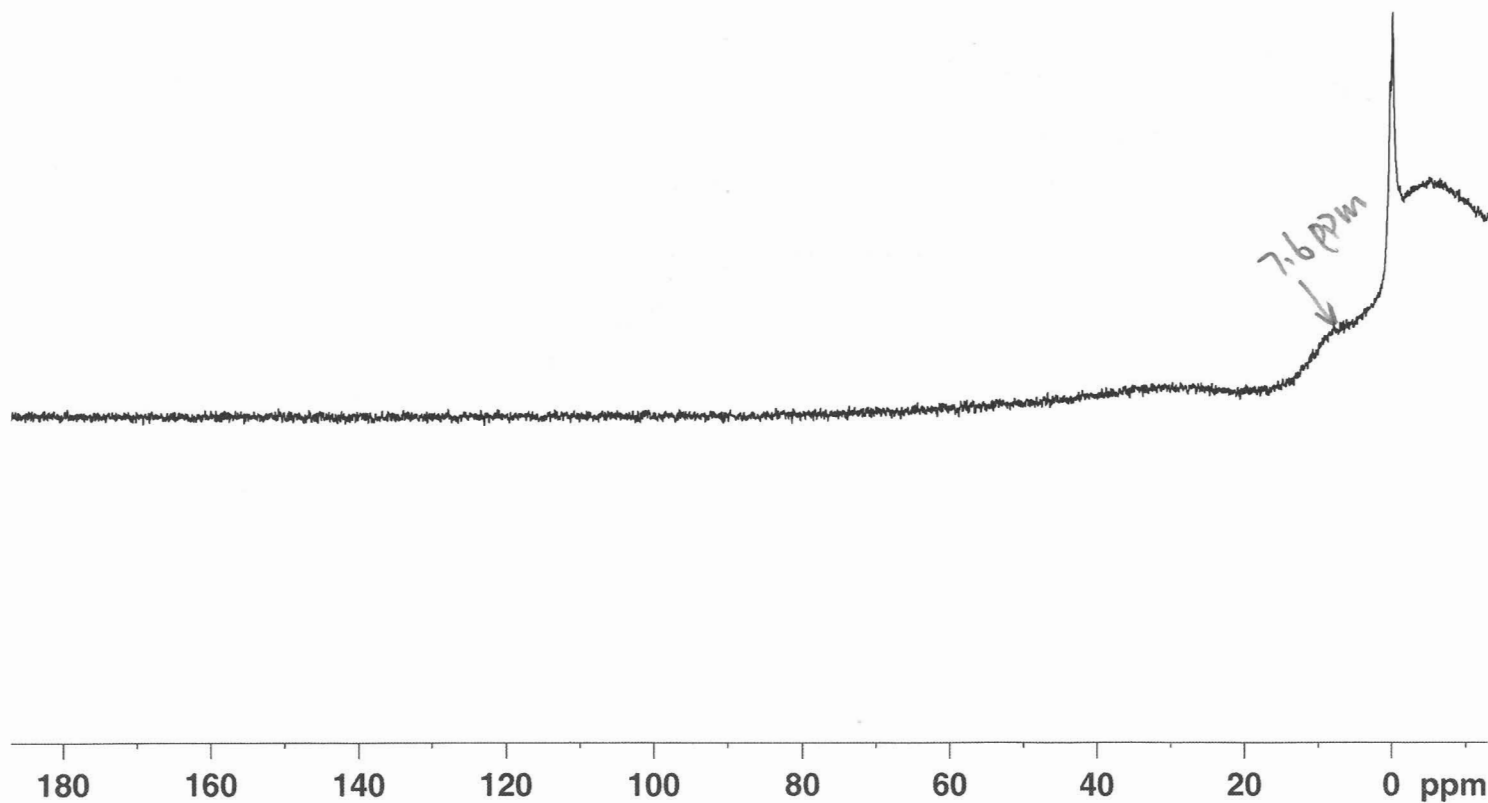


Current Data Parameters
NAME JC-III-8IQBA+Fru-11.1-11B
EXPNO 1
PROCNO 1

F2 - Acquisition Parameters
Date_ 20091022
Time 18.02
INSTRUM spect
PROBHD 5 mm PABBO BB-
PULPROG zg30
TD 16384
SOLVENT CDCl3
NS 121
DS 0
SWH 50125.312 Hz
FIDRES 3.059406 Hz
AQ 0.1634804 sec
RG 1024
DW 9.975 usec
DE 25.00 usec
TE 296.0 K
D1 2.00000000 sec
MCREST 0.00000000 sec
MCWRK 0.01500000 sec

===== CHANNEL f1 =====
NUC1 11B
P1 5.00 usec
PL1 0.00 dB
SFO1 128.3876799 MHz

F2 - Processing parameters
SI 32768
SF 128.3776050 MHz
WDW EM
SSB 0
LB 4.00 Hz
GB 0
PC 1.40



^{11}B NMR of 5-IQBA (pH = 1.6)

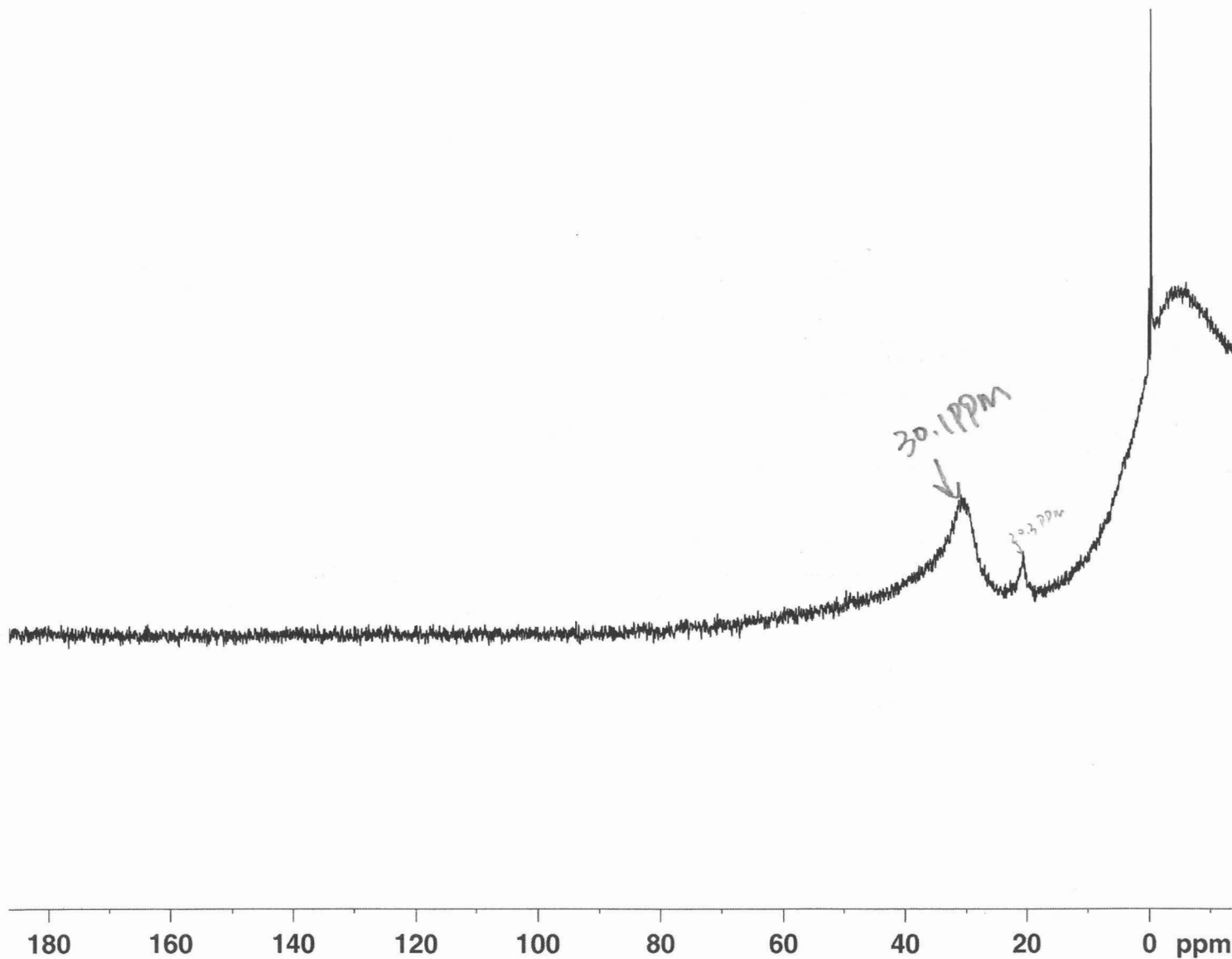


Current Data Parameters
NAME JC-III-5-IQBA-1.6-11B
EXPNO 1
PROCNO 1

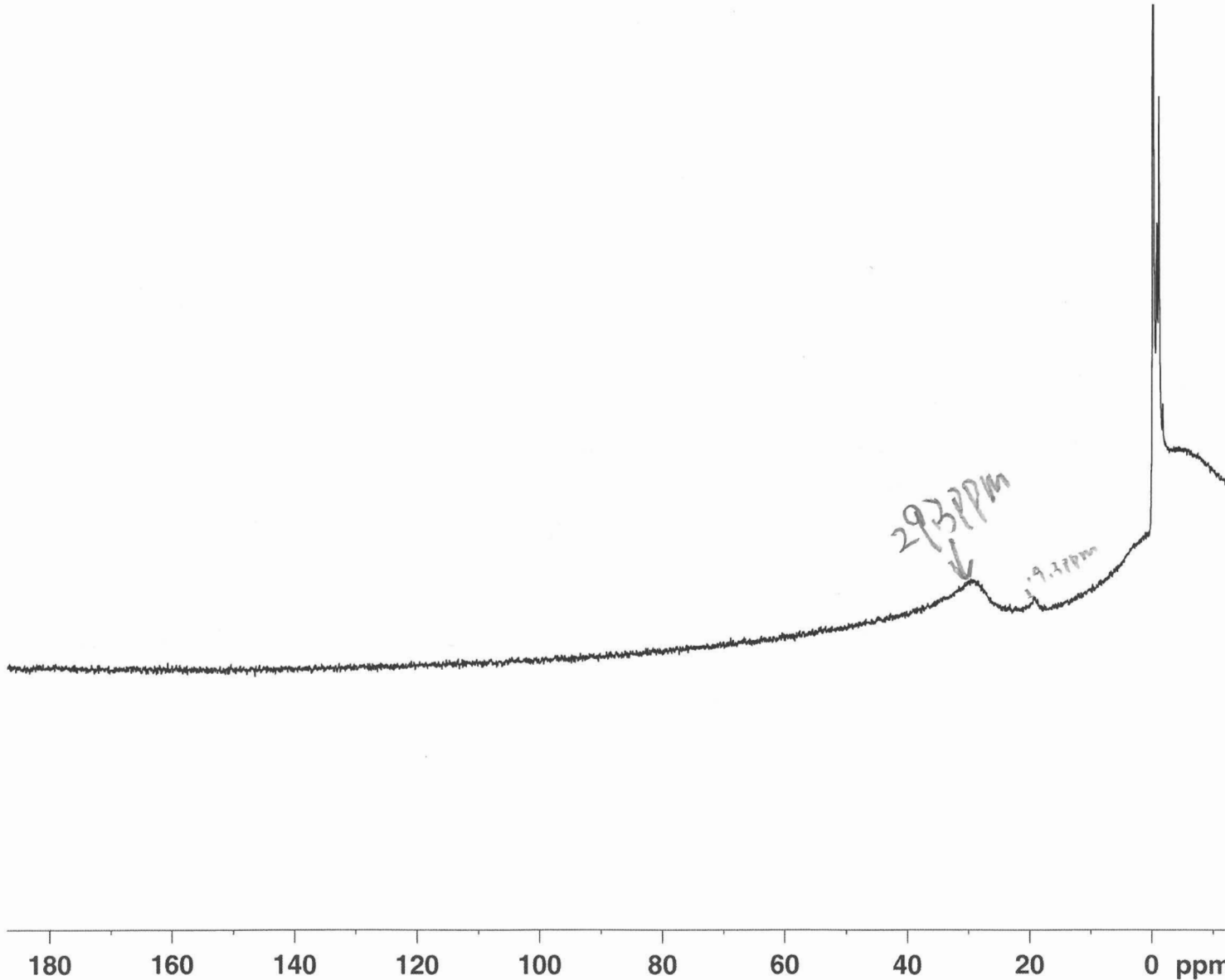
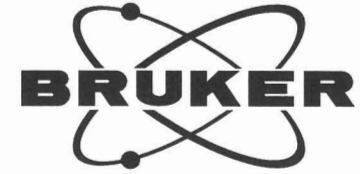
F2 - Acquisition Parameters
Date_ 20091023
Time 13.52
INSTRUM spect
PROBHD 5 mm PABBO BB-
PULPROG zg30
TD 16384
SOLVENT MeOD
NS 111
DS 0
SWH 50125.312 Hz
FIDRES 3.059406 Hz
AQ 0.1634804 sec
RG 1024
DW 9.975 usec
DE 25.00 usec
TE 296.1 K
D1 2.00000000 sec
MCREST 0.00000000 sec
MCWRK 0.01500000 sec

==== CHANNEL f1 =====
NUC1 11B
P1 5.00 usec
PL1 0.00 dB
SFO1 128.3876799 MHz

F2 - Processing parameters
SI 32768
SF 128.3772381 MHz
WDW EM
SSB 0
LB 4.00 Hz
GB 0
PC 1.40



¹¹B NMR of 5-IQBA (pH = 7.3)



Current Data Parameters
NAME JC-III-5-IQBA-7.3-11B
EXPNO 1
PROCNO 1

F2 - Acquisition Parameters
Date_ 20091023
Time 14.05
INSTRUM spect
PROBHD 5 mm PABBO BB-
PULPROG zg30
TD 16384
SOLVENT MeOD
NS 111
DS 0
SWH 50125.312 Hz
FIDRES 3.059406 Hz
AQ 0.1634804 sec
RG 1024
DW 9.975 usec
DE 25.00 usec
TE 296.2 K
D1 2.00000000 sec
MCREST 0.00000000 sec
MCWRK 0.01500000 sec

==== CHANNEL f1 =====
NUC1 11B
P1 5.00 usec
PL1 0.00 dB
SFO1 128.3876799 MHz

F2 - Processing parameters
SI 32768
SF 128.3774477 MHz
WDW EM
SSB 0
LB 4.00 Hz
GB 0
PC 1.40

^{11}B NMR of 5-IQBA (pH = 12.8)



Current Data Parameters

NAME JC-III-5-IQBA-12.8-11B
EXPNO 1
PROCNO 1

F2 - Acquisition Parameters

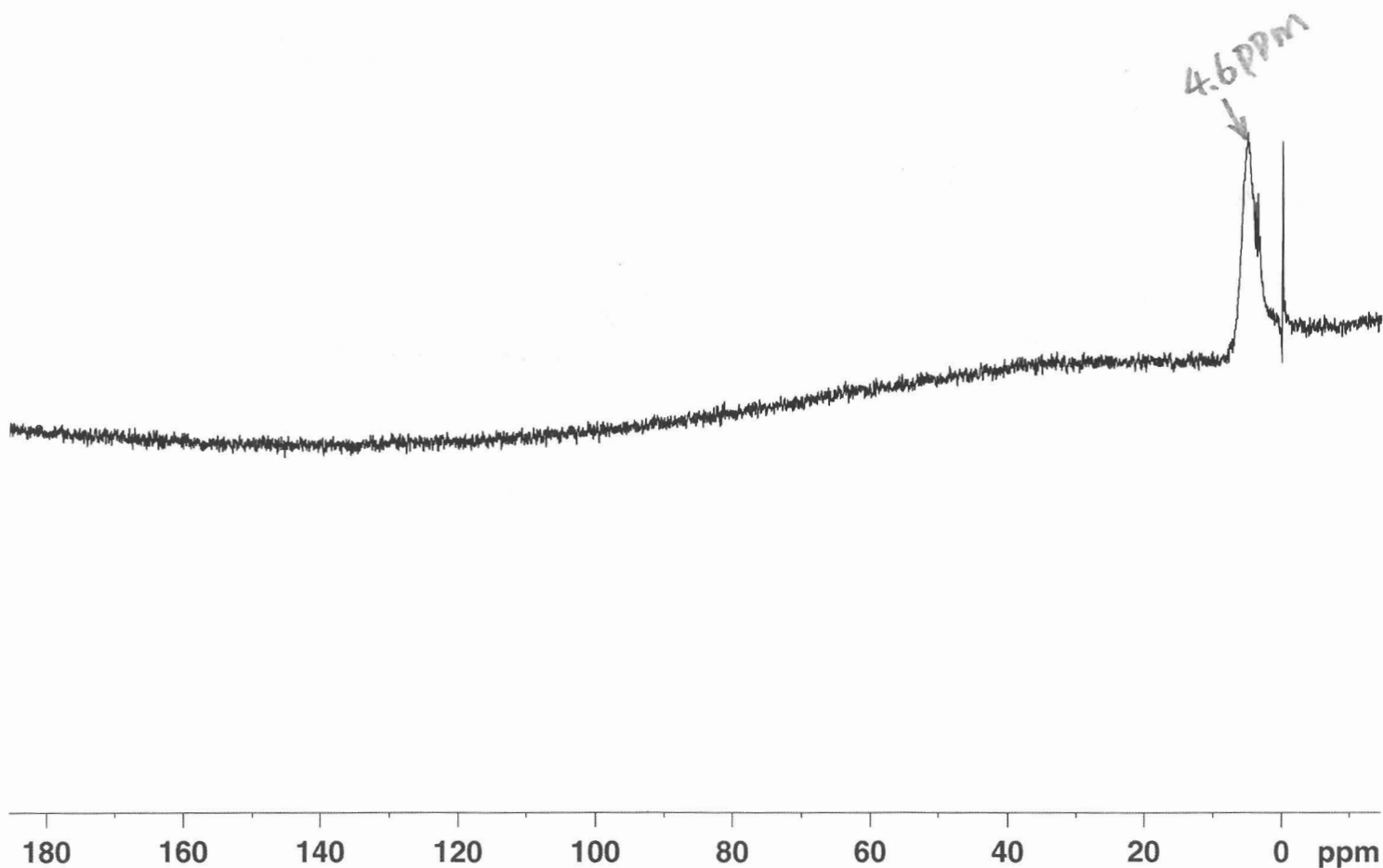
Date_ 20091023
Time 14.16
INSTRUM spect
PROBHD 5 mm PABBO BB-
PULPROG zg30
TD 16384
SOLVENT CDCl3
NS 113
DS 0
SWH 50125.312 Hz
FIDRES 3.059406 Hz
AQ 0.1634804 sec
RG 2896.3
DW 9.975 usec
DE 25.00 usec
TE 296.2 K
D1 2.0000000 sec
MCREST 0.0000000 sec
MCWRK 0.0150000 sec

==== CHANNEL f1 =====

NUC1 11B
P1 5.00 usec
PL1 0.00 dB
SFO1 128.3876799 MHz

F2 - Processing parameters

SI 32768
SF 128.3772396 MHz
WDW EM
SSB 0
LB 4.00 Hz
GB 0
PC 1.40



^{11}B NMR of fructose ester of 5-IQBA (pH = 2.1)

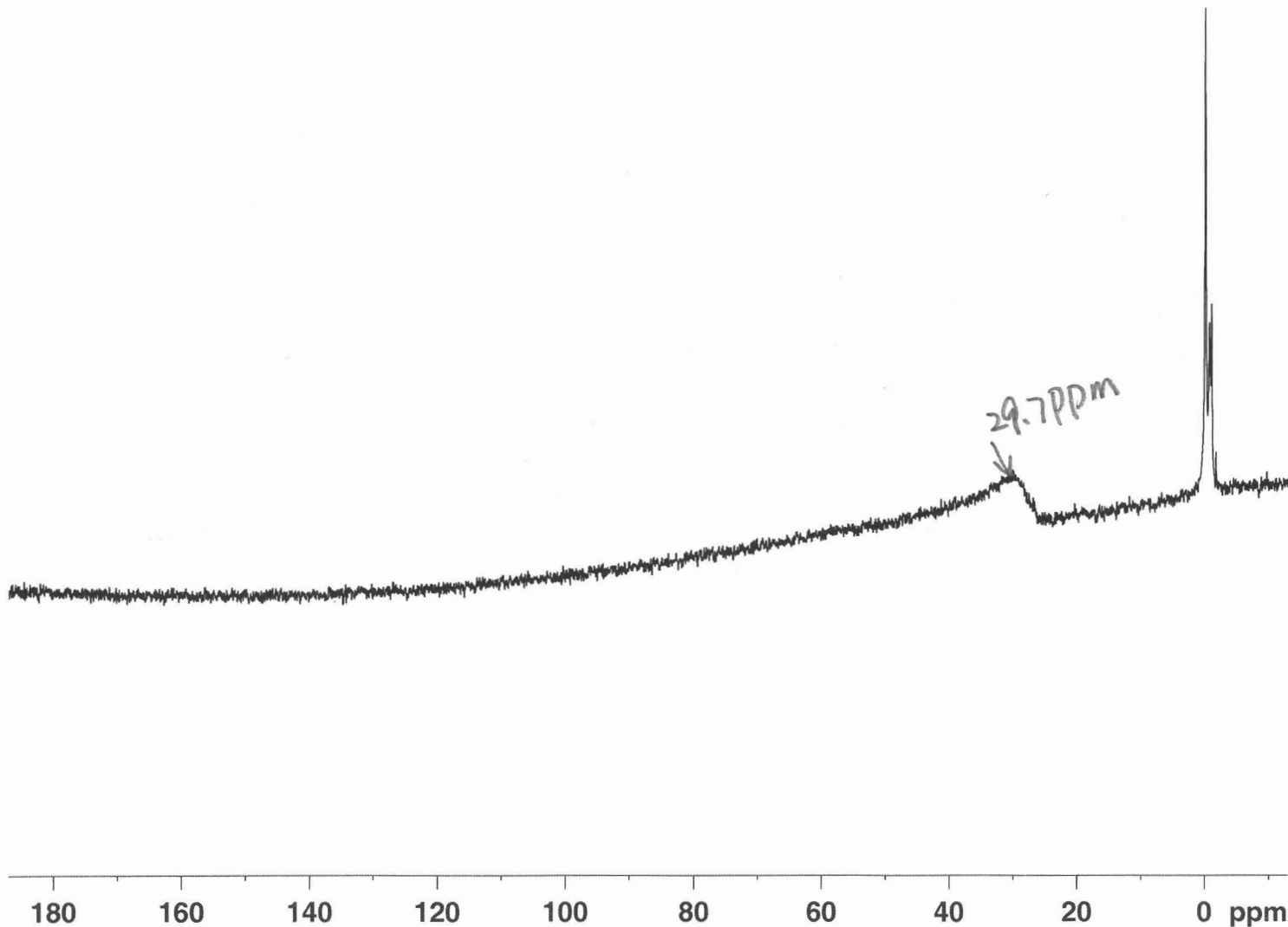


Current Data Parameters
NAME JC-III-5-IQBA+Fru-2.1-11B
EXPNO 1
PROCNO 1

F2 - Acquisition Parameters
Date_ 20091023
Time 17.58
INSTRUM spect
PROBHD 5 mm PABBO BB-
PULPROG zg30
TD 16384
SOLVENT MeOD
NS 67
DS 0
SWH 50125.312 Hz
FIDRES 3.059406 Hz
AQ 0.1634804 sec
RG 2896.3
DW 9.975 usec
DE 25.00 usec
TE 296.0 K
D1 2.00000000 sec
MCREST 0.00000000 sec
MCWRK 0.01500000 sec

=====
CHANNEL f1
NUC1 11B
P1 5.00 usec
PL1 0.00 dB
SFO1 128.3876799 MHz

F2 - Processing parameters
SI 32768
SF 128.3776511 MHz
WDW EM
SSB 0
LB 4.00 Hz
GB 0
PC 1.40



¹¹B NMR of fructose ester of 5-IQBA (pH = 7.6)

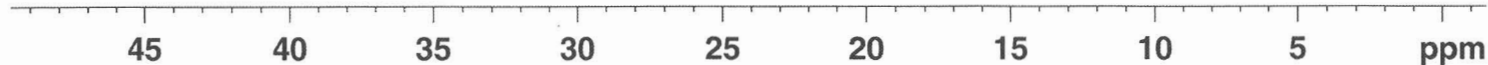
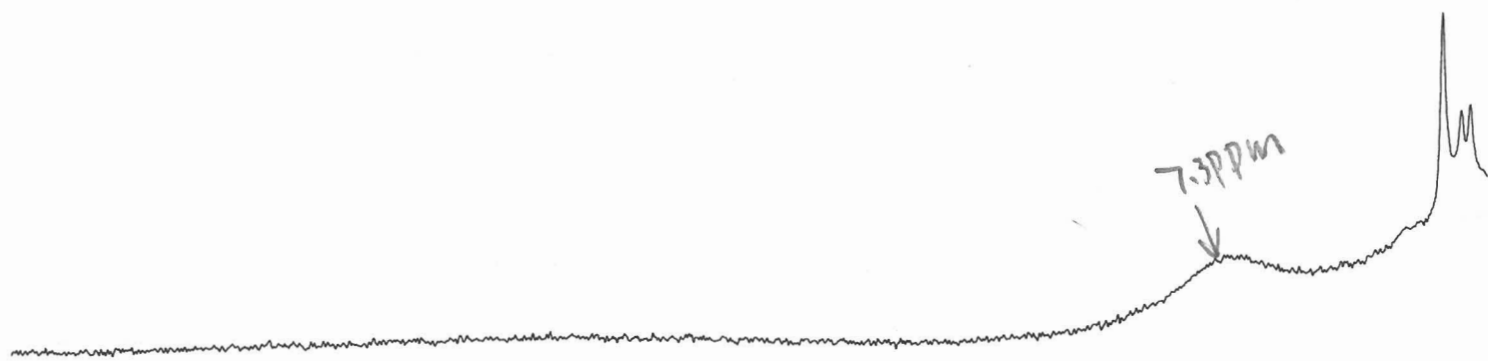


Current Data Parameters
NAME JC-III-5-IQBA+Fru-7.6-11B
EXPNO 1
PROCNO 1

F2 - Acquisition Parameters
Date_ 20091023
Time 18.23
INSTRUM spect
PROBHD 5 mm PABBO BB-
PULPROG zg30
TD 16384
SOLVENT CDC13
NS 138
DS 0
SWH 50125.312 Hz
FIDRES 3.059406 Hz
AQ 0.1634804 sec
RG 1024
DW 9.975 usec
DE 25.00 usec
TE 296.0 K
D1 2.00000000 sec
MCREST 0.00000000 sec
MCWRK 0.01500000 sec

=====
CHANNEL f1
NUC1 11B
P1 5.00 usec
PL1 0.00 dB
SFO1 128.3876799 MHz

F2 - Processing parameters
SI 32768
SF 128.3774477 MHz
WDW EM
SSB 0
LB 4.00 Hz
GB 0
PC 1.40



^{11}B NMR of fructose ester of 5-IQBA (pH = 11.7)

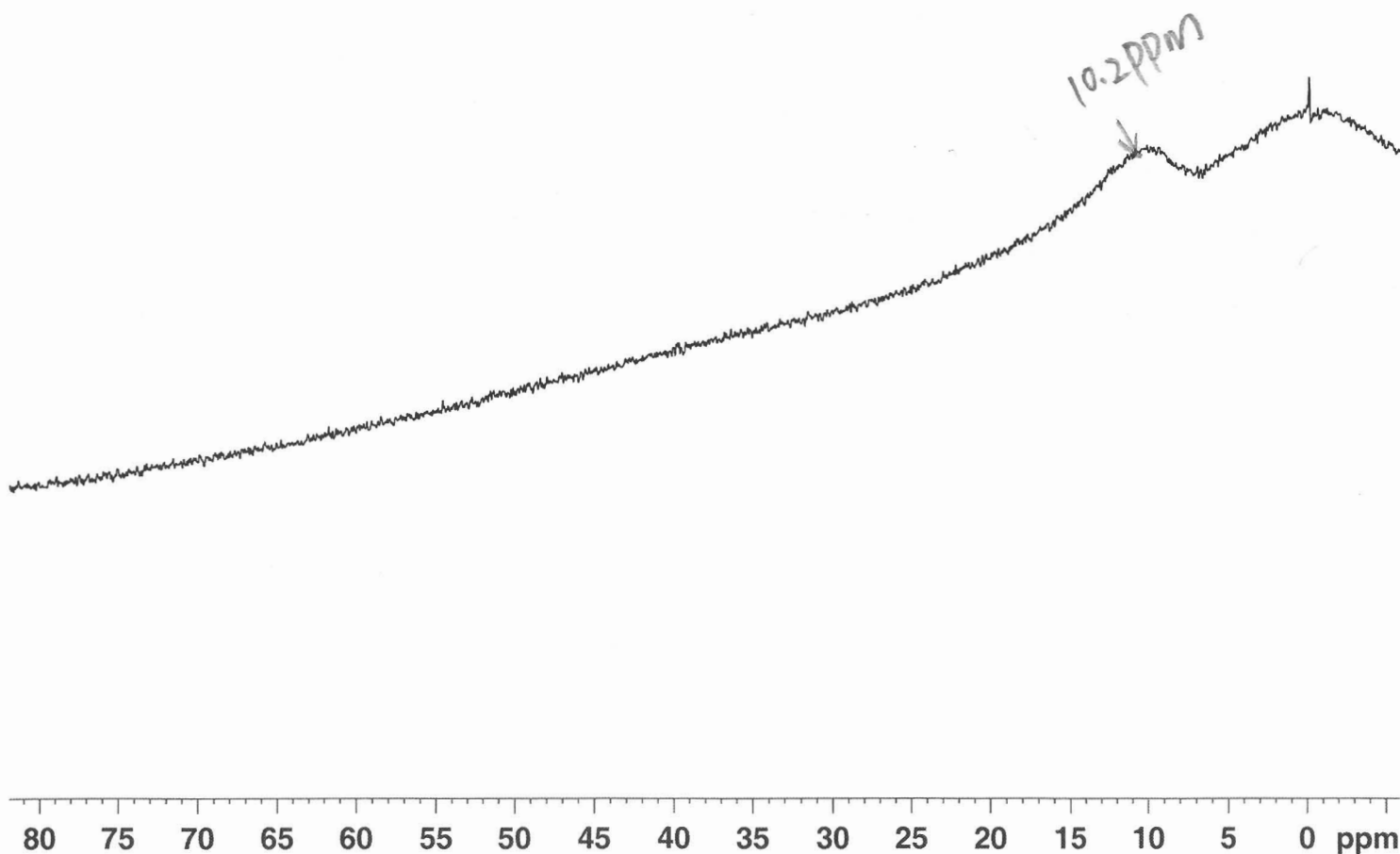


Current Data Parameters
NAME JC-III-5-IQBA+Fru-11.7-11B
EXPNO 1
PROCNO 1

F2 - Acquisition Parameters
Date_ . 20091023
Time 18.08
INSTRUM spect
PROBHD 5 mm PABBO BB-
PULPROG zg30
TD 16384
SOLVENT CDC13
NS 107
DS 0
SWH 50125.312 Hz
FIDRES 3.059406 Hz
AQ 0.1634804 sec
RG 1024
DW 9.975 usec
DE 25.00 usec
TE 296.0 K
D1 2.00000000 sec
MCREST 0.00000000 sec
MCWRK 0.01500000 sec

==== CHANNEL f1 =====
NUC1 11B
P1 5.00 usec
PL1 0.00 dB
SFO1 128.3876799 MHz

F2 - Processing parameters
SI 32768
SF 128.3772412 MHz
WDW EM
SSB 0
LB 4.00 Hz
GB 0
PC 1.40



^{11}B NMR of 4-IQBA (pH = 1.5)

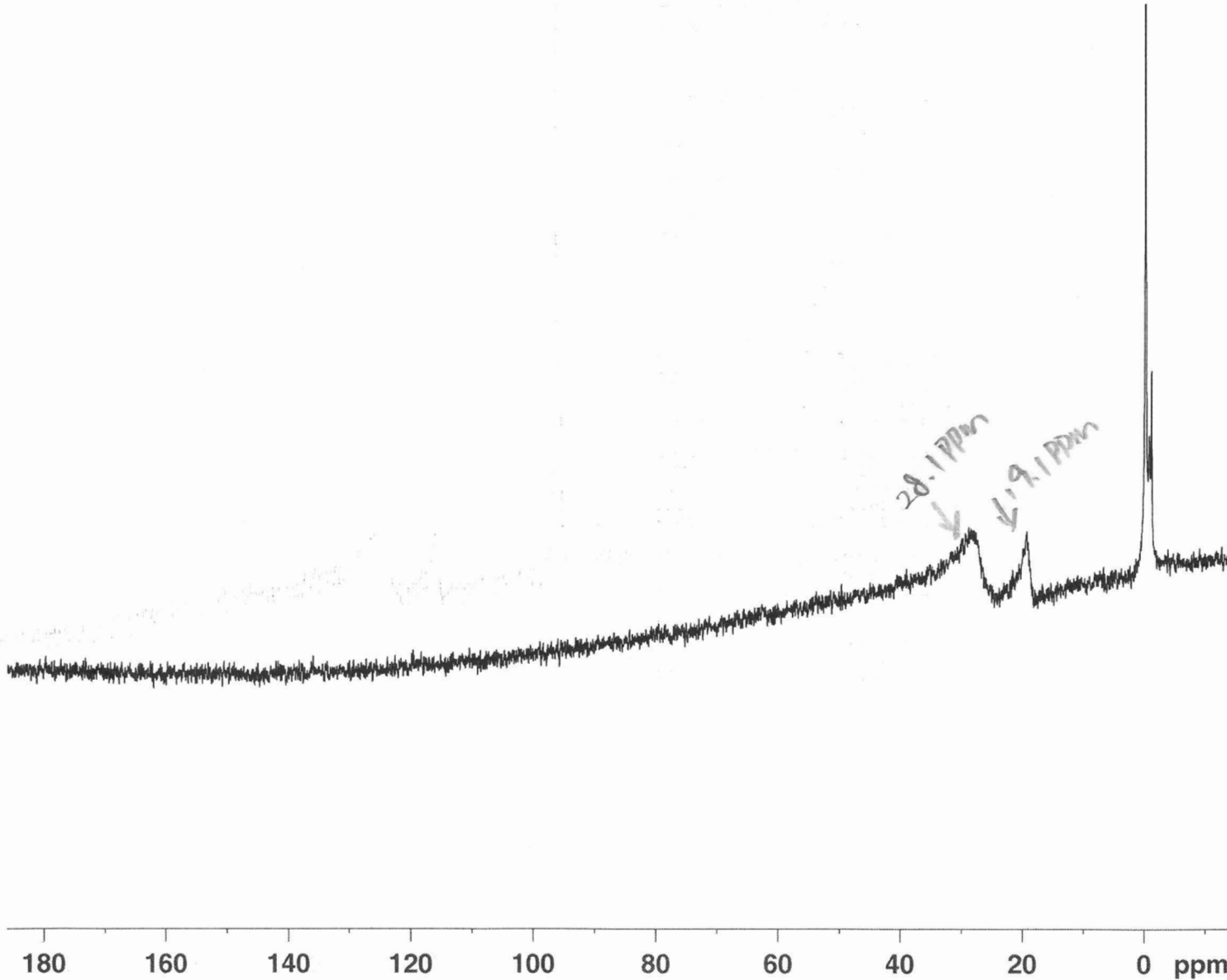


Current Data Parameters
NAME JC-III-4-IQBA-1.5-11B-2
EXPNO 1
PROCNO 1

F2 - Acquisition Parameters
Date_ 20091106
Time 17.01
INSTRUM spect
PROBHD 5 mm PABBO BB-
PULPROG zg30
TD 16384
SOLVENT MeOD
NS 53
DS 0
SWH 50125.312 Hz
FIDRES 3.059406 Hz
AQ 0.1634804 sec
RG 2896.3
DW 9.975 usec
DE 25.00 usec
TE 296.7 K
D1 2.00000000 sec
MCREST 0.00000000 sec
MCWRK 0.01500000 sec

==== CHANNEL f1 =====
NUC1 11B
P1 5.00 usec
PL1 0.00 dB
SF01 128.3876799 MHz

F2 - Processing parameters
SI 32768
SF 128.3776450 MHz
WDW EM
SSB 0
LB 4.00 Hz
GB 0
PC 1.40



<

¹¹B NMR of 4-IQBA (pH = 5.7)

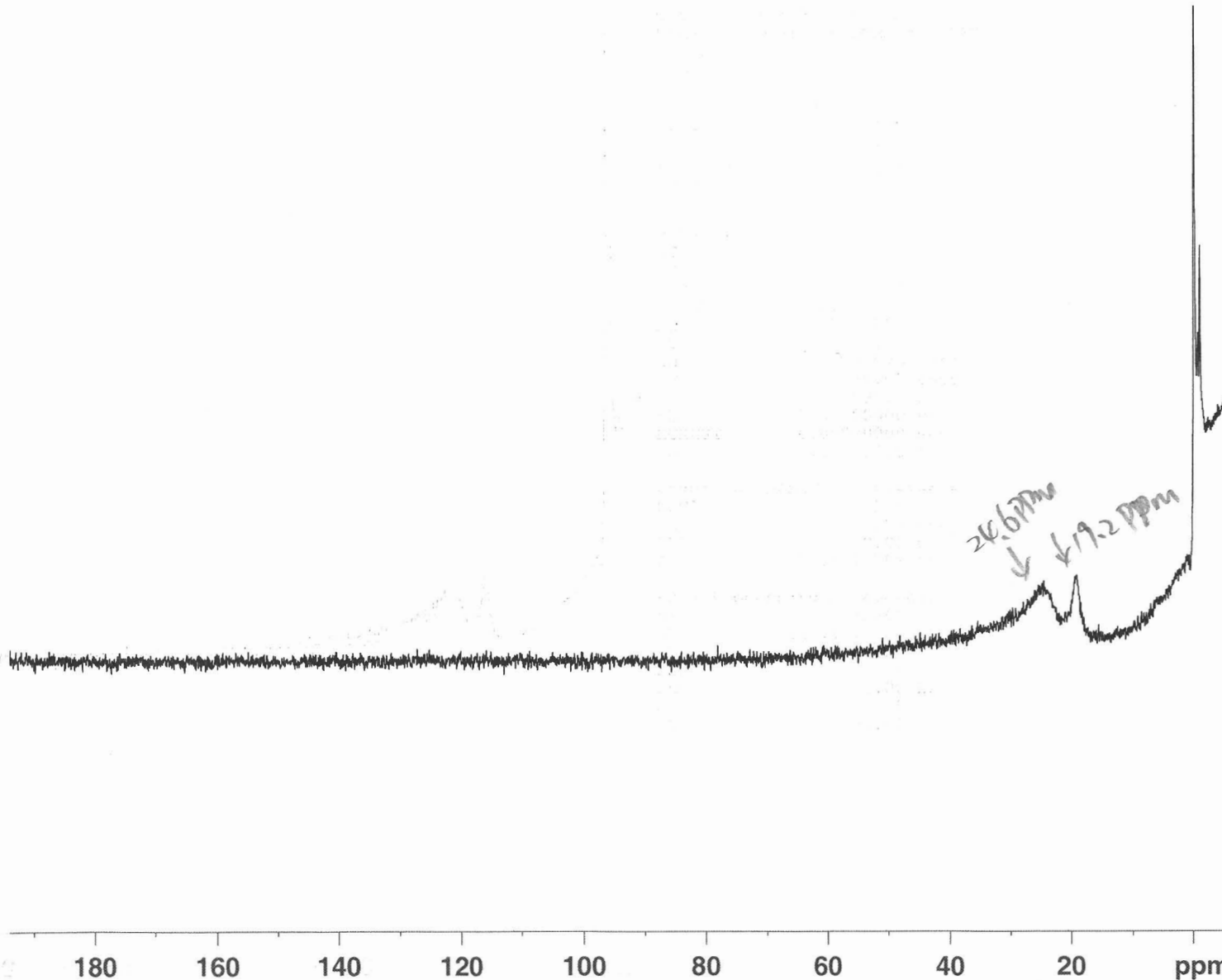


Current Data Parameters
NAME JC-III-4-IQBA-5.7-11B
EXPNO 1
PROCNO 1

F2 - Acquisition Parameters
Date_ 20091106
Time 16.39
INSTRUM spect
PROBHD 5 mm PABBO BB-
PULPROG zg30
TD 16384
SOLVENT MeOD
NS 68
DS 0
SWH 50125.312 Hz
FIDRES 3.059406 Hz
AQ 0.1634804 sec
RG 1024
DW 9.975 usec
DE 25.00 usec
TE 296.7 K
D1 2.00000000 sec
MCREST 0.00000000 sec
MCWRK 0.01500000 sec

==== CHANNEL f1 =====
NUC1 11B
P1 5.00 usec
PL1 0.00 dB
SFO1 128.3876799 MHz

F2 - Processing parameters
SI 32768
SF 128.3776404 MHz
WDW EM
SSB 0
LB 4.00 Hz
GB 0
PC 1.40



190 180 160 140 120 100 80 60 40 20 ppm

^{11}B NMR of 4-IQBA (pH = 12.2)

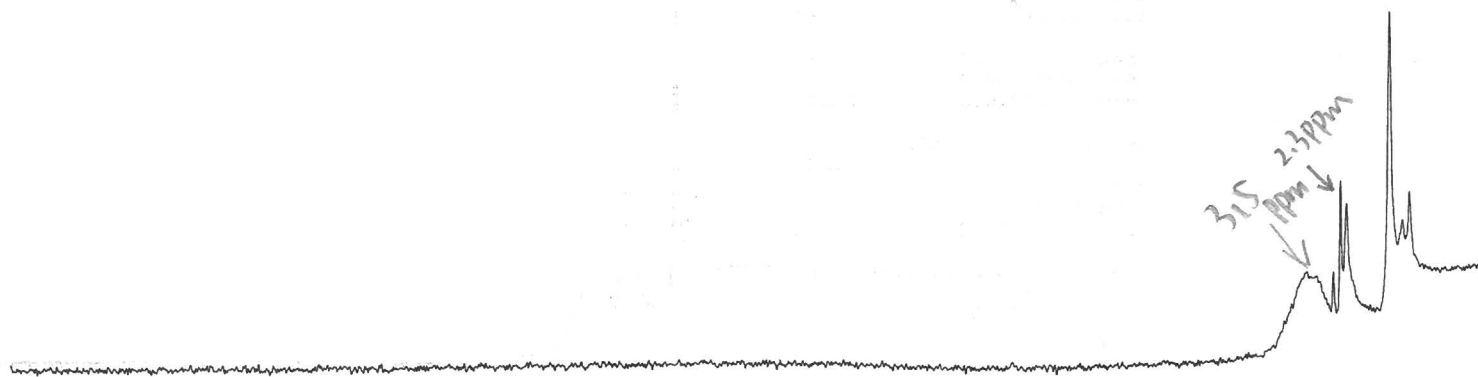


Current Data Parameters
NAME JC-III-4-IQBA-12.2-11B
EXPNO 1
PROCNO 1

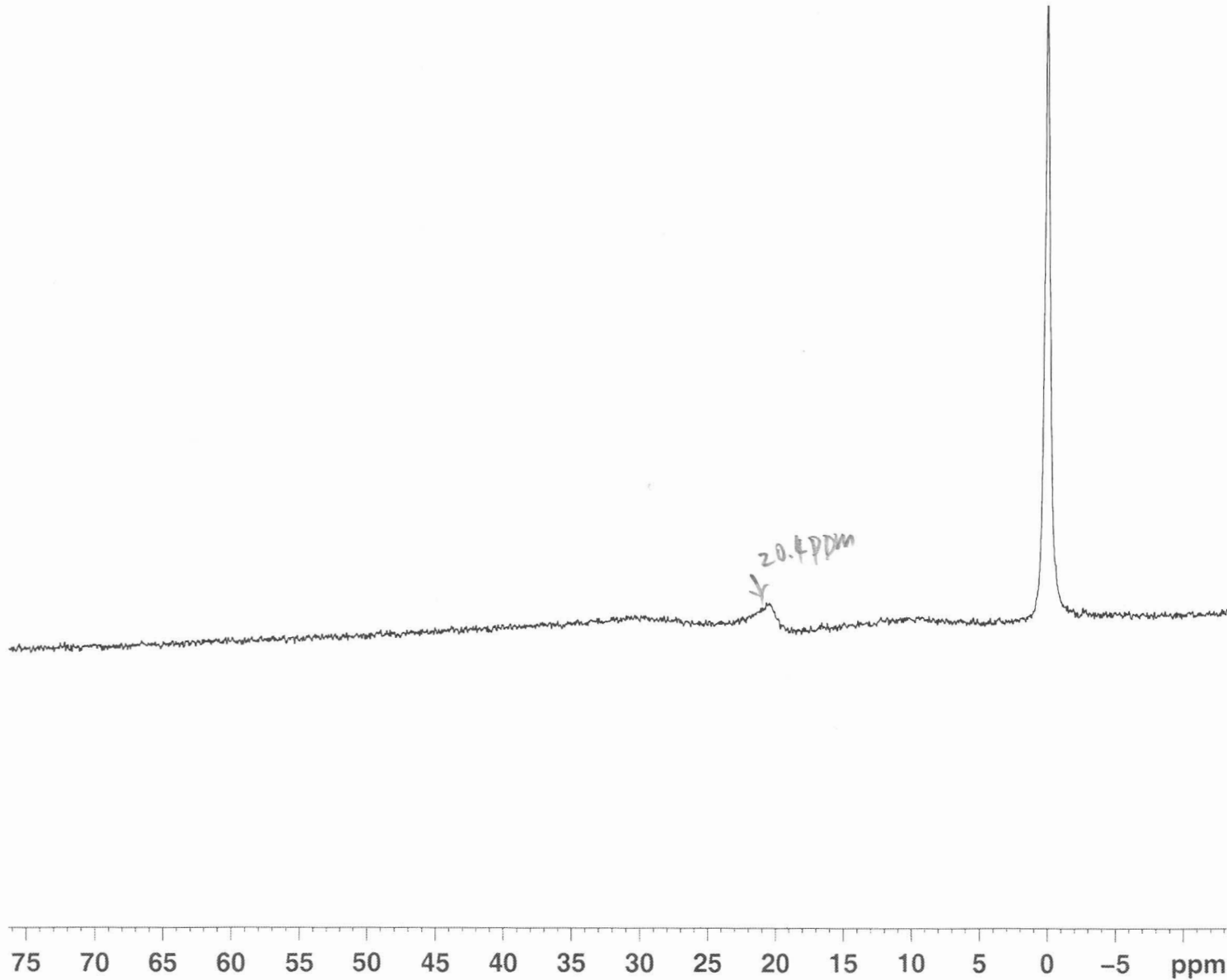
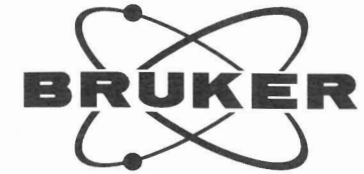
F2 - Acquisition Parameters
Date_ 20091106
Time 16.49
INSTRUM spect
PROBHD 5 mm PABBO BB-
PULPROG zg30
TD 16384
SOLVENT MeOD
NS 68
DS 0
SWH 50125.312 Hz
FIDRES 3.059406 Hz
AQ 0.1634804 sec
RG 1024
DW 9.975 usec
DE 25.00 usec
TE 296.7 K
D1 2.00000000 sec
MCREST 0.00000000 sec
MCWRK 0.01500000 sec

==== CHANNEL f1 =====
NUC1 11B
P1 5.00 usec
PL1 0.00 dB
SFO1 128.3876799 MHz

F2 - Processing parameters
SI 32768
SF 128.3776450 MHz
WDW EM
SSB 0
LB 4.00 Hz
GB 0
PC 1.40



^{11}B NMR of fructose ester of 4-IQBA (pH = 2.0)



Current Data Parameters
NAME JC-III-4-IQBA+Fru-1.98-11B
EXPNO 1
PROCNO 1

F2 - Acquisition Parameters
Date_ 20100110
Time 15.50
INSTRUM spect
PROBHD 5 mm PABBO BB-
PULPROG zg30
TD 16384
SOLVENT D2O
NS 53
DS 0
SWH 50125.312 Hz
FIDRES 3.059406 Hz
AQ 0.1634804 sec
RG 2896.3
DW 9.975 usec
DE 25.00 usec
TE 297.1 K
D1 2.00000000 sec
MCREST 0.00000000 sec
MCWRK 0.01500000 sec

==== CHANNEL f1 =====
NUC1 11B
P1 5.00 usec
PL1 0.00 dB
SF01 128.3876799 MHz

F2 - Processing parameters
SI 32768
SF 128.3776924 MHz
WDW EM
SSB 0
LB 4.00 Hz
GB 0
PC 1.40

¹¹B NMR of fructose ester of 4-IQBA (pH = 6.6)

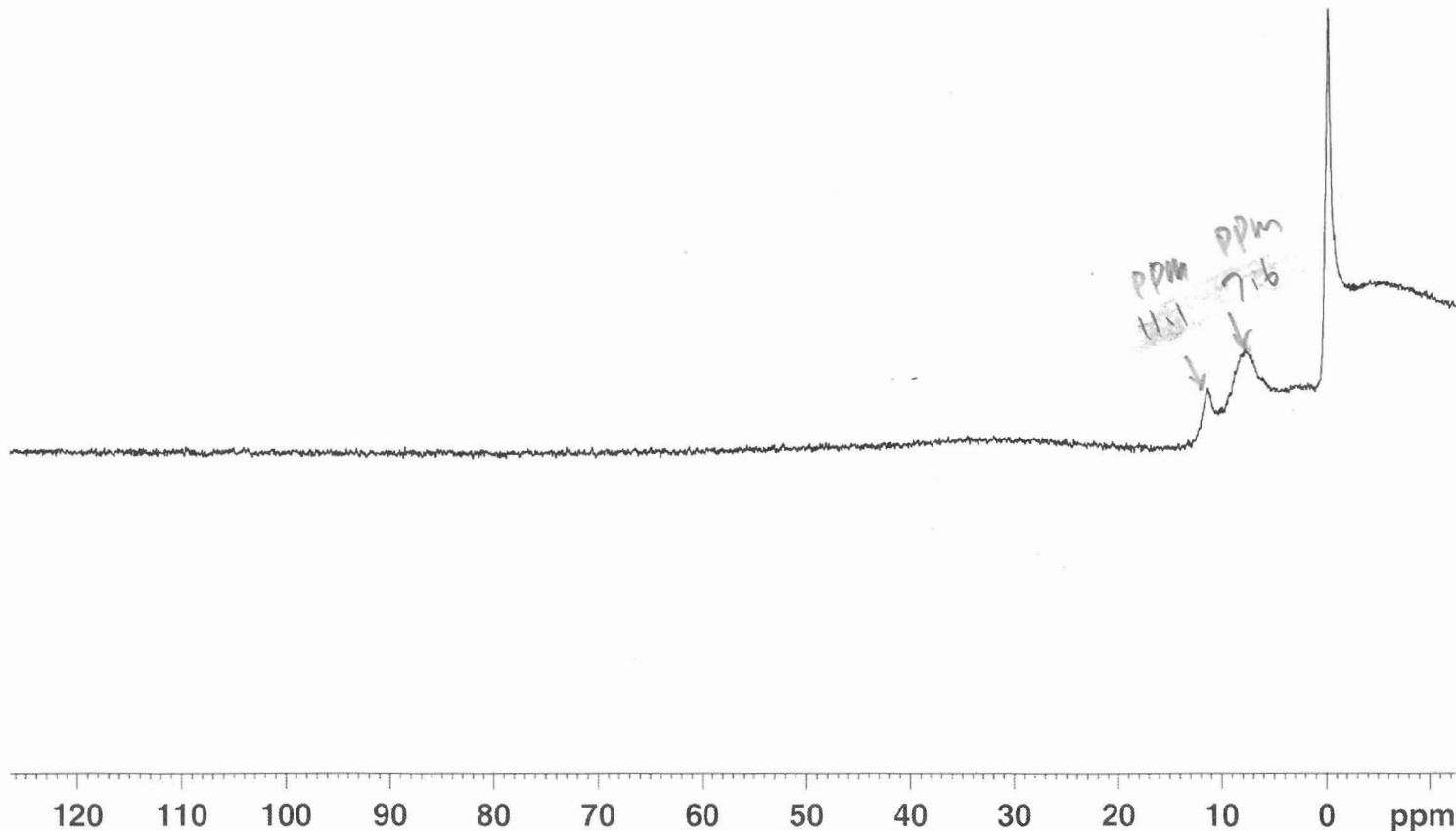


Current Data Parameters
NAME JC-III-4-IQBA+Fru-6.57-11B
EXPNO 1
PROCNO 1

F2 - Acquisition Parameters
Date_ 20100110
Time 16.10
INSTRUM spect
PROBHD 5 mm PABBO BB-
PULPROG zg30
TD 16384
SOLVENT CDCl3
NS 115
DS 0
SWH 50125.312 Hz
FIDRES 3.059406 Hz
AQ 0.1634804 sec
RG 1024
DW 9.975 usec
DE 25.00 usec
TE 297.2 K
D1 2.00000000 sec
MCREST 0.00000000 sec
MCWRK 0.01500000 sec

==== CHANNEL f1 =====
NUC1 11B
P1 5.00 usec
PL1 0.00 dB
SFO1 128.3876799 MHz

F2 - Processing parameters
SI 32768
SF 128.3775700 MHz
WDW EM
SSB 0
LB 4.00 Hz
GB 0
PC 1.40



^{11}B NMR of fructose ester of 4-IQBA (pH = 12.0)

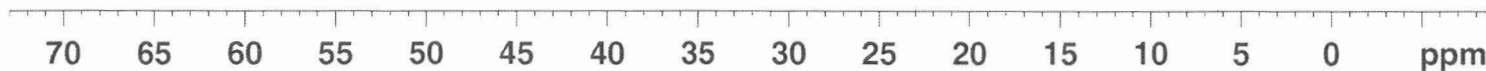


Current Data Parameters
NAME JC-III-4-IQBA+Fru-11.98-11B
EXPNO 1
PROCNO 1

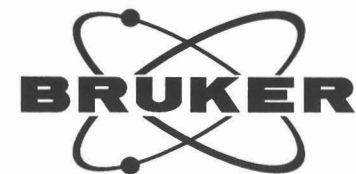
F2 - Acquisition Parameters
Date_ 20100110
Time 16.39
INSTRUM spect
PROBHD 5 mm PABBO BB-
PULPROG zg30
TD 16384
SOLVENT CDCl3
NS 204
DS 0
SWH 50125.312 Hz
FIDRES 3.059406 Hz
AQ 0.1634804 sec
RG 1024
DW 9.975 usec
DE 25.00 usec
TE 297.2 K
D1 2.00000000 sec
MCREST 0.00000000 sec
MCWRK 0.01500000 sec

==== CHANNEL f1 =====
NUC1 11B
P1 5.00 usec
PL1 0.00 dB
SFO1 128.3876799 MHz

F2 - Processing parameters
SI 32768
SF 128.3775563 MHz
WDW EM
SSB 0
LB 4.00 Hz
GB 0
PC 1.40



^{11}B NMR of 6-IQBA (pH = 1.6)

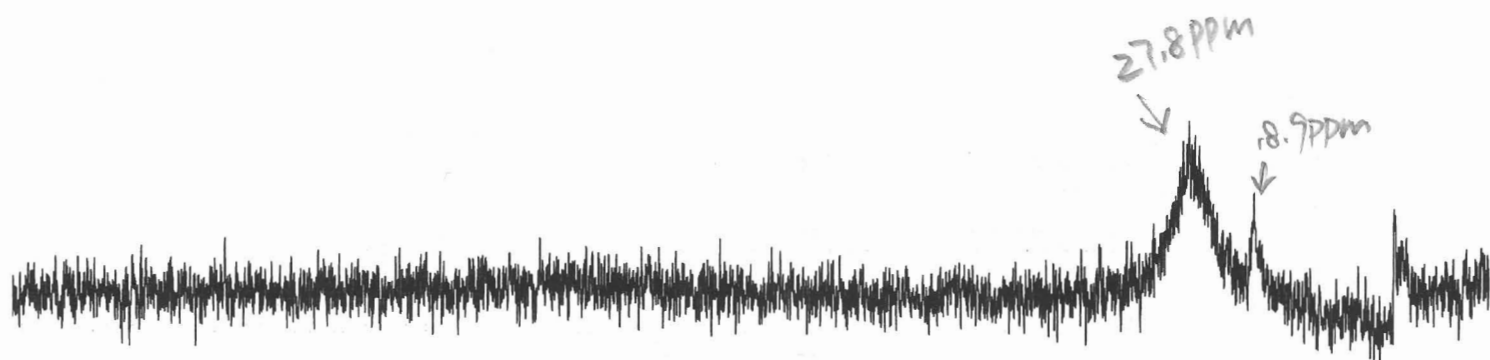


Current Data Parameters
NAME JC-III-6-IQBA-1.6-11B
EXPNO 1
PROCNO 1

F2 - Acquisition Parameters
Date_ 20091026
Time 17.47
INSTRUM spect
PROBHD 5 mm PABBO BB-
PULPROG zg30
TD 16384
SOLVENT MeOD
NS 55
DS 0
SWH 50125.312 Hz
FIDRES 3.059406 Hz
AQ 0.1634804 sec
RG 3251
DW 9.975 usec
DE 25.00 usec
TE 295.6 K
D1 2.00000000 sec
MCREST 0.00000000 sec
MCWRK 0.01500000 sec

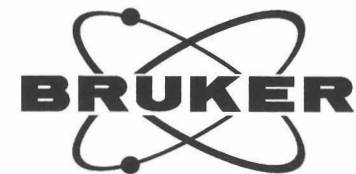
==== CHANNEL f1 =====
NUC1 11B
P1 5.00 usec
PL1 0.00 dB
SFO1 128.3876799 MHz

F2 - Processing parameters
SI 32768
SF 128.3774675 MHz
WDW EM
SSB 0
LB 4.00 Hz
GB 0
PC 1.40



180 160 140 120 100 80 60 40 20 0 ppm

^{11}B NMR of 6-IQBA (pH = 7.6)

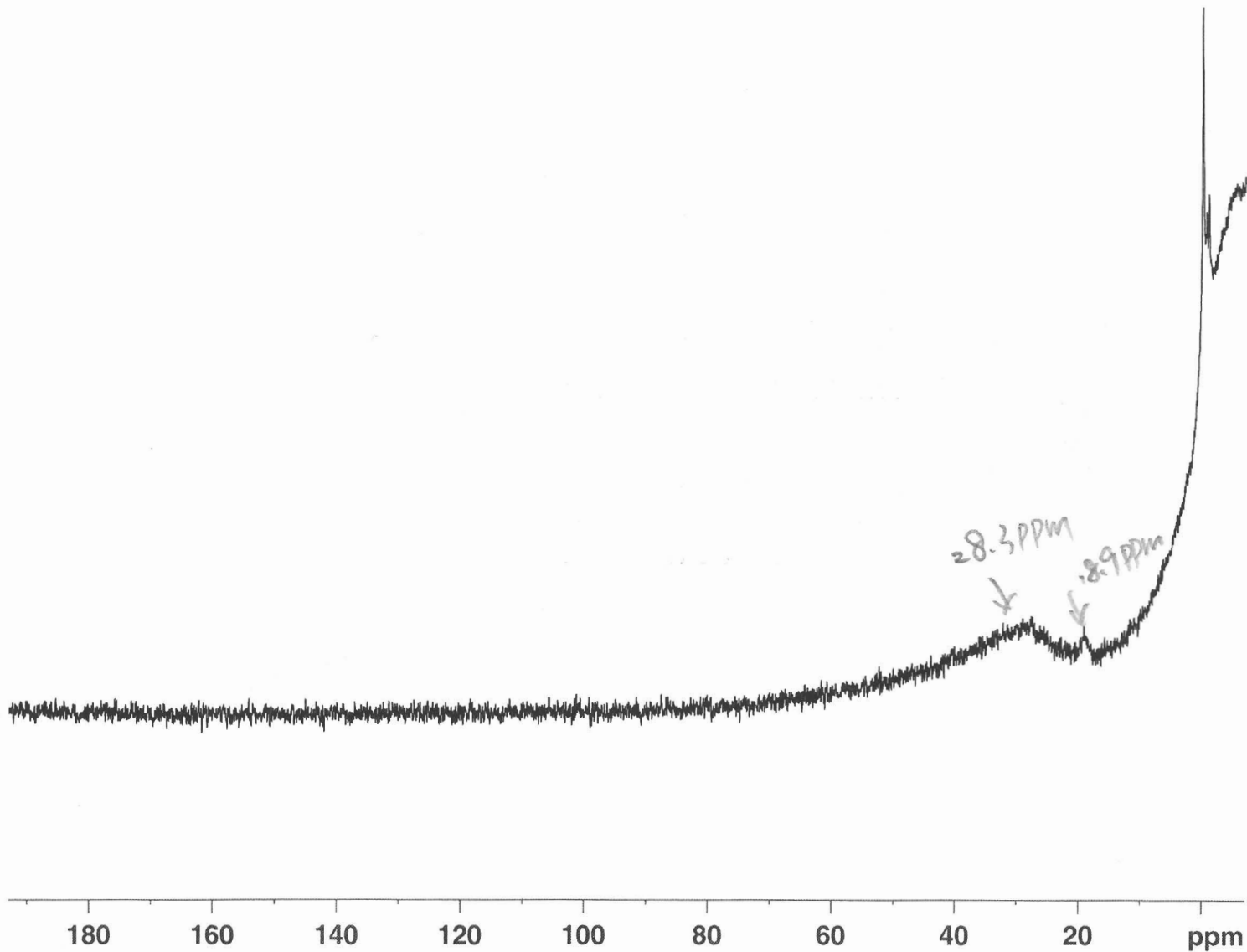


Current Data Parameters
NAME JC-III-6-IQBA-7.6-11B
EXPNO 1
PROCNO 1

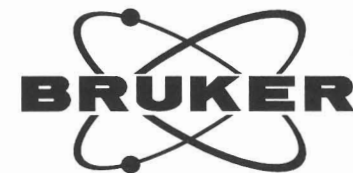
F2 - Acquisition Parameters
Date_ 20091026
Time 18.08
INSTRUM spect
PROBHD 5 mm PABBO BB-
PULPROG zg30
TD 16384
SOLVENT CDC13
NS 119
DS 0
SWH 50125.312 Hz
FIDRES 3.059406 Hz
AQ 0.1634804 sec
RG 1024
DW 9.975 usec
DE 25.00 usec
TE 295.7 K
D1 2.00000000 sec
MCREST 0.00000000 sec
MCWRK 0.01500000 sec

==== CHANNEL f1 =====
NUC1 11B
P1 5.00 usec
PL1 0.00 dB
SFO1 128.3876799 MHz

F2 - Processing parameters
SI 32768
SF 128.3774798 MHz
WDW EM
SSB 0
LB 4.00 Hz
GB 0
PC 1.40



¹¹B NMR of 6-IQBA (pH = 12.6)

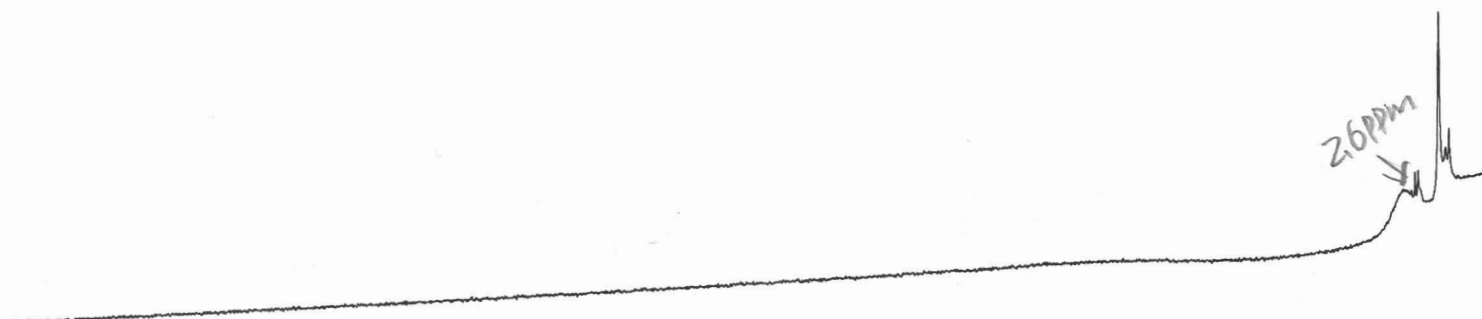


Current Data Parameters
NAME JC-III-6-IQBA-12.6-11B
EXPNO 1
PROCNO 1

F2 - Acquisition Parameters
Date_ 20091026
Time 18.23
INSTRUM spect
PROBHD 5 mm PABBO BB-
PULPROG zg30
TD 16384
SOLVENT CDC13
NS 184
DS 0
SWH 50125.312 Hz
FIDRES 3.059406 Hz
AQ 0.1634804 sec
RG 1024
DW 9.975 usec
DE 25.00 usec
TE 295.7 K
D1 2.00000000 sec
MCREST 0.00000000 sec
MCWRK 0.01500000 sec

=====
CHANNEL f1
NUC1 11B
P1 5.00 usec
PL1 0.00 dB
SFO1 128.3876799 MHz

F2 - Processing parameters
SI 32768
SF 128.3774461 MHz
WDW EM
SSB 0
LB 4.00 Hz
GB 0
PC 1.40



^{11}B NMR of fructose ester of 6-IQBA (pH = 1.5)

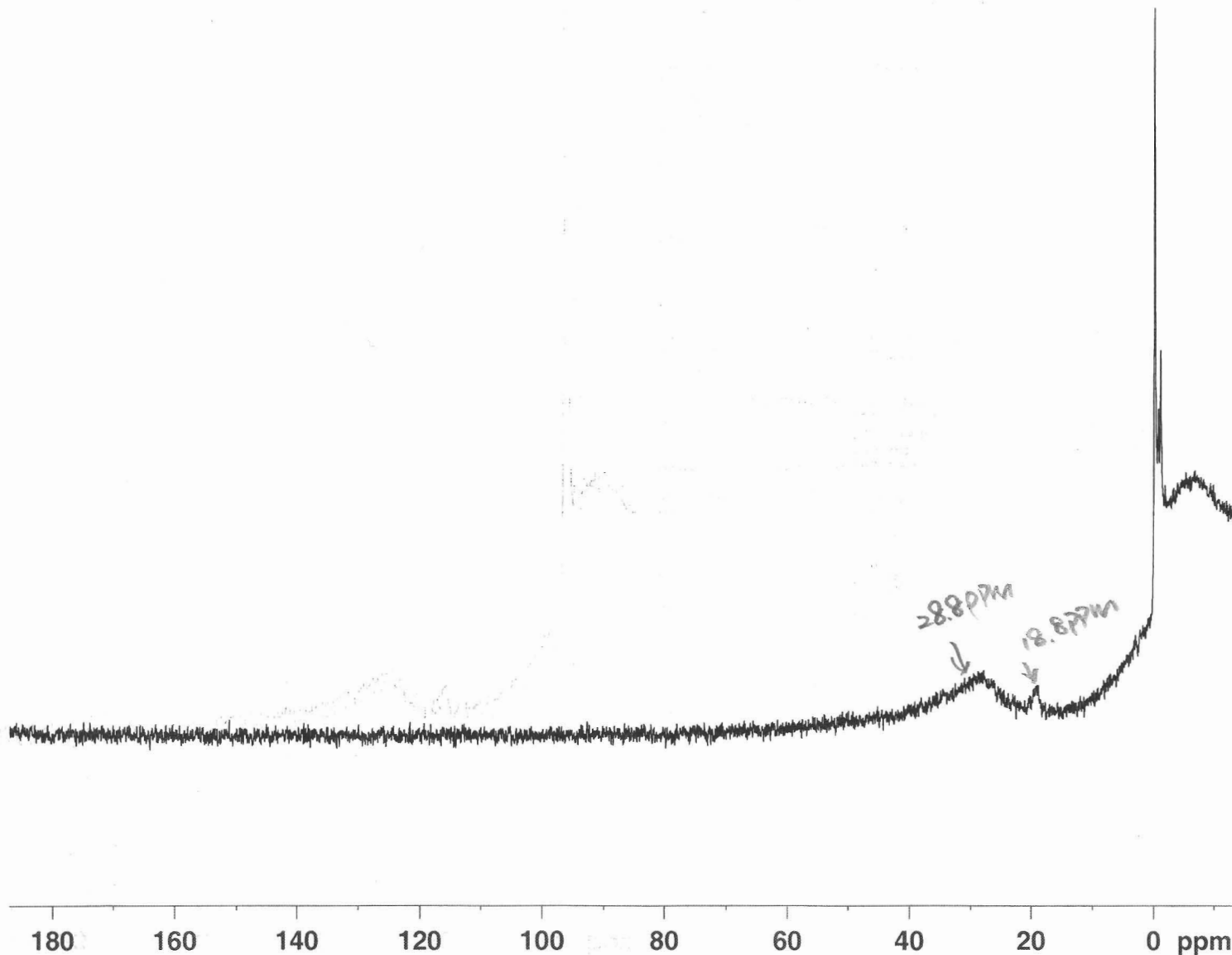


Current Data Parameters
NAME JC-III-6-IQBA+Fru-1.5-11B
EXPNO 1
PROCNO 1

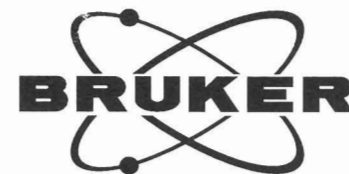
F2 - Acquisition Parameters
Date_ 20091105
Time 15.12
INSTRUM spect
PROBHD 5 mm PABBO BB-
PULPROG zg30
TD 16384
SOLVENT MeOD
NS 42
DS 0
SWH 50125.312 Hz
FIDRES 3.059406 Hz
AQ 0.1634804 sec
RG 1024
DW 9.975 usec
DE 25.00 usec
TE 296.2 K
D1 2.00000000 sec
MCREST 0.00000000 sec
MCWRK 0.01500000 sec

==== CHANNEL f1 =====
NUC1 11B
P1 5.00 usec
PL1 0.00 dB
SFO1 128.3876799 MHz

F2 - Processing parameters
SI 32768
SF 128.3776511 MHz
WDW EM
SSB 0
LB 4.00 Hz
GB 0
PC 1.40



^{11}B NMR of fructose ester of 6-IQBA (pH = 5.7)

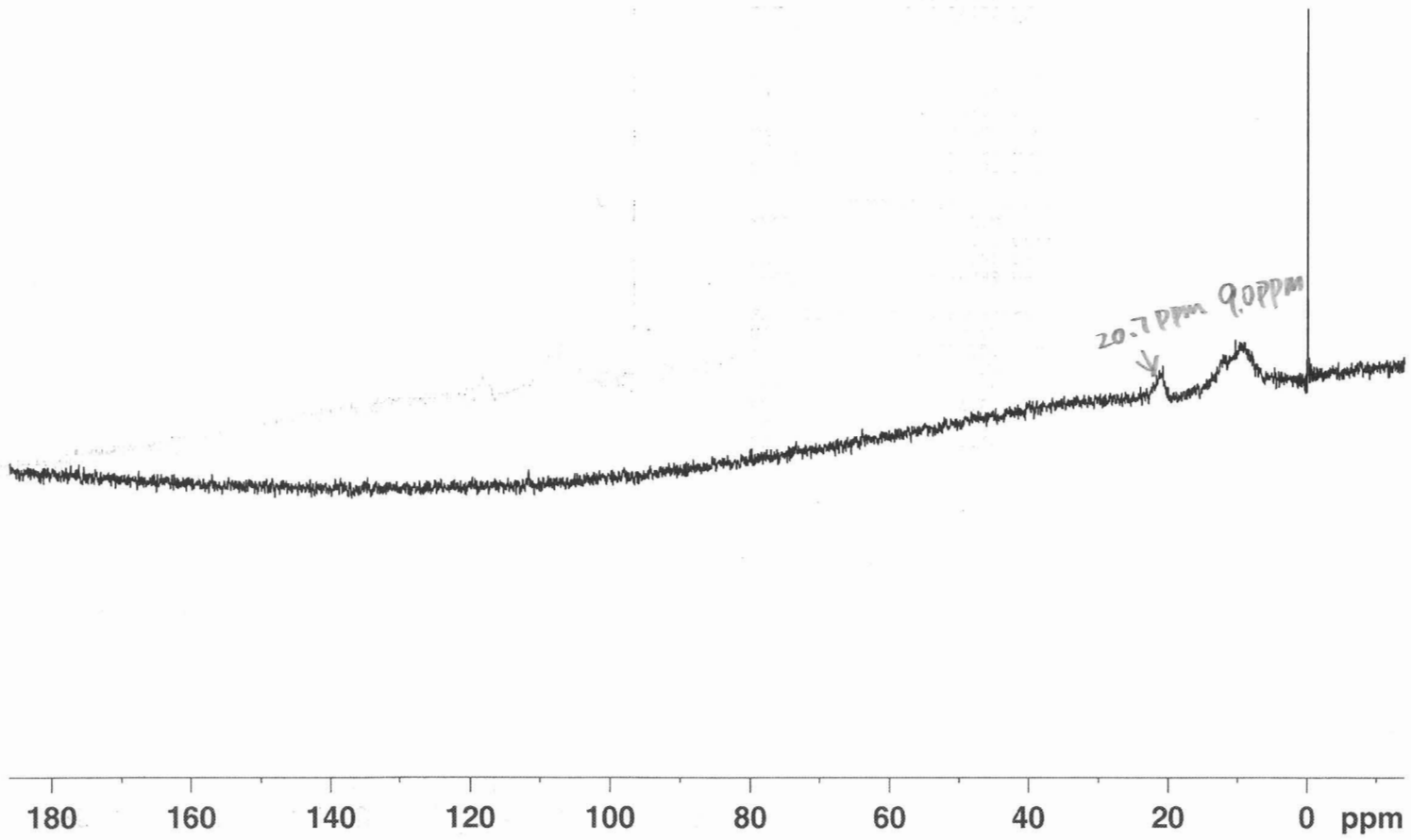


Current Data Parameters
NAME JC-III-6-IQBA+Fru-5.7-11B
EXPNO 1
PROCNO 1

F2 - Acquisition Parameters
Date_ 20091105
Time 15.22
INSTRUM spect
PROBHD 5 mm PABBO BB-
PULPROG zg30
TD 16384
SOLVENT MeOD
NS 82
DS 0
SWH 50125.312 Hz
FIDRES 3.059406 Hz
AQ 0.1634804 sec
RG 2896.3
DW 9.975 usec
DE 25.00 usec
TE 296.2 K
D1 2.0000000 sec
MCREST 0.0000000 sec
MCWRK 0.0150000 sec

==== CHANNEL f1 =====
NUC1 11B
P1 5.00 usec
PL1 0.00 dB
SFO1 128.3876799 MHz

F2 - Processing parameters
SI 32768
SF 128.3774354 MHz
WDW EM
SSB 0
LB 4.00 Hz
GB 0
PC 1.40



^{11}B NMR of fructose ester of 6-IQBA (pH = 12.1)

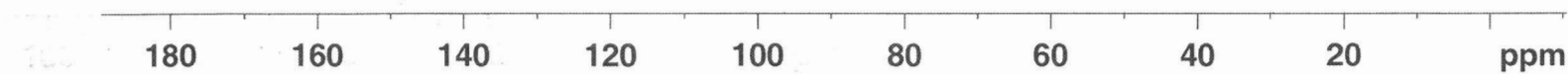


Current Data Parameters
NAME JC-III-6-IQBA+Fru-12.1-11B
EXPNO 1
PROCNO 1

F2 - Acquisition Parameters
Date_ 20091105
Time 15.30
INSTRUM spect
PROBHD 5 mm PABBO BB-
PULPROG zg30
TD 16384
SOLVENT MeOD
NS 200
DS 0
SWH 50125.312 Hz
FIDRES 3.059406 Hz
AQ 0.1634804 sec
RG 1024
DW 9.975 usec
DE 25.00 usec
TE 296.2 K
D1 2.00000000 sec
MCREST 0.00000000 sec
MCWRK 0.01500000 sec

==== CHANNEL f1 =====
NUC1 11B
P1 5.00 usec
PL1 0.00 dB
SFO1 128.3876799 MHz

F2 - Processing parameters
SI 32768
SF 128.3774507 MHz
WDW EM
SSB 0
LB 4.00 Hz
GB 0
PC 1.40



Stability test of B-TTP analogues 18-21 in PCR and denature condition

HPLC condition: column: Agilent, 5 μ m, 4.6 x 250 mm LN PR045204; flow rate: 0.6 mL/min;

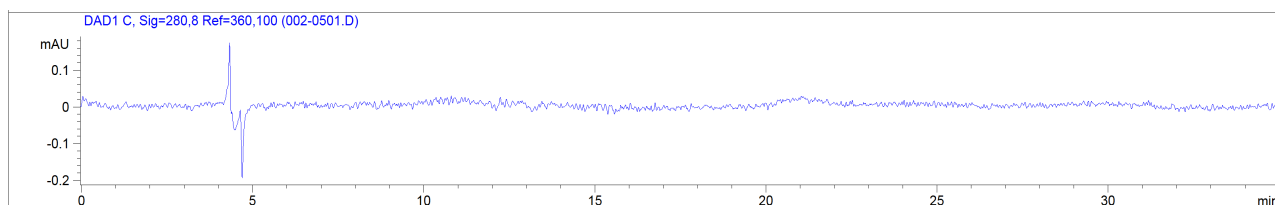
Solvents: A: 0.1 M NH₄HCO₃, B: MeOH; program: 0-35 min 25% (B%); Temp 20 °C,
monitor wavelength: 280 nm.

PCR condition: Initially denaturing at 94 °C for 2 min, followed by three cycles of 94 °C for 1 min, 46 °C for 1 min, and 72 °C for 1 min, then hold at 4 °C.

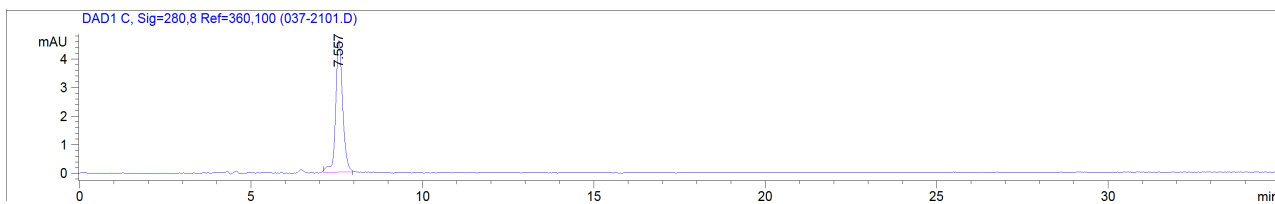
Denature condition: 95 °C for 7 min.

B-TTP analogue 18 (Figure S3.1):

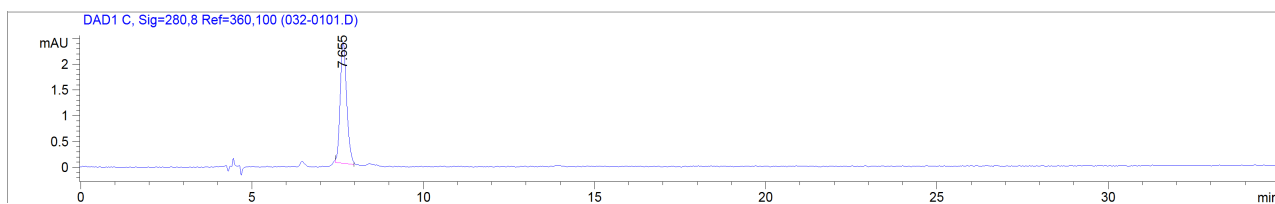
Blank injection (Figure S3.1-a)



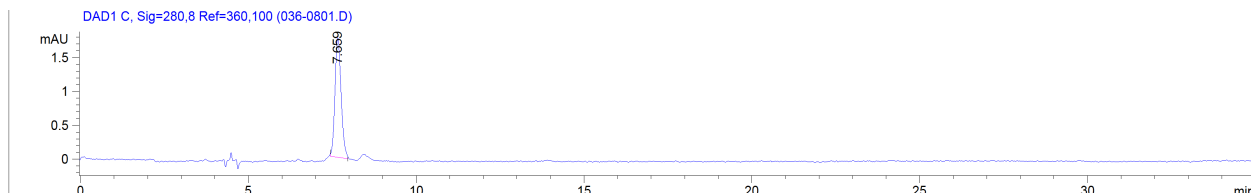
B-TTP analogue 18 (Figure S3.1-b)



B-TTP analogue 18 after subjecting to PCR conditions (Figure S3.1-c)

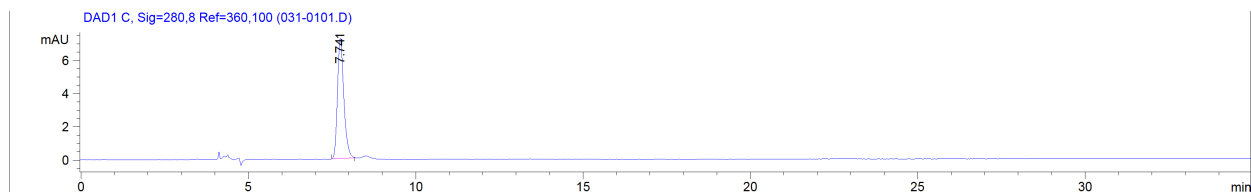


B-TTP analogue 18 after subjecting to denaturing condition (Figure S3.1-d)

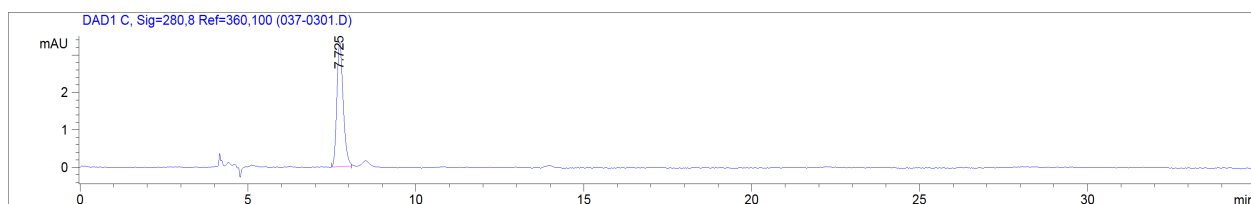


B-TTP analogue 19 (Figure S3.2):

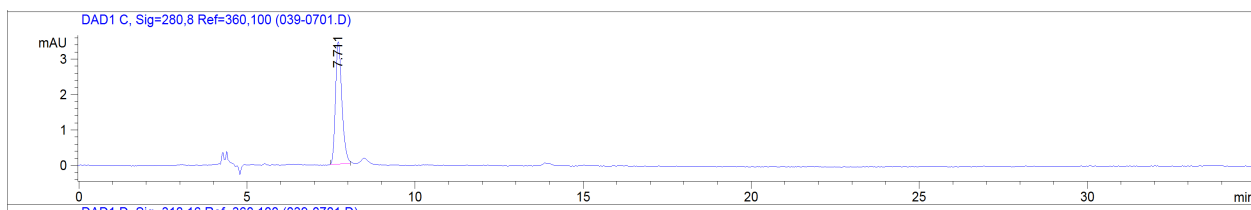
B-TTP analogue 19 (Figure S3.2-a)



B-TTP analogue 19 after subjecting to PCR conditions (Figure S3.2-b)

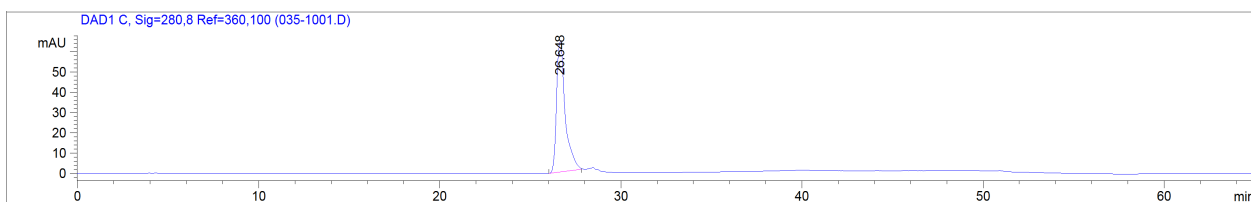


B-TTP analogue 19 after subjecting to denaturing condition (Figure S3.2-c)

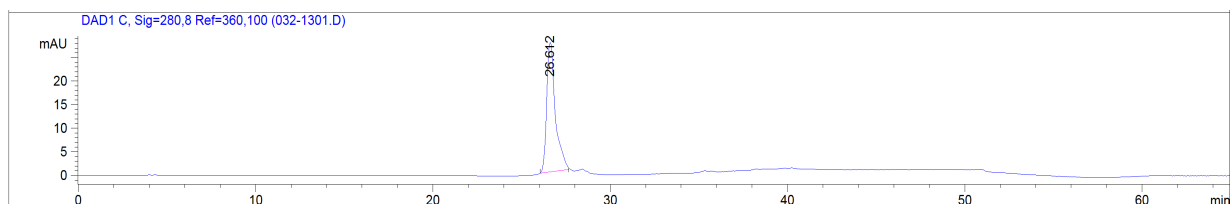


B-TTP analogue 20 (Figure S3.3):

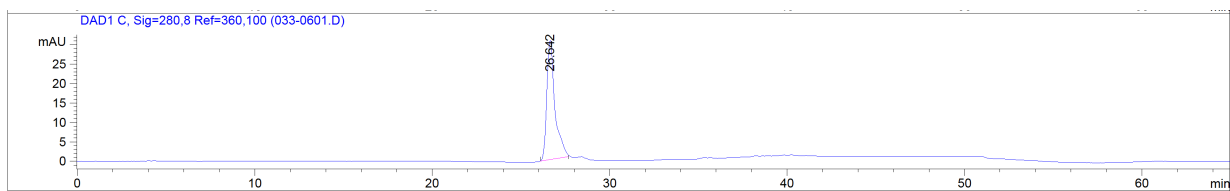
B-TTP analogue 20 (Figure S3.3-a)



B-TTP analogue 20 after subjecting to PCR conditions (Figure S3.3-b)

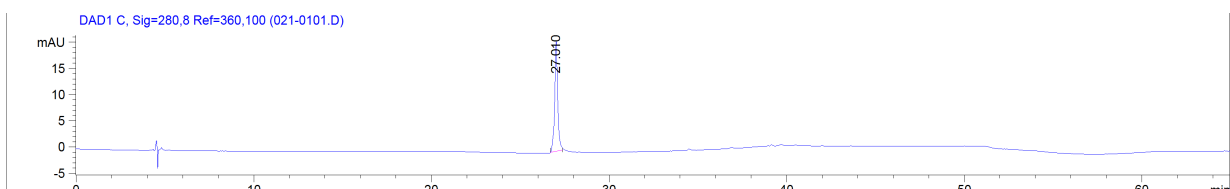


B-TTP analogue 20 after subjecting to denaturing conditions (Figure S3.3-c)

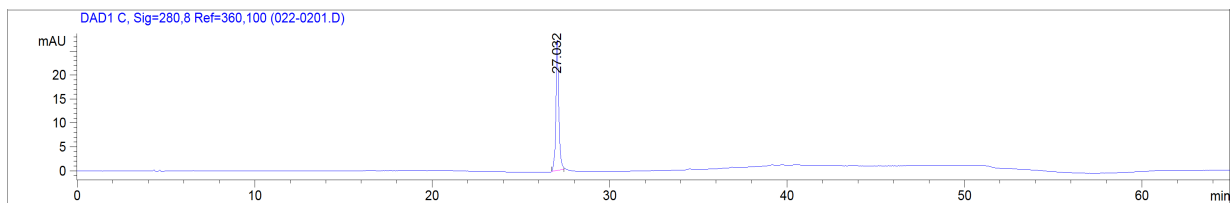


B-TTP analogue (Figure S3.4):

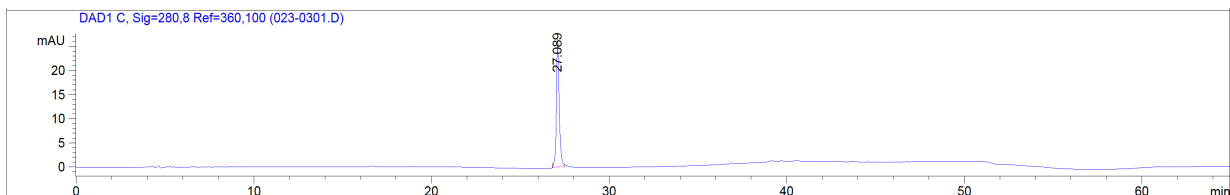
B-TTP analogue 21 (Figure S3.4-a)



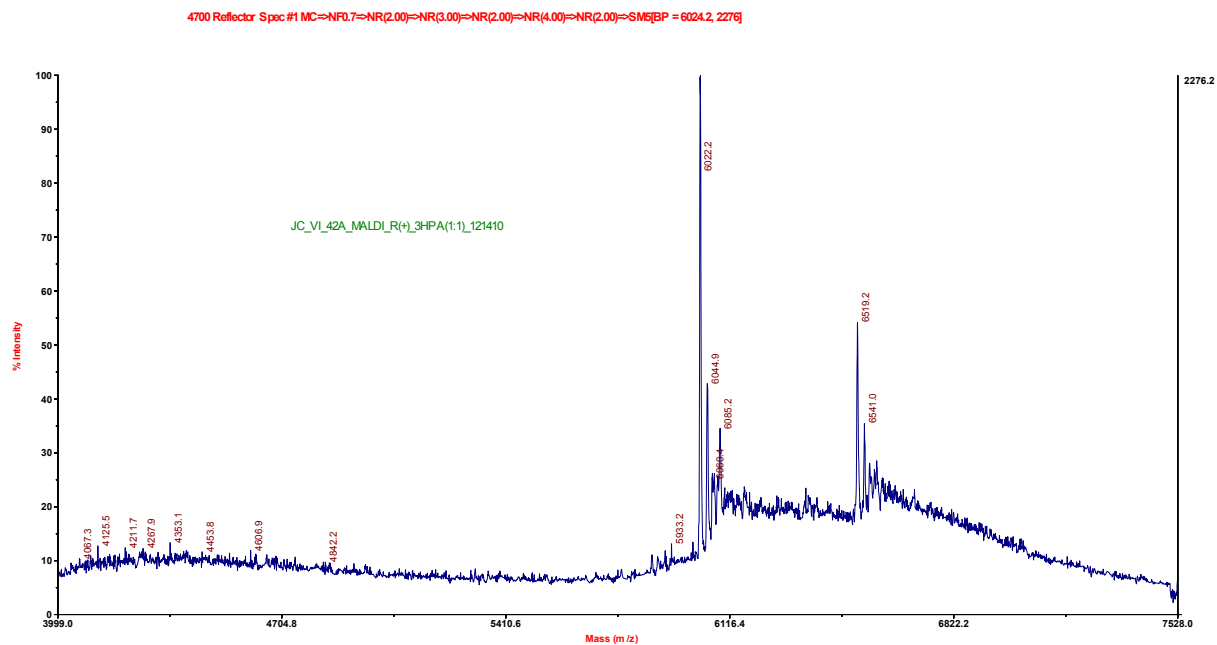
B-TTP analogue 21 after subjecting to PCR conditions (Figure S3.4-b)



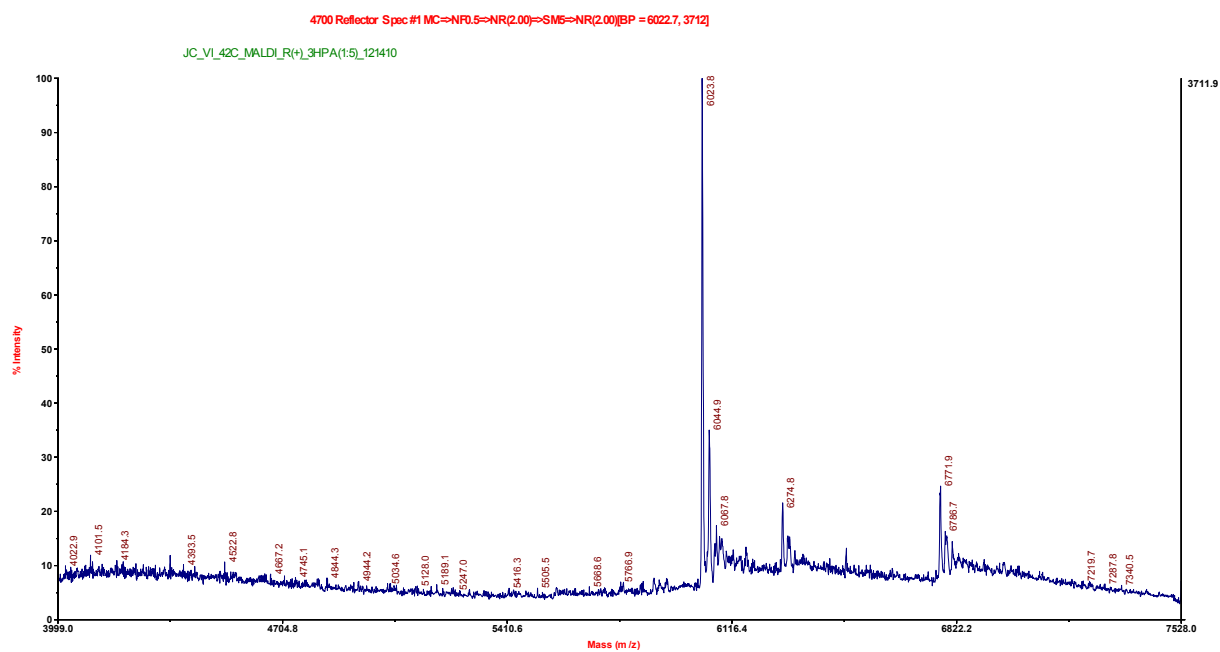
B-TTP analogue 21 after subjecting to denaturing conditions (Figure S3.4-c)



MALDI-TOF-MS of primer extension product (90-mer) using natural NTPs (Figure S3.5)

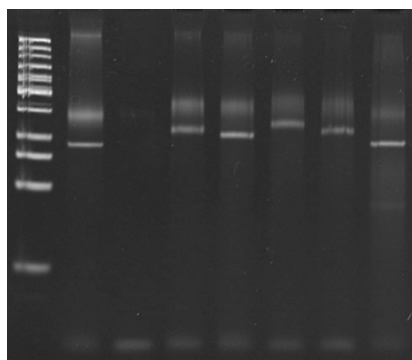


MALDI-TOF-MS of primer extension product using B-TTP analogue 18 (Figure S3.6)

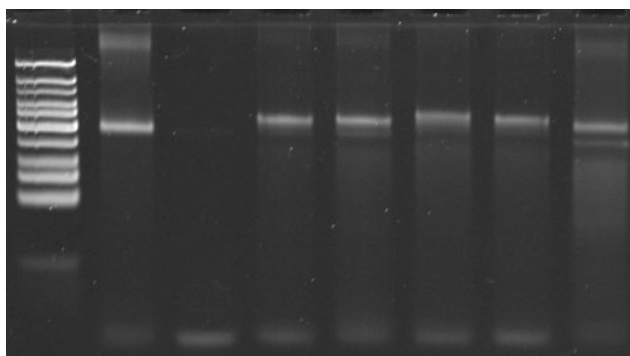


Full pictures of Figure 3.4.

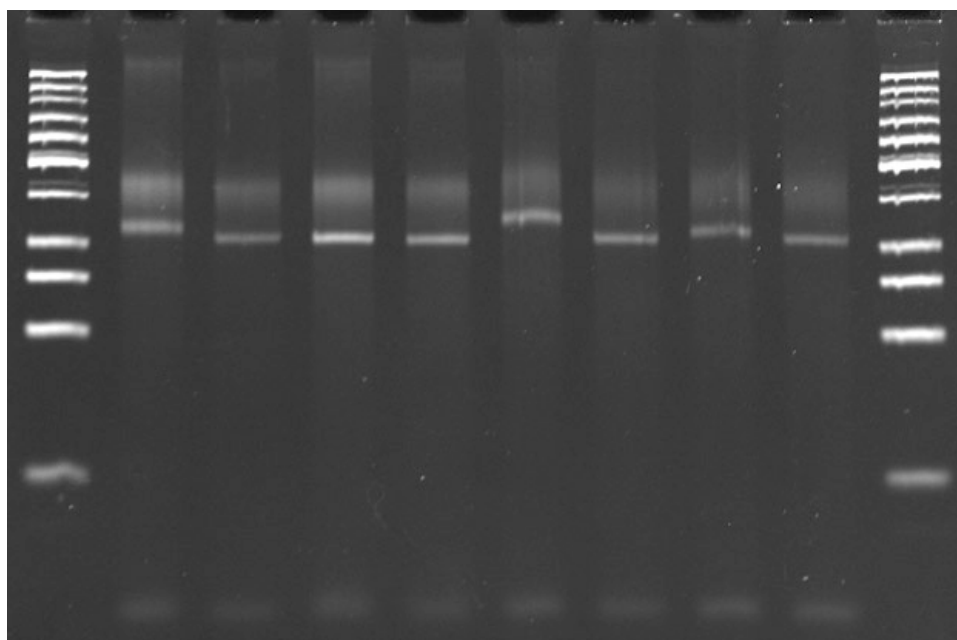
A



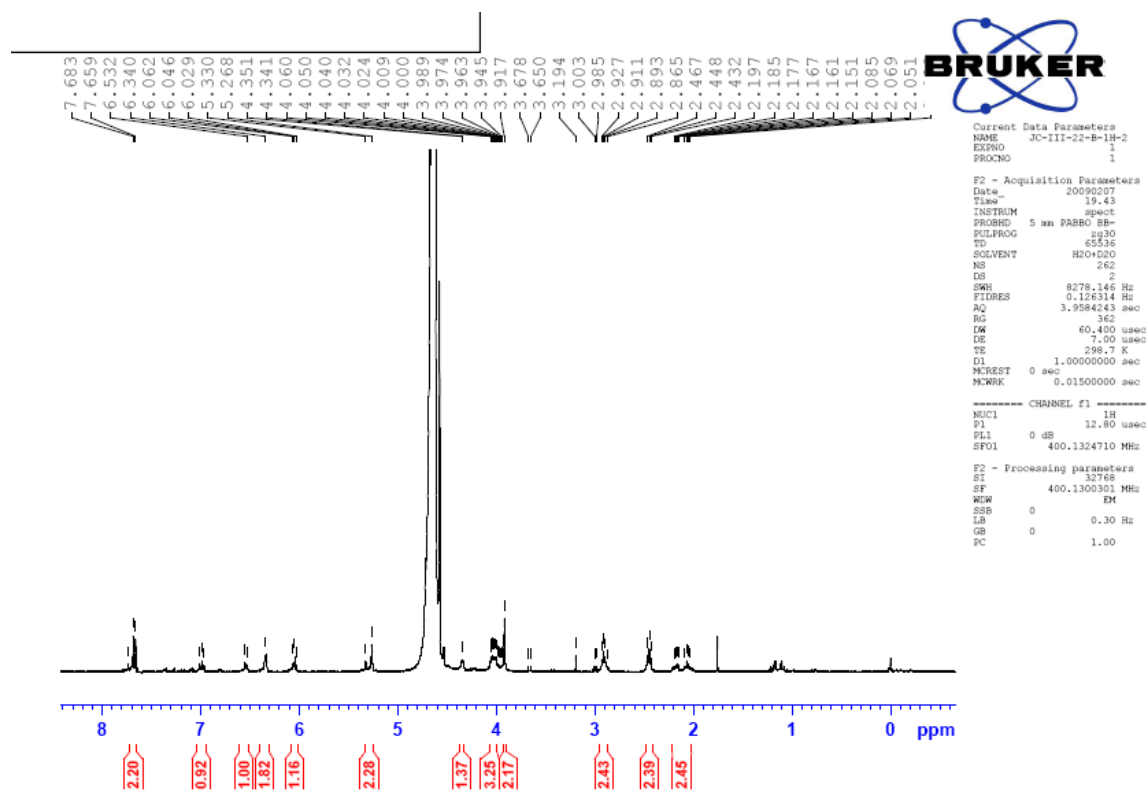
B



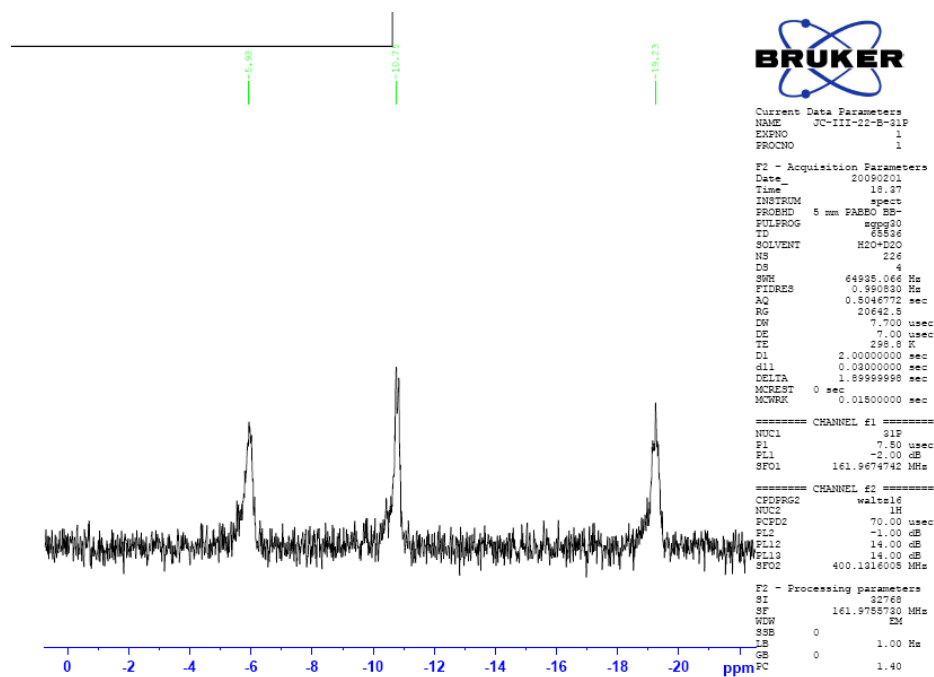
C



¹H NMR of B-TTP analogue 18 (Figure S3.7-a)



³¹P NMR of B-TTP analogue 18 (Figure S3.7-b)

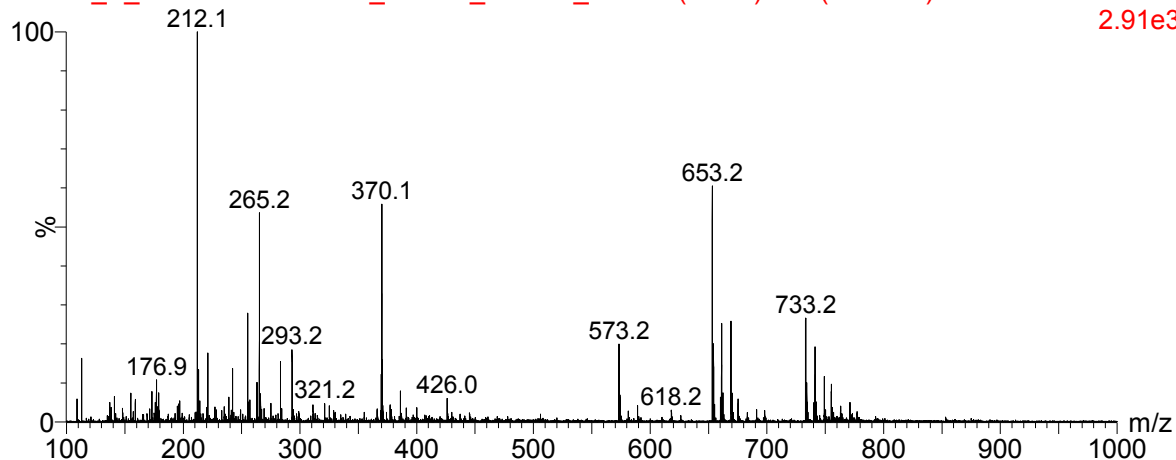
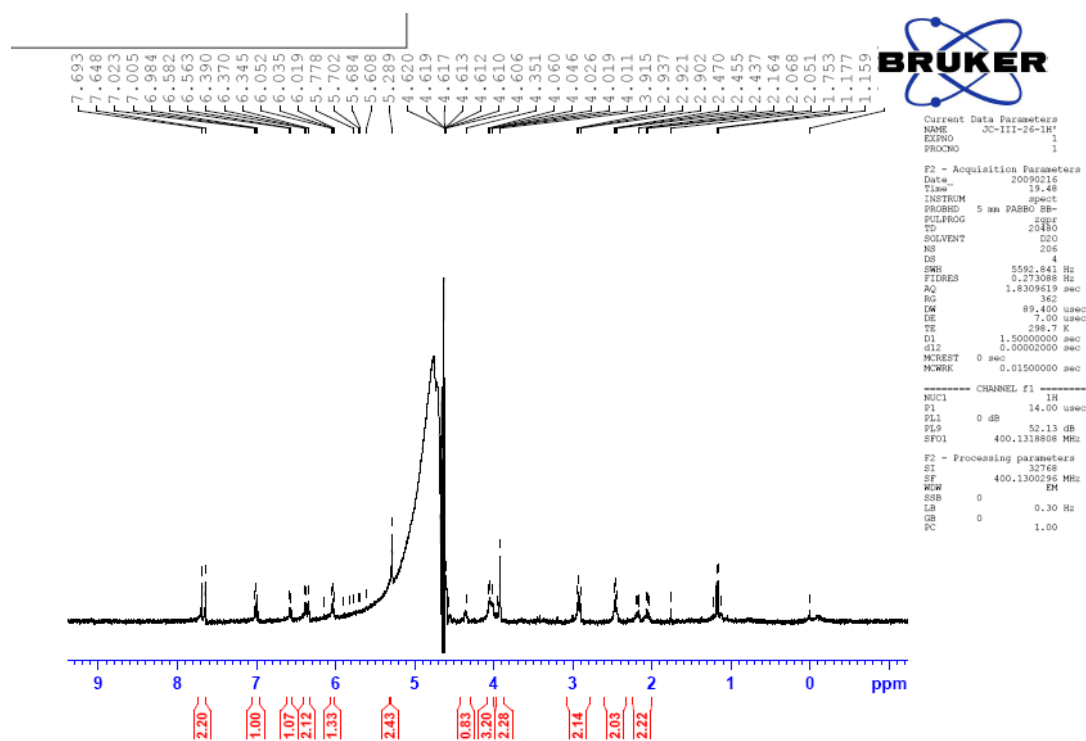


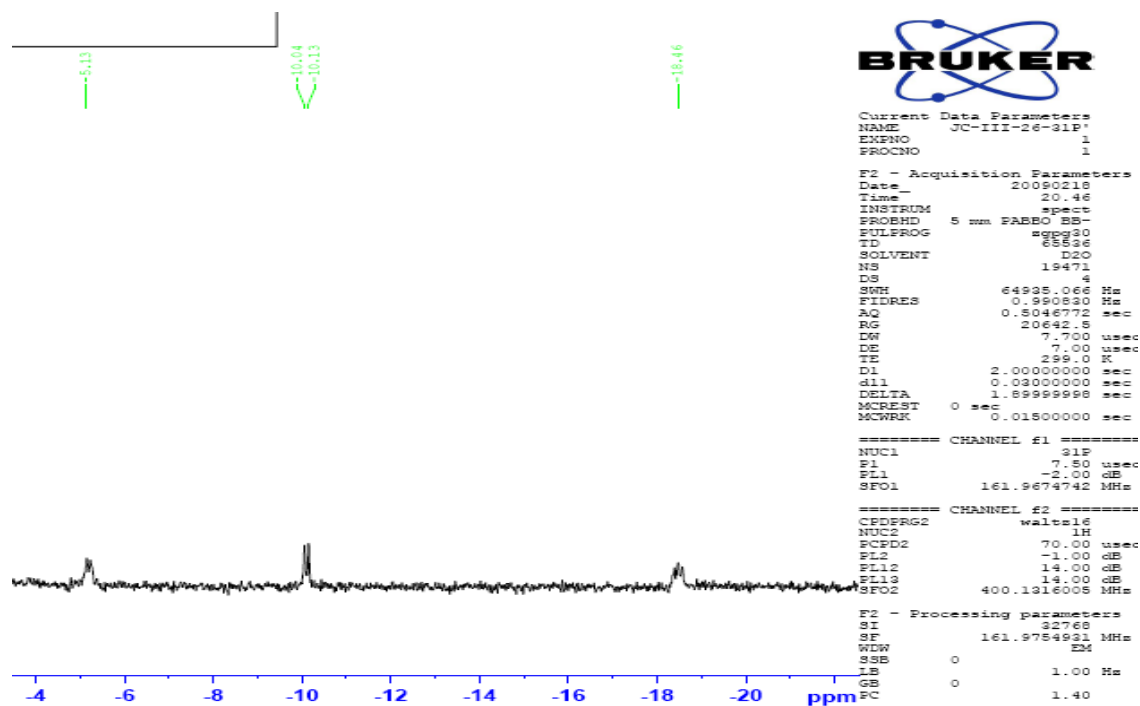
ESI-MS of B-TTP analogue 18 (Figure S3.7-c)

50%MeOH+0.5%NH4OH

14:30:50 17-Feb-2011

JERRY_B_TTP ANALOGUE 2_WANG_021711_01 203 (3.782) Cm (202:288)

TOF MS ES-
2.91e3 ^1H NMR of B-TTP analogue 19 (Figure S3.8-a)

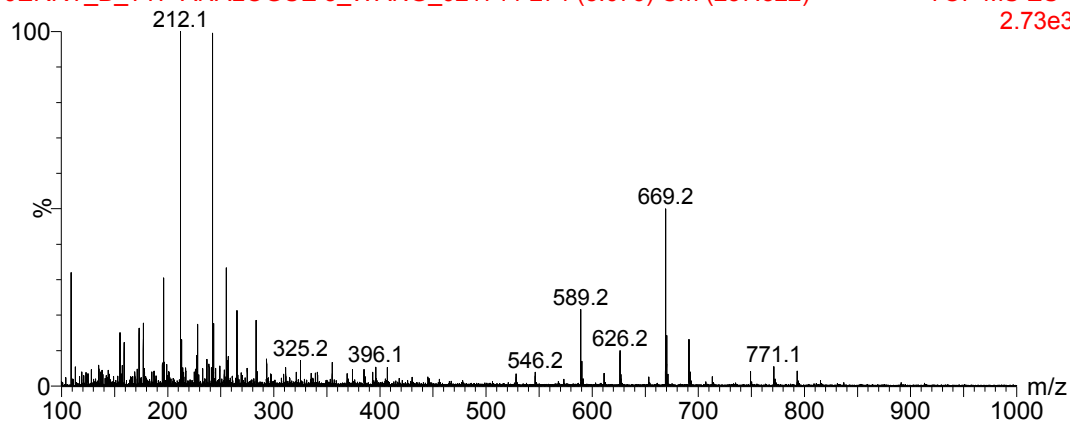
³¹P NMR of B-TTP analogue 19 (Figure S3.8-b)

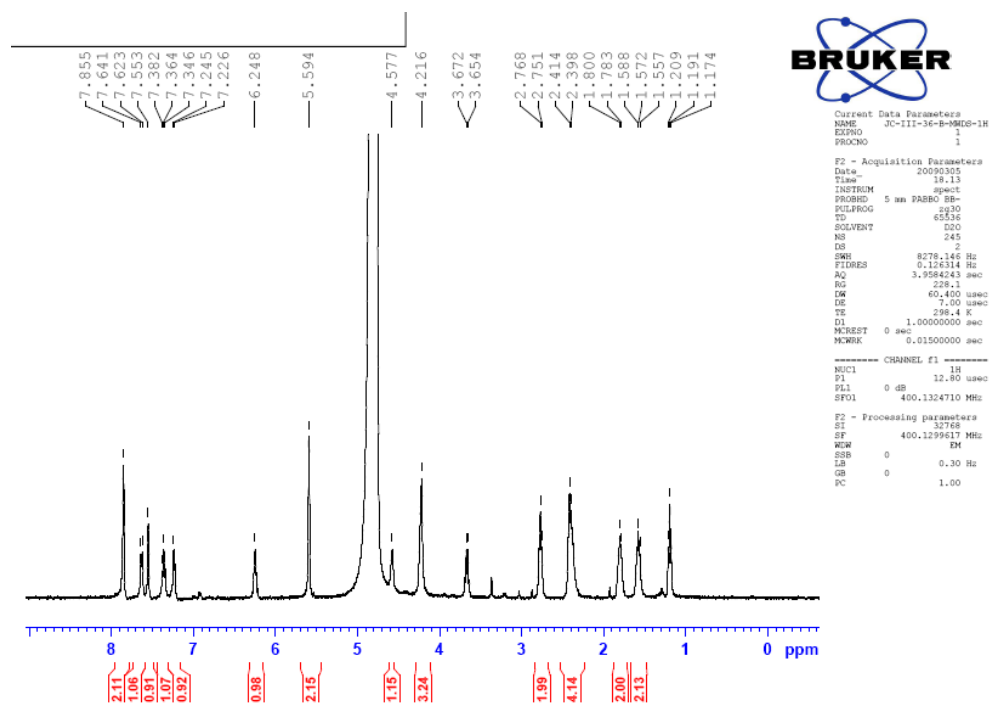
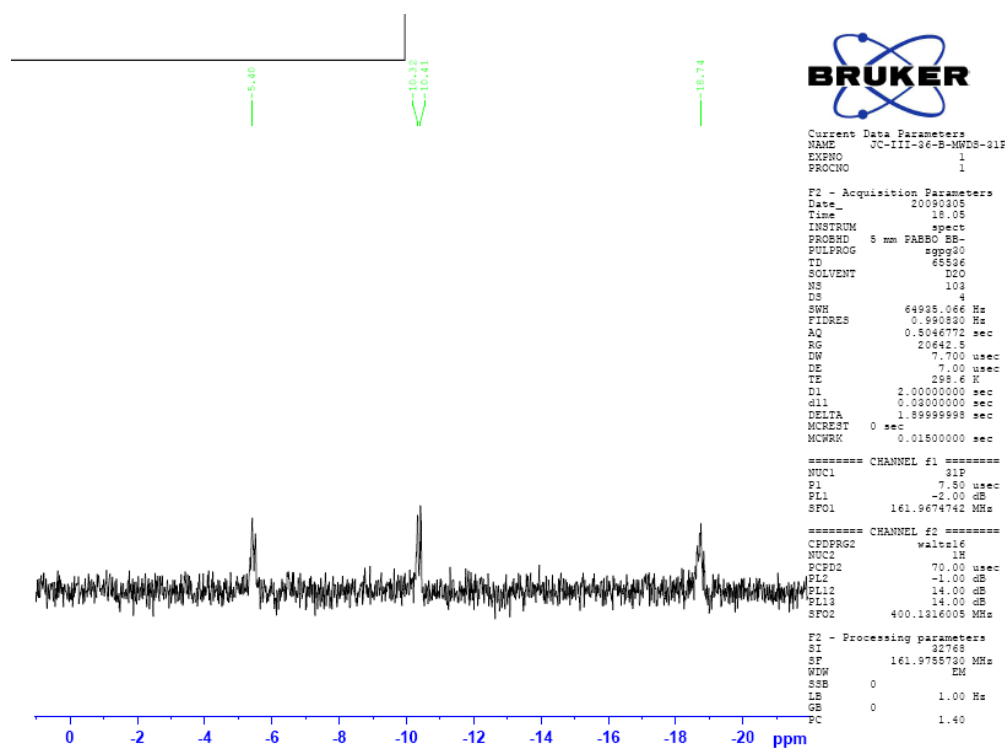
ESI-MS of B-TTP analogue 19 (Figure S3.8-c)

50%MeOH+0.5%NH4OH

14:41:31 17-Feb-2011

JERRY_B_TTP ANALOGUE 3_WANG_021711 274 (5.076) Cm (237:322)

TOF MS ES-
2.73e3

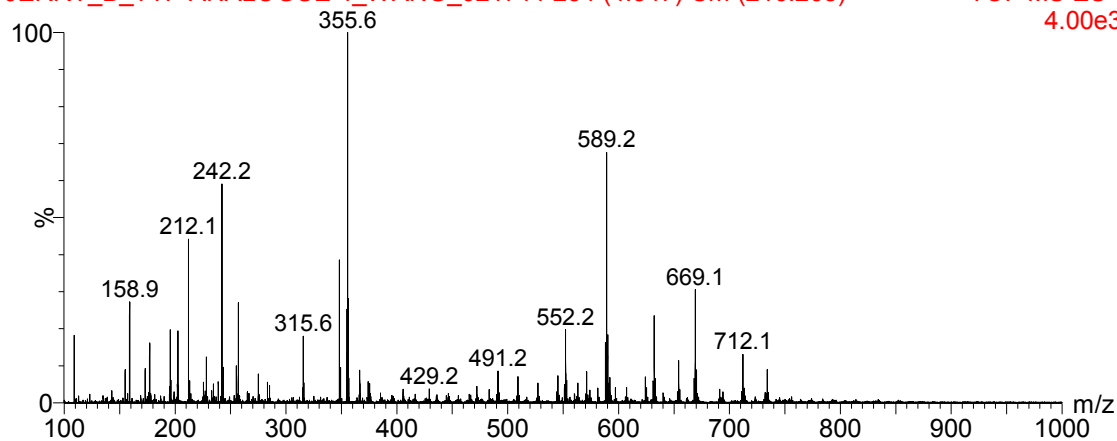
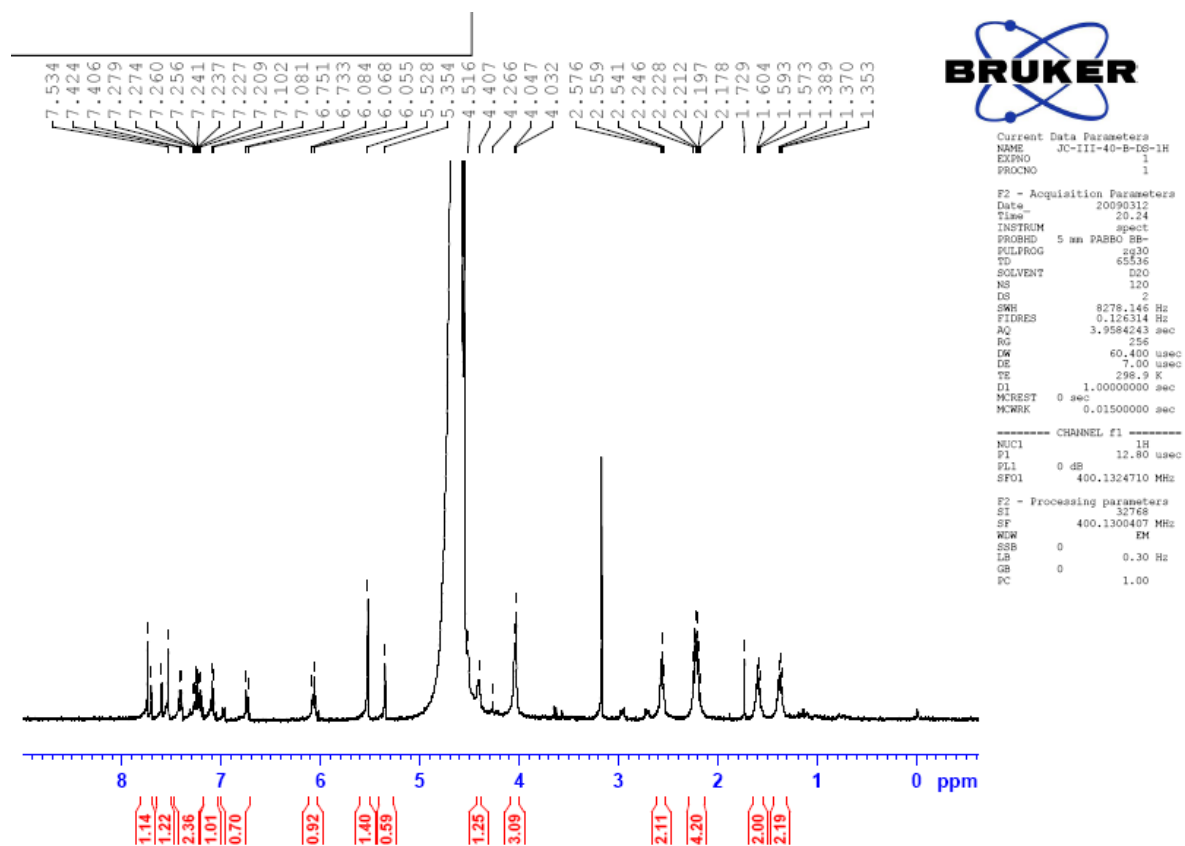
¹H NMR of B-TTP analogue 20 (Figure S3.9-a)³¹P NMR of B-TTP analogue 20 (Figure S3.9-b)

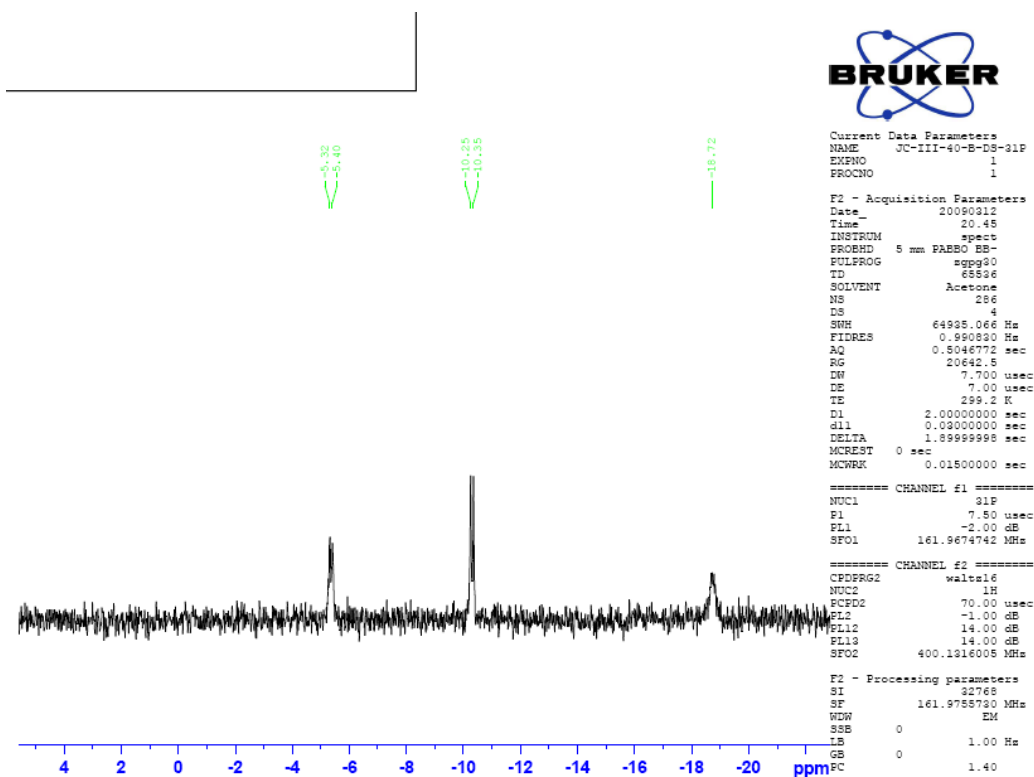
ESI-MS of B-TTP analogue 20 (Figure S3.9-c)

50%MeOH+0.5%NH4OH

14:57:06 17-Feb-2011

JERRY_B_TTP ANALOGUE 4_WANG_021711 234 (4.347) Cm (216:268)

TOF MS ES-
4.00e3¹H NMR of B-TTP analogue 21 (Figure S3.10-a)

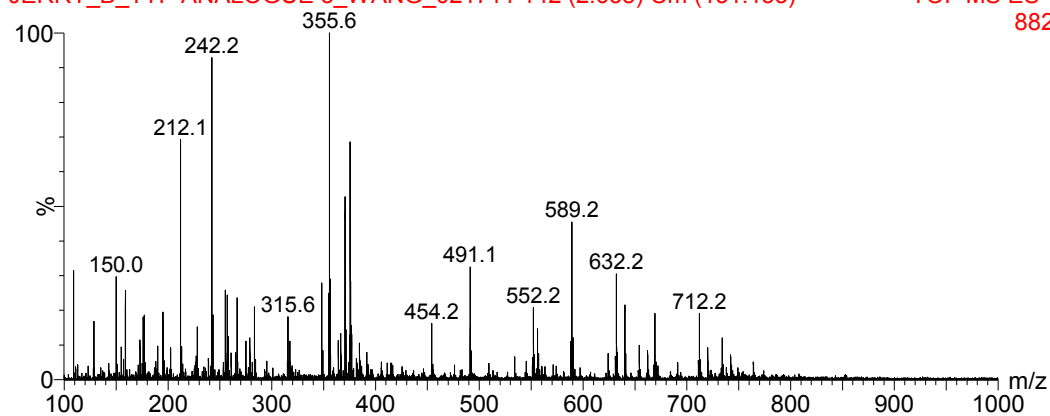
³¹P NMR of B-TTP analogue 21 (Figure S3.10-b)

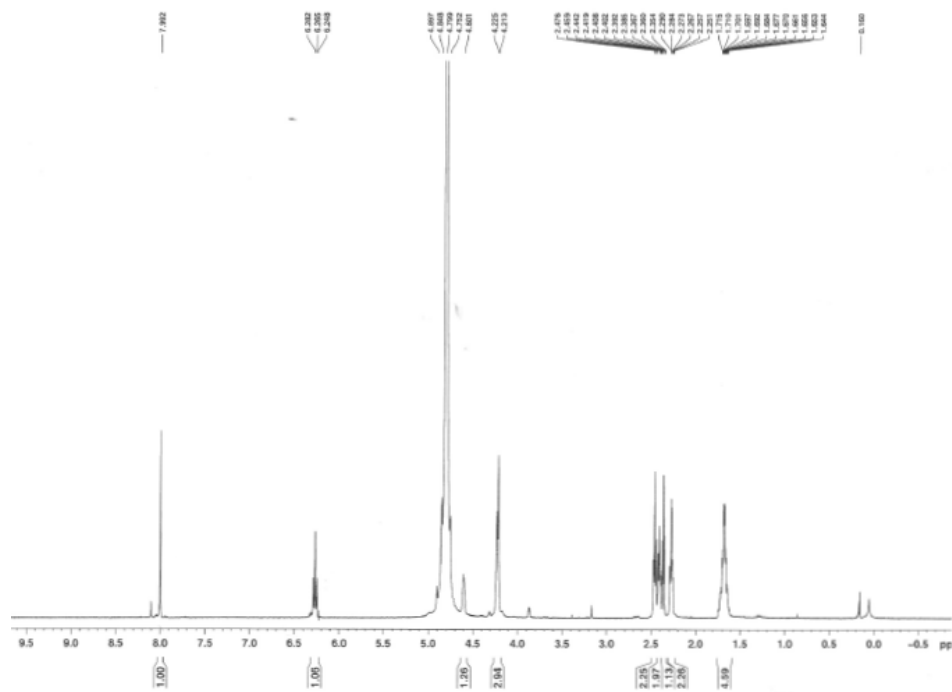
ESI-MS of B-TTP analogue 21 (Figure S3.10-c)

50%MeOH+0.5%NH4OH

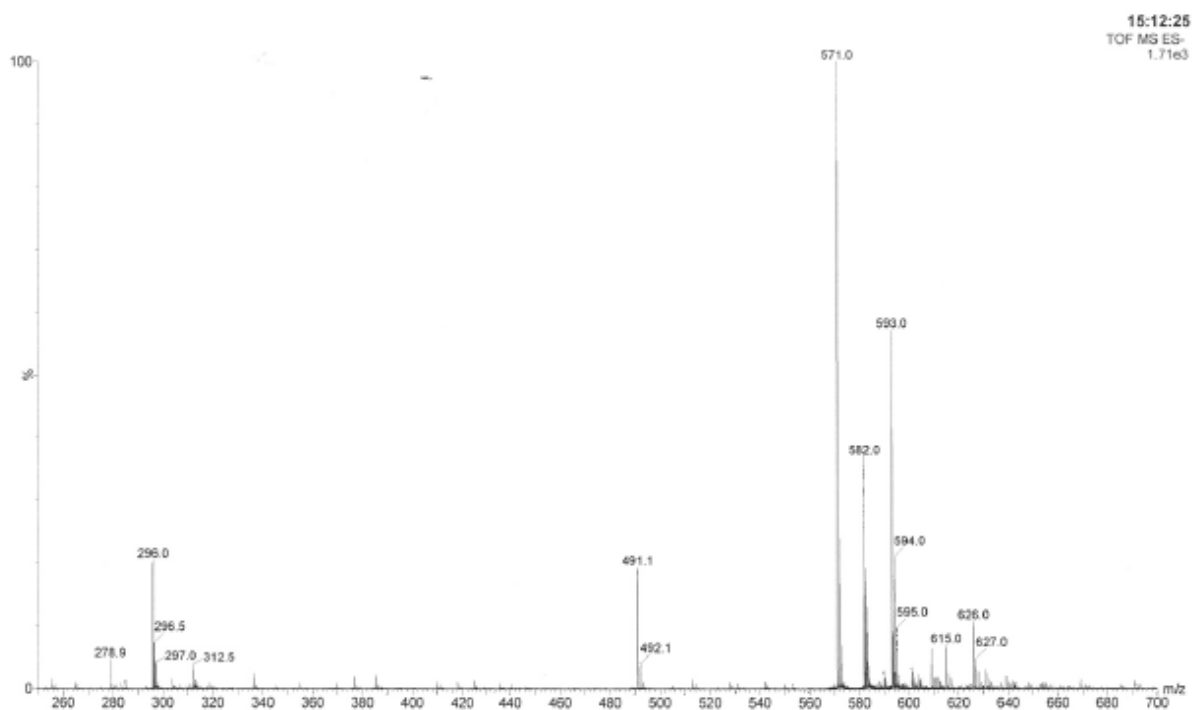
15:05:23 17-Feb-2011

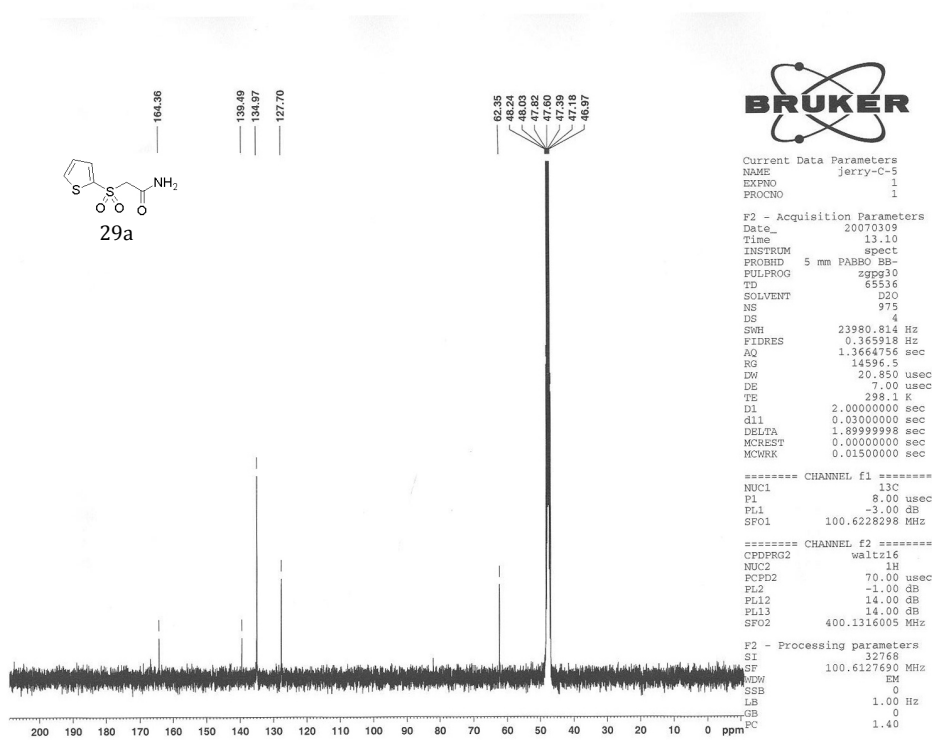
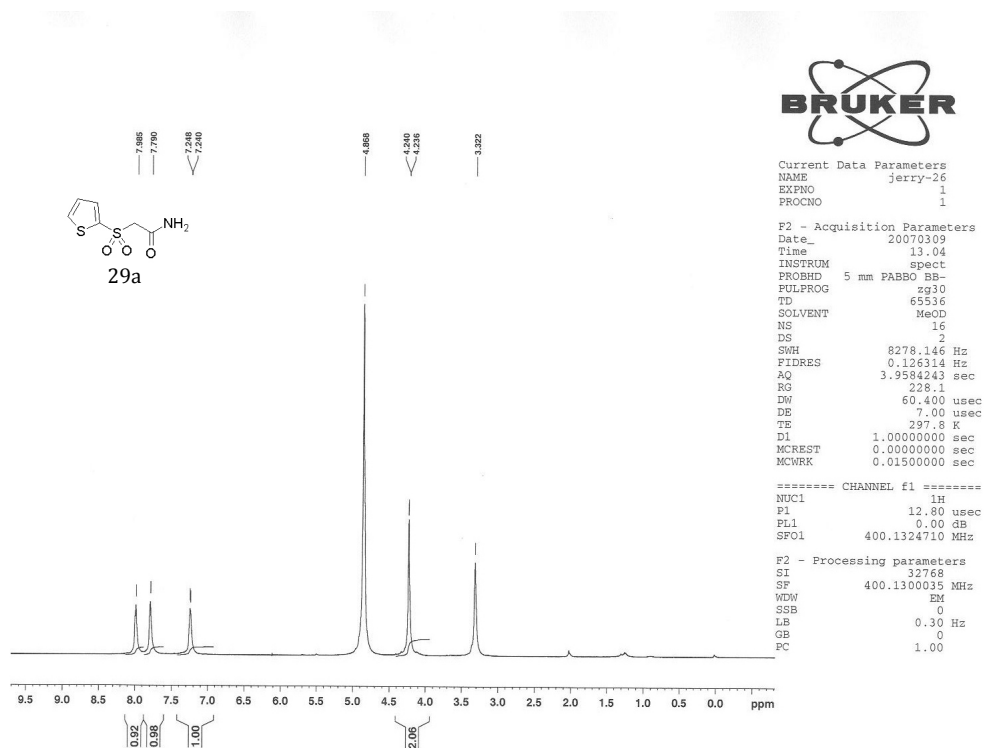
JERRY_B_TTP ANALOGUE 5_WANG_021711 142 (2.638) Cm (131:153)

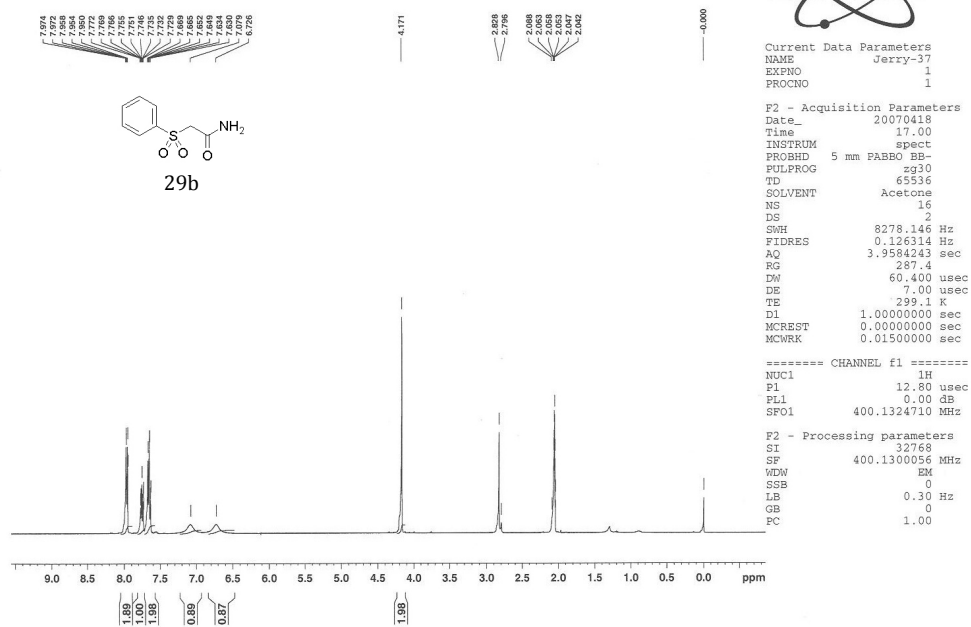
TOF MS ES-
882

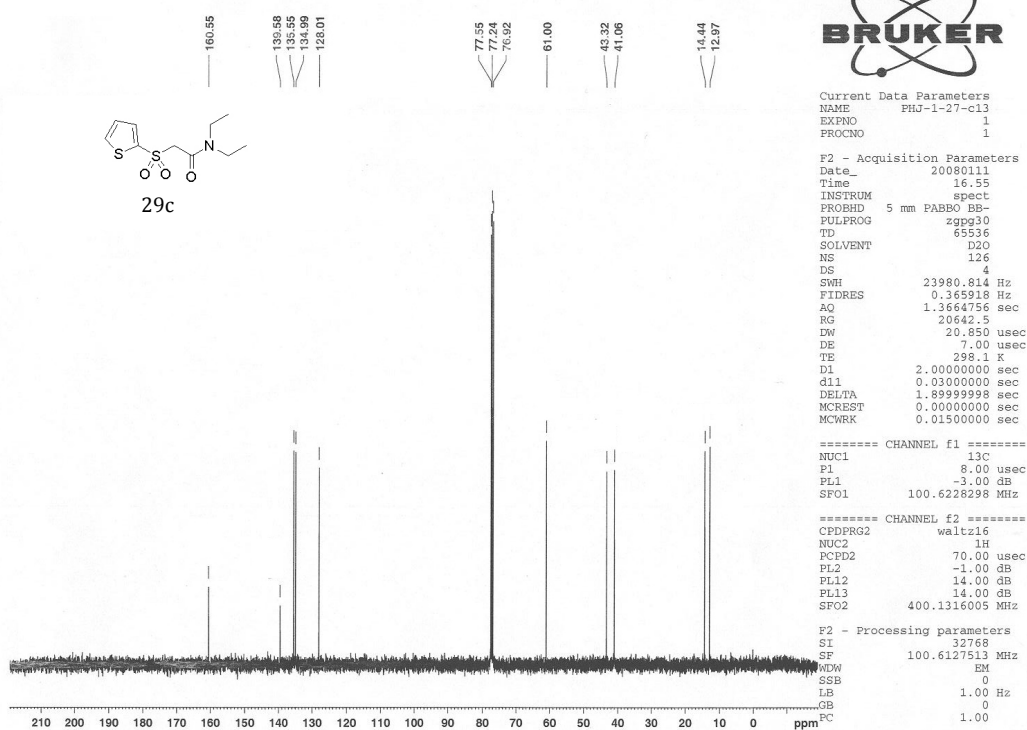
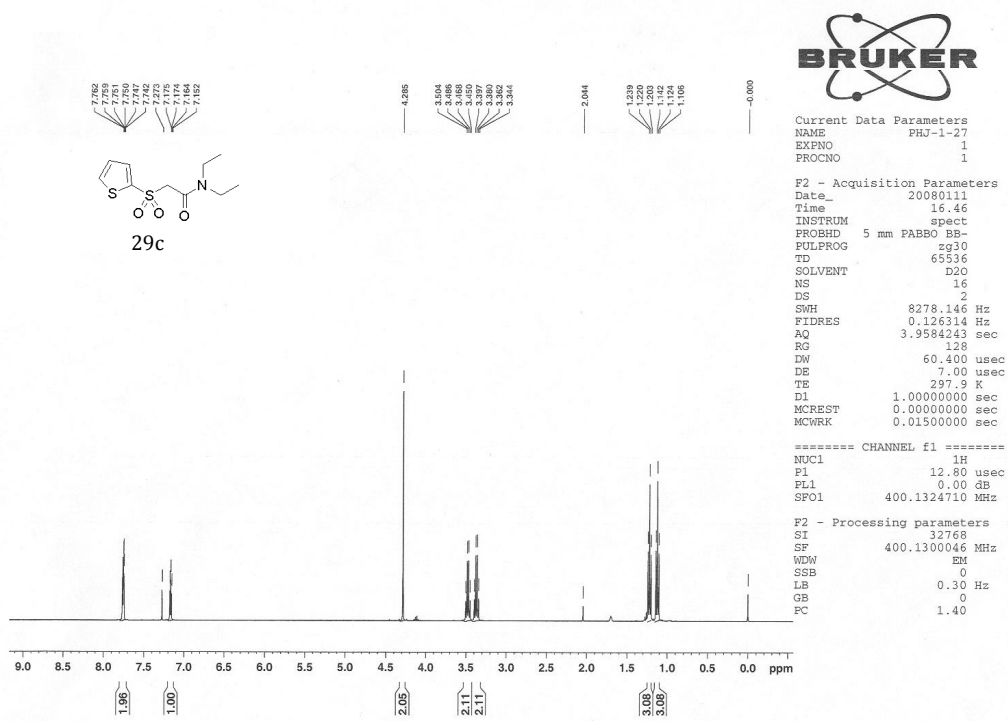
^1H NMR of M(C)-TTP (Figure S3.11-a)

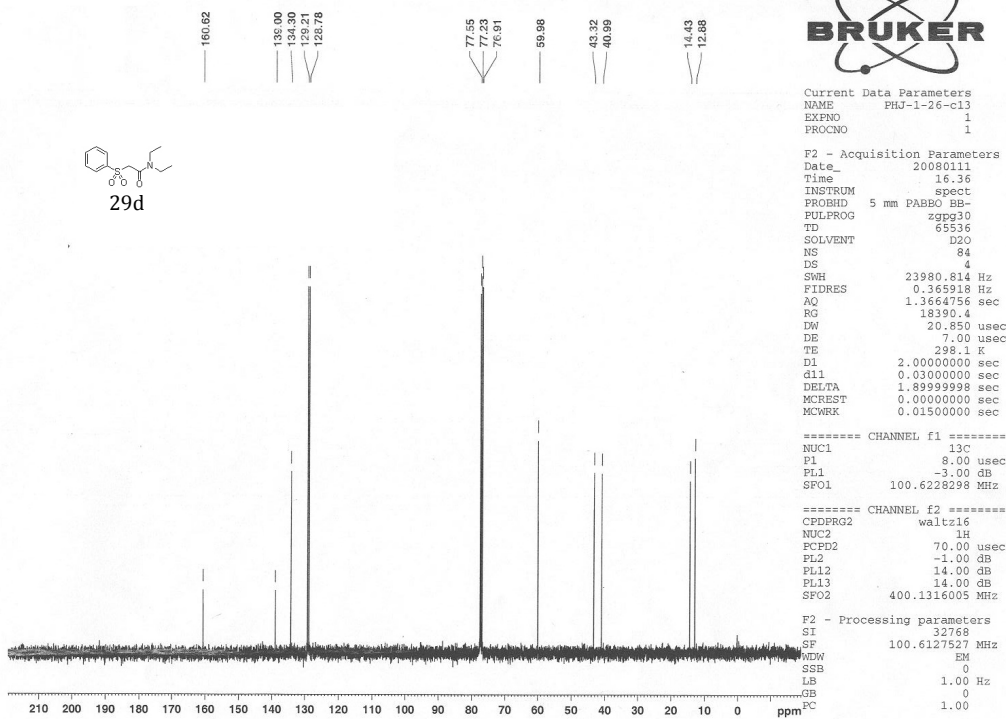
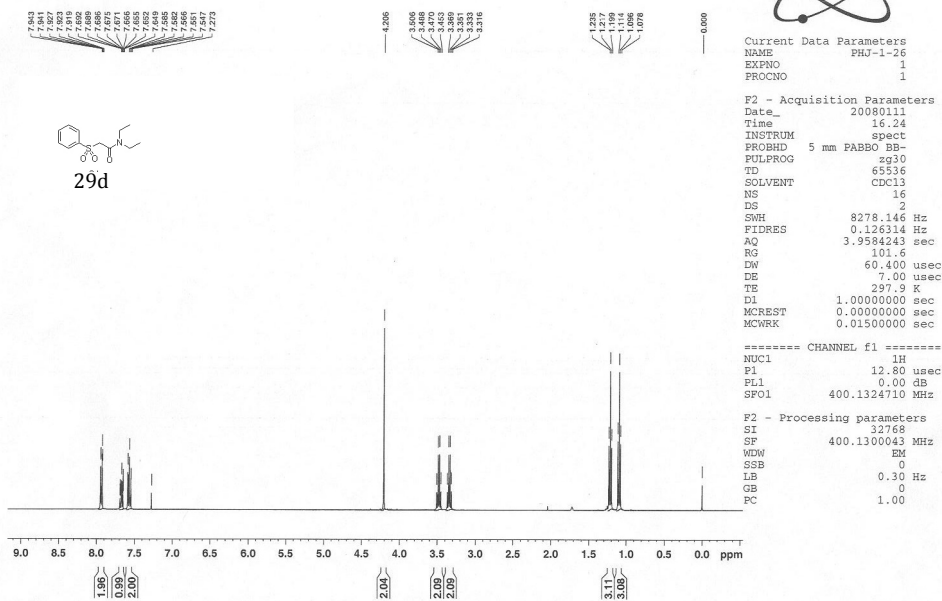
ESI-MS of M(C)-TTP (Figure S3.11-c)

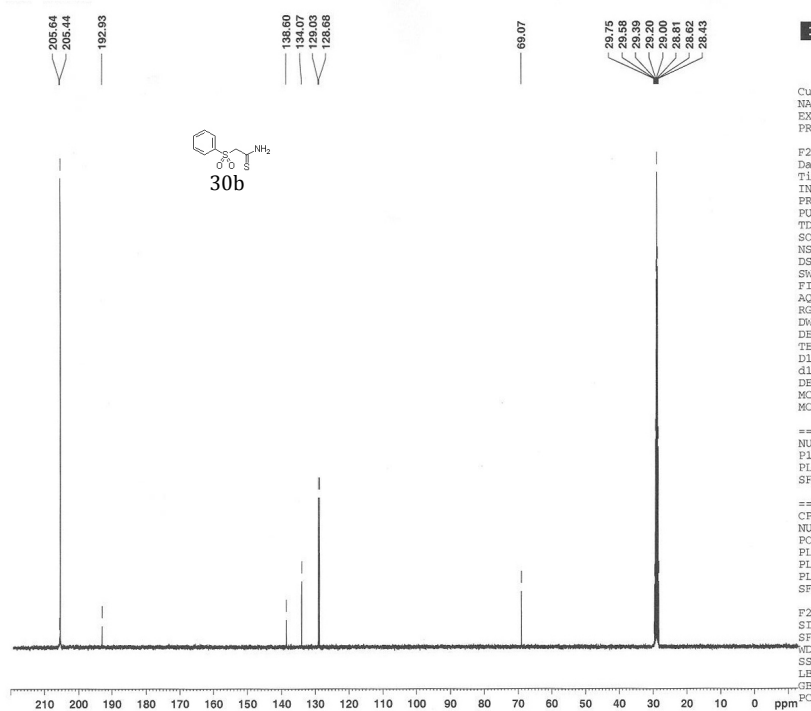
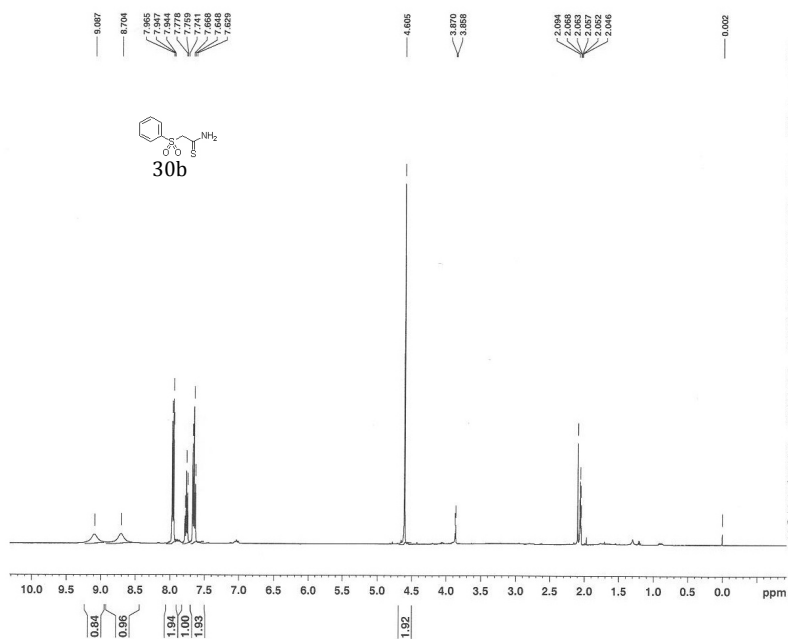


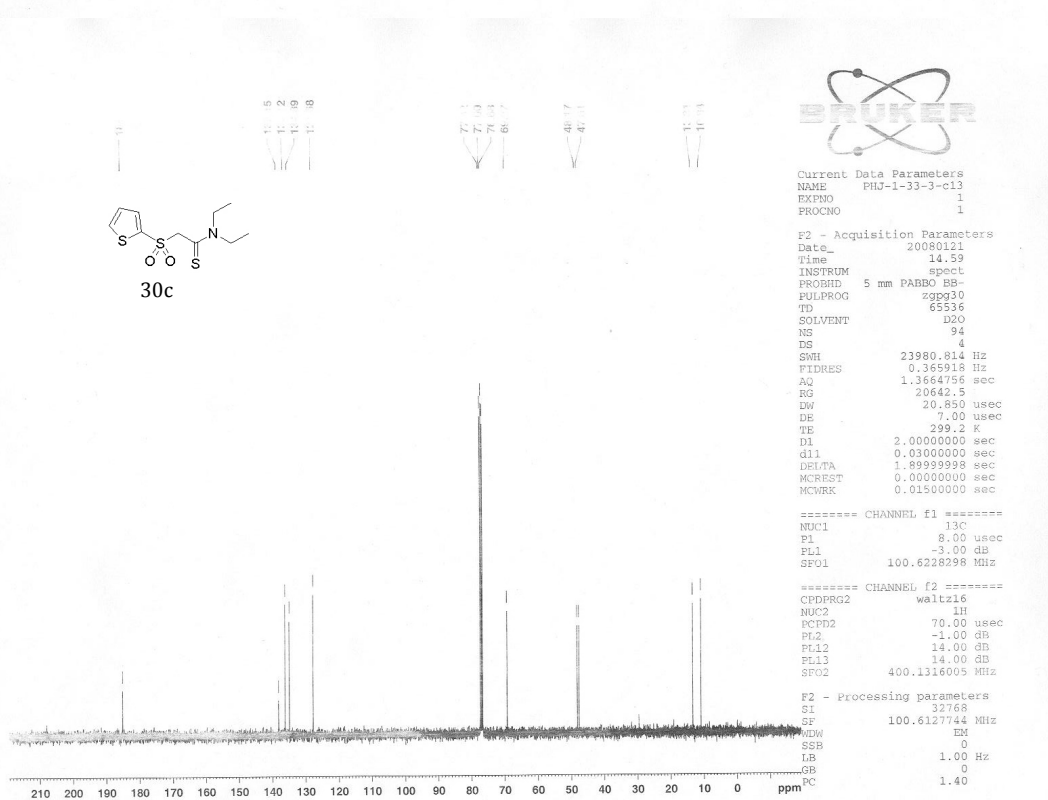
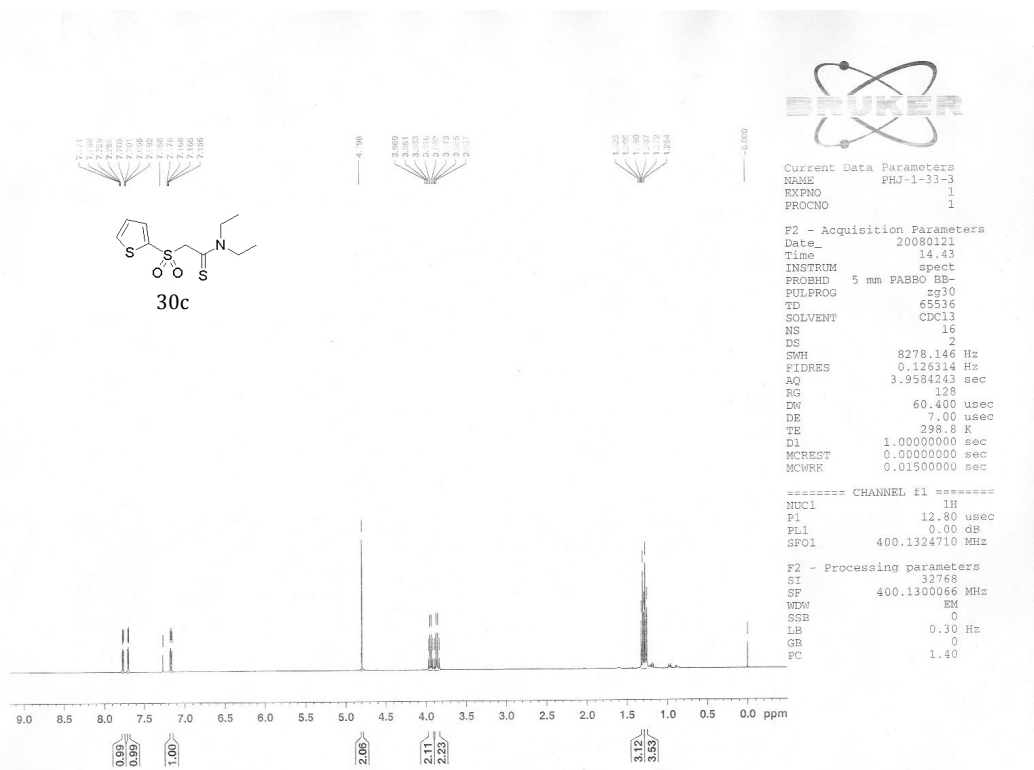
¹HNMR and ¹³CNMR spectra of tested compounds in chapter 4

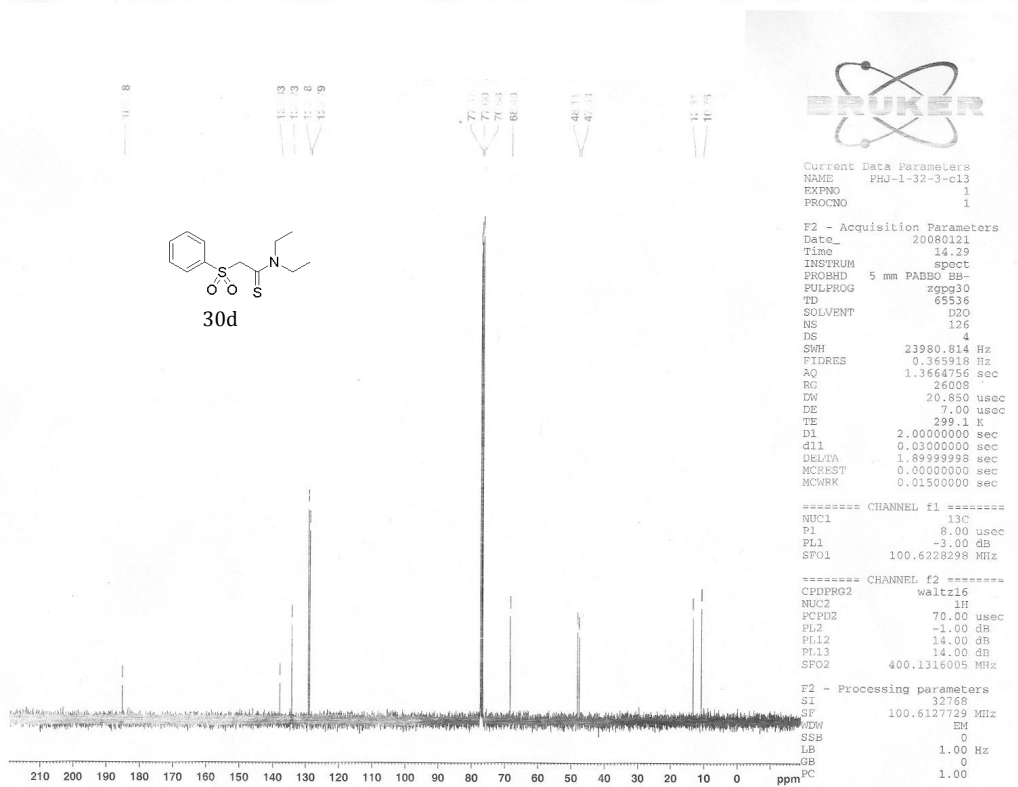
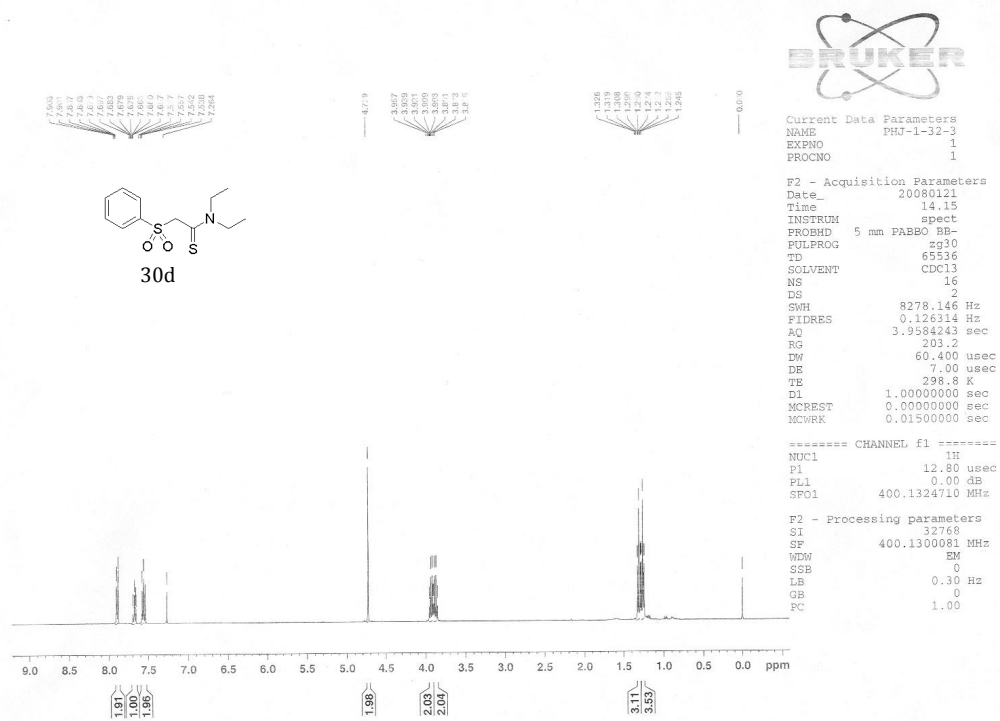


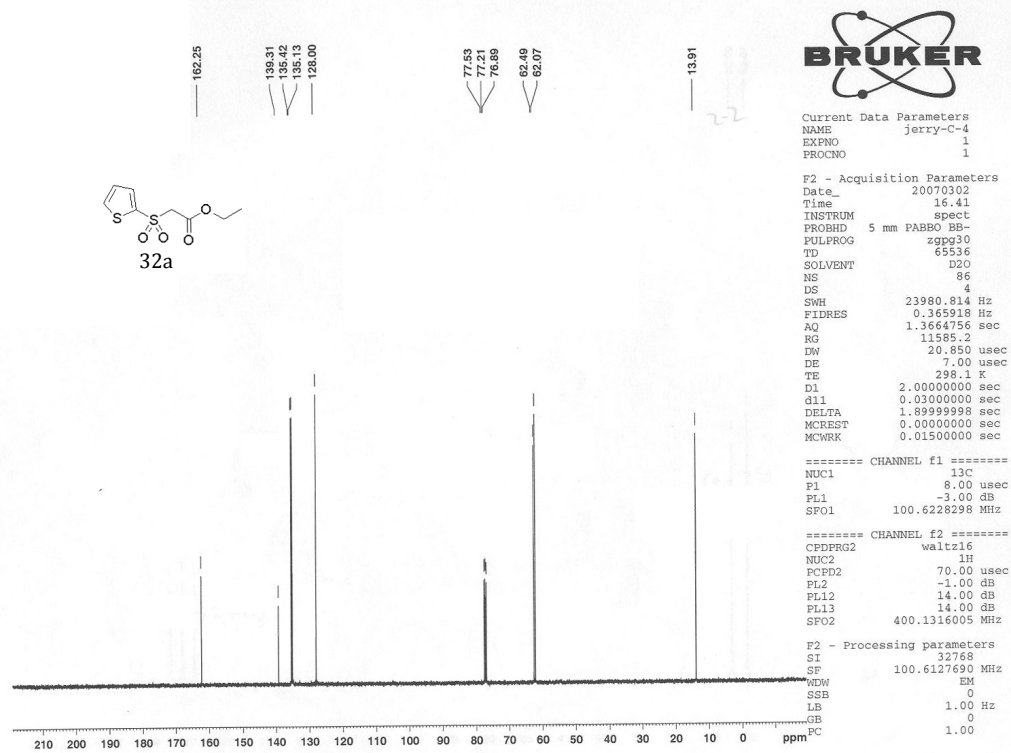
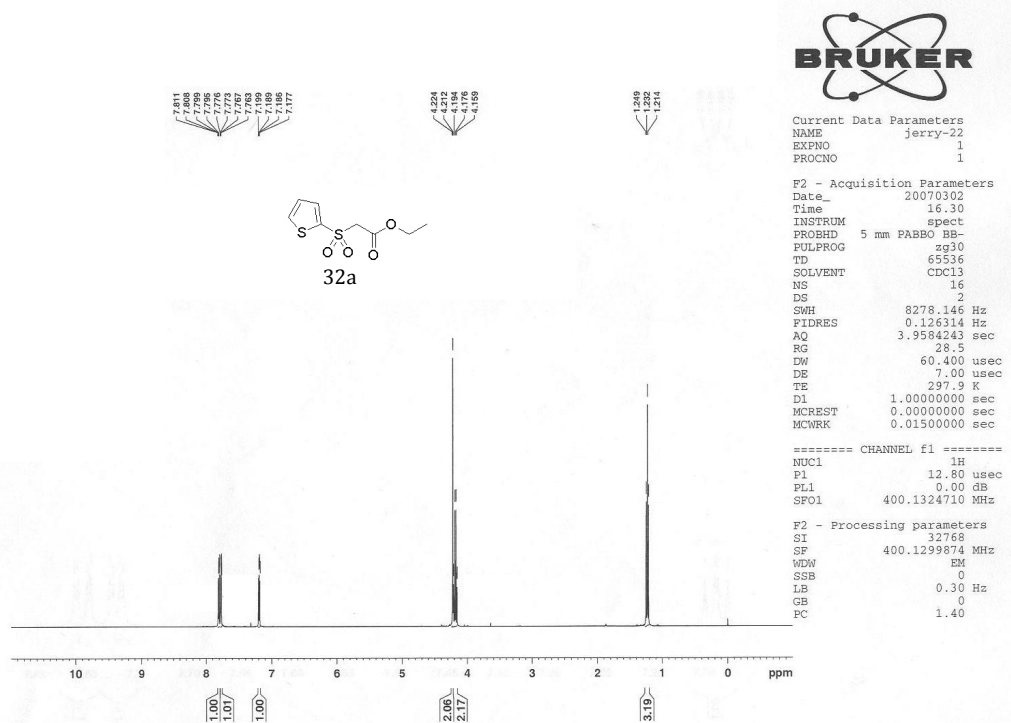


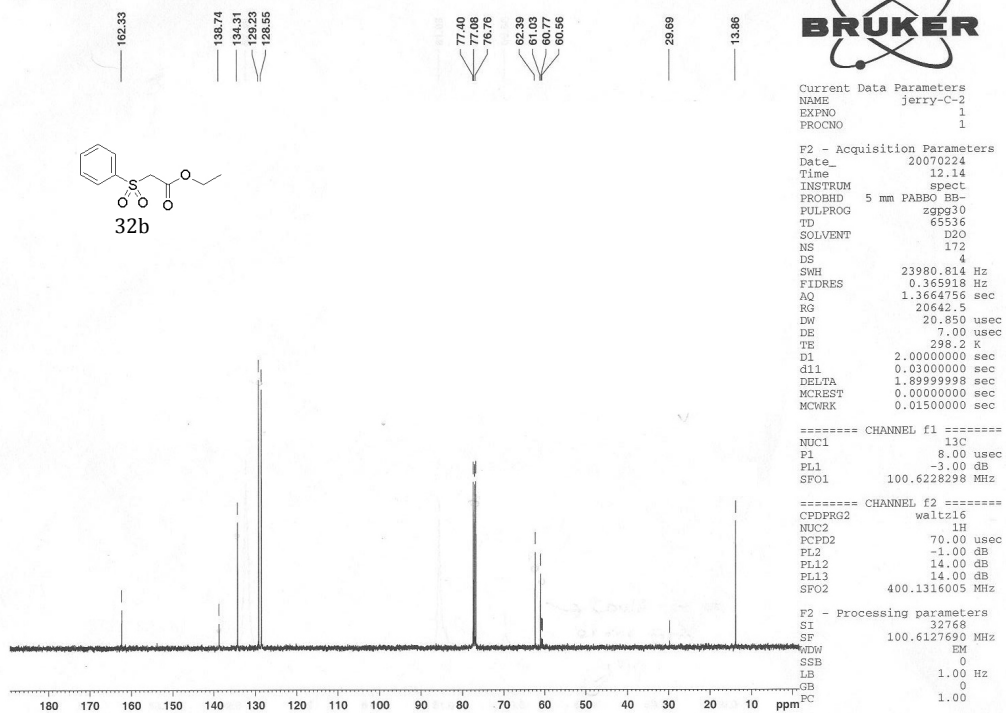
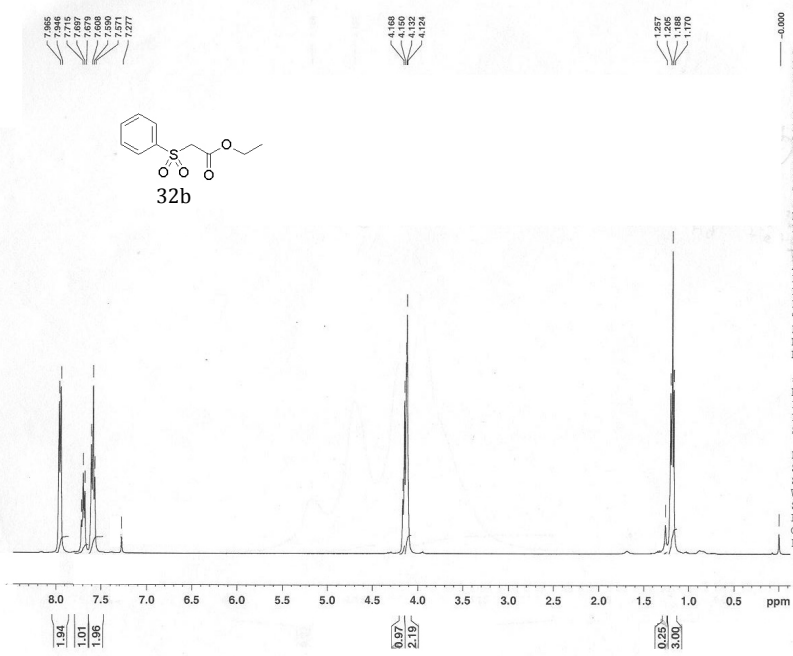


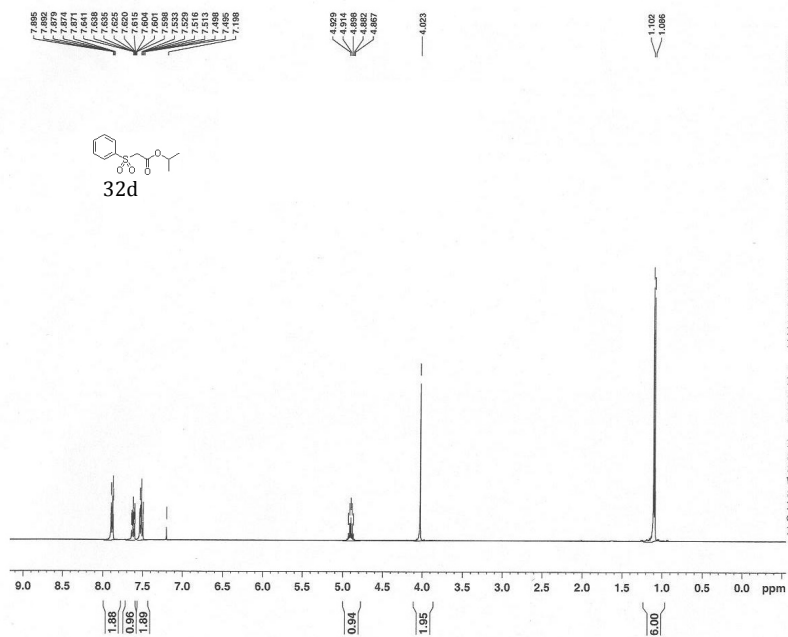










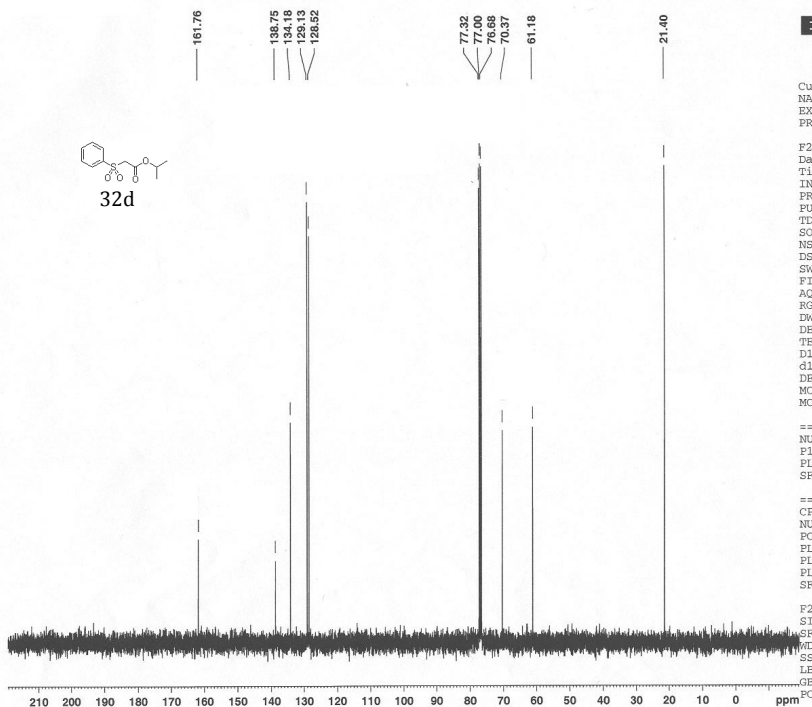


Current Data Parameters
NAME phj-1-12
EXPNO 1
PROCNO 1

F2 - Acquisition Parameters
Date_ 20071212
Time 14.13
INSTRUM spect
PROBHD 5 mm PABBO BB-
PULPROG zg30
TD 65536
SOLVENT CDCl3
NS 16
DS 2
SWH 8278.146 Hz
FIDRES 0.126314 Hz
AQ 3.9584243 sec
RG 128
DW 60.400 usec
DE 7.00 usec
TE 297.8 K
D1 1.0000000 sec
MCREST 0.0000000 sec
MCWRK 0.0150000 sec

===== CHANNEL f1 =====
NUC1 1H
P1 12.80 usec
PL1 0.00 dB
SFO1 400.1324710 MHz

F2 - Processing parameters
SI 32768
SF 400.1300344 MHz
WDW EM
SSB 0
LB 0.30 Hz
GB 0
FC 1.00



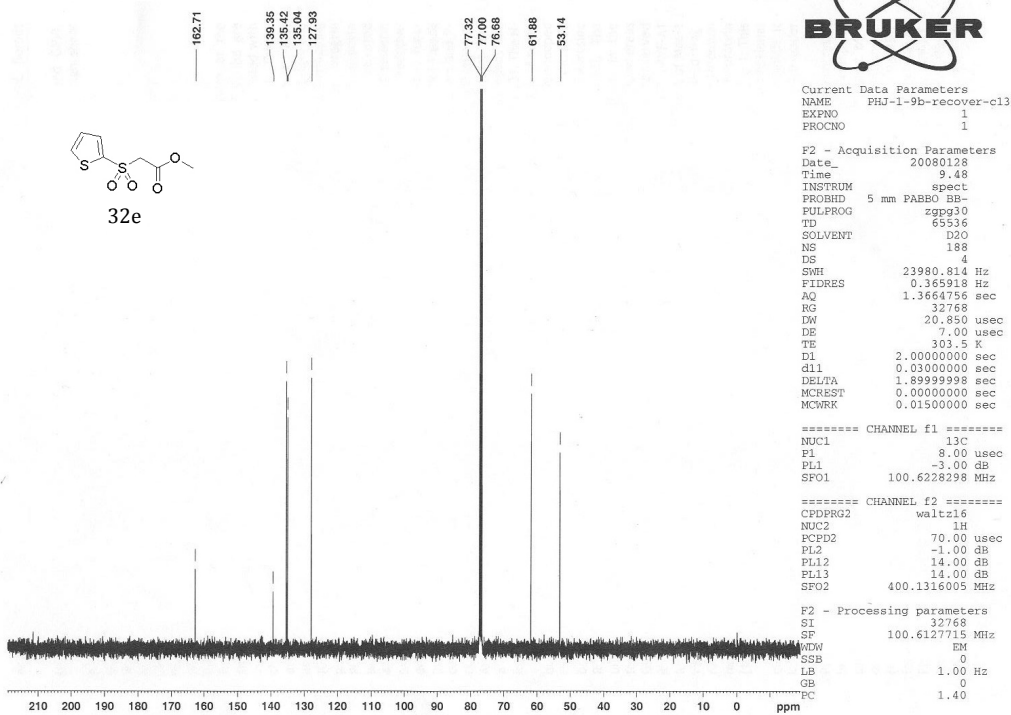
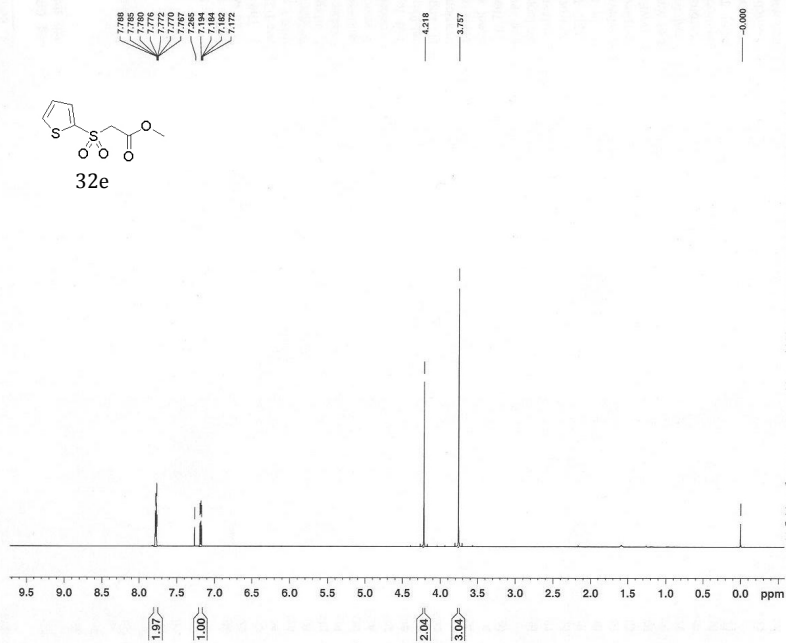
Current Data Parameters
NAME phj-1-12 17
EXPNO 2
PROCNO 1

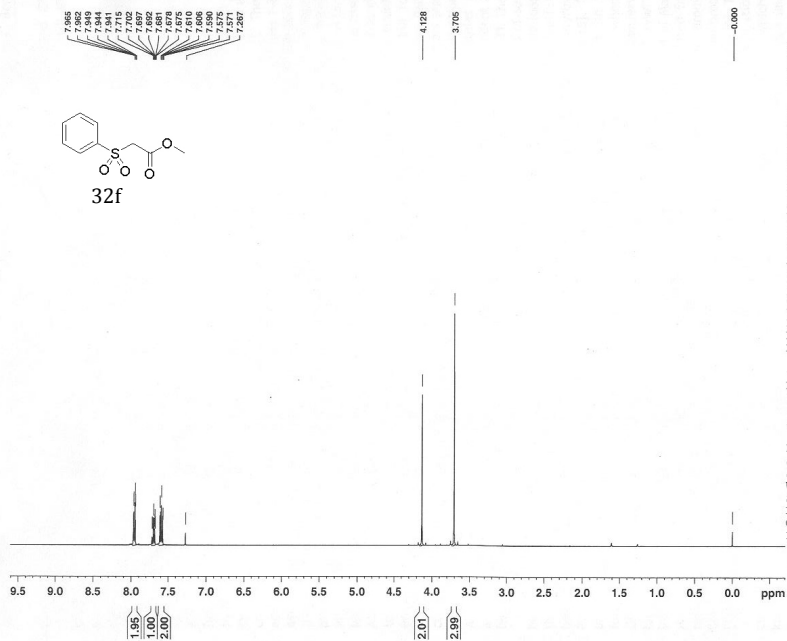
F2 - Acquisition Parameters
Date_ 20071212
Time 14.41
INSTRUM spect
PROBHD 5 mm PABBO BB-
PULPROG zgpg30
TD 65536
SOLVENT D2O-CDCl3
NS 54
DS 4
SWH 23980.814 Hz
FIDRES 0.365918 Hz
AQ 1.3664756 sec
RG 16384
DW 20.850 usec
DE 7.00 usec
TE 298.1 K
D1 2.0000000 sec
d11 0.0300000 sec
DELTA 1.89999998 sec
MCREST 0.0000000 sec
MCWRK 0.0150000 sec

===== CHANNEL f1 =====
NUC1 13C
P1 8.00 usec
PL1 -3.00 dB
SFO1 100.6228298 MHz

===== CHANNEL f2 =====
CPDPRG2 waltz16
NUC2 1H
PCPD2 70.00 usec
PL2 -1.00 dB
PL12 14.00 dB
PL13 14.00 dB
SFO2 400.1316005 MHz

F2 - Processing parameters
SI 32768
SF 100.6127751 MHz
WDW EM
SSB 0
LB 1.00 Hz
GB 0
FC 1.00



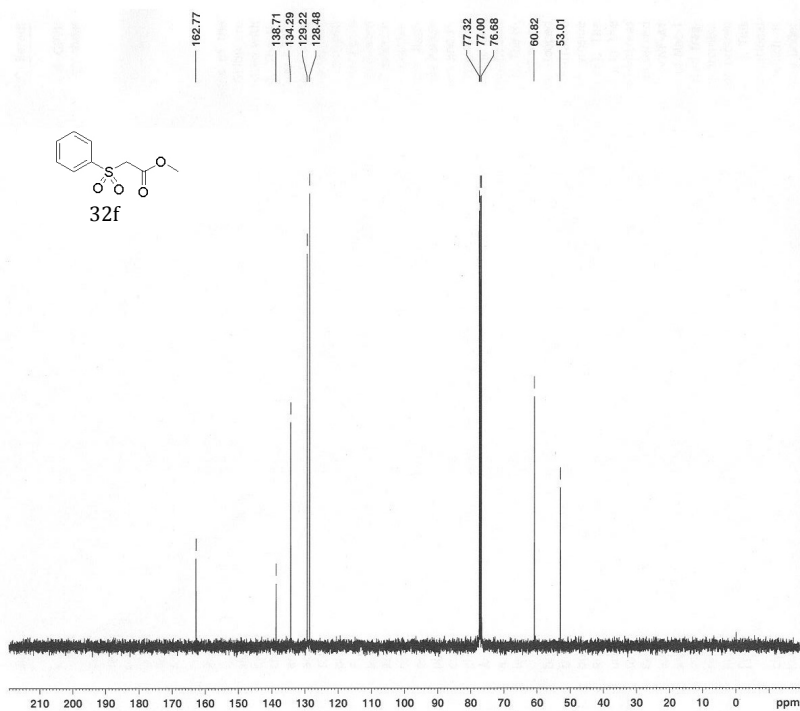


Current Data Parameters
NAME PHJ-1-9a-recover
EXPNO 1
PROCNO 1

F2 - Acquisition Parameters
Date_ 20080128
Time 9.15
INSTRUM spect
PROBHD 5 mm PABBO BB-
PULPROG zg30
TD 65536
SOLVENT CDCl3
NS 16
DS 2
SWH 8278.146 Hz
FIDRES 0.126314 Hz
AQ 3.9584243 sec
RG 181
DW 60.400 usec
DE 7.00 usec
TE 304.7 K
D1 1.00000000 sec
MCREST 0.00000000 sec
MCWRK 0.01500000 sec

===== CHANNEL f1 =====
NUC1 1H
P1 12.80 usec
PL1 0.00 dB
SFO1 400.1324710 MHz

F2 - Processing parameters
SI 32768
SF 400.1300068 MHz
WDW EM
SSB 0
LB 0.30 Hz
GB 0
PC 1.00



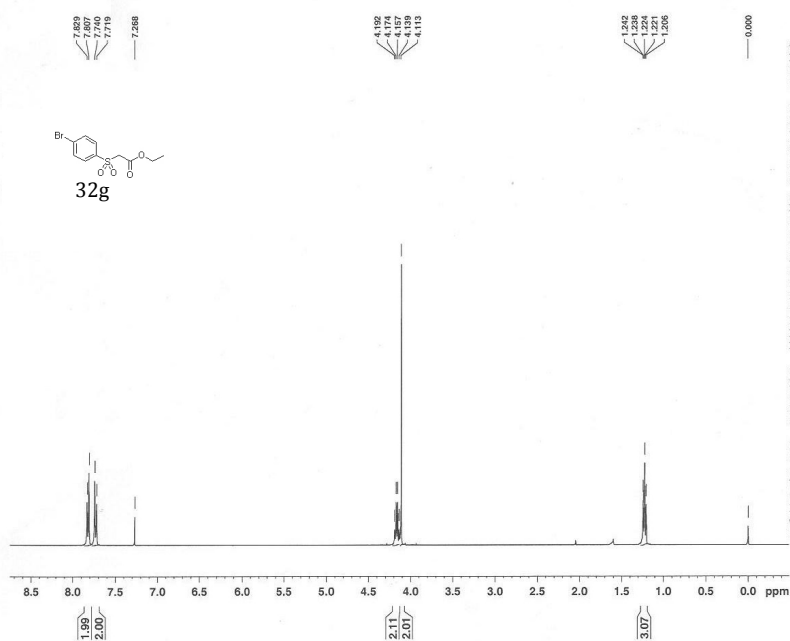
Current Data Parameters
NAME PHJ-1-9a-recover-cl3
EXPNO 1
PROCNO 1

F2 - Acquisition Parameters
Date_ 20080128
Time 9.25
INSTRUM spect
PROBHD 5 mm PABBO BB-
PULPROG zgpg30
TD 65536
SOLVENT D2O
NS 140
DS 4
SWH 23980.814 Hz
FIDRES 0.365918 Hz
AQ 1.3664756 sec
RG 14596.5
DW 20.850 usec
DE 7.00 usec
TE 304.5 K
D1 2.00000000 sec
d11 0.03000000 sec
DELTA 1.89999998 sec
MCREST 0.00000000 sec
MCWRK 0.01500000 sec

===== CHANNEL f1 =====
NUC1 13C
P1 8.00 usec
PL1 -3.00 dB
SFO1 100.6228298 MHz

===== CHANNEL f2 =====
CPDPRG2 waltz16
NUC2 1H
PCPD2 70.00 usec
PL2 -1.00 dB
PL12 14.00 dB
PL13 14.00 dB
SFO2 400.1316005 MHz

F2 - Processing parameters
SI 32768
SF 100.6127729 MHz
WDW EM
SSB 0
LB 1.00 Hz
GB 0
PC 1.40

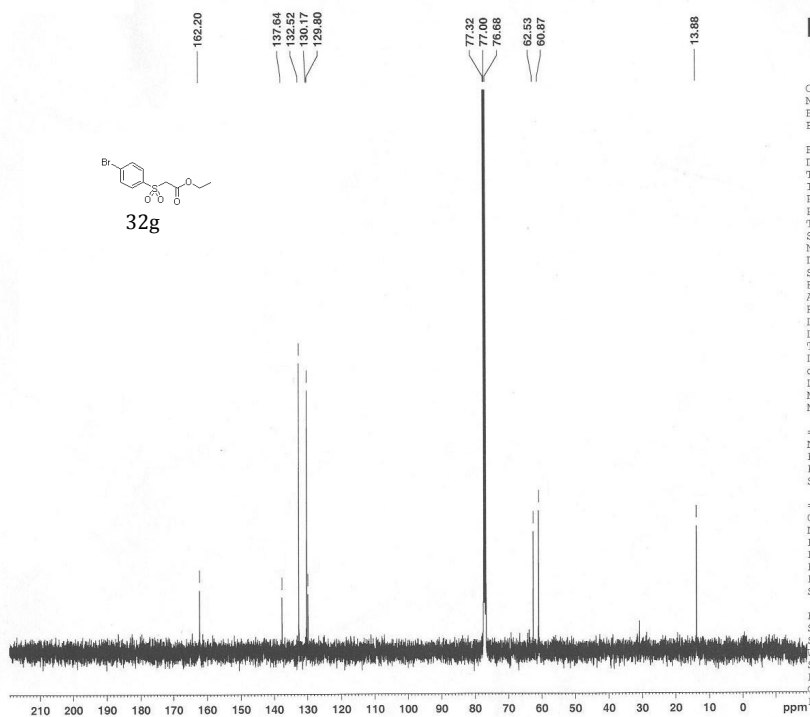


Current Data Parameters
 NAME PHJ-1-56
 EXPNO 1
 PROCNO 1

F2 - Acquisition Parameters
 Date_ 20080328
 Time 11.21
 INSTRUM spect
 PROBHD 5 mm PABBO BB-
 PULPROG zg30
 TD 65536
 SOLVENT CDC13
 NS 16
 DS 2
 SWH 8278.146 Hz
 FIDRES 0.126314 Hz
 AQ 3.9584243 sec
 RG 161.3
 DW 60.400 usec
 DE 7.00 usec
 TE 299.4 K
 D1 1.0000000 sec
 MCREST 0.0000000 sec
 MCWRK 0.0150000 sec

===== CHANNEL f1 =====
 NUC1 1H
 P1 12.80 usec
 PL1 0.00 dB
 SFO1 400.1324710 MHz

F2 - Processing parameters
 SI 32768
 SF 400.1300063 MHz
 WDW EM
 SSB 0
 LB 0.30 Hz
 GB 0
 PC 1.00



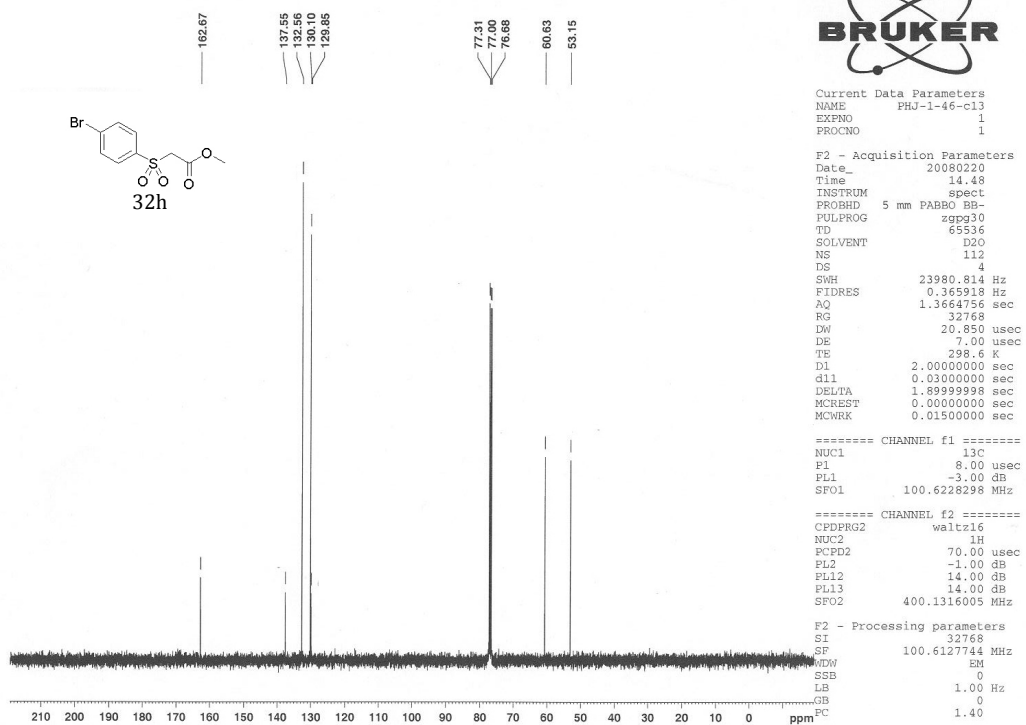
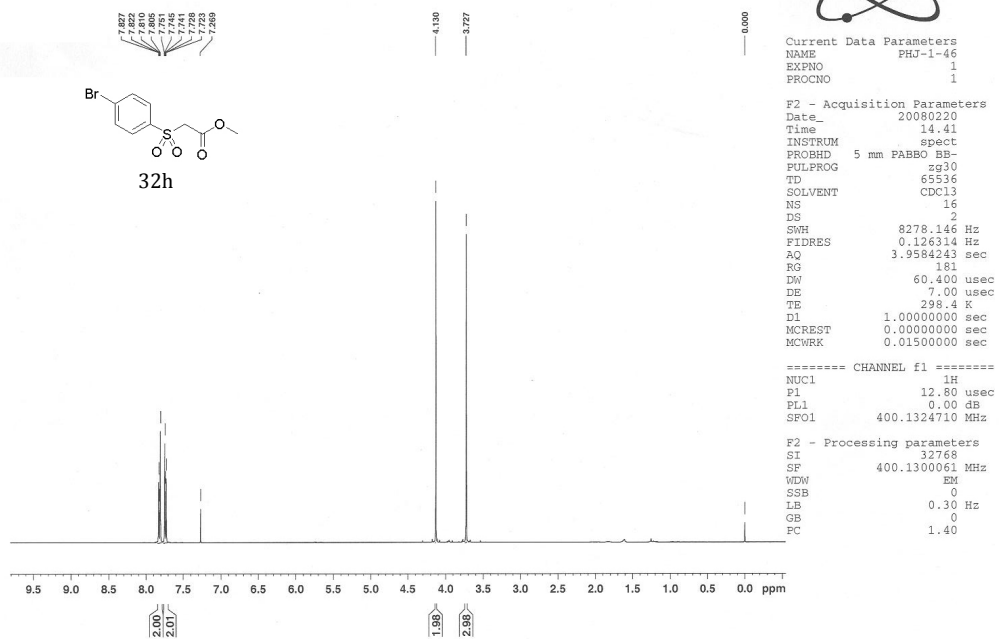
Current Data Parameters
 NAME PHJ-1-49-cl3-2
 EXPNO 1
 PROCNO 1

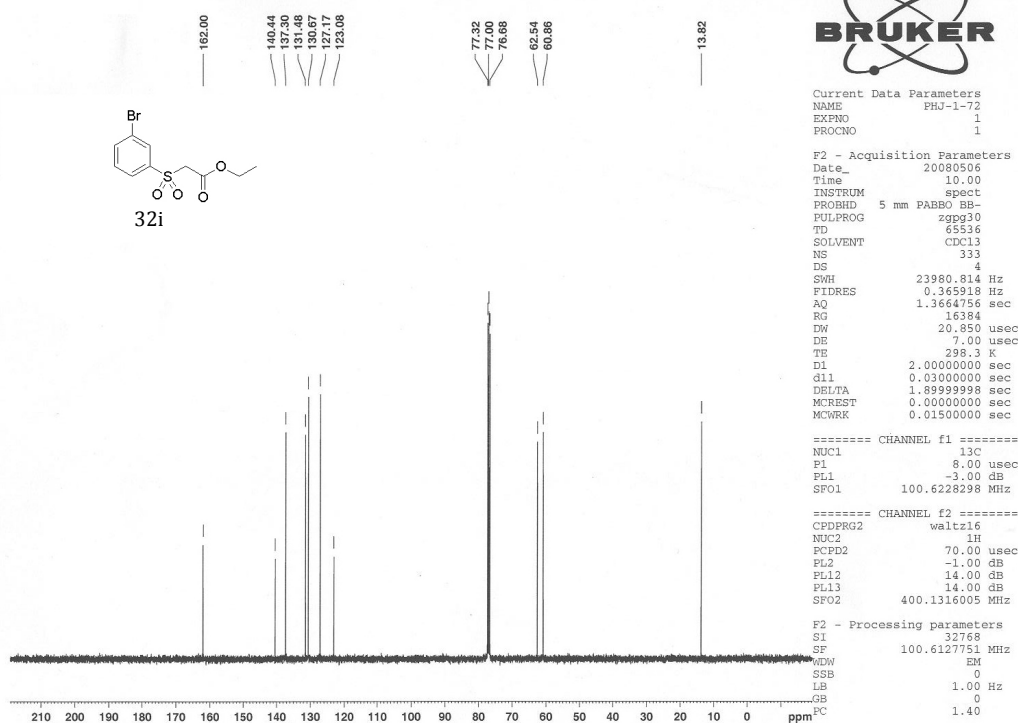
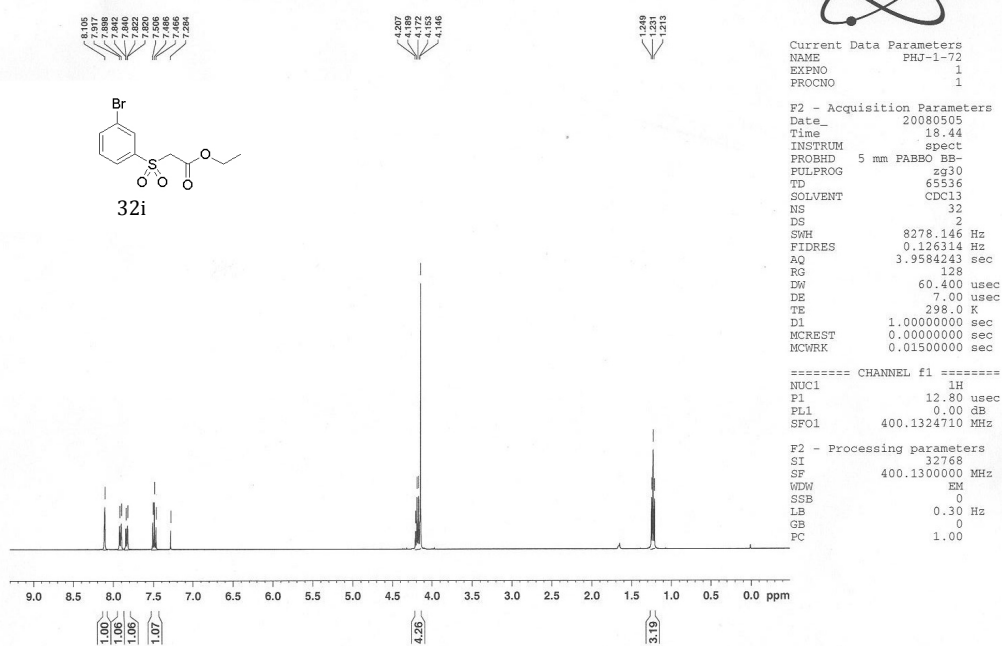
F2 - Acquisition Parameters
 Date_ 20080306
 Time 13.24
 INSTRUM spect
 PROBHD 5 mm PABBO BB-
 PULPROG zgpg30
 TD 65536
 SOLVENT D2O
 NS 374
 DS 4
 SWH 23980.814 Hz
 FIDRES 0.365918 Hz
 AQ 1.3664756 sec
 RG 10321.3
 DW 20.850 usec
 DE 7.00 usec
 TE 297.9 K
 D1 2.0000000 sec
 d11 0.0300000 sec
 DELTA 1.89999998 sec
 MCREST 0.0000000 sec
 MCWRK 0.0150000 sec

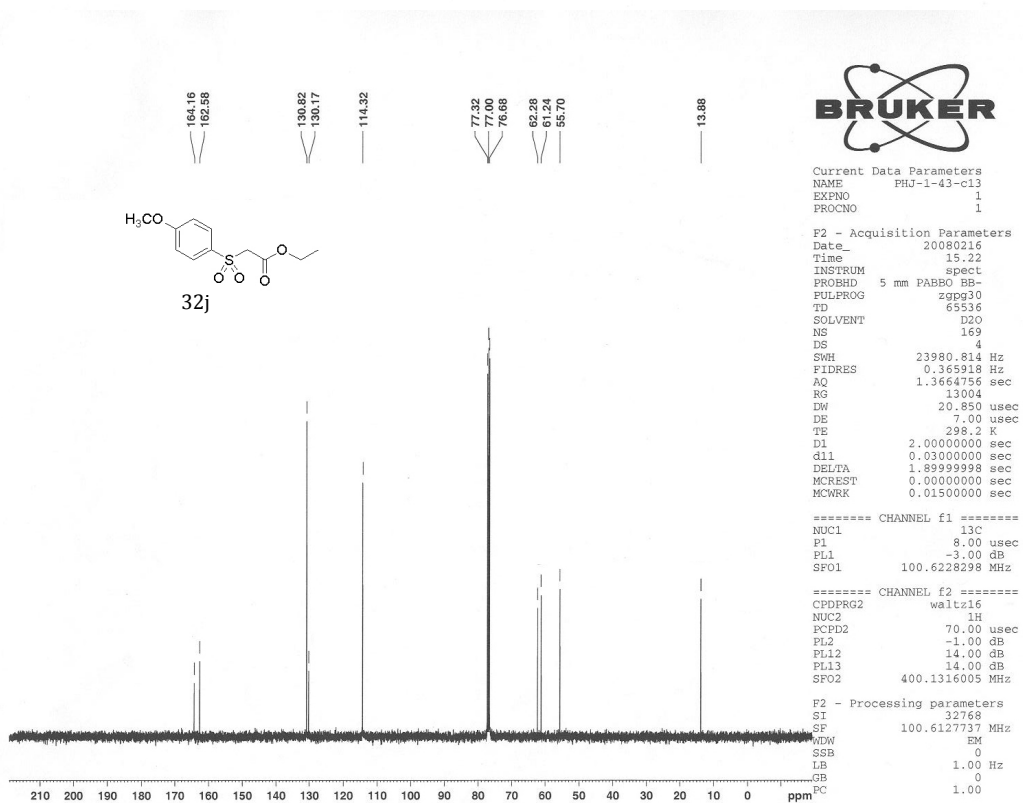
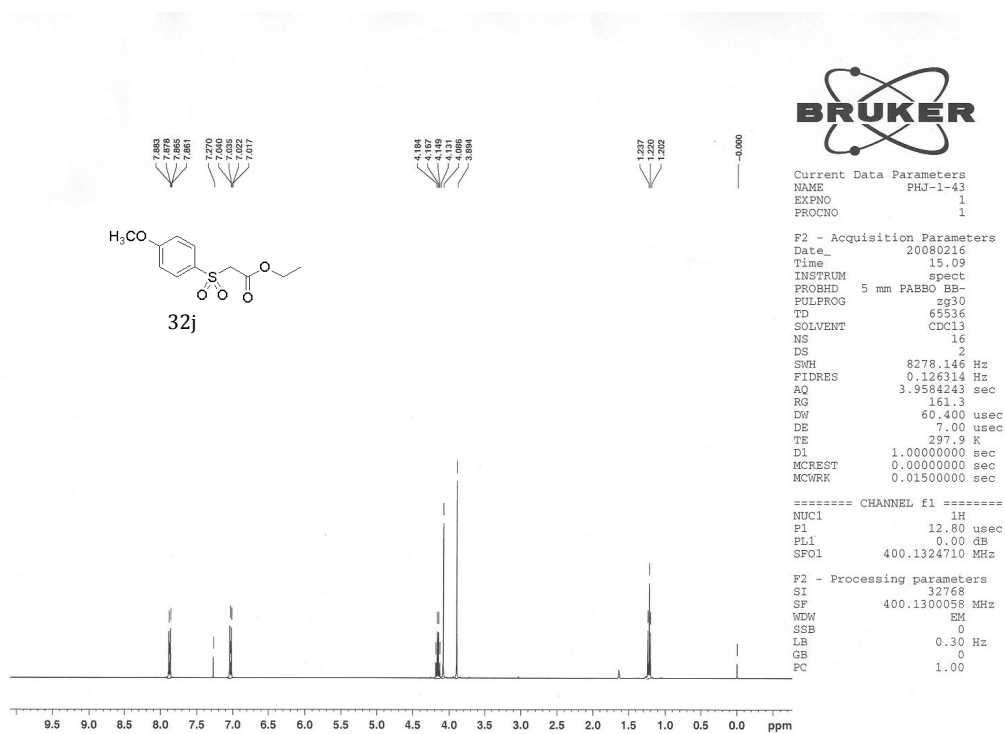
===== CHANNEL f1 =====
 NUC1 13C
 P1 8.00 usec
 PL1 -3.00 dB
 SFO1 100.6228298 MHz

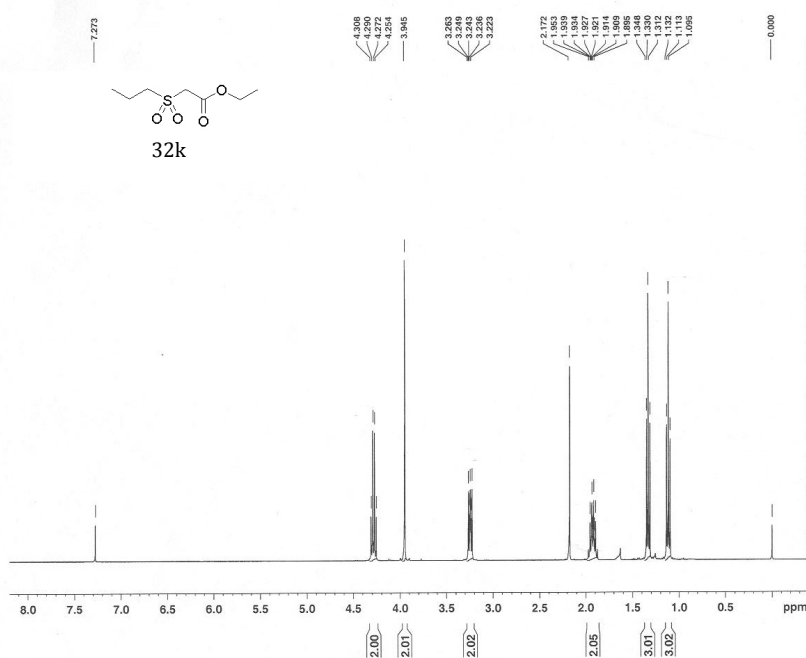
===== CHANNEL f2 =====
 CHOPRG2 waltz16
 NUC2 1H
 PCPD2 70.00 usec
 PL2 -1.00 dB
 PL12 14.00 dB
 PL13 14.00 dB
 SFO2 400.1316005 MHz

F2 - Processing parameters
 SI 32768
 SF 100.6127722 MHz
 WDW EM
 SSB 0
 LB 1.00 Hz
 GB 0
 PC 1.40







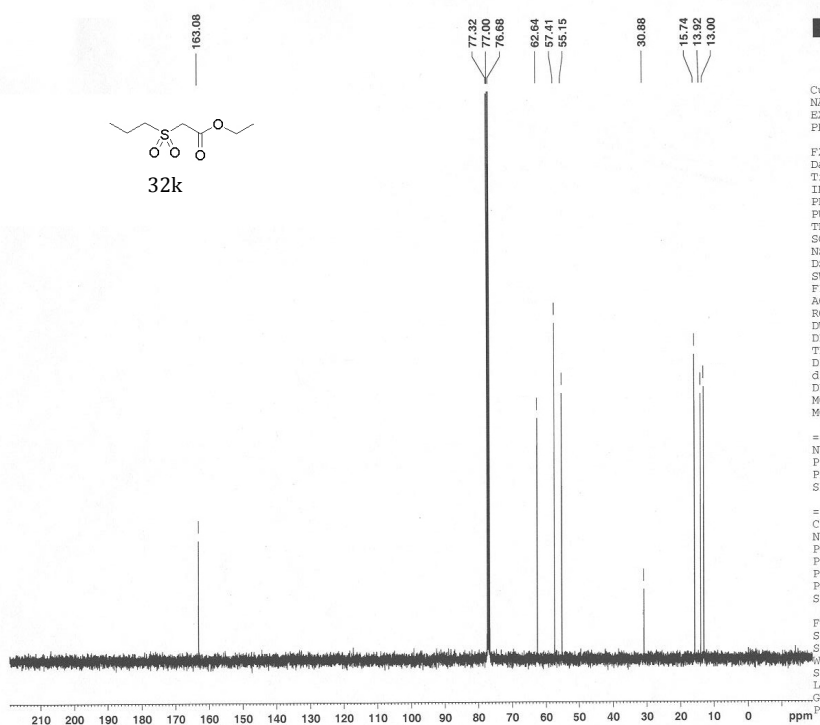


Current Data Parameters
 NAME PHU-1-50
 EXPNO 1
 PROCNO 1

F2 - Acquisition Parameters
 Date_ 20080306
 Time 10.31
 INSTRUM spect
 PROBHD 5 mm PABBO BB-
 PULPROG zg30
 TD 65536
 SOLVENT CDCl3
 NS 16
 DS 2
 SWH 8278.146 Hz
 FIDRES 0.126314 Hz
 AQ 3.9584243 sec
 RG 128
 DW 60.400 usec
 DE 7.00 usec
 TE 297.8 K
 D1 1.0000000 sec
 MCREST 0.0000000 sec
 MCWRK 0.01500000 sec

===== CHANNEL f1 =====
 NUC1 1H
 P1 12.80 usec
 PL1 0.00 dB
 SFO1 400.1324710 MHz

F2 - Processing parameters
 SI 32768
 SF 400.1300043 MHz
 WDW EM
 SSB 0
 LB 0.30 Hz
 GB 0
 PC 1.00



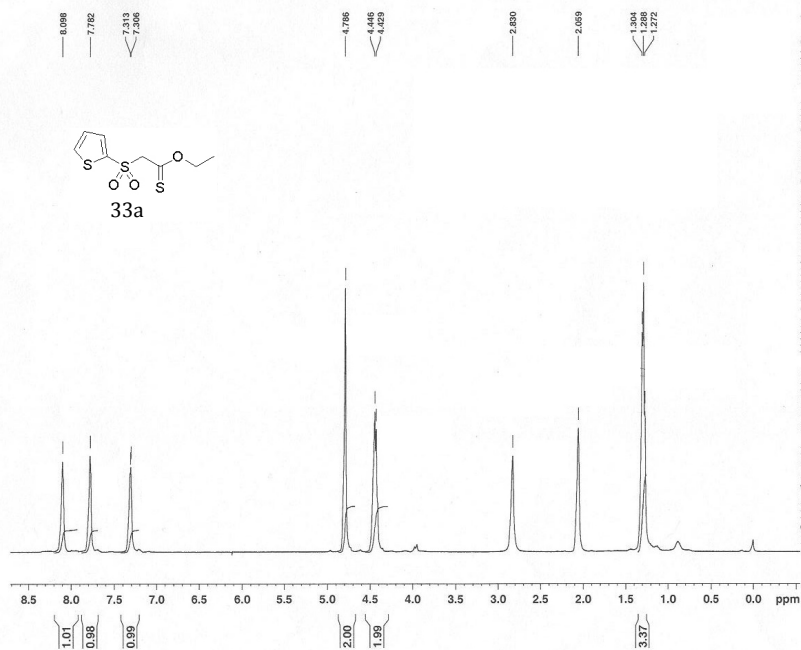
Current Data Parameters
 NAME PHU-1-50-cl3
 EXPNO 1
 PROCNO 1

F2 - Acquisition Parameters
 Date_ 20080306
 Time 10.53
 INSTRUM spect
 PROBHD 5 mm PABBO BB-
 PULPROG zgpg30
 TD 65536
 SOLVENT D2O
 NS 273
 DS 4
 SWH 23980.814 Hz
 FIDRES 0.365918 Hz
 AQ 1.3664756 sec
 RG 11585.2
 DW 20.850 usec
 DE 7.00 usec
 TE 298.1 K
 D1 2.0000000 sec
 d11 0.0300000 sec
 DELTA 1.8999998 sec
 MCREST 0.0000000 sec
 MCWRK 0.01500000 sec

===== CHANNEL f1 =====
 NUC1 13C
 P1 8.00 usec
 PL1 -3.00 dB
 SFO1 100.6228298 MHz

===== CHANNEL f2 =====
 CPDPRG2 waltz16
 NUC2 1H
 PCPD2 70.00 usec
 PL2 -1.00 dB
 PL12 14.00 dB
 PL13 14.00 dB
 SFO2 400.1316005 MHz

F2 - Processing parameters
 SI 32768
 SF 100.6127737 MHz
 WDW EM
 SSB 0
 LB 1.00 Hz
 GB 0
 PC 1.00

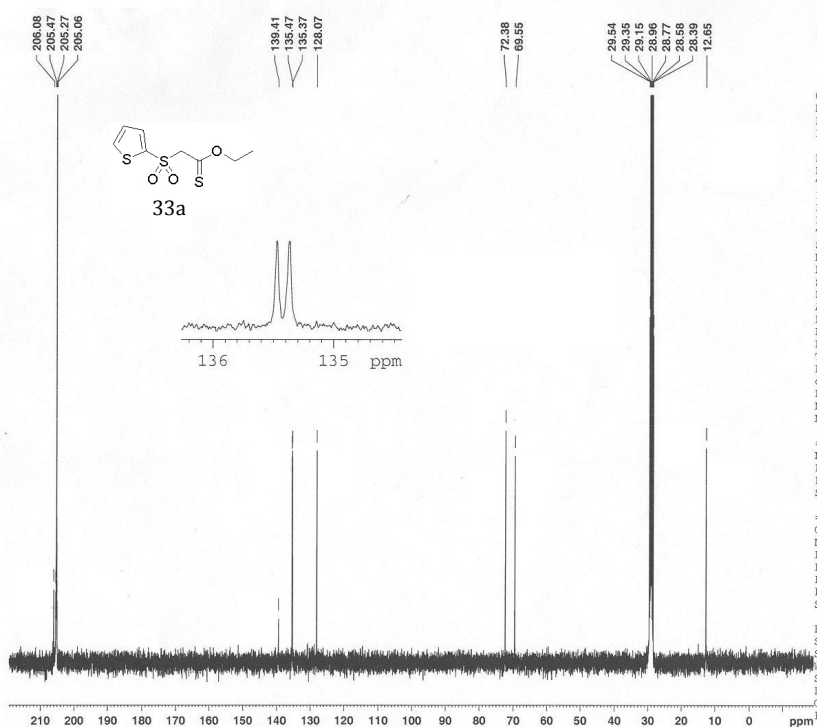


Current Data Parameters
 NAME Jerry-48
 EXPNO 1
 PROCNO 1

F2 - Acquisition Parameters
 Date_ 20070507
 Time 10.21
 INSTRUM spect
 PROBHD 5 mm PABBO BB-
 PULPROG zg30
 TD 65536
 SOLVENT Acetone
 NS 16
 DS 2
 SWH 8278.146 Hz
 FIDRES 0.126314 Hz
 AQ 3.9584243 sec
 RG 203.2
 DW 60.400 usec
 DE 7.00 usec
 TE 298.2 K
 D1 1.00000000 sec
 MCREST 0.00000000 sec
 MCWRK 0.01500000 sec

==== CHANNEL f1 =====
 NUC1 1H
 P1 12.80 usec
 PL1 0.00 dB
 SFO1 400.1324710 MHz

F2 - Processing parameters
 SI 32768
 SF 400.1300038 MHz
 WDW EM
 SSB 0
 LB 0.30 Hz
 GB 0
 FC 1.00



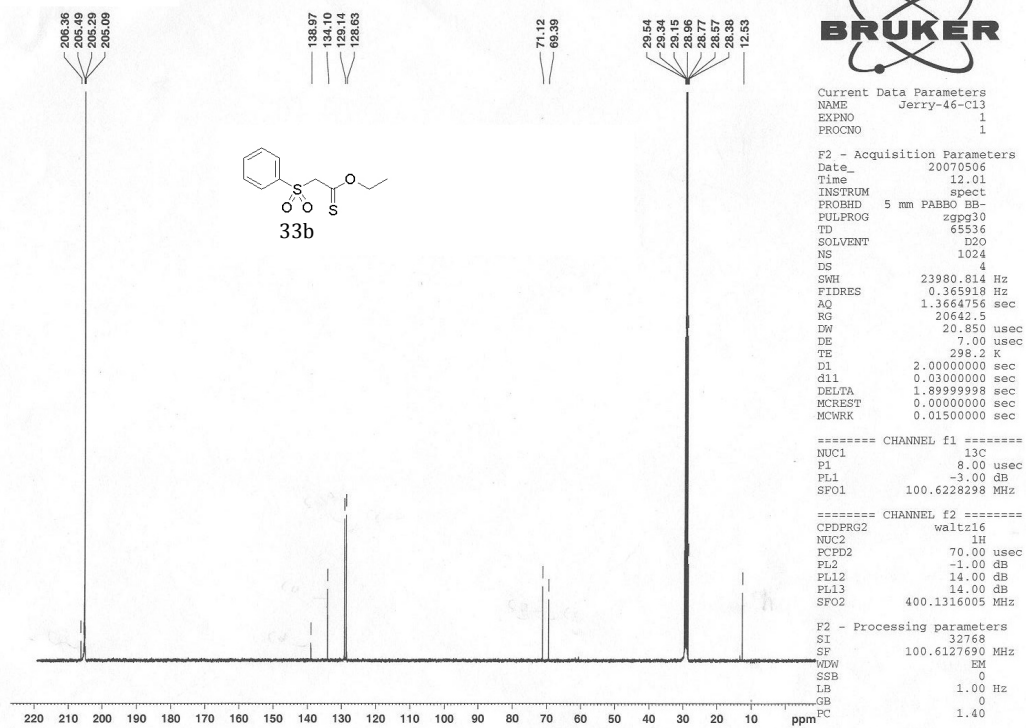
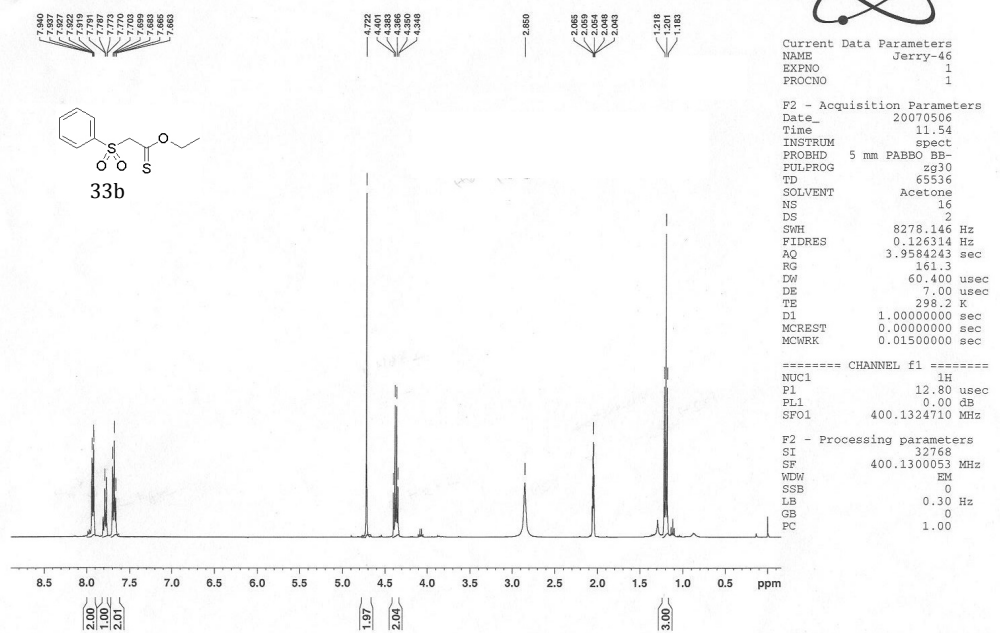
Current Data Parameters
 NAME Jerry-48-Cl3
 EXPNO 1
 PROCNO 1

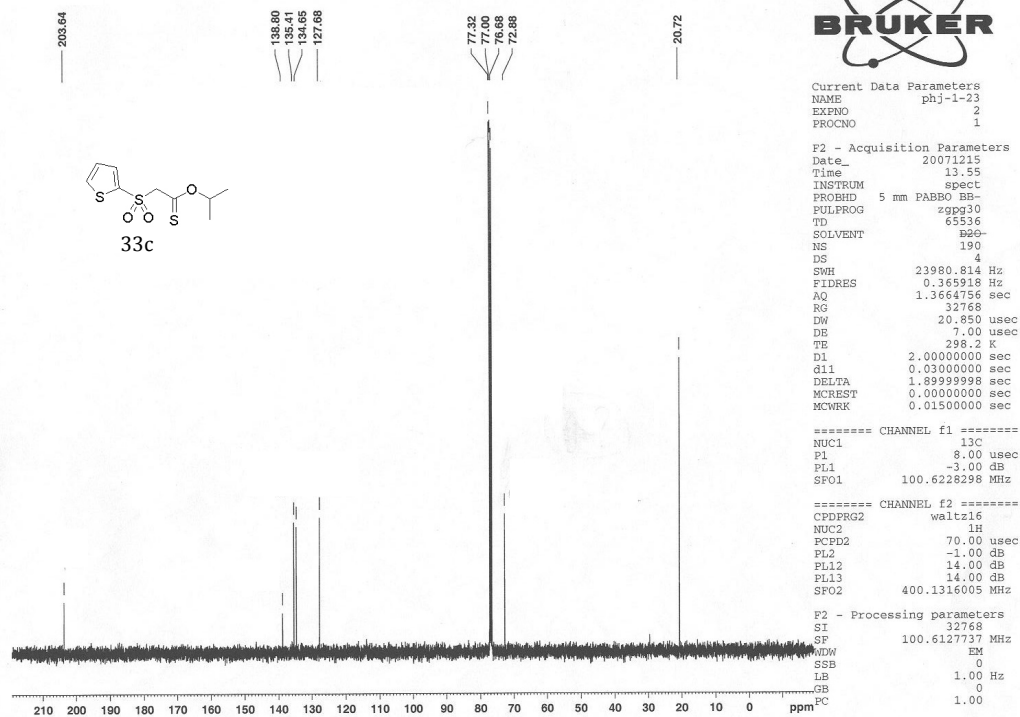
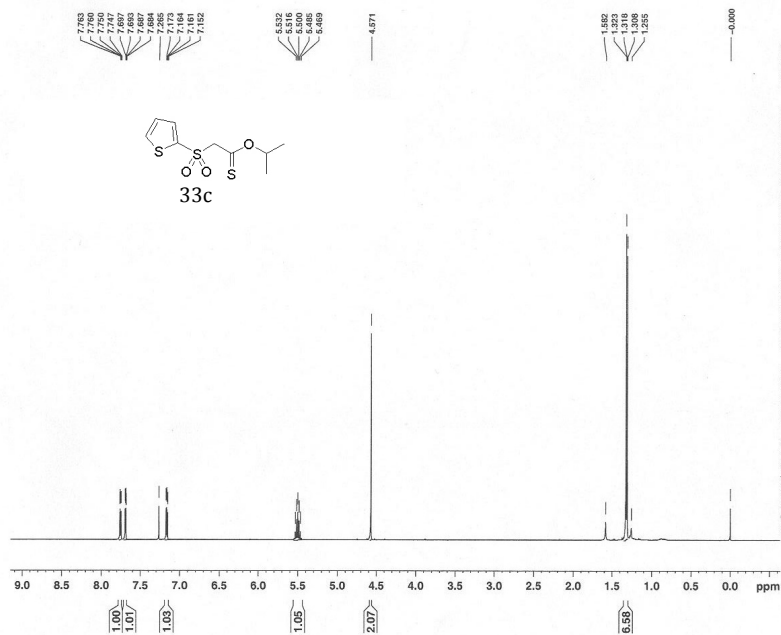
F2 - Acquisition Parameters
 Date_ 20070507
 Time 10.29
 INSTRUM spect
 PROBHD 5 mm PABBO BB-
 PULPROG zgpg30
 TD 65536
 SOLVENT D2O
 NS 441
 DS 4
 SWH 23980.814 Hz
 FIDRES 0.365918 Hz
 AQ 1.3664756 sec
 RG 23170.5
 DW 20.850 usec
 DE 7.00 usec
 TE 298.2 K
 D1 2.00000000 sec
 d11 0.03000000 sec
 DELTA 1.89999998 sec
 MCREST 0.00000000 sec
 MCWRK 0.01500000 sec

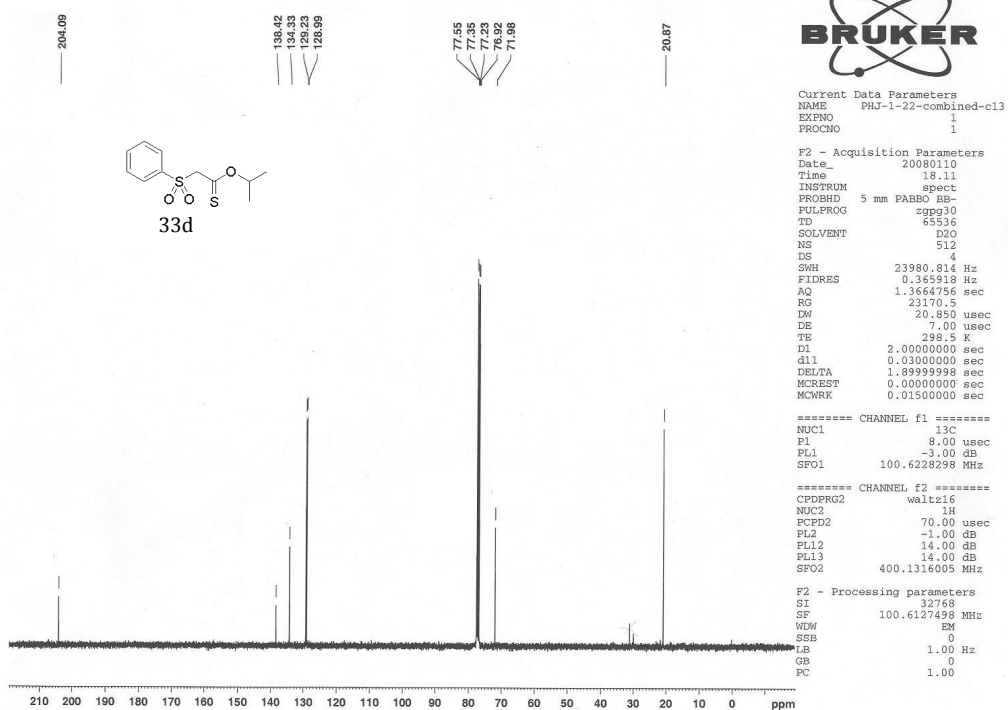
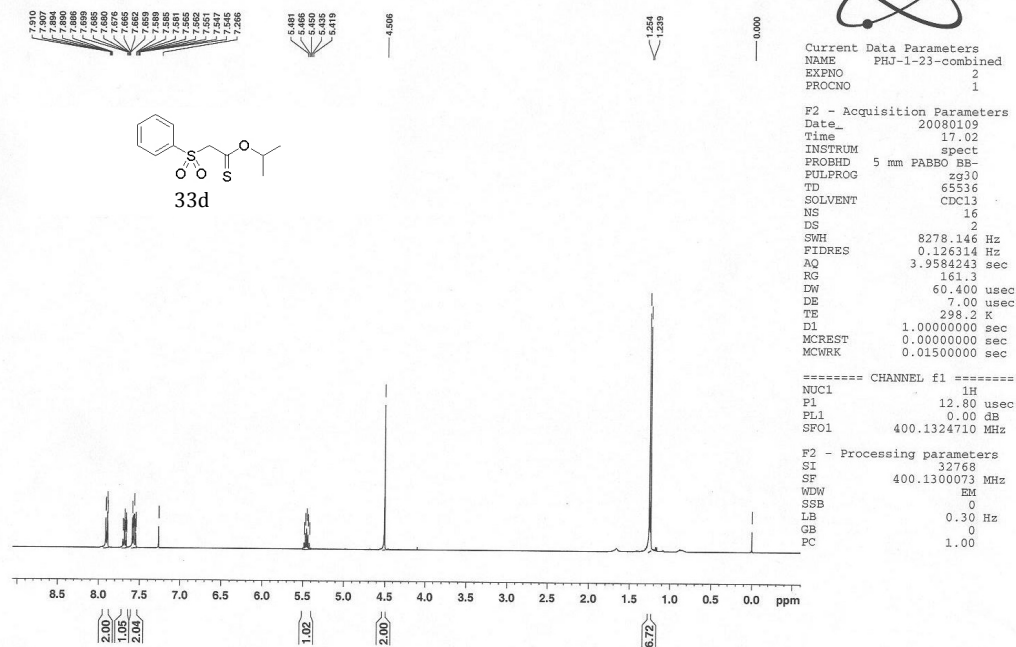
==== CHANNEL f1 =====
 NUC1 13C
 P1 8.00 usec
 PL1 -3.00 dB
 SFO1 100.6228298 MHz

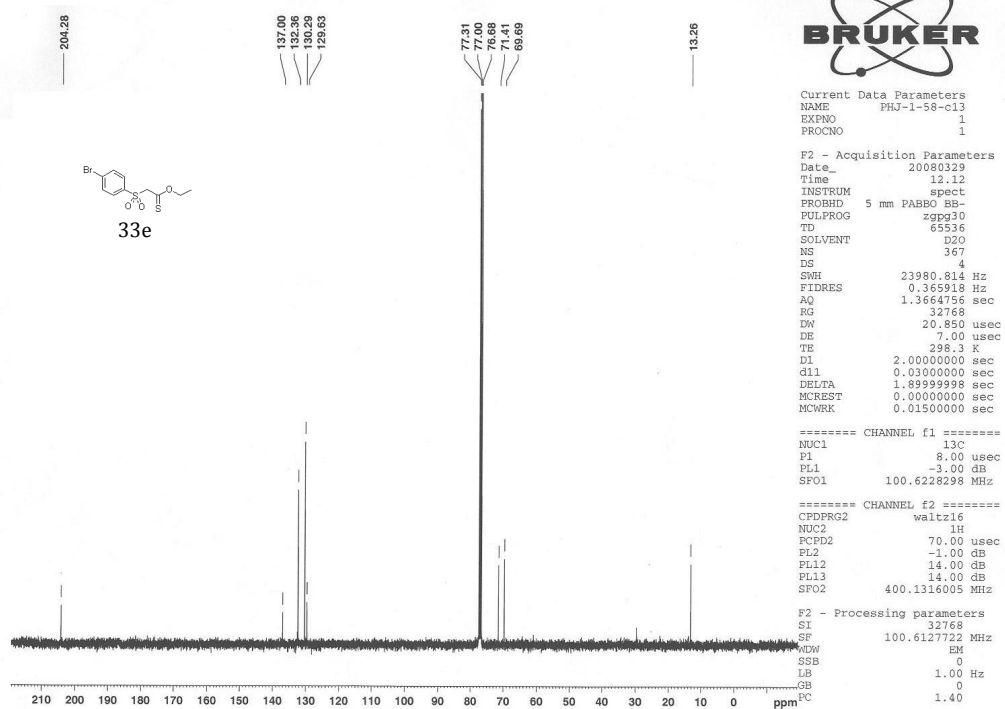
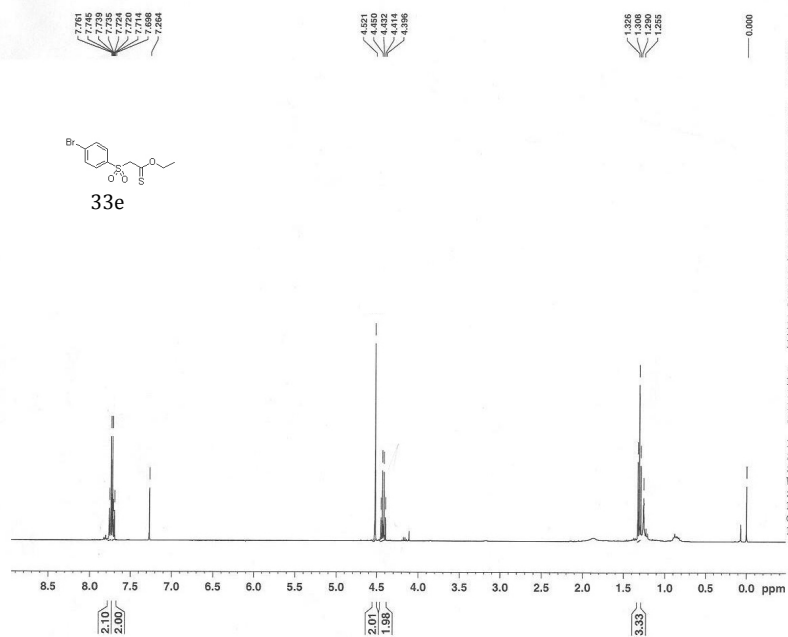
==== CHANNEL f2 =====
 CPDPRG2 waltz16
 NUC2 1H
 PCPD2 70.00 usec
 FL2 -1.00 dB
 PL12 14.00 dB
 PL13 14.00 dB
 SFO2 400.1316005 MHz

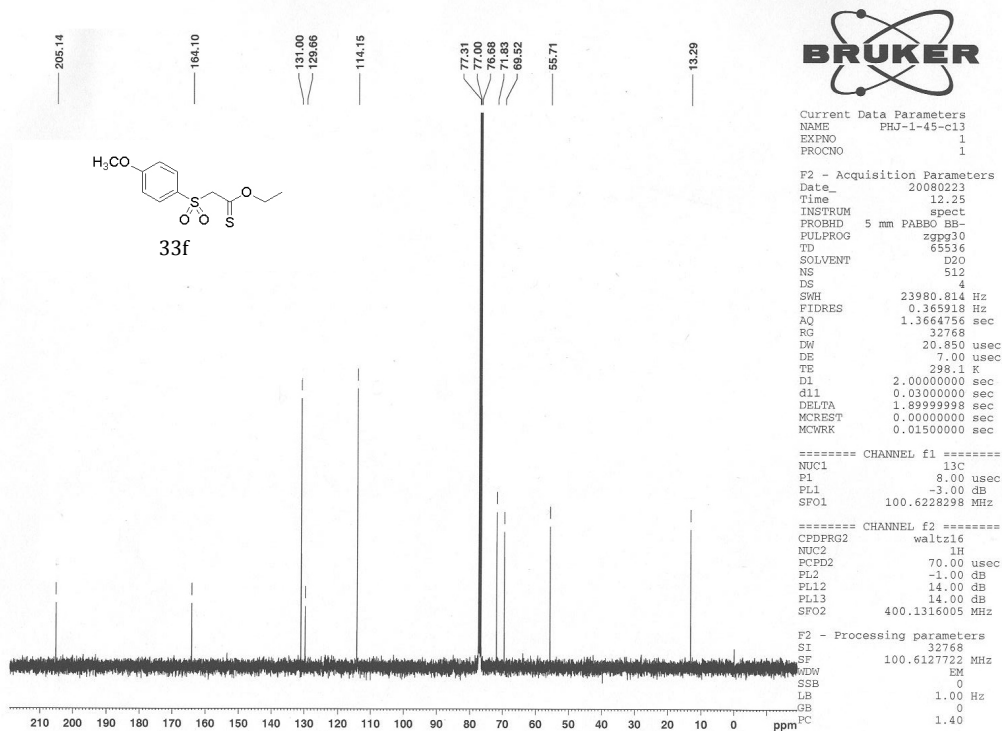
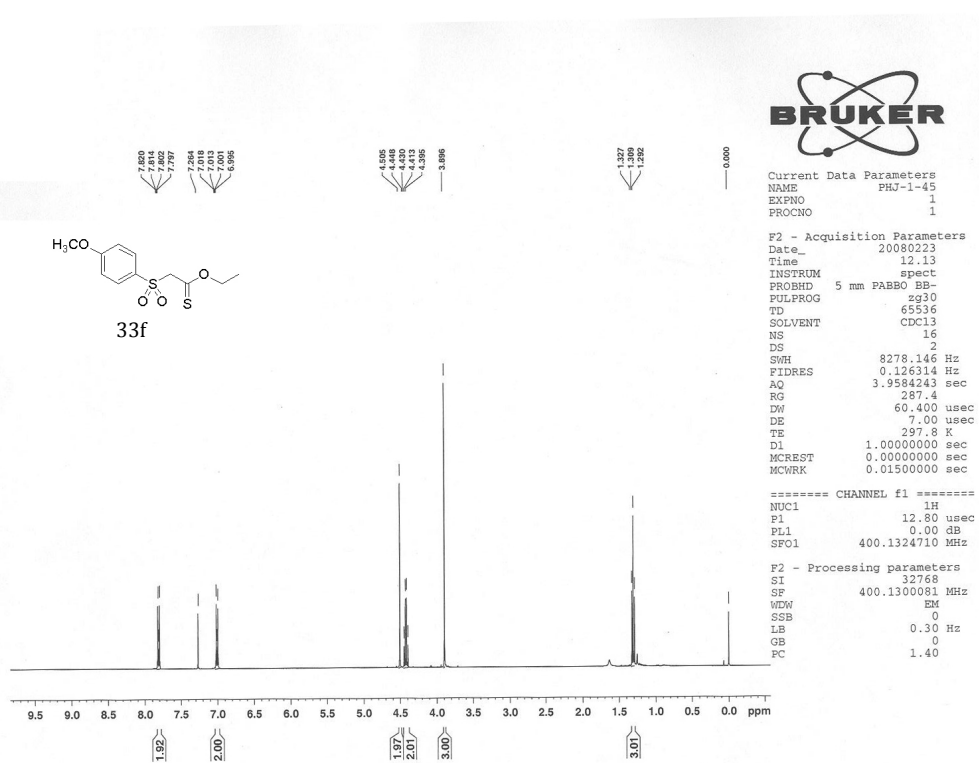
F2 - Processing parameters
 SI 32768
 SF 100.6127690 MHz
 WDW EM
 SSB 0
 LB 1.00 Hz
 GB 0
 FC 1.00

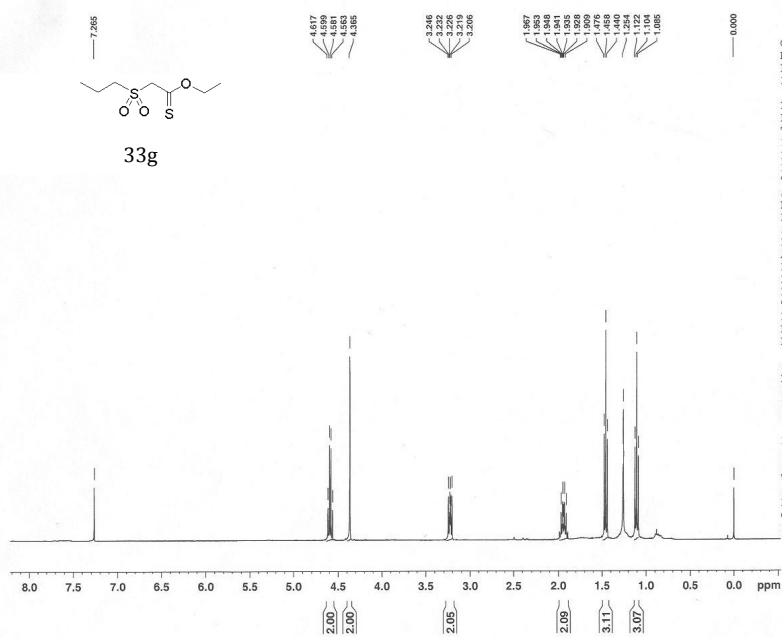










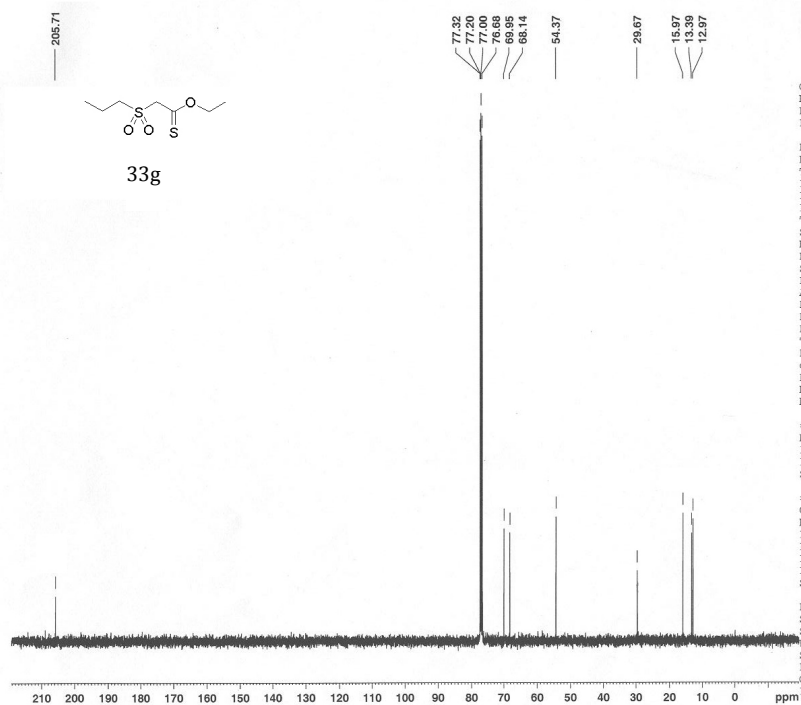


Current Data Parameters
 NAME PHJ-1-57
 EXPNO 1
 PROCNO 1

F2 - Acquisition Parameters
 Date_ 20080329
 Time 12.23
 INSTRUM spect
 PROBHD 5 mm PABBO BB-
 PULPROG zg30
 TD 65536
 SOLVENT D2O
 NS 16
 DS 2
 SWH 8278.146 Hz
 FIDRES 0.126314 Hz
 AQ 3.9584243 sec
 RG 181
 DW 60.400 usec
 DE 7.00 usec
 TE 298.0 K
 D1 1.0000000 sec
 MCREST 0.0000000 sec
 MCWRK 0.0150000 sec

----- CHANNEL f1 -----
 NUC1 1H
 P1 12.80 usec
 PL1 0.00 dB
 SFO1 400.1324710 MHz

F2 - Processing parameters
 SI 32768
 SF 400.1300076 MHz
 WDW EM
 SSB 0
 LB 0.30 Hz
 GB 0
 PC 1.40



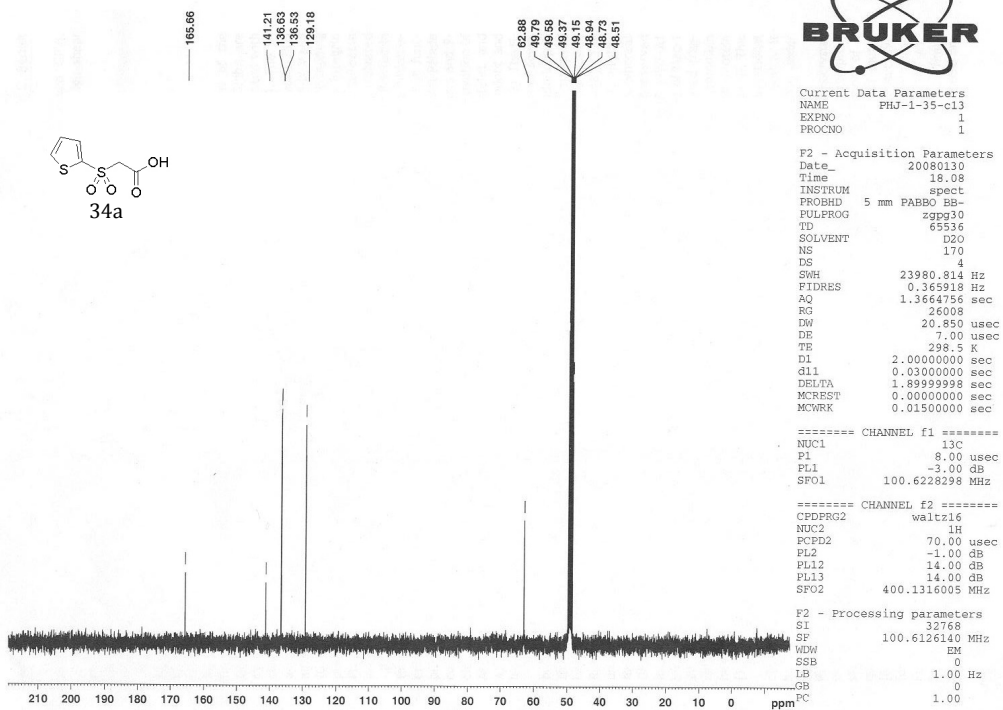
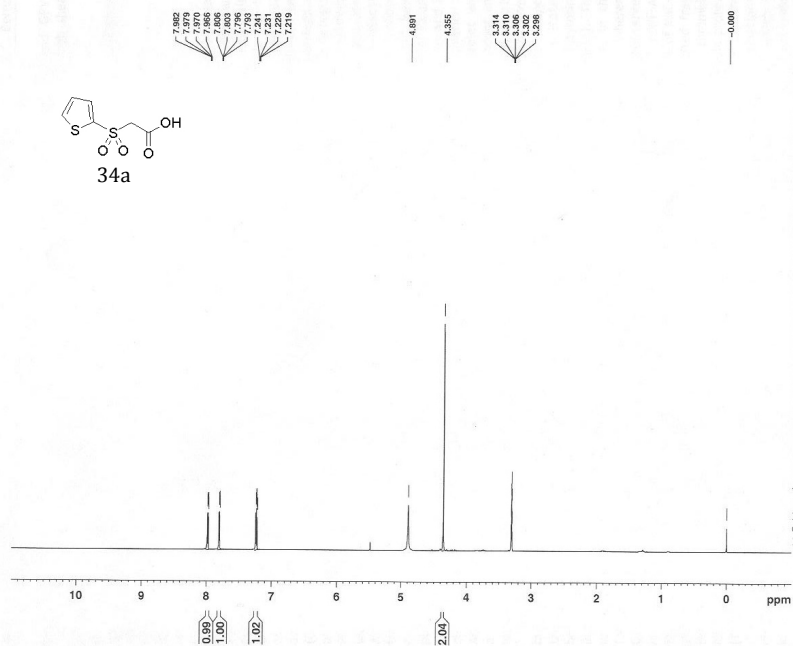
Current Data Parameters
 NAME PHJ-1-57-cl3
 EXPNO 1
 PROCNO 1

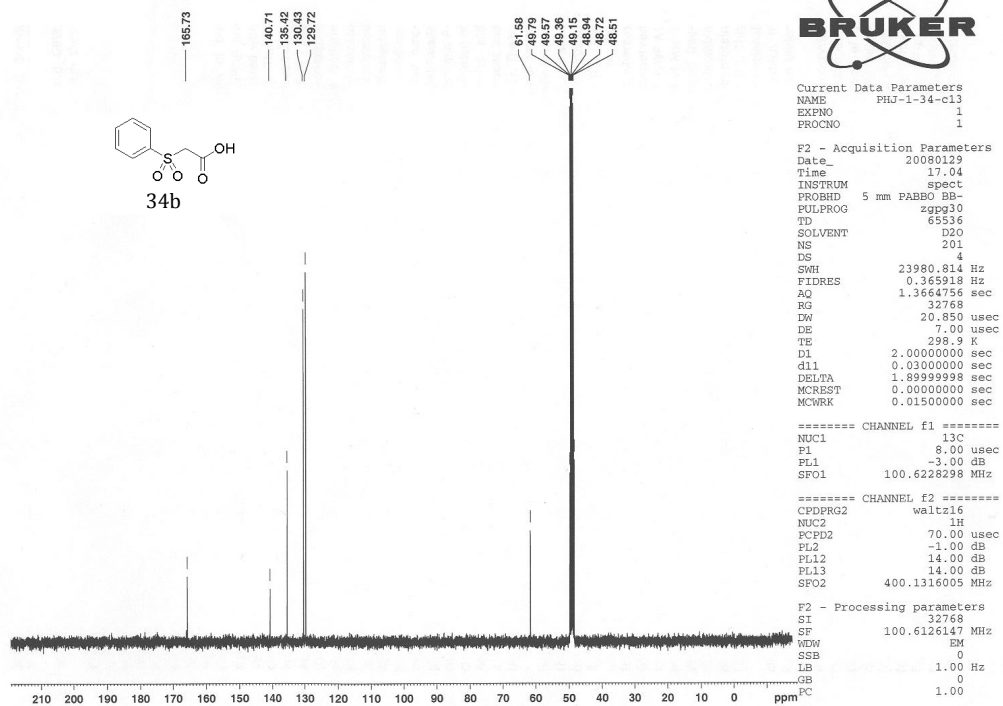
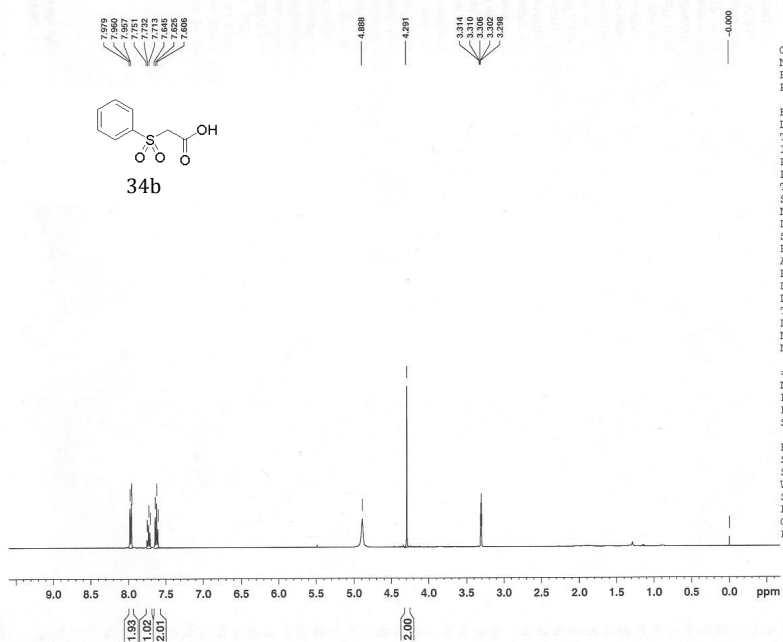
F2 - Acquisition Parameters
 Date_ 20080329
 Time 12.38
 INSTRUM spect
 PROBHD 5 mm PABBO BB-
 PULPROG zgpg30
 TD 65536
 SOLVENT D2O
 NS 330
 DS 4
 SWH 23980.814 Hz
 FIDRES 0.365918 Hz
 AQ 1.3664756 sec
 RG 32768
 DW 20.850 usec
 DE 7.00 usec
 TE 298.2 K
 D1 2.0000000 sec
 d11 0.0300000 sec
 DELTA 1.8999998 sec
 MCREST 0.0000000 sec
 MCWRK 0.0150000 sec

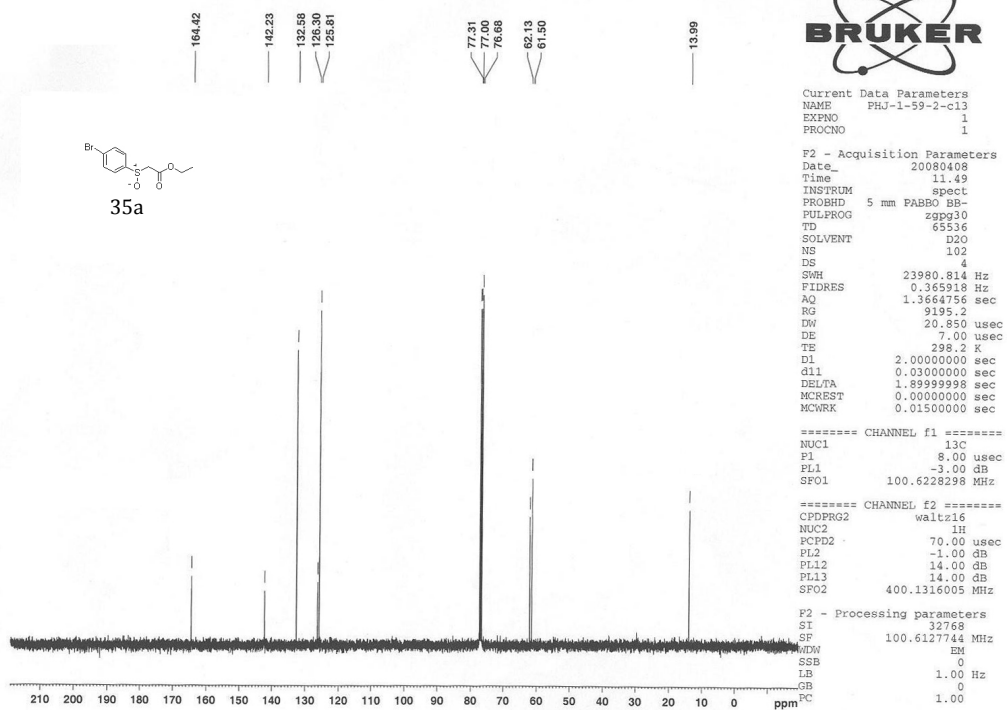
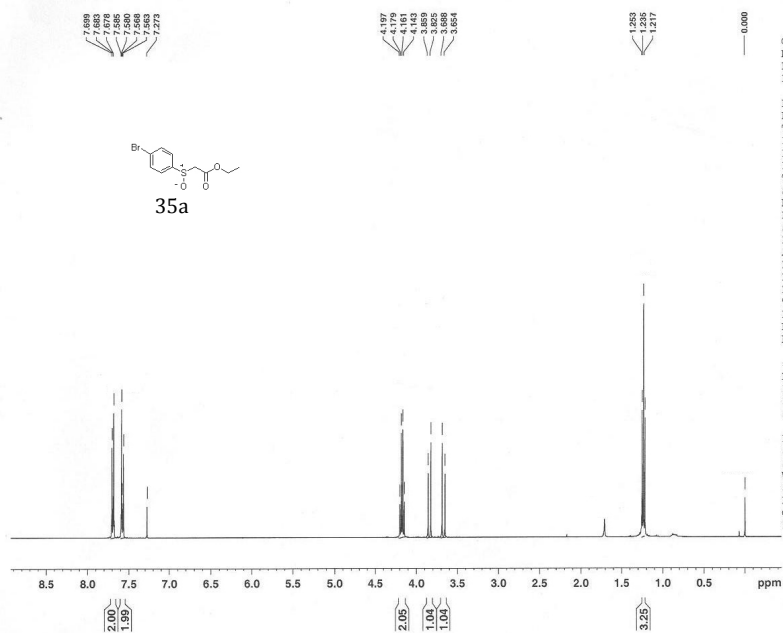
----- CHANNEL f1 -----
 NUC1 13C
 P1 8.00 usec
 PL1 -3.00 dB
 SFO1 100.6228298 MHz

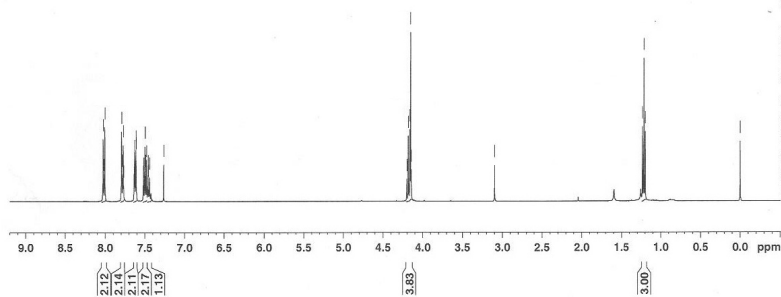
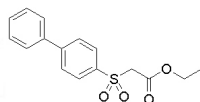
----- CHANNEL f2 -----
 CPDPRG2 waltz16
 NUC2 1H
 PCPD2 70.00 usec
 PL2 -1.00 dB
 PL12 14.00 dB
 PL13 14.00 dB
 SFO2 400.1316005 MHz

F2 - Processing parameters
 SI 32768
 SF 100.6127722 MHz
 WDW EM
 SSB 0
 LB 1.00 Hz
 GB 0
 PC 1.00







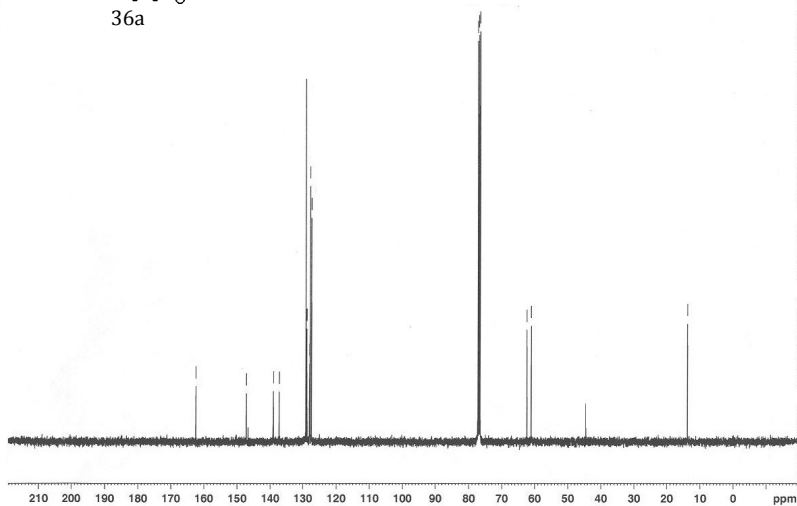
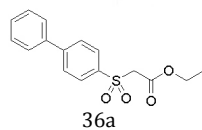
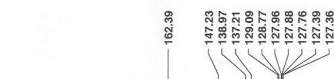


Current Data Parameters
 NAME PHJ-1-65-maj
 EXPNO 1
 PROCNO 1

F2 - Acquisition Parameters
 Date_ 20080428
 Time 10.49
 INSTRUM spect
 PROBHD 5 mm PABBO BB-
 PULPROG zg30
 TD 65536
 SOLVENT CDCl3
 NS 16
 DS 2
 SWH 8278.146 Hz
 FIDRES 0.126314 Hz
 AQ 3.9584243 sec
 RG 203.2
 DW 60.400 usec
 DE 7.00 usec
 TE 298.0 K
 D1 1.0000000 sec
 MCREST 0.0000000 sec
 MCWRK 0.0150000 sec

==== CHANNEL f1 =====
 NUC1 1H
 P1 12.80 usec
 PL1 0.00 dB
 SFO1 400.1324710 MHz

F2 - Processing parameters
 SI 32768
 SF 400.1300096 MHz
 WDW EM
 SSB 0
 LB 0.30 Hz
 GB 0
 FC 1.00



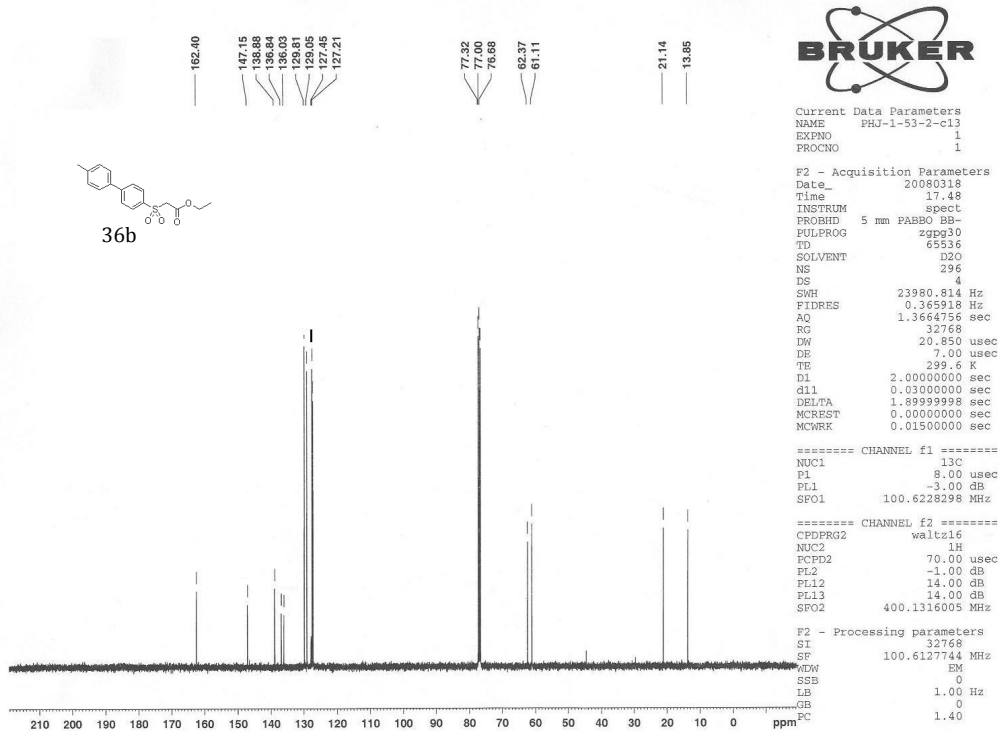
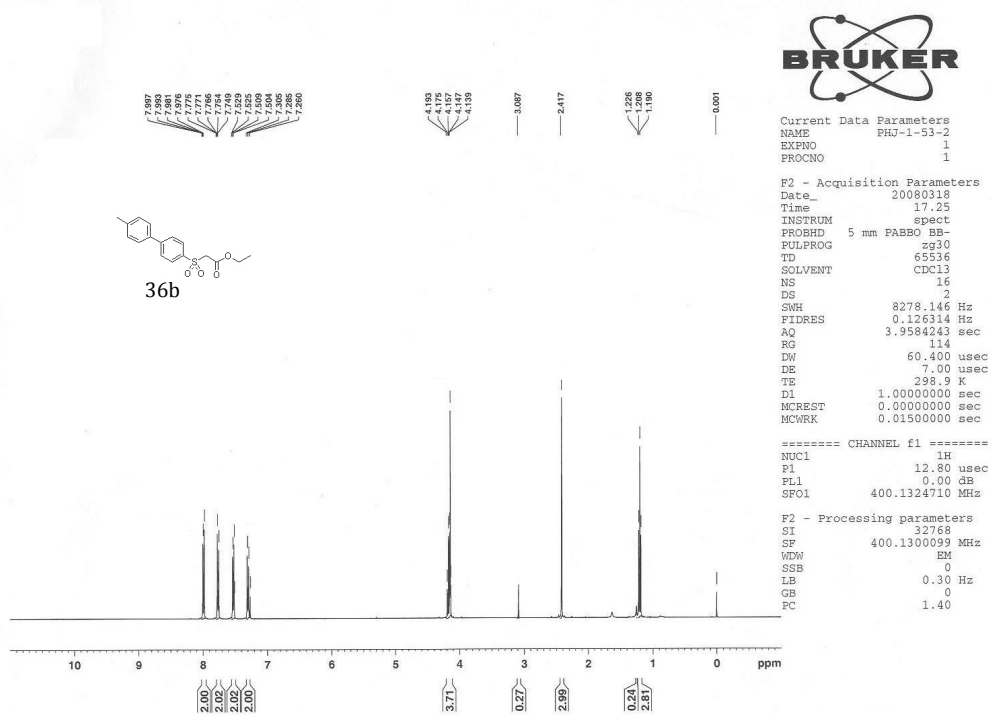
Current Data Parameters
 NAME PHJ-1-65-cl3
 EXPNO 1
 PROCNO 1

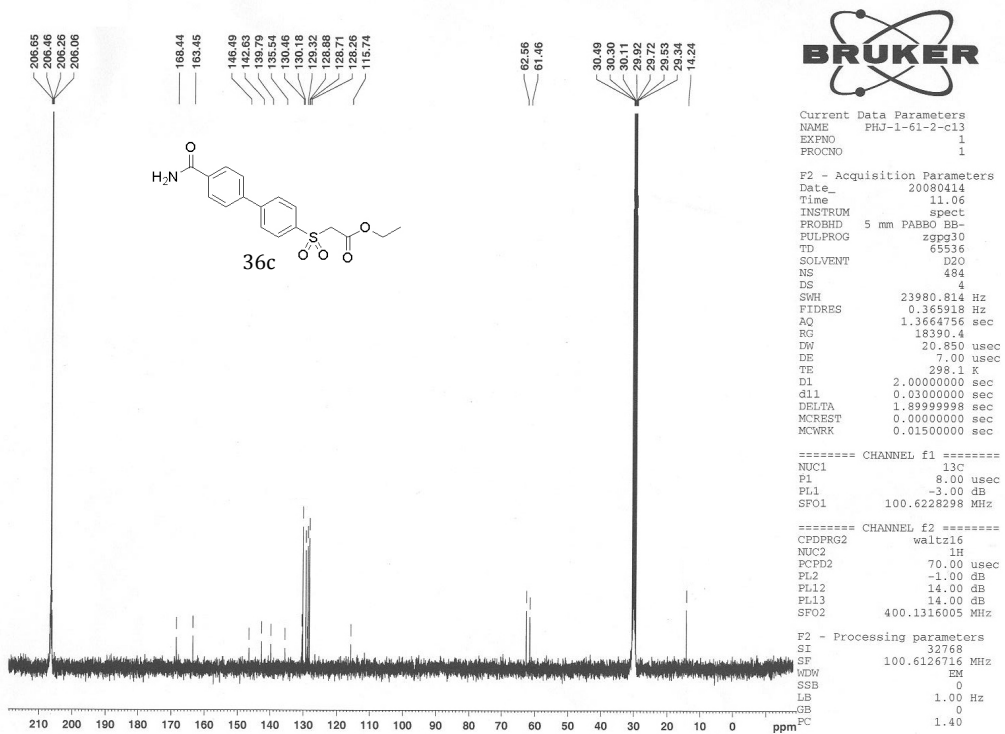
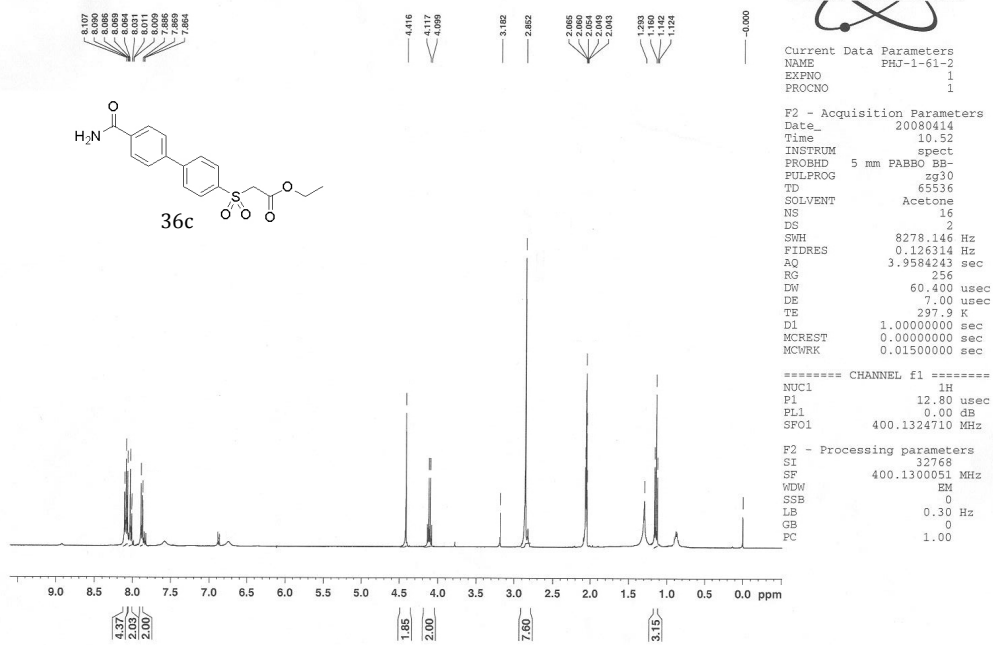
F2 - Acquisition Parameters
 Date_ 20080426
 Time 11.28
 INSTRUM spect
 PROBHD 5 mm PABBO BB-
 PULPROG zgpg30
 TD 65536
 SOLVENT D2O
 NS 401
 DS 4
 SWH 23980.814 Hz
 FIDRES 0.365918 Hz
 AQ 1.3664756 sec
 RG 20642.5
 DW 20.850 usec
 DE 7.00 usec
 TE 300.1 K
 D1 2.0000000 sec
 d11 0.0300000 sec
 DELTA 1.8999998 sec
 MCREST 0.0000000 sec
 MCWRK 0.0150000 sec

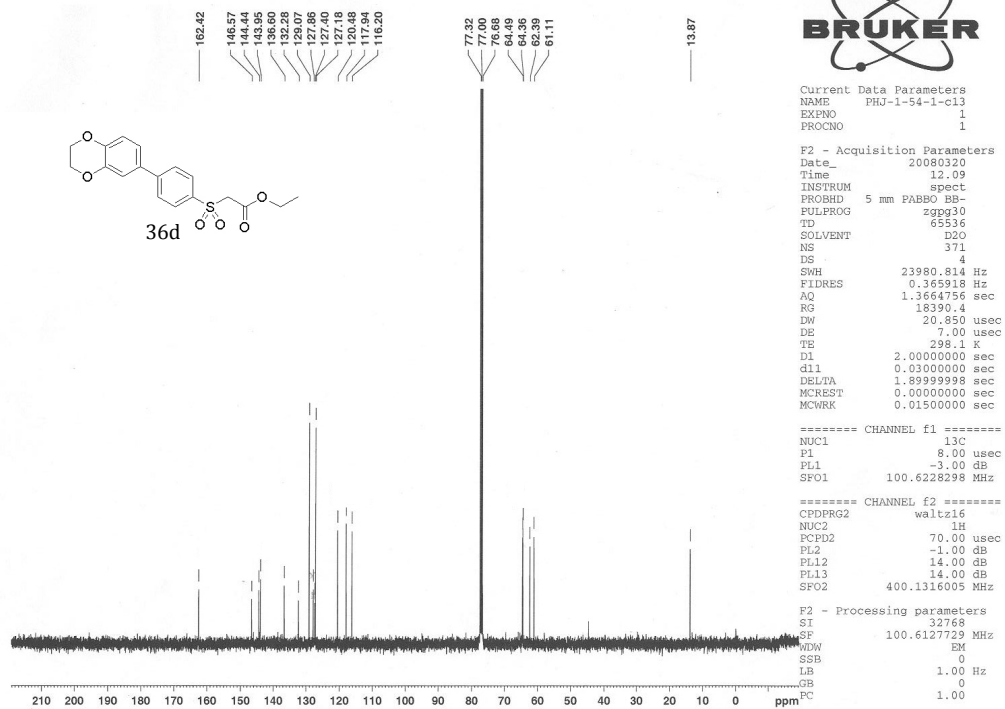
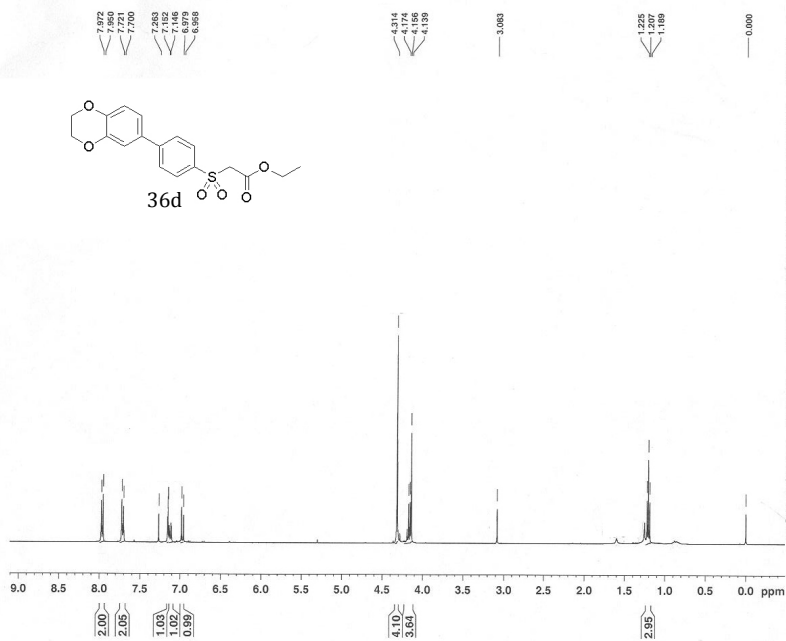
==== CHANNEL f1 =====
 NUC1 13C
 P1 8.00 usec
 PL1 -3.00 dB
 SFO1 100.6228298 MHz

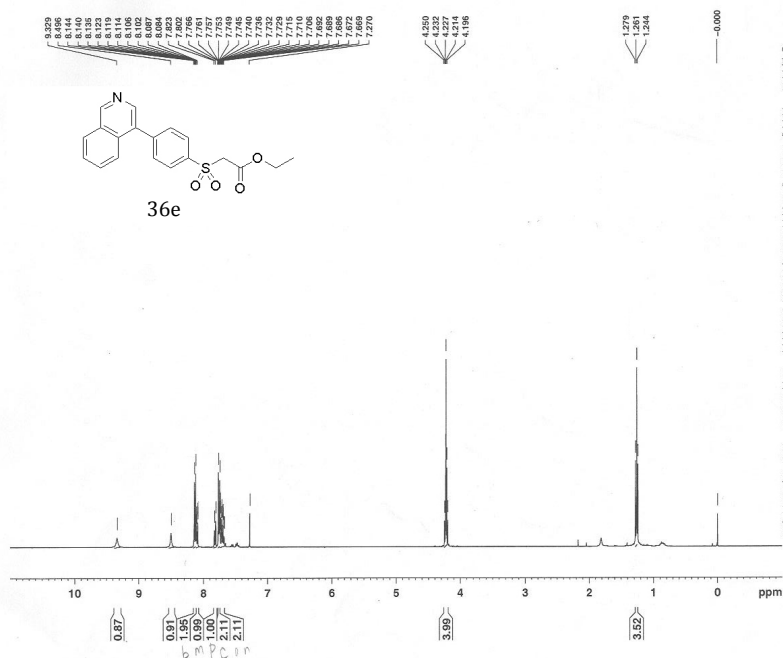
==== CHANNEL f2 =====
 CPDPRG2 waltz16
 NUC2 1H
 BCPD2 70.00 usec
 PL2 -1.00 dB
 PL12 14.00 dB
 PL13 14.00 dB
 SFO2 400.1316005 MHz

F2 - Processing parameters
 SI 32768
 SF 100.6127737 MHz
 WDW EM
 SSB 0
 LB 1.00 Hz
 GB 0
 FC 1.40







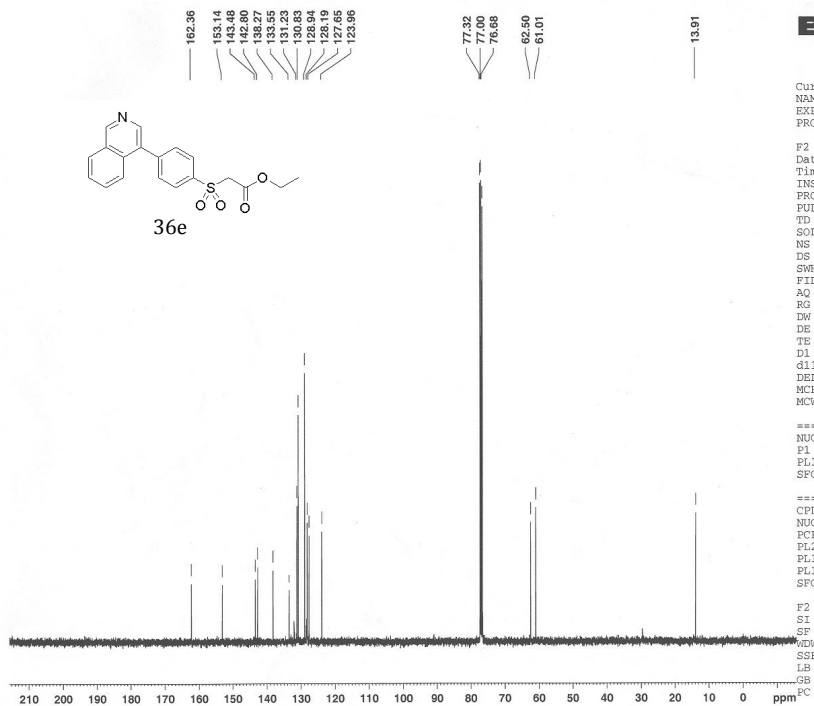


Current Data Parameters
NAME PHJ-1-60
EXPNO 1
PROCNO 1

F2 - Acquisition Parameters
Date_ 20080410
Time 9.32
INSTRUM spect
PROBHD 5 mm PABBO BB-
PULPROG zg30
TD 65536
SOLVENT CDC13
NS 16
DS 2
SWH 8278.146 Hz
FIDRES 0.126314 Hz
AQ 3.9584243 sec
RG 161.3
DW 60.400 usec
DE 7.00 usec
TE 298.2 K
D1 1.00000000 sec
MCREST 0.00000000 sec
MCWRK 0.01500000 sec

===== CHANNEL f1 =====
NUC1 1H
P1 12.80 usec
PL1 0.00 dB
SFO1 400.1324710 MHz

F2 - Processing parameters
SI 32768
SF 400.1300056 MHz
WDW EM
SSB 0
LB 0.30 Hz
GB 0
FC 1.00



Current Data Parameters
NAME PHJ-1-60-cl3
EXPNO 1
PROCNO 1

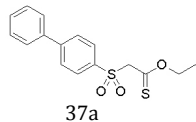
F2 - Acquisition Parameters
Date_ 20080410
Time 10.18
INSTRUM spect
PROBHD 5 mm PABBO BB-
PULPROG zgpg30
TD 65536
SOLVENT D2O
NS 512
DS 4
SWH 23980.814 Hz
FIDRES 0.365918 Hz
AQ 1.3664756 sec
RG 43004
DW 20.850 usec
DE 7.00 usec
TE 298.2 K
D1 2.00000000 sec
d11 0.03000000 sec
DELTA 1.89999998 sec
MCREST 0.00000000 sec
MCWRK 0.01500000 sec

===== CHANNEL f1 =====
NUC1 13C
P1 8.00 usec
PL1 -3.00 dB
SFO1 100.6228298 MHz

===== CHANNEL f2 =====
CPDPRG2 waltz16
NUC2 1H
PCPD2 70.00 usec
PL2 -1.00 dB
PL12 14.00 dB
PL13 14.00 dB
SFO2 400.1316005 MHz

F2 - Processing parameters
SI 32768
SF 100.6127737 MHz
WDW EM
SSB 0
LB 1.00 Hz
GB 0
FC 1.00

7.962
7.947
7.930
7.900
7.796
7.747
7.730
7.614
7.596
7.580
7.564
7.474
7.470
7.455
7.455
7.416
7.434
7.284



4.585
4.486
4.439
4.413

1.312
1.307
1.290
1.272
1.266

0.004
0.004

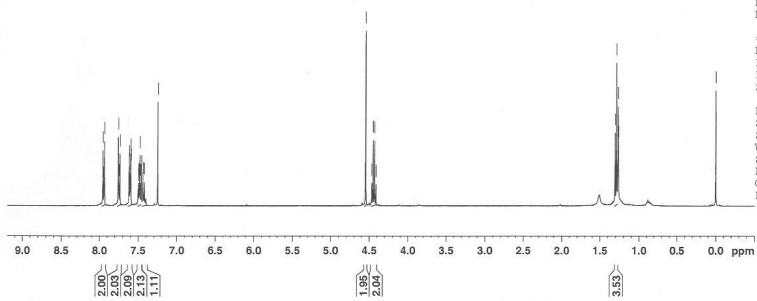


Current Data Parameters
NAME PHJ-1-66-tb15-
EXPNO 1
PROCNO 1

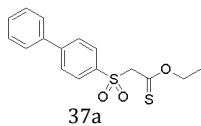
F2 - Acquisition Parameters
Date_ 20080430
Time 9.40
INSTRUM spect
PROBHD 5 mm PABBO BB-
PULPROG zg30
TD 65536
SOLVENT CDCl3
NS 32
DS 2
SWH 8278.146 Hz
FIDRES 0.126314 Hz
AQ 3.9584243 sec
RG 512
DW 60.400 usec
DE 7.00 usec
TE 333.2 K
D1 1.0000000 sec
MCREST 0.0000000 sec
MCVRK 0.0150000 sec

***** CHANNEL f1 *****
NUC1 1H
P1 12.80 usec
PL1 0.00 dB
SFO1 400.1324710 MHz

F2 - Processing parameters
SI 32768
SF 400.1300152 MHz
WDW EM
SSB 0
LB 0.30 Hz
GB 0
PC 1.00



204.70



147.14
139.00
136.54
136.54
129.12
128.79
127.60
127.40

77.32
77.20
77.08
76.88
71.63
69.59

13.25



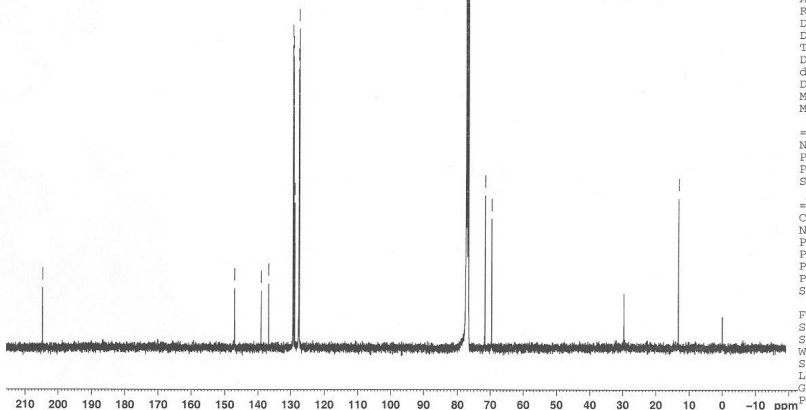
Current Data Parameters
NAME PHJ-1-66-tb15-cl3-2
EXPNO 1
PROCNO 1

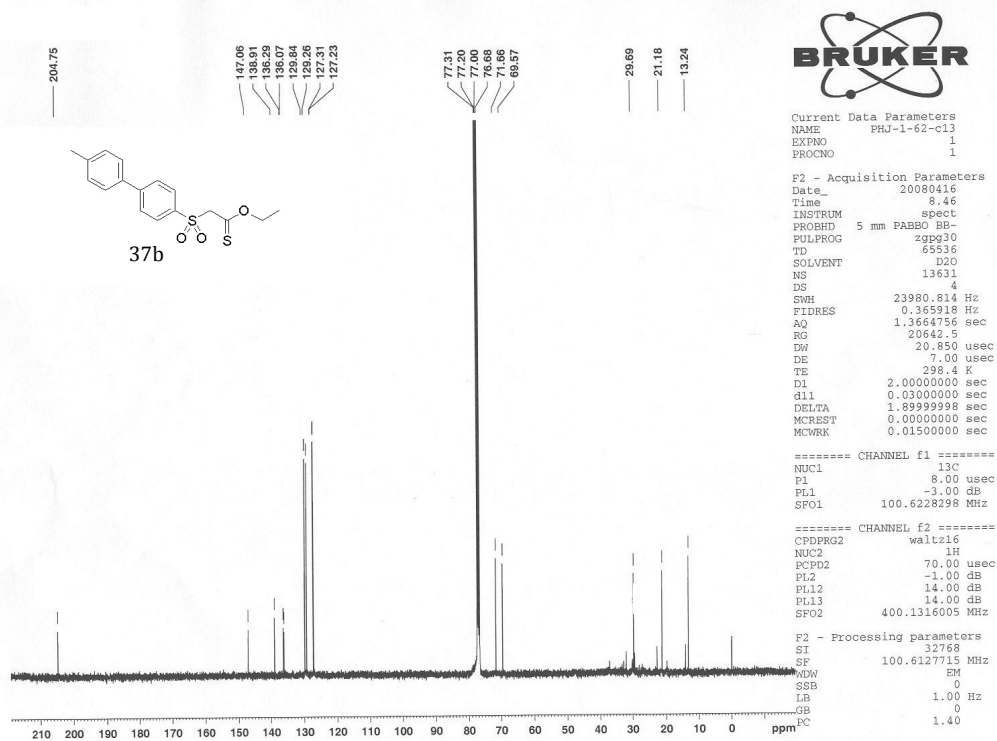
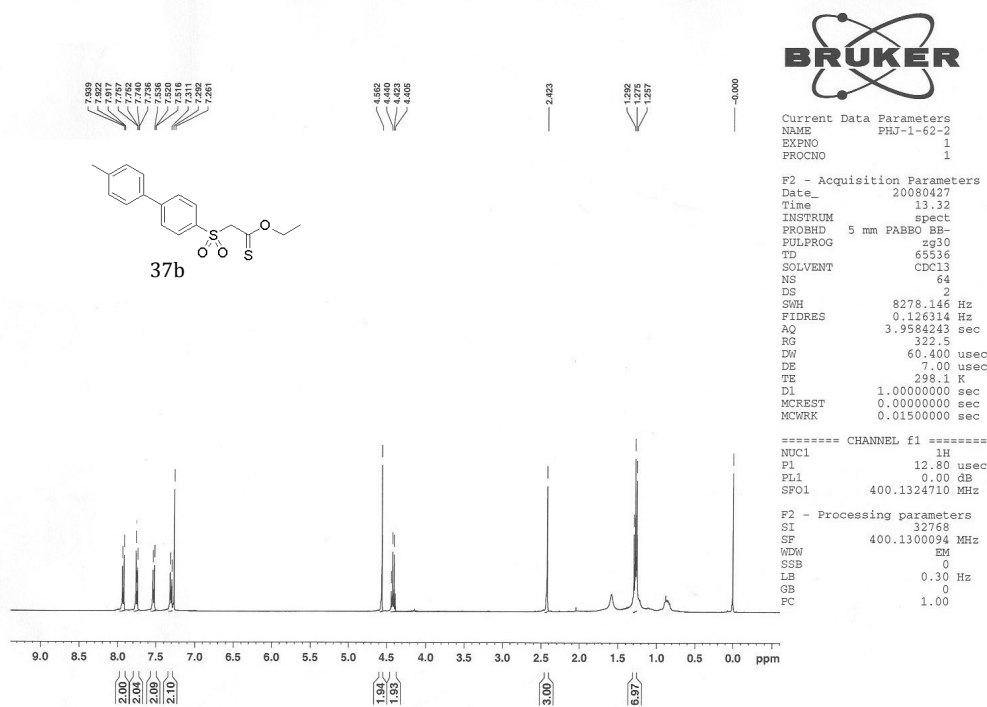
F2 - Acquisition Parameters
Date_ 20080502
Time 9.41
INSTRUM spect
PROBHD 5 mm PABBO BB-
PULPROG zgpg30
TD 65536
SOLVENT CDCl3
NS 14668
DS 4
SWH 23980.814 Hz
FIDRES 0.365918 Hz
AQ 1.3664756 sec
RG 14596.5
DW 20.850 usec
DE 7.00 usec
TE 298.5 K
D1 2.0000000 sec
d11 0.0300000 sec
DELTA 1.89999998 sec
MCREST 0.0000000 sec
MCVRK 0.0150000 sec

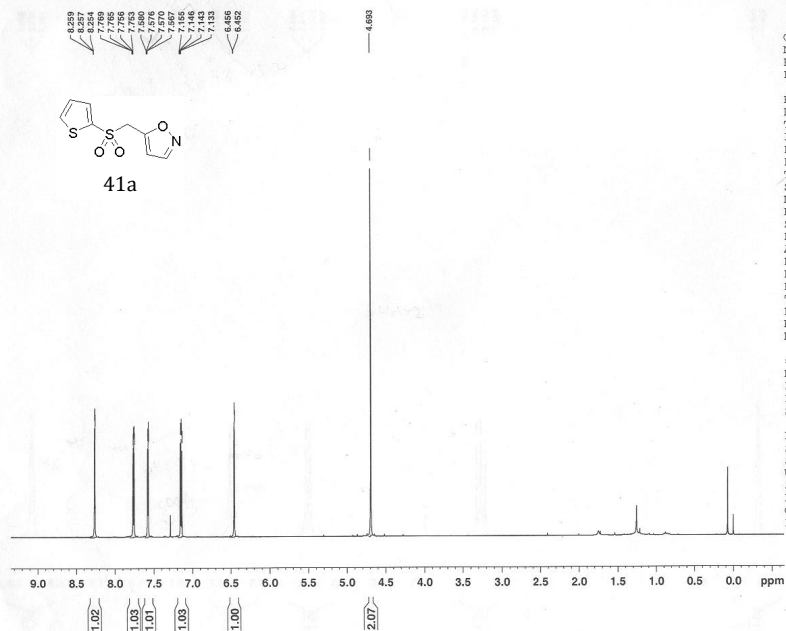
***** CHANNEL f1 *****
NUC1 13C
P1 8.00 usec
PL1 -3.00 dB
SFO1 100.6228298 MHz

***** CHANNEL f2 *****
CPDPRG2 waltz16
NUC2 1H
PCPD2 70.00 usec
PL2 -1.00 dB
PL12 14.00 dB
PL13 14.00 dB
SFO2 400.1316005 MHz

F2 - Processing parameters
SI 32768
SF 100.6127715 MHz
WDW EM
SSB 0
LB 1.00 Hz
GB 0
PC 1.40





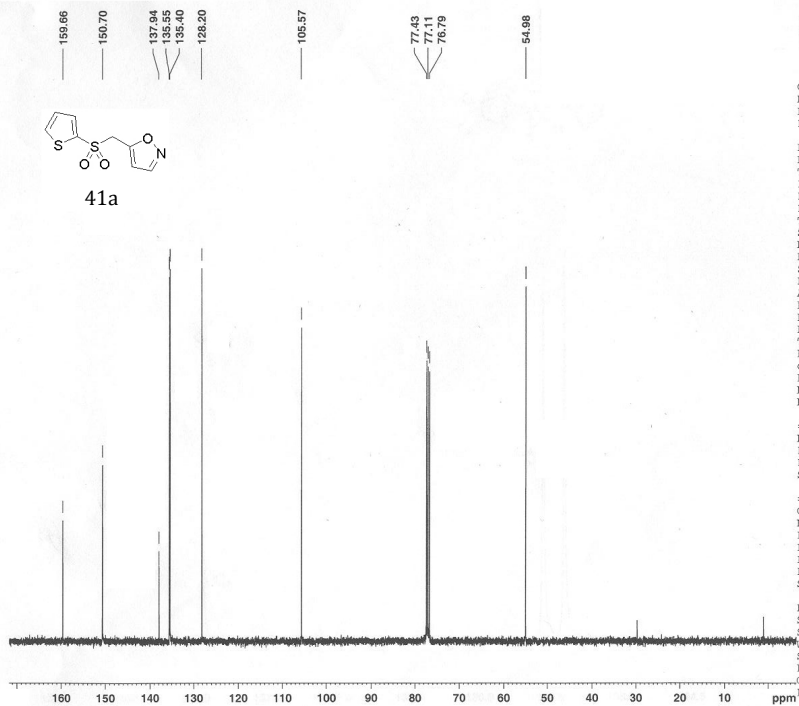


Current Data Parameters
NAME jerry-27
EXPNO 1
PROCNO 1

F2 - Acquisition Parameters
Date_ 20070309
Time 16.41
INSTRUM spect
PROBHD 5 mm PABBO BB-
PULPROG zg30
TD 65536
SOLVENT CDCl3
NS 16
DS 2
SWH 8278.146 Hz
FIDRES 0.126314 Hz
AQ 3.9584243 sec
RG 101.6
DW 60.400 usec
DE 7.00 usec
TE 297.9 K
D1 1.0000000 sec
MCREST 0.0000000 sec
MCWRK 0.0150000 sec

===== CHANNEL f1 =====
NUC1 1H
P1 12.80 usec
PL1 0.00 dB
SFO1 400.1324710 MHz

F2 - Processing parameters
SI 32768
SF 400.1300005 MHz
WDW EM
SSB 0
LB 0.30 Hz
GB 0
PC 1.00



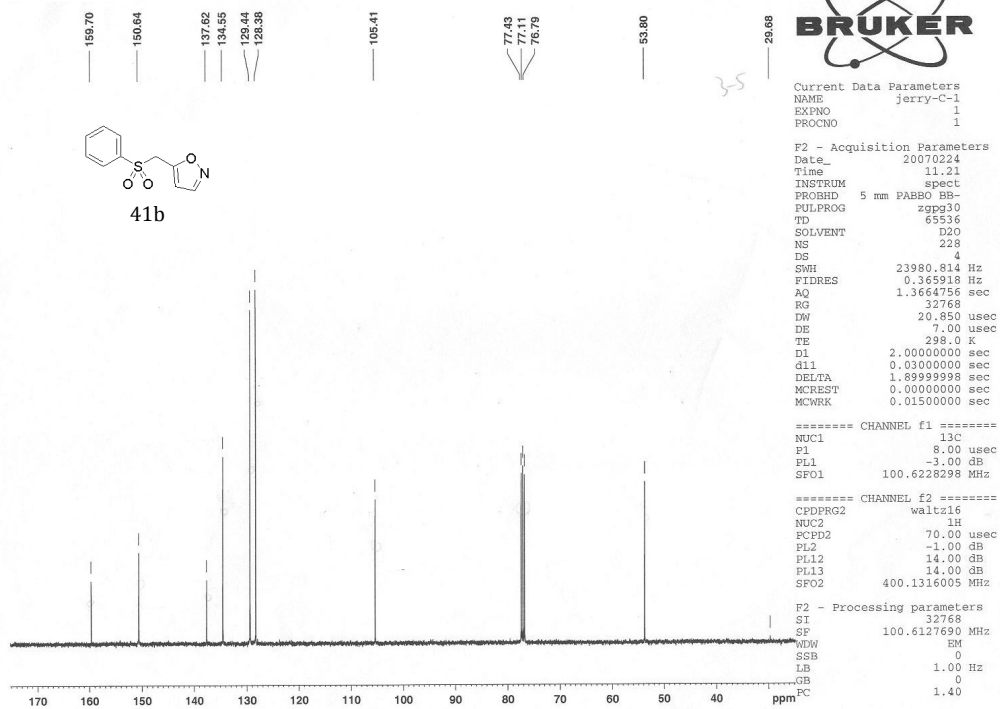
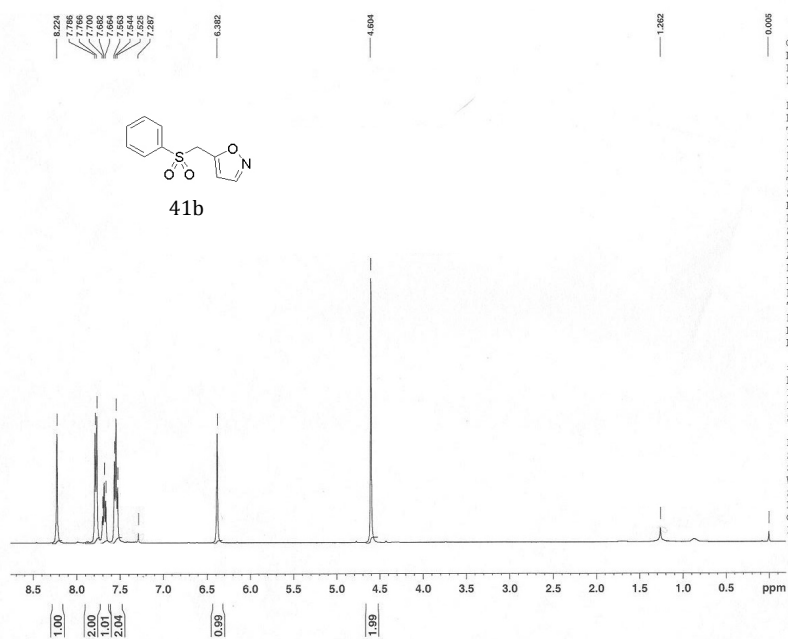
Current Data Parameters
NAME jerry-C-6
EXPNO 1
PROCNO 1

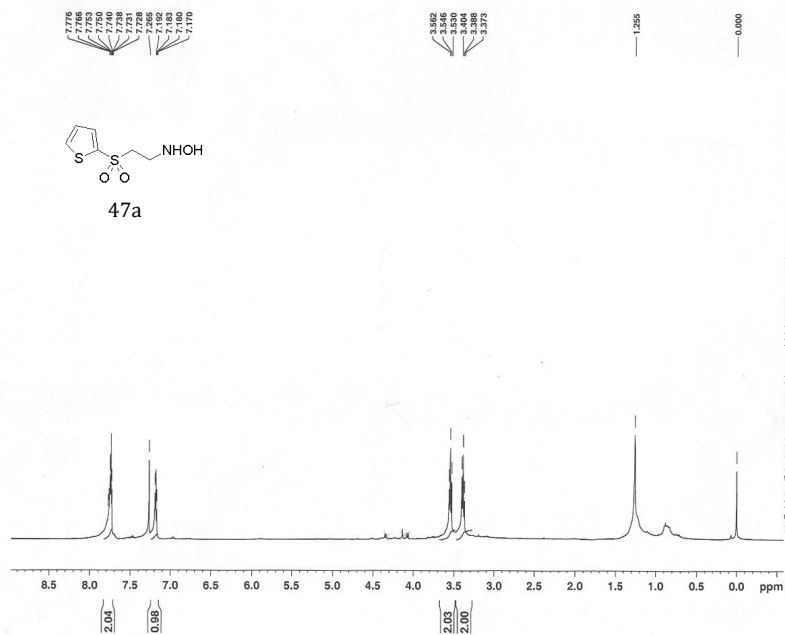
F2 - Acquisition Parameters
Date_ 20070309
Time 16.51
INSTRUM spect
PROBHD 5 mm PABBO BB-
PULPROG zgpg30
TD 65536
SOLVENT D2O
NS 177
DS 4
SWH 23980.814 Hz
FIDRES 0.365918 Hz
AQ 1.3664756 sec
RG 32768
DW 20.850 usec
DE 7.00 usec
TE 298.2 K
D1 2.0000000 sec
d11 0.0300000 sec
DELTA 1.8999999 sec
MCREST 0.0000000 sec
MCWRK 0.0150000 sec

===== CHANNEL f1 =====
NUC1 13C
P1 8.00 usec
PL1 -3.00 dB
SFO1 100.6228298 MHz

===== CHANNEL f2 =====
CPDPRG2 waltz16
NUC2 1H
PCPD2 70.00 usec
PL2 -1.00 dB
PL12 14.00 dB
PL13 14.00 dB
SFO2 400.1316005 MHz

F2 - Processing parameters
SI 32768
SF 100.6127690 MHz
WDW EM
SSB 0
LB 1.00 Hz
GB 0
PC 1.40



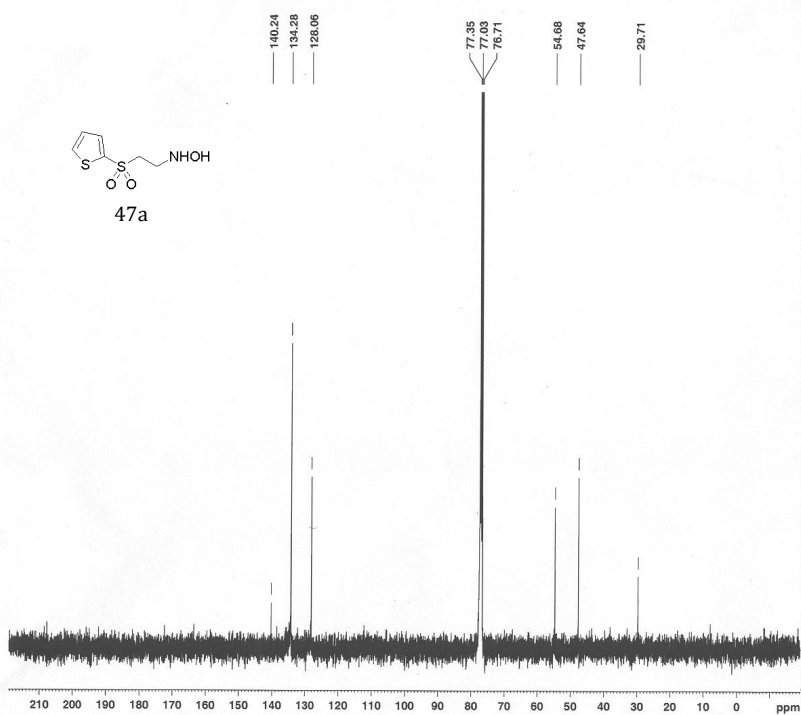


Current Data Parameters
 NAME JC-I-122d
 EXPNO 1
 PROCNO 1

F2 - Acquisition Parameters
 Date_ 20070630
 Time 12.22
 INSTRUM spect
 PROBHD 5 mm PABBO BB-
 PULPROG zg30
 TD 65536
 SOLVENT CDC13
 NS 64
 DS 2
 SWH 8278.146 Hz
 FIDRES 0.126314 Hz
 AQ 3.9584243 sec
 RG 256
 DW 60.400 usec
 DE 7.00 usec
 TE 297.4 K
 D1 1.00000000 sec
 MCREST 0.00000000 sec
 MCWRK 0.01500000 sec

==== CHANNEL f1 =====
 NUC1 1H
 P1 12.80 usec
 PL1 0.00 dB
 SFO1 400.1324710 MHz

F2 - Processing parameters
 SI 32768
 SF 400.1300071 MHz
 WDW EM
 SSB 0
 LB 0.30 Hz
 GB 0
 PC 1.40



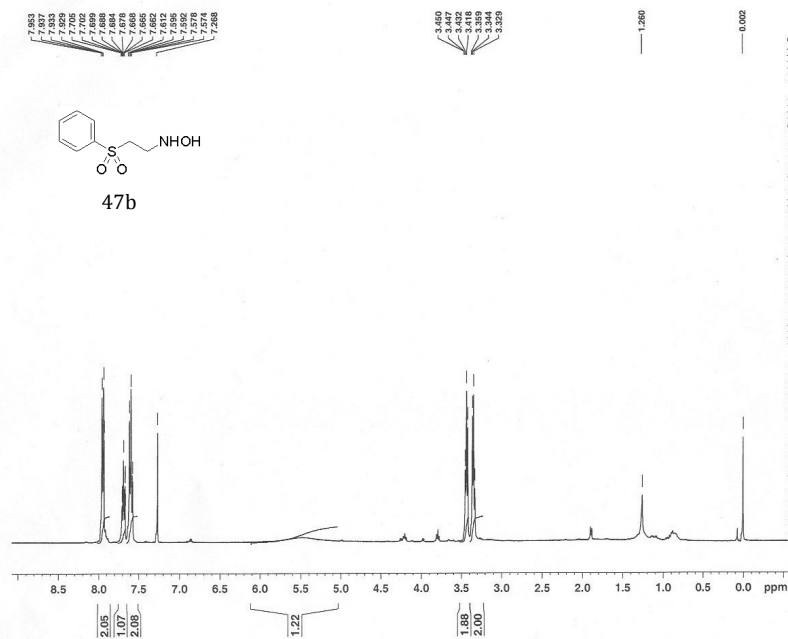
Current Data Parameters
 NAME JC-I-122d-C13
 EXPNO 1
 PROCNO 1

F2 - Acquisition Parameters
 Date_ 20070630
 Time 12.34
 INSTRUM spect
 PROBHD 5 mm PABBO BB-
 PULPROG zgpg30
 TD 65536
 SOLVENT D2O
 NS 1536
 DS 4
 SWH 23980.814 Hz
 FIDRES 0.365918 Hz
 AQ 1.3664756 sec
 RG 13004
 DW 20.850 usec
 DE 7.00 usec
 TE 297.6 K
 D1 2.00000000 sec
 d11 0.03000000 sec
 DELTA 1.89999998 sec
 MCREST 0.00000000 sec
 MCWRK 0.01500000 sec

==== CHANNEL f1 =====
 NUC1 13C
 P1 8.00 usec
 PL1 -3.00 dB
 SFO1 100.6228298 MHz

==== CHANNEL f2 =====
 CDPGR2 waltz16
 NUC2 1H
 PCPD2 70.00 usec
 PL2 -1.00 dB
 PL12 14.00 dB
 PL13 14.00 dB
 SFO2 400.1316005 MHz

F2 - Processing parameters
 SI 32768
 SF 100.6127690 MHz
 WDW EM
 SSB 0
 LB 1.00 Hz
 GB 0
 PC 1.40

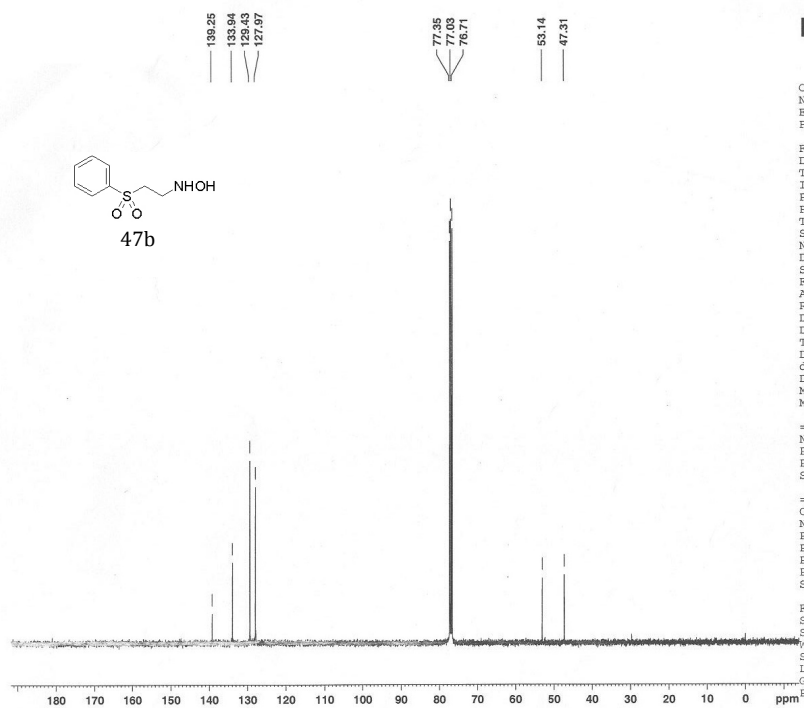


Current Data Parameters
NAME JC-I-119-2c
EXPNO 1
PROCNO 1

F2 - Acquisition Parameters
Date_ 20070623
Time 12.15
INSTRUM spect
PROBHD 5 mm PABBO BB-
PULPROG zg30
TD 65536
SOLVENT CDCl3
NS 16
DS 2
SWH 8278.146 Hz
FIDRES 0.126314 Hz
AQ 3.9584243 sec
RG 256
DW 60.400 usec
DE 7.00 usec
TE 298.2 K
DI 1.00000000 sec
MCREST 0.00000000 sec
MCVRK 0.01500000 sec

===== CHANNEL f1 =====
NUC1 1H
P1 12.80 usec
PL1 0.00 dB
SFO1 400.1324710 MHz

F2 - Processing parameters
SI 32768
SF 400.1300061 MHz
WDW EM
SSB 0
LB 0.30 Hz
GB 0
PC 1.00



Current Data Parameters
NAME JC-I-119-2c-C13
EXPNO 1
PROCNO 1

F2 - Acquisition Parameters
Date_ 20070623
Time 12.23
INSTRUM spect
PROBHD 5 mm PABBO BB-
PULPROG zgpg30
TD 65536
SOLVENT D2O
NS 1281
DS 4
SWH 23980.814 Hz
FIDRES 0.365918 Hz
AQ 1.3664756 sec
RG 16384
DW 20.850 usec
DE 7.00 usec
TE 298.2 K
DI 2.00000000 sec
d11 0.03000000 sec
DELTA 1.89999998 sec
MCREST 0.00000000 sec
MCVRK 0.01500000 sec

===== CHANNEL f1 =====
NUC1 13C
P1 8.00 usec
PL1 -3.00 dB
SFO1 100.6228298 MHz

===== CHANNEL f2 =====
CFPRG2 waltz16
NUC2 1H
PCPD2 70.00 usec
PL2 -1.00 dB
PL12 14.00 dB
PL13 14.00 dB
SFO2 400.1316005 MHz

F2 - Processing parameters
SI 32768
SF 100.6127690 MHz
WDW EM
SSB 0
LB 1.00 Hz
GB 0
PC 1.40